



D 2019

U. PORTO
FEUP FACULDADE DE ENGENHARIA
UNIVERSIDADE DO PORTO

SULFAMETHOXAZOLE BIODEGRADATION

AN UNCOMMON PROPERTY WITH POTENTIAL APPLICATION FOR WASTEWATER TREATMENT

ANA C. REIS

TESE DE DOUTORAMENTO APRESENTADA

À FACULDADE DE ENGENHARIA DA UNIVERSIDADE DO PORTO EM JULHO DE 2019

ÁREA CIENTÍFICA EM ENGENHARIA DO AMBIENTE



Sulfamethoxazole biodegradation, an uncommon property with potential application for wastewater treatment

Dissertation presented to the Faculdade de Engenharia – Universidade do Porto to attain the degree of PhD in Environment Engineering

By

Ana C. Reis

Under the supervision of Professor Olga Cristina Pastor Nunes

Under the co-supervision of Professor Philippe François Xavier Corvini

Under the co-supervision of Professor Célia Maria Manaia Rodrigues

Laboratório de Engenharia de Processos, Ambiente, Biotecnologia e Energia -
LEPABE

Departamento de Engenharia Química

Faculdade de Engenharia da Universidade do Porto

Portugal

Porto, Setembro 2019

“Wisdom is not a product of schooling but of the lifelong attempt to acquire it.”

Albert Einstein

To my husband, parents, and brother for always being there for me...

Acknowledgments

When I first embarked on this Ph.D. journey, more than 4 years ago, I could have never predicted all the ups and downs that awaited me around the corner. However, looking back fills my heart with gratitude. First and foremost I am grateful to my husband, my brother and my parents. You have supported me unconditionally and often reminded me of what is truly essential in life. You have been my rock in the “downs” and the ones I’ve always called to celebrate my “ups”.

A very special thanks to Dr. Olga Nunes, for encouraging and guiding me since the very beginning of this project and for challenging me to become a better researcher every day. Thank you also to LEPABE and to the Faculty of Engineering for providing me with space and conditions to carry out my work. I am especially grateful to Prof. Dr. Philippe Corvini for having me in his lab at the FHNW (Basel, Switzerland) and for the continued support even throughout the most uncertain periods of this Ph.D. Working under your guidance has widened and matured my perspective both personally and professionally. I am also very grateful to Dr. Boris Kolvenbach for always keeping your door open and for still finding the time to help. Lastly, a special thanks to Dr. Célia Manaia, for always being receptive and supportive along this journey. It was a pleasure to work and learn with all of you!

A very heartfelt thank you to all of my colleagues both in Porto and Basel for always being available to share a cup of coffee and lots of advice. A special mention to Dr. Rita Lopes, Dr. Patrícia Reis, Vera Sousa, Sara Teixeira, Dr. Joana Bondoso, Marta Pedrosa, Mário Sousa, Mafalda Paiva, Teresa Viana, Diana Salvador, Nuno Moreira, Dr. Luísa Barreiros and Dr. Rita Lado, thank you for making the lab at FEUP such a fun and great place to be. Thank you to my colleagues at ESB, Dr. Ivone Moreira, Dr. Catarina Ferreira, Carlos Rocha, and Gonçalo Macedo for the patience and for wise advice. And to my colleagues in Basel, Dr. Danuta Cichocka, Marta Woźniak-Karczewska, Dr. Monika Čvančarová, Federica Bonacci, Ying Liu, Kevin Kroll, Dr. Markus Lenz, Riccardo Perri, David Cayon, Sebastian Hedwig,

Acknowledgements

Erik Amman, Dr. Nora Corvini, Dr. Aleksandra Galic, Melissa Amrein and Dr. Benjamin Ricken for creating such a melting pot of cultures and for making the lab at FHNW such a dynamic place to be. Also, a very special thanks to the always optimistic and energetic, Dr. Ana Tskhvediani, it has been wonderful to share an office with you!

A special mention to Anna Weston (FHNW) for all the advice on qPCR and RNA extraction, to Dr. Mohamed Chami (Uni Basel) for all the support with the TEM analysis and to Prof. Dr. Peter Vandamme (UGhent) for kindly supplying multiple *Achromobacter* spp. strains for phage host range infection studies.

I am also grateful to all technical staff: Sílvia Faia, Paula Pinheiro, Liliana Pereira, and Dr. Carla Ferreira, your support has been vital in all the steps of the way. Moreover, I want to thank the administrative staff at both institutions, especially Fátima Faustino (FEUP) and François Vogel (FHNW) for all the patience and for coming out of your way multiple times to help me navigate the administrative and bureaucratic tasks.

My deepest gratitude goes to all of those special people who left us. I wish you were all here to celebrate with me. Also, to my friends outside of academia for helping keep things in perspective and to regain my focus when things seemed lost. Lastly, I thank God for taking care of me during this intense and life-changing journey. Without His blessing, this thesis would not have been born.

Lastly, I wish to thank the Fundação para a Ciência e Tecnologia (FCT) for my Ph.D. grant (SFRH/BD/95814/2013). This work was financially supported by:

- (i) Beyond pollutant removal - understanding the biochemical mechanism of sulfonamide degradation in wastewater and the role of *ipso*-substitution (Swiss National Science Foundation grant No. 160332);
- (ii) Project UID/EQU/00511/2013-LEPABE (Laboratory for Process Engineering, Environment, Biotechnology and Energy – EQU/00511) by FEDER funds through

Programa Operacional Competitividade e Internacionalização – COMPETE2020
and by national funds through FCT - Fundação para a Ciência e a Tecnologia;

(iii) Project “LEPABE-2-ECO-INNOVATION” – NORTE-01-0145-FEDER-000005,
funded by Norte Portugal Regional Operational Programme (NORTE 2020), under
PORTUGAL 2020 Partnership Agreement, through the European Regional
Development Fund (ERDF);

(iv) Project UID/EQU/00511/2019 - Laboratory for Process Engineering,
Environment, Biotechnology and Energy – LEPABE funded by national funds
through FCT/MCTES (PIDDAC).



Abstract

Sulfonamides were the first fully synthetic antibiotics successfully applied to therapy. The intensive and sometimes imprudent use of these antimicrobials has made them ubiquitous micropollutants and resulted in the onset and spread of resistance. Despite the increasing levels of resistance, this class of antibiotics is still invaluable for modern veterinary medicine and animal husbandry, and it remains useful for the treatment of a selected number of infections in humans.

In recent years our knowledge of the biological transformation of these drugs has been steadily increasing. Current research on this topic has shown that sulfonamides can be transformed mostly by acetylation, hydroxylation, deamination, and oxidation of the primary amine. These molecules were also found to be susceptible to biodegradation through reactions such as the *ipso*-hydroxylation and subsequent cleavage of the sulfonamide bond. An increasing minority of *Actinobacteria* isolates has been reported to catalyze this reaction and to partially mineralize the sulfonamide molecule. Sulfonamide-mineralizing strains from the *Microbacterium* and *Arthrobacter* genera have been shown to carry a conserved gene cluster consisting of a sulfonamide monooxygenase (*sadA*), 4-aminophenol monooxygenase (*sadB*) and an FMN-reductase (*sadC*).

Achromobacter denitrificans PR1, a *Proteobacteria* enriched and isolated from activated sludge, was previously described as a sulfamethoxazole-degrader (SMX). Nevertheless, later studies revealed that some colonies spontaneously lost the ability to metabolize this antibiotic. This instability and our lack of knowledge regarding the dissemination of the *sad* cluster motivated further genomic and metabolic analysis with this culture. Thus, two main goals were defined for this thesis: (i) characterization of the metabolic pathway for SMX degradation; and (ii) determination of the genetic determinants linked to the degradation of this antibiotic.

The study of the metabolic pathway for SMX degradation revealed that *ipso*-hydroxylation of the molecule was the underlying mechanism of SMX transformation in the culture containing *A. denitrificans* PR1. As previously described in *Microbacterium* sp. BR1, this reaction led to the release of 3-amino-5-methylisoxazole (3A5MI), as a dead-end metabolite, and 4-aminophenol (4AP) that serves as carbon and energy source. Interestingly, this reaction also caused molecular rearrangements that led to the accumulation of 3 additional dead-end metabolites. These rearrangements comprised (i) an NIH shift of the sulfonyl group leading to the formation of 5-amino-2-hydroxybenzenesulfonic acid; (ii) a Baeyer-Villiger rearrangement resulting from the migration of the sulfo-methylisoxazole moiety to the oxygen atom of the hydroxyl group; and (iii) an unspecific hydroxylation at *meta* or *ortho* position of the benzene ring. Some of these reactions had been previously observed for *ipso*-hydroxylation of other aromatic substrates. Nevertheless, they were described for sulfonamides here for the first time.

The assessment of *A. denitrificans* PR1 metabolic instability led to the discovery of a low-abundance and slow-growing actinobacterium. This new strain, named strain GP, displayed a syntrophic behavior and was unable to grow independently from the *Proteobacteria*.

Noticeably, SMX and 4AP were only degraded by the consortium of the two bacteria but not by axenic cultures of *A. denitrificans* PR1, suggesting that strain GP played a crucial role in this process. To assess the nature of the syntrophic relationship in this two-member sulfonamide-degrading consortium, two independent approaches were used. In the first study several different media, co-factors and culture conditions were tested. In the second study, an *in silico* comparative genomics approach was used.

The findings obtained in both studies indicate that strain GP represents a new species and possibly even a new genus within the *Microbacteriaceae* family. Noticeably, it did not display a significant genome reduction as commonly observed in other syntrophs. Instead,

this strain showed a moderate loss of genes linked to tetrapyrrole and heme biosynthesis and appeared to lack thiol transporters, essential to maintain the redox balance in the periplasm. This reduction would avert the synthesis of cytochromes, essential for aerobic growth. Nevertheless, exogenous heme, catalase and even addition of *A. denitrificans* PR1 supernatant and crude cell extract failed to produce isolated colonies of the *Actinobacteria*. Comparison of the genome of strain GP and *A. denitrificans* PR1 revealed that only the first one harbored homologs of the genes previously linked to sulfonamide metabolism: *sadA*, *sadB*, and *sadC*. Interestingly, strain GP carried *sadA* within a transposable element flanked by a *yceI* transporter, an SOS-response peptidase, and an IS1380 family transposase, while *sadB* and *sadC* were dispersed into other regions of its genome. A similar transposon was observed in the sulfadiazine-degraders *Arthrobacter* sp. D2 and D4, while a single isolated copy of the IS1380 transposase was also found in the genome of *Microbacterium* sp. BR1, far from its *sadABC* cluster.

The findings obtained in this thesis indicate that syntrophs may play an essential role in the elimination of sulfonamides in the environment. Furthermore, the detection of a similar transposable element in different *Actinobacteria* suggests that *sadA* may be mobile. Thus, further studies are necessary to assess the risk of horizontal gene transference (HGT) of these determinants and the subsequent risks for human and animal health.

Resumo

As sulfonamidas foram os primeiros antibióticos usados com sucesso na medicina. O seu uso intensivo e, por vezes, imprudente tornou-os micropoluentes globais e levou ao desenvolvimento e disseminação de vários mecanismos de resistência. Hoje, esta classe de antibióticos continua a ser importante para a medicina veterinária, pecuária e no tratamento dum número limitado de infeções bacterianas em pacientes humanos.

O conhecimento sobre a transformação e degradação biológica destes antibióticos tem vindo a aumentar nos últimos anos. Atualmente sabemos que as sulfonamidas podem ser transformadas por acetilação, hidroxilação, desaminação e oxidação da amina primária. Estas moléculas são também suscetíveis à biodegradação por *ipso*-hidroxilação que resulta na clivagem do grupo sulfonamida e parcial mineralização da molécula. A metabolização e mineralização destes antibióticos tem sido observada numa crescente minoria de isolados do filo *Actinobacteria*. Estas estirpes, dos géneros *Microbacterium* e *Arthrobacter*, possuem um operão conservado que consiste numa sulfonamida monooxigenase (*sadA*), numa 4-aminofenol monooxigenase (*sadB*) e numa FMN redutase (*sadC*).

A estirpe *Achromobacter denitrificans* PR1, uma *Proteobacteria* enriquecida e isolada de lamas ativadas, foi previamente descrita como um organismo degradador de sulfametoxazole (SMX). No entanto, estudos posteriores revelaram que algumas colónias desta bactéria perdiam espontaneamente a capacidade de metabolizar o antibiótico. Essa instabilidade metabólica e a falta de conhecimento relativamente à disseminação deste operão motivaram estudos adicionais com esta estirpe. Com base nisto, definiram-se dois objetivos fundamentais para esta tese: (i) a caracterização da via metabólica e (ii) identificação dos genes envolvidos na degradação deste antibiótico.

O estudo da via metabólica da degradação do SMX revelou que a cultura contendo a *A. denitrificans* PR1 transformava o SMX por *ipso*-hidroxilação. Como descrito anteriormente para o *Microbacterium* sp. BR1, esta reação levou à formação de 3-amino-5-metilisoxazol

(3A5MI), como produto final da reação, e 4-aminofenol (4AP) que serve de fonte de carbono e energia. Curiosamente, esta reação provocou rearranjos moleculares adicionais que levaram à acumulação de outros 3 metabolitos. Estes rearranjos consistiram em: (i) um “NIH shift” do grupo sulfonilo que resultou na formação de ácido 5-amino-2-hidroxi-benzenossulfónico; (ii) um rearranjo de Baeyer-Villiger resultando na migração do grupo sulfo-metilisoxazole para o átomo de oxigénio do grupo hidroxilo; e (iii) uma hidroxilação inespecífica na posição *ortho* ou *meta* do anel de benzeno. Alguns destes metabolitos foram previamente observados como resultado da *ipso*-hidroxilação de outros substratos aromáticos. Contudo, estes rearranjos nunca tinham sido observados em sulfonamidas.

A avaliação da instabilidade metabólica da *A. denitrificans* PR1 levou à descoberta da presença de uma actinobactéria de baixa abundância e crescimento lento na mesma cultura. Esta nova estirpe, denominada por estirpe GP, aparentou ser um microrganismo sintrófico dependente do contacto constante com a *A. denitrificans* PR1.

Curiosamente, o SMX e o 4AP apenas foram degradados pelo consórcio das duas bactérias e nunca por culturas puras da *A. denitrificans* PR1. O que indica que a estirpe GP desempenha um papel importante neste processo. Duas abordagens independentes foram usadas para avaliar a natureza da dependência metabólica da estirpe GP e o processo de degradação de sulfonamidas neste consórcio. No primeiro estudo, testaram-se diferentes meios de cultura, co-fatores e condições de crescimento. O segundo estudo, focou-se numa abordagem de genómica comparativa *in silico*.

Os resultados obtidos em ambos os estudos indiciam que a estirpe GP representa uma nova espécie e, possivelmente, um novo género dentro da família das *Microbacteriaceae*. Contudo, esta bactéria não apresentou um genoma reduzido como é frequentemente observado em microrganismos sintróficos. Ao invés disso esta estirpe mostrou apenas uma perda moderada de genes associados à síntese de tetrapirroles e heme e ao

transporte de tiol, estes últimos essenciais para a regulação do equilíbrio redox no periplasma. A perda destes genes poderá estar associada à perda da capacidade de sintetizar citocromos, vitais para o crescimento em aerobiose. No entanto, a incorporação de heme, catalase e mesmo de sobrenadante e extratos celulares da *A. denitrificans* PR1 não permitiu a formação de colónias isoladas e puras desta *Actinobacteria*.

A comparação do genoma da estirpe GP e *A. denitrificans* PR1 revelou que apenas a primeira contém genes homólogos ao operão *sadABC*, recentemente ligados ao metabolismo de sulfonamidas noutras *Actinobacteria*. Curiosamente, na estirpe GP o gene *sadA* encontra-se codificado dentro de um transposão contendo um transportador *yceI*, uma proteína de resposta SOS e uma transposase da família IS1380, enquanto o *sadB* e *sadC* se encontram dispersos por outras regiões do seu genoma.

Um transposão similar foi detetado nos genomas dos degradadores de sulfadiazina, *Arthrobacter* sp. D2 e D4. Também, uma cópia isolada do gene que codifica a transposase IS1380 foi detetada no genoma do *Microbacterium* sp. BR1, longe do seu operão *sadABC*.

Os resultados obtidos nesta tese indicam que os microrganismos sintróficos podem desempenhar um papel importante na eliminação das sulfonamidas do ambiente. Para além disso, a deteção de um transposão similar entre diferentes *Actinobacteria* sugere que a *sadA* pode ser adquirida por transferência horizontal. Deste modo, estudos adicionais são necessários para avaliar o risco de transferência horizontal (HGT) dos genes do operão *sadABC* e potenciais consequências para a saúde humana e animal.

Publications

The content of this thesis is partially published in:

A.C. Reis, B.A. Kolvenbach, P.F.-X. Corvini, M. Chami, L. Gales, C. Egas, O.C. Nunes. “Comparative genomics of *Leucobacter* spp. reveals moderate gene loss in sulfonamide-degrader strain GP”. BMC Genomics. Under revision.

A. Tskhvediani¹, **A.C. Reis**¹, M. Chami, P. Vandamme, B.A. Kolvenbach, O.C. Nunes, M. Tediashvili, P.F.-X. Corvini. “*Achromobacter* phage vB_Ade_ART as a biocontrol tool in a sulfamethoxazole-degradation consortium”. Manuscript in preparation.

A.C. Reis, Boris A. Kolvenbach, Olga C. Nunes, Philippe F.X. Corvini (2018). “Biodegradation of antibiotics: the new resistance determinants – part II”. New Biotechnology. 54:13-27. doi: 10.1016/j.nbt.2019.08.003.

A.C. Reis, Boris A. Kolvenbach, Olga C. Nunes, Philippe F.X. Corvini (2018). “Biodegradation of antibiotics: the new resistance determinants – part I”. New Biotechnology. 54:34-51. doi: 10.1016/j.nbt.2019.08.002.

A.C. Reis, M. Čvančarová, Y. Liu, M. Lenz, T. Hettich, B.A. Kolvenbach, P.F.-X. Corvini, Olga C. Nunes (2018). “Biodegradation of sulfamethoxazole by a bacterial consortium of *Achromobacter denitrificans* PR1 and *Leucobacter* sp. GP”. Applied Microbiology and Biotechnology. Applied Microbiology and Biotechnology. 102(23):10299-10314. doi: 10.1007/s00253-018-9411-9.

P.Y. Nguyen, A.F. Silva, **A.C. Reis**, O.C. Nunes, A.M. Rodrigues, J.E. Rodrigues, V.V. Cardoso, M.J. Benoliel, M.A.M. Reis, Adrian Oehmen, G. Carvalho (2019). “Bioaugmentation of membrane bioreactor with *Achromobacter denitrificans* strain PR1 for enhanced sulfamethoxazole removal in wastewater”. Science of the Total Environment. 648:44-55, doi: 10.1016/j.scitotenv.2018.08.100.

¹ These authors contributed equally to this work

A.C. Reis, K. Kroll, M. Gomila, B.A. Kolvenbach, P.F.X. Corvini, O.C. Nunes (2017). "Complete Genome Sequence of *Achromobacter denitrificans* PR1". *Genome Announcements*. 5(31), e00762-17, doi: 10.1128/genomeA.00762-17.

P.Y. Nguyen, G. Carvalho, **A.C. Reis**, O.C. Nunes, M.A.M. Reis, A. Oehmen (2017). "Impact of biogenic substrates on sulfamethoxazole biodegradation kinetics by *Achromobacter denitrificans* strain PR1". *Biodegradation*. 28(2-3):205-217. doi: 10.1007/s10532-017-9789-6.

Oral communications

A.C. Reis, A. Tskhvediani, B.A. Kolvenbach, P.F.X. Corvini, O.C. Nunes (2018). Role of unculturable bacteria in sulfamethoxazole degradation. In Book of Abstracts of Joint Conference EBC-VII & ISEB, Chania, Crete, Greece, 25th-28th June (Oral presentation, O170, session: Emerging Contaminants in Soils, Sediments and Groundwater).

A.C. Reis, M. Čvančarová, K. Kroll, B.A. Kolvenbach, P.F.X. Corvini, O.C. Nunes (2017). Metabolic cooperation in a sulfamethoxazole-degrading consortium composed by *Achromobacter denitrificans* PR1 and an unculturable bacterium from the Microbacteriaceae family. In Book of Abstracts of Joint Annual Meeting 2017 SSM|SSI|SSHH|SSTMP|SSTTM, Basel, Switzerland, August 30th to September 1st. (Oral presentation, O40, session: Environmental Microbiology).

A.C. Reis, K. Kroll, M. Čvančarová, B.A. Kolvenbach, P.F.X. Corvini, O.C. Nunes (2016). Comparative genomic analysis of *Achromobacter denitrificans* PR1, a sulfonamide degrading bacterium. In Book of Abstracts of ISEB2016, Barcelona, Spain, June 1st-3rd. (Oral presentation, session: Environmental Processes and Microbial Advances).

List of Contents

Acknowledgments.....	v
Abstract.....	ix
Resumo	xiii
Publications.....	xvi
Oral communications	xviii
List of Contents	xix
List of Tables	xxii
List of Figures	xxiii
List of Abbreviations	xxvii
Chapter 1 General Introduction	2
1.1 Consequences of the antibiotic era	2
1.2 A brief history of sulfonamide antibiotics.....	4
1.3 Sulfamethoxazole biotransformation	7
1.4 Sulfamethoxazole biodegradation	10
1.4.1 Cleavage of the sulfonamide bond.....	10
1.4.2 Cleavage of the isoxazole ring.....	12
1.5 Biotransformation and biodegradation of other sulfonamides.....	15
1.6 Sulfonamide degradation by ligninolytic enzymes	18
1.7 Feasibility of bioaugmentation and bioremediation to attenuate sulfonamides contamination	19
1.8 Microbial cooperation and pollutant degradation	20
1.9 Main objectives of this study	24
Chapter 2 Roadmap for the thesis	25
Chapter 3 Complete genome sequence of <i>Achromobacter denitrificans</i> PR1	31
3.1 Abstract.....	32
3.2 Genome Announcement.....	32
3.3 Nucleotide accession number.....	36
Chapter 4 Biodegradation of sulfamethoxazole by a bacterial consortium of <i>Achromobacter denitrificans</i> PR1 and <i>Leucobacter</i> sp. GP	37
4.1 Abstract.....	38
4.2 Introduction	38
4.3 Materials and methods.....	41
4.3.1.1 Chemicals	41
4.3.2 Microorganisms and culture conditions.....	41
4.3.3 Attempts at purification of <i>Leucobacter</i> sp. strain GP	43
4.3.4 16S rRNA metagenomics sequencing.....	44
4.3.5 16S rRNA gene clone libraries	45

List of contents

4.3.6	Role of strain GP in the SMX-degrading consortium.....	46
4.3.7	Detection and sequencing of genes related to the metabolism of sulfonamides	46
4.3.8	Quantitative PCR (qPCR) and reverse transcriptase qPCR (RT-qPCR)	47
4.3.9	Identification of metabolites.....	49
4.4	Results.....	54
4.4.1	Identification of <i>Leucobacter</i> sp. strain GP	54
4.4.2	Role of the members of the sulfamethoxazole-degrading consortium	58
4.4.3	Elucidation of the metabolic pathway	59
4.4.4	Detection and expression of the <i>sadABC</i> cluster in the consortium.....	70
4.4.5	Functional classification of the sulfonamide monooxygenase SadA	71
4.5	Discussion	72
Chapter 5 Isolation and characterization of <i>Achromobacter</i> phage vB_Ade_ART, a novel phage with potential medical and environmental application.....		77
5.1	Abstract.....	78
5.2	Introduction	78
5.3	Materials and methods.....	81
5.3.1	Bacterial strains and culture conditions.....	81
5.3.2	Determination of antibiotic resistance phenotypes for <i>Achromobacter</i> spp.	82
5.3.3	Bacteriophage isolation, propagation and culturing conditions	82
5.3.4	Efficiency of plating (EOP)	83
5.3.5	Infection parameters.....	83
5.3.6	Electron microscopy.....	84
5.3.7	Bacteriophage DNA extraction, genome sequencing and assembly.....	85
5.3.8	Genome annotation and phylogenetic analysis	86
5.3.9	Bacterial consortium DNA extraction and quantitative PCR (qPCR)	87
5.3.10	Effect of the bacteriophage in a sulfonamide-degrading consortium	87
5.4	Results and discussion	87
5.4.1	Isolation of the bacteriophage	87
5.4.2	Morphological analysis.....	88
5.4.3	Infection parameters.....	89
5.4.4	Phage host range determination	89
5.4.5	Phage stability	91
5.4.6	Taxonomic classification and genomic analysis	94
5.4.7	Effect of phage in the sulfonamide-degrading consortium	99
5.5	Conclusions	102
Chapter 6 Comparative genomics reveals a novel genetic organization of the <i>sad</i> cluster in the sulfonamide-degrader '<i>Candidatus</i> <i>Leucobacter sulfamidivorax</i>' strain GP		103
6.1	Abstract.....	104
6.2	Background	105

6.3	Results and discussion	107
6.3.1	Morphological and physiological characterization of the consortium.....	107
6.3.2	Analysis of the metagenome-assembled genome of strain GP	111
6.3.3	Analysis of mobile and conjugative elements	113
6.3.4	Phylogenetic analysis	117
6.3.5	Core and softcore genome of <i>Leucobacter</i> spp.	124
6.3.6	Estimation of gene loss in strain GP	129
6.3.7	Unique genes shared between sulfonamide degraders.....	134
6.3.8	Taxonomic classification of strain GP	144
6.3.9	Description of ' <i>Candidatus</i> <i>Leucobacter</i> sulfamidivorax'	145
6.4	Conclusions	146
6.5	Methods.....	146
6.5.1	Culture conditions and DNA extraction.....	146
6.5.2	Physiological characterization of the consortium	147
6.5.3	Microscopy	148
6.5.4	<i>Leucobacter</i> spp. type strains whole-genome sequencing and assembly	149
6.5.5	Whole consortium sequencing.....	149
6.5.6	Metagenome-assembled genome (MAG) of strain GP	150
6.5.7	Genome annotation, completeness, and mobile genetic elements	151
6.5.8	Phylogenetic analysis of strain GP.....	152
6.5.9	<i>Leucobacter</i> spp. core and pangenome analysis.....	153
6.5.10	Whole genome comparisons and evolution of the SadABC complex	154
Chapter 7 General Discussion		157
7.1	Antibiotic degraders: a threat or an opportunity?.....	158
7.2	A sulfonamide-degrading two-member consortium and dependency of strain GP	160
7.3	Pathway and genes involved in sulfamethoxazole degradation	163
7.4	Potential application for bioaugmentation.....	165
Chapter 8 Main Conclusions		167
Chapter 9 Proposal for additional and future work.....		171
References.....		175

List of Tables

Table 1.1. - General chemical structure of the most commonly used sulfonamide antibiotics, composed by an aniline moiety, a sulfonamide group and a heterocyclic moiety (R), adapted from Ingerslev and Halling-Sørensen (2000).....	6
Table 1.2. - Microbial communities and single bacterial strains able to degrade the antibiotic sulfamethoxazole.....	14
Table 3.1 - Sequences of the primers used to circularize the genome of <i>A. denitrificans</i> strain PR1.....	33
Table 4.1 - Primers and conditions used for the end-point amplification of <i>sadA</i> , <i>sadB</i> and <i>sadC</i> genes...	47
Table 4.2 - Primers, PCR conditions, and efficiency for the qPCR experiments.....	49
Table 4.3 - Taxonomic classification of representative OTU in the SMX-degrading consortium obtained with RDP classifier and confirmed with NCBI BLAST against the 16S ribosomal RNA database, and pairwise sequence similarity of each representative OTU with the 16S rRNA gene sequence of strains PR1 or GP retrieved from the clone libraries.....	56
Table 4.4 - Inter-species pairwise similarity between <i>Leucobacter</i> sp. GP and other, validly described, <i>Leucobacter</i> spp. was determined based on the global alignment in the EzBioCloud webserver (Yoon et al. 2017).....	57
Table 4.5 - Metabolites detected by LC-MS (Ion Trap) during SMX degradation in resting cells of the microbial consortium. Oxygen atoms in red represent probable atoms originated from the incorporation of atmospheric O ₂ . N.d., not determined; (*) metabolite confirmed with a standard; (!) M1 could not be fragmented in positive mode (ESI ⁺), therefore, the product ions correspond to fragmentation in negative mode (ESI ⁻).....	65
Table 5.1 - List of <i>Achromobacter</i> spp. strains used in this study. Sequence type (ST) was retrieved from sequences publicly available at the <i>Achromobacter</i> pubMLST database (www.pubmlst.org/achromobacter ; Jolley and Maiden, 2010). N.A. means not available.....	80
Table 5.2 - Core genes of the <i>Jwrvirus</i> genus as determined by core/pangenomic analysis. *, these genes are not annotated in GenBank, the nucleotide position of the coding sequence is presented instead.....	95
Table 5.3 - Genes unique to <i>Achromobacter</i> phage vB_Ade_ART within the <i>Jwrvirus</i> genus as determined by core/pangenomic analysis and manual curation of the results.....	96
Table 5.4 - Viability (log CFU/ml) of strain PR1 determined by plating after 90 min incubation in mineral medium (MMSY - SMX) at different MOI.....	101
Table 6.1 - List of named species of the <i>Leucobacter</i> genus used in the phylogenetic and comparative studies. Assembly quality was calculated using QUASt (Konstantinidis and Tiedje 2005) with a minimum contig size set to 200 bp. Completeness and contamination were computed with CheckM (Parks et al. 2015). 16S rRNA pairwise similarity was computed with the global alignment tool in the EzBioCloud web server (Yoon et al. 2017). Strains sequenced in this study are shown in bold.....	112
Table 6.2 - Mean coverage and GC content per strain and contig in the metagenome assembly of the consortium consisting of <i>Achromobacter denitrificans</i> PR1 and ' <i>Candidatus</i> <i>Leucobacter sulfamidivorax</i> '.....	113
Table 6.3 - Genes and corresponding conserved domains linked to integrative, conjugative and resistance elements found in contigs 5, 7 and 9 from the draft assembly of strain GP. Families and E-values in bold indicate the best hits obtained with CONJscan (Abby et al. 2014). n.a., not applicable.....	115
Table 6.4 - List of all bacterial strain used for comparative genomics. (T) type strain; (*) sulfonamide degraders; N.A. not available; (bold) strains sequenced in this study; (!) available on Github ; * the 16S rRNA gene sequence of this strain has a gap between positions 706 and 761; ** no rRNA was annotated in this sequence; cells highlighted in orange indicate strain for which the genome sequence became available after November 2018, and, therefore were not included in the comparative genomics studies to assess gene loss in strain GP.....	118
Table 6.5 - Complete and near-complete (1 block missing = 1 ortholog gene missing) modules of the softcore genome of <i>Leucobacter</i> spp. and strain GP reconstructed <i>in silico</i> with KEGG Mapper (Kanehisa et al. 2017).....	126
Table 6.6 - Essential genes missing from the draft genome of strain GP identified by core/pangenome analysis with GET_HOMOLOGUES (Contreras-Moreira and Vinuesa 2013).....	130

List of Figures

Figure 1.1 - Vicious cycle for the development of antibiotic resistance and degradation in bacteria and the potential interplay between these two mechanisms on the development and spread of new mechanisms of resistance. The WWTP image is courtesy of the Integration and Application Network (ian.umces.edu/symbols); vectors graphics are designed by FreePik (www.freepik.com); the molecular structure is from tetX enzyme - PDB ID 2XD0 (Volkers et al. 2011) - obtained from RCSB PDB (www.rcsb.org).....	4
Figure 1.2 - Summary of the main metabolites detected during biotransformation (orange arrows) and biodegradation (dark arrows) of SMX by individual bacteria and complex microbial communities under aerobic and anaerobic conditions.	13
Figure 1.3 - Sulfanilamide degradation in biological-activated-carbon filter system described by Liao et al. (2016).	16
Figure 1.4 - Biodegradation of sulfadiazine and sulfamethazine by several bacterial strains under aerobic conditions.	18
Figure 3.1 - ANI (a) and AAI (b) heatmaps comparing values between all fully sequenced strains of <i>A. denitrificans</i> : NBRC 15125T (GCA_001571365); USDA-ARS-USMARC-56712 (GCA_001514355); DP_1 (GCA_002192685); NCTC8582 (GCA_900444675); MT3 (GCA_001945385); NCTC3233 (GCA_900444685) and UBA1869 (GCA_002338195). Presence/absence heatmap (c) for antibiotic resistance proteins found in each strain against aminoglycosides (AadA2), beta-lactams (Oxa-258), phenicolts (CatB3 and CmlA1), sulfonamides (Sul1, Sul2), tetracyclines (TetC) and multidrug resistance efflux pumps (AdeF, AxyX, AxyY, OprZ).	34
Figure 3.2 - Genome-wide nucleotide comparison (BLASTn) between fully sequenced strains of <i>A. denitrificans</i> . Strain PR1 genome is the innermost black circle and rings correspond, from inside out, to the draft/complete genome assemblies of strains: NBRC 15125 ^T (GCA_001571365); USDA-ARS-USMARC-56712 (GCA_001514355); DP_1 (GCA_002192685); NCTC8582 (GCA_900444675); MT3 (GCA_001945385); NCTC3233 (GCA_900444685) and UBA1869 (GCA_002338195). Within each ring, zones with higher transparency correspond to lower nucleotide identity. Gaps in the alignment correspond to the unique regions found in the genome of strain PR1. Relevant antibiotic resistance genes of strain PR1 are indicated in red. The plot was generated with BRIG (Alikhan et al. 2011).	35
Figure 4.1 - Picture of the microbial consortium taken under a magnifying glass with bright field after 11 days of incubation on BHI-SMX-agar, yellow colonies of the <i>Leucobacter</i> sp. GP (red arrows) growing attached to the beige colonies of <i>A. denitrificans</i> PR1.	55
Figure 4.2 - Abundance of strains PR1 and GP, respectively, during growth of the consortium in MMSY medium with SMX as a supplementary carbon source. a: growth of both strains over time in MMSY with 0.6 mM of SMX. b: abundance of both strains after 7 h incubation with different SMX concentrations. SMX concentration (●); 3A5MI concentration (▲); 16S rRNA gene copy number of strain PR1 per ml of culture or ng of DNA (white bars); 16S rRNA gene copy number of strain GP per ml of culture or ng of DNA (grey bars). Values are the mean of triplicates and error bars represent standard deviation.	58
Figure 4.3 - Degradation of SMX (●) by the microbial consortium in resting cells assays with the concomitant release of the dead-end product 3A5MI (▲), sulfur species (sulfite and sulfate, dark yellow ◆) and ammonium ions (dark red ◇). Values are the mean of triplicates and error bars represent standard deviation.....	59
Figure 4.4 - Mass spectrum of 3-amino-5-methylisoxazole product ion recorded in positive mode with possible sum formula annotation.	60
Figure 4.5 - Extracted ion chromatogram (EIC) of some of the main metabolites identified throughout this study recorded in negative mode (-ESI).	61
Figure 4.6 - Mass spectrum of sulfamethoxazole product ion recorded in positive mode with possible sum formula annotation.	62
Figure 4.7 - Mass spectrum of M1 product ion recorded in negative mode with possible sum formula annotation.....	62
Figure 4.8 - Mass spectrum of M2 product ion recorded in positive mode with possible sum formula annotation.....	63
Figure 4.9 - Mass spectrum of M3 product ion recorded in positive mode with possible sum formula annotation.....	63
Figure 4.10 - Mass spectrum of 5-amino-2-hydroxybenzenesulfonic acid (M4) product ion recorded in positive mode with possible sum formula annotation.....	67

Figure 4.11 – Product ion (QTOF) mass spectra of [M - H] ⁻ of metabolite M5 and possible molecular structure.....	68
Figure 4.12 – Degradation of sulfamethoxazole (a), 4-aminophenol (b) and sulfanilic acid (c) in resting cells conditions by the microbial consortium (●), axenic cultures of strain PR1 (△) and in abiotic controls (◆). Values are the mean of triplicates and error bars represent standard deviation.	69
Figure 4.13 – Release of ¹⁴ C-4AP (white bars) during the consumption of ¹⁴ C-SMX (green bars) in assays spiked (a) and non-spiked (b) with 1 mM of non-labelled 4AP. Values are the mean of triplicates and error bars represent standard deviation.	70
Figure 4.14 – Agarose gel electrophoresis of the PCR products obtained from the amplification of <i>sad</i> cluster. <i>sadA</i> (1-5), <i>sadB</i> (6-10) and <i>sadC</i> (11-15). 1/6/11: Consortium. 2/7/12: Consortium after alkaline lysis. 3/8/13: <i>Microbacterium</i> sp. BR1 (positive control). 4/9/14: <i>A. denitrificans</i> PR1 (negative control). 5/10/15: Blank.	71
Figure 4.15 – Proposed metabolic pathway for sulfamethoxazole degradation in microbial consortium between <i>Leucobacter</i> sp. strain GP and <i>Achromobacter denitrificans</i> PR1, oxygen atoms marked in red represent atoms originating from atmospheric O ₂ , as confirmed in assays with ¹⁸ O ₂	75
Figure 5.1 – Electron micrographs of the bacteriophage vB_Ade_ART negatively stained in (a) and frozen hydrated in (b). The magnification in (a) is 17500 and in (b) is 24000x.	88
Figure 5.2 – Adsorption (a) and one-step growth cycle (b) of <i>Achromobacter</i> phage vB_Ade_ART. Values for adsorption are plotted as percentage of free PFU and one-step growth cycle (PFU/ml) is plotted in logarithmic scale. All values are the mean of triplicates, and the error bars represent the standard deviation.	89
Figure 5.3 – Phylogenetic tree derived from 16S rRNA gene sequence analysis, showing the relationship between all type strains of the genus <i>Achromobacter</i> . Type strains of <i>Kerstersia</i> , <i>Taylorella</i> and <i>Burkholderia</i> genera were used as outgroups. The maximum likelihood phylogenetic tree based on the 16S rRNA gene was inferred with the Jukes-Cantor model from 1000 bootstrap replicates in MEGA6 software (Tamura et al. 2013). Bootstrap values at or above 50%, are indicated at branch points. The scale bar indicates the number of substitutions per site. Strain names in bold indicate the species used in this study, strains with a circle next to the tip of the branch indicate the species that could be infected by <i>Achromobacter</i> phage vB_Ade_ART.	90
Figure 5.4 – Antibiotic resistance pattern and bacteriophage host range for different strains of the genus <i>Achromobacter</i> . For both antibiotics and phage red represents resistant, yellow intermediate and green susceptible phenotypes.	91
Figure 5.5 – Active phage particles after incubation under different pH values (a), temperature (b) and the presence of organic solvents (c). Control conditions correspond to pH 7 at 22 °C in the absence of organic solvents. Values for PFU/ml are in logarithmic scale and represent the mean of three replicates and error bars represent the standard deviation.	93
Figure 5.6 – Phylogenomic GBDP tree from representative phages from the <i>Siphoviridae</i> family inferred using the balanced minimum evolution method based on the D4 formula (Meier-Kolthoff et al. 2017). Pseudo-bootstrap support values were generated from 100 replications, values above 50% are indicated at branch points. Tree was rooted at the midpoint and visualized with FigTree. Scale bar represents the number of substitutions per site.	97
Figure 5.7 – Circular representation of the genome of <i>Achromobacter</i> phage vB_Ade_ART obtained with BRIG (Alikhan et al. 2011). The beginning of the genome is placed on the leftmost side of the virion DNA. The genomes of the closest relatives were aligned with BLAST+ and are represented as follows: <i>Achromobacter</i> phage 83-24 (orange), <i>Achromobacter</i> phage JWR (green) and <i>Burkholderia</i> phage BcepGomr (blue). Genes from the queuosine biosynthetic cluster are represented in red; genes possibly involved in recombination are represented in black.	98
Figure 5.8 – Phage titer at different multiplicity of infection (MOI) in <i>Achromobacter denitrificans</i> PR1 and in the consortium between this strain and <i>Leucobacter</i> sp. GP. Values for phage titer in PFU/ml in strain PR1 (white bars) and in the microbial consortium (orange bars) are in logarithmic scale and represent the mean of triplicates and error bars the standard deviation.	100
Figure 5.9 – Effect of phage vB_Ade_ART in the abundance of <i>Leucobacter</i> sp. strain GP in the consortium with <i>A. denitrificans</i> strain PR1 after 48 h of incubation in MMSY with 0.6 mM SMX. Values for 16S rRNA gene copies per ml for strain PR1 (white bars) and strain GP (orange bars) are in logarithmic scale. Degradation of SMX (●) is represented as the percentage of antibiotic concentration decrease. Abiotic controls present negligible degradation of SMX. At all MOI, phage titer after 48 h is of 9.85 ± 0.30 log PFU/ml. All values are the mean of triplicates and error bars represent the standard deviation. Significant differences in strain GP / strain PR1 ratio are indicated by a, b, c, d, e and f (from higher to lower values of the mean) as determined by one-way ANOVA and the Tukey test at p < 0.05.	101

Figure 6.1 - Electron micrographs of frozen hydrated <i>Achromobacter denitrificans</i> strain PR1 (a) and strain GP (b). Micrographs of negatively stained <i>A. denitrificans</i> PR1 showing the presence of peritrichous flagella (c and d). PM - Plasma membrane; OM - Outer membrane; FG - Flagellum; CW - Cell wall; C - Carbon support grid.....	108
Figure 6.2 - Fluorescence microscopy composite images of DAPI-stained cells of the microbial consortium (blue) and (A) cells hybridized with the modified ActORD1 FISH probe (stains strain GP, 5' fluorophore: FAM, green) or with (B) cells hybridized with Alca2 FISH probe (stains strain PR1; 5' fluorophore: Cy3, orange/red).....	109
Figure 6.3 - Abundance of strain PR1 and strain GP after 15 h incubation at different pH and salinity in DLB and at different temperatures in MMSY. The values for copies of the 16S rRNA gene per ml are plotted in logarithmic scale for strains PR1 (white) and GP (orange). Values are the mean values of triplicates and the error bars represent the standard deviation. Significant differences in strain GP abundance are indicated by a, b, c and d (from higher to lower values of the mean) as determined by two-way ANOVA and the Tukey test at $p < 0.05$ within each tested condition (pH, temperature and salinity) (R Core Team 2015).	110
Figure 6.4 - Abundance of strain PR1 and strain GP after 15 h incubation in different media. The values for copies of the 16S rRNA gene per ml are plotted in logarithmic scale for strains PR1 (white) and GP (orange). Values are the mean values of triplicates, and the error bars the standard deviation. Significant differences in strain GP abundance (16S rRNA copy numbers of strain GP divided by those of PR1) are indicated by a, b, c and d (from higher to lower values of the mean) as determined by one-way ANOVA and the Tukey test at $p < 0.05$ among all tested media (R Core Team 2015).	111
Figure 6.5 - Cladogram of the 16S rRNA gene inferred from maximum likelihood estimation with MEGA6 with the best-fitting model: TN93+G+I (Tamura et al. 2013). <i>Leucobacter</i> spp. strains sequenced in this study are marked with an asterisk, and sulfonamide degraders are shown in bold. The tree was rooted at the outgroup and visualized with FigTree. The scale bar represents the number of expected substitutions per site. Bootstrap values were inferred from 1000 replicates, values above 70% are shown at the corresponding nodes.....	121
Figure 6.6 - ANI (a), AAI (b) and POCP (c) heatmaps comparing values between strain GP and validly named species of the <i>Leucobacter</i> genus at the time of the analysis.	122
Figure 6.7 - Phylogenomic relationships between the <i>Leucobacter</i> genus and strain GP inferred from concatenated amino acid alignments of 400 universal proteins obtained with PhyloPhlAn (Segata et al. 2013). Representative members of genera <i>Microbacterium</i> , <i>Leifsonia</i> , <i>Gulosibacter</i> , <i>Agromyces</i> and <i>Arthrobacter</i> were included as the outgroup. <i>Leucobacter</i> spp. strains sequenced in this study are marked with an asterisk, and sulfonamide degraders are shown in bold. Node labels indicate local support values obtained with FastTree using the Shimodaira-Hasegawa test (Shimodaira 2002). The scale bar represents the number of expected substitutions per site. The tree was rooted at the outgroup node and visualized with FigTree.	123
Figure 6.8 - Presence/absence heatmap representation and dendrograms of the 12,998 orthologs gene clusters found in the pangenome of <i>Leucobacter</i> spp. and strain GP obtained with the GET_HOMOLOGUES package (Contreras-Moreira and Vinuesa 2013). Each column represents a different gene cluster which can be absent (white) or present (blue) in each strain. As paralogs were included in the analysis, some clusters have more than one homolog per genome, and these are shown in darker blue.	128
Figure 6.9 - Representation of the genetic organization of the sad cluster in sulfonamide degraders: <i>Microbacterium</i> sp. strains BR1 and CJ77, <i>Arthrobacter</i> sp. strains D2 and D4 and strain GP. Scaffolds or contig numbers and locus are shown next to the DNA backbone.	135
Figure 6.10 - Heatmaps representing amino acid identity (BLASTp) of the SadABC complex and Ycel transporter among isolates from the <i>Microbacterium</i> genus (strains BR1, C488, SDZm4 and CJ77), <i>Arthrobacter</i> genus (strains D2 and D4) and strain GP.....	137
Figure 6.11 - Maximum likelihood phylogenetic trees inferred from amino acid alignments with MEGA6 (Tamura et al. 2013) of (a) SadA, (b) SadB, (c) SadC, (d) Ycel transporter and (e) IS1380/IS3/IS4 transposases shared between sulfonamide degraders. Strain GP is shown in bold; sulfonamide degraders are marked with an asterisk (*); and structural homologs to these enzymes obtained with SWISS-MODEL (Waterhouse et al. 2018) are shown in bright blue. Node labels indicate ML bootstrap support above 50% (in bold) / NJ bootstrap support values above 50% / Bayesian posterior probabilities above 70%. The scale bar represents the number of expected substitutions per site. The tree was rooted at the midpoint and visualized with FigTree.	139
Figure 6.12 - Amino acid alignment with MUSCLE (Edgar 2004) of Acyl-CoA domains: <i>N</i> -terminal (a), middle (b) and <i>C</i> -terminal (c); between SadA and SadB homologs in <i>Microbacterium</i> sp. BR1, <i>Arthrobacter</i> sp. D2 and D4 and strain GP (SadB1: D3X82_00235; SadB2: D3X82_03160). Conserved regions within SadA	

and SadB and highlighted in green and conserved regions shared between all proteins are marked with an asterisk..... 140

Figure 6.13 – Pairwise alignment with BLASTp of the regions of the substrate binding pocket of XiaF (accession number 5LVW) and each homolog of SadA (a) and SadB (b) in strains GP, *Microbacterium* sp. BR1 and *Arthrobacter* sp. D2 and D4. Conserved regions between the different SadA and SadB homologs are highlighted in green, non-conserved residues are highlighted in red. Residues shared by all sequences are marked with an asterisk. The diagrams were designed with Excel 2013..... 143

Figure 6.14 – Close-up of the substrate-binding pocket of XiaF (PDB: 5LVW) bound to FADH₂ and indole obtained by Kugel et al. (2017). FADH₂ is the co-factor, indole the substrate and S121 and I237 are the residues that are modified in SadA of *Microbacterium* sp. BR1 and strain GP. The ribbon (a) and electrostatic surface potential (b) diagrams have been prepared with PyMol (Schrödinger 2002). In b negative potential is shown in red and positive potential in blue. 144

List of Abbreviations

16S rRNA	16S Ribosomal Ribonucleic Acid
3A5MI	3-amino-5-methylisoxazole
4AP	4-aminophenol
AMO	Ammonia-Monooxygenase
AMP	Ampicillin
Anammox	ANAerobic AMMonium OXidation
ANI	Average Nucleotide Identity
ANOVA	Analysis of variance
AOB	Ammonia-Oxidizing Bacteria
ARB	Antibiotic Resistant Bacteria
ARG	Antibiotic Resistance Genes
ATU	Allylthiourea
BCCM/LMG	LMG Bacteria Collection of the Laboratory for Microbiology of the University of Ghent, Belgian Coordinated Collections of Microorganisms
BHI-SMX-agar	25% diluted BHI with 0.6 mM SMX and 15 g/l agar
BLAST	Basic Local Alignment Search Tool
BRIG	BLAST Ring Image Generator
CCUG	Culture Collection of the University of Gothenburg
CDS	Coding Sequences
CFU	Colony Forming Unit
CHL	Chloramphenicol
CIP	Ciprofloxacin
CLSI	Clinical & Laboratory Standards Institute
Cryo-TEM	Cryogenic electron microscopy
C _t	Threshold cycle

Abbreviations

CTAB	Cetyltrimethylammonium Bromide
DDH	DNA-DNA Hybridization
DHFR	Dihydrofolate reductase
DHPS	Dihydropteroate synthase
DMSO	Dimethyl sulfoxide
DNA	Deoxyribonucleic Acid
dNTP	Deoxyribonucleotide triphosphate
DOX	Doxycycline
DSM	German Collection of Microorganisms and Cell Cultures
EDTA	Ethylenediaminetetraacetic Acid
EIC	Extracted Ion Chromatogram
EOP	Efficiency of Plating
$E_{\text{reference}}$	PCR efficiency of the reference gene
ERY	Erythromycin
ESI	Electrospray Ionization
E_{target}	PCR efficiency of the target gene
FMN	Flavin Mononucleotide
<i>folP</i>	Gene encoding for Dihydropteroate Synthase
G+C	Guanine plus Cytosine
GBDP	Genome-BLAST Distance Phylogeny
GCA	GenBank assembly accession number
GC-MS	Gas chromatography–mass spectrometry
GEN	Gentamicin
GO	Gene Ontology
HGT	Horizontal Gene Transfer
HPLC	High-Performance Liquid Chromatography
HQ	Hydroquinone

HRT	Hydraulic Retention Time
IC	Ion chromatography
LA	Lysogeny Broth
LC-MS	Liquid chromatography–mass spectrometry
LPSN	List of Prokaryotic names with Standing in Nomenclature
MAG	Metagenome-assembled genome
MEGA	Molecular Evolutionary Genetics Analysis
MLST	MultiLocus Sequence Typing
MMBN	Mineral medium B with ammonium sulfate
MMSY	MMBN with 7 mM succinate and 0.2 g/l yeast extract
MMSY+SMX	MMSY with 0.6 mM SMX
MOI	Multiplicity of infection
MS	Mass spectrometry
MS2	Product Ion Scan
NCBI	National Center for Biotechnology Information
ONT	Oxford Nanopore Technologies
ORF	Open-Reading Frame
OTU	Operational Taxonomic Unit
PASC	PAirwise Sequence Comparison
PB	Phosphate Buffer
PCR	Polymerase Chain Reaction
PDB	Protein Data Bank
PE	2-phenylethanol
PFGE	Pulsed Field Gel Electrophoresis
PFU	Plaque-Forming Unit
pVOGs	Prokaryotic Virus Orthologous Groups
PY-BHI	BHI with peptone and yeast extract

Abbreviations

Q	Phred Quality Score
qPCR	Quantitative Polymerase Chain Reaction
R2A	R2 Agar culture medium
RAST	Rapid Annotation using Subsystem Technology
RAxML	Randomized Axelerated Maximum Likelihood
RDP	Ribosomal Database Project
RNA	RiboNucleic Acid
RQ	Relative Quantification
rRNA	Ribosomal RiboNucleic Acid
RT	Room Temperature
RT-qPCR	Reverse Transcription Quantitative Polymerase Chain Reaction
SA	Sulfanilic acid
SadA	Sulfonamide Monooxygenase
SadB	4-aminophenol Monooxygenase
SadC	FMN Reductase
SDZ	Sulfadiazine
SMC	Spent Mushroom Compost
SMX	Sulfamethoxazole
SPE	Solid-Phase Extraction
ST	Sequence type
<i>sul1-4</i>	Genes encoding a drug-resistant dihydropteroate synthase (resistance to sulfonamides)
TE	Tris Buffer with EDTA
TEM	Transmission Electron Microscopy
THB	1,2,4-Trihydroxybenzene
TOC	Total Organic Carbon
tRNA	Transfer RiboNucleic Acid

TSA	Tryptic Soy Agar
TSB	Tryptic Soy Broth
UHPLC-QTOF-MS	Ultra-Performance Liquid Chromatography Quadrupole Time-Of-Flight Mass Spectrometry
UV	Ultraviolet radiation
WWTP	Wastewater Treatment Plant

Chapter 1

General Introduction

Part of this section is retrieved from the manuscript:

A.C. Reis, Boris A. Kolvenbach, Olga C. Nunes, Philippe F.X. Corvini (2018). "Biodegradation of antibiotics: the new resistance determinants – part I". *New Biotechnology*. 54:34-51, doi:10.1016/j.nbt.2019.08.002.

1.1 Consequences of the antibiotic era

The discovery of antibiotics and their introduction into clinical use in the early 20th century has revolutionized modern human and veterinary medicine. The advent of antibiotics had great impact on human and veterinary health, but also, as has been discovered over the past decade, on the environment.

Current human and animal medicine practices rely heavily on the availability of antibiotics. However, the intense and sometimes imprudent use of these antimicrobial compounds has led to a widespread environmental contamination with residues of the parent compounds or metabolites thereof (Berendonk et al. 2015; Petrie et al. 2015), which in turn may favour the development and spread of antibiotic resistance (Aminov 2010; van Hoek et al. 2011).

Because antibiotics often leave the body unaltered, antibiotic residues as well as antibiotic-resistant bacteria (ARB) and antibiotic resistance genes (ARG), end up in excreta. Via manure application onto agricultural fields and the wastewater treatment process they contaminate soil and different water bodies, respectively (FAO 2014; Berendonk et al. 2015; Petrie et al. 2015). Today it is generally recognized that wastewater treatment plants (WWTP) and animal farming are both potential sources of ARGs and ARBs. Here the constant exposure of bacteria at high cell densities to antibiotics residues and other stressful conditions may promote the development and spread of resistance (Teuber 2001; Rizzo et al. 2013; Manaia et al. 2016) (Fig. 1.1). Therefore, antibiotics are being regarded as emerging pollutants, causing the proliferation of ARBs and ARGs in both clinical and environmental settings (Baquero et al. 2008; Kemper 2008; Kümmerer 2009; Martinez 2009; Carvalho et al. 2015). To tackle the problem of antibiotic resistance and contamination we have to go beyond the mere optimization of current treatment processes in wastewater treatment plants; first, we need to understand how the presence of resistance and the degradation of antibiotics correlate in natural populations.

Both knowledge and research on antibiotic resistance are extensive (Blair et al. 2015). Furthermore, many studies have been dedicated to the degradation of antibiotics. However, few of these studies have described and characterize microorganisms that can use antibiotics as carbon and energy source, i.e., "antibiotrophs" (Dantas et al. 2008; Barnhill et al. 2010). Research on degradation and subsistence has been intensified in the last decade, but knowledge on these antibiotic degraders is still scarce, and their role in the environment poorly understood. Beyond their value as tools for bioremediation and biological treatment in WWTP, understanding these organisms may also be a way to understand the evolution of resistance (Fig. 1.1). Recent studies suggest that antibiotic degraders can protect susceptible members of the microbial community by removing the antibiotic and thus abolishing the need of the latter to acquire resistance genes of their own (Nicoloff and Andersson 2016; Sorg et al. 2016). This mechanism, known as indirect resistance, poses serious risks in clinical settings and it is often linked to antibiotic therapy failures. However, we lack knowledge of the role of this mechanism in environmental settings. Research on antibiotic degradation could hold the key to understand the equilibrium between resistance and susceptibility and the evolution of resistance itself.

For sulfonamides especially the subsistence phenotype has been established, as many heterotrophic bacteria were found to use these drugs as carbon and energy source. Furthermore, the enzymes responsible for this transformation have been identified. Some of these sulfonamide-degrading bacteria were found to carry additional resistance genes (e.g., *sul1*), raising important questions regarding the interactions between degradation and traditional resistance mechanisms. However, many studies fail to explore the molecular basis of antibiotic degradation. Hence, it is still unclear if antibiotic degradation evolves strictly in antibiotic-resistant bacteria (i.e., those who already carry traditional resistance genes) or if the evolution of these two mechanisms is independent.

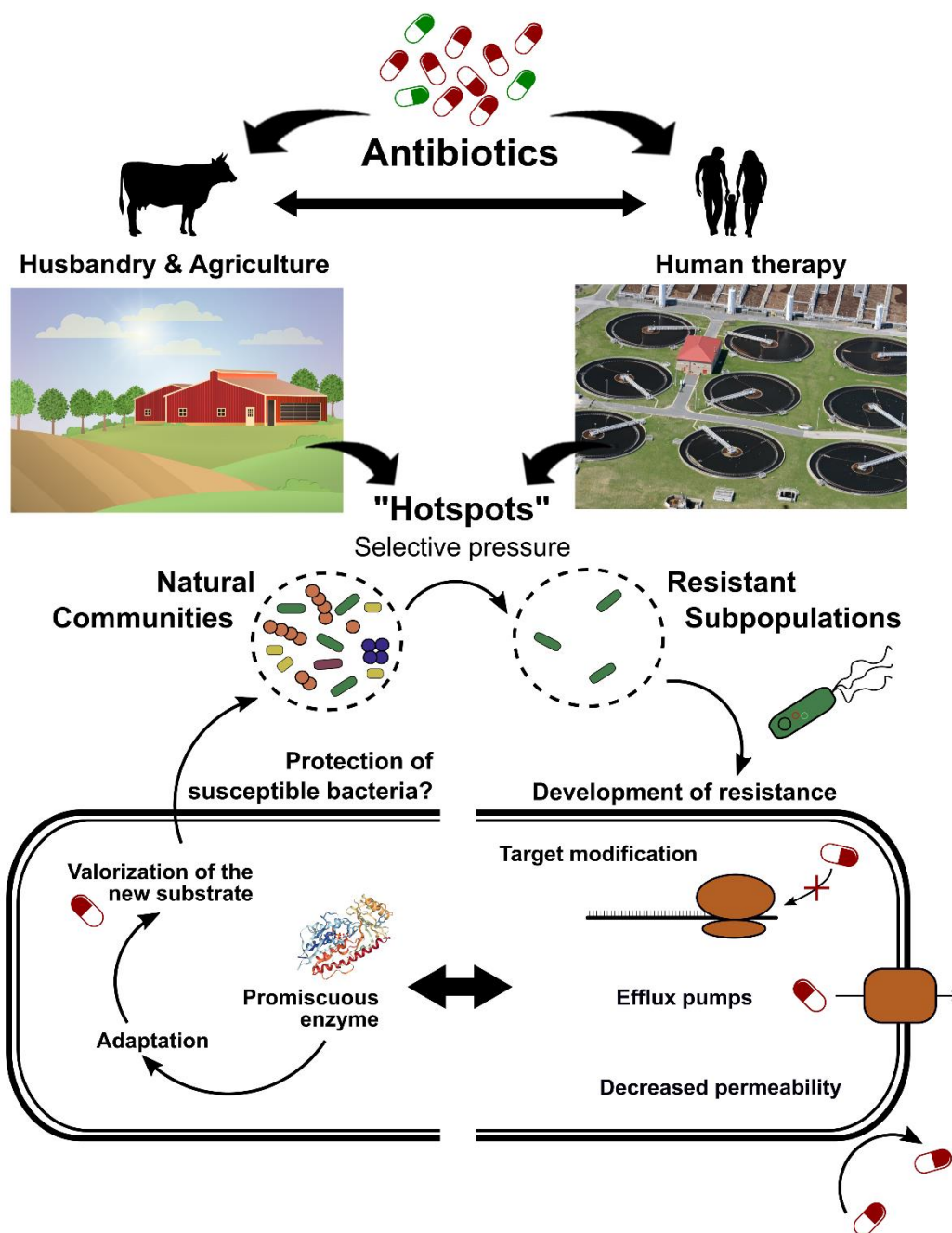


Figure 1.1. - Vicious cycle for the development of antibiotic resistance and degradation in bacteria and the potential interplay between these two mechanisms on the development and spread of new mechanisms of resistance. The WWTP image is courtesy of the Integration and Application Network (ian.umces.edu/symbols); vectors graphics are designed by FreePik (www.freepik.com); the molecular structure is from tetX enzyme - PDB ID 2XDO (Volkers et al. 2011) - obtained from RCSB PDB (www.rcsb.org).

1.2 A brief history of sulfonamide antibiotics

Since the discovery of the antimicrobial properties of sulfanilamide in the 1930s by the German pathologist and bacteriologist Gerhard Domagk, sulfonamides have had a long

history of success. These synthetic antibiotics are structural analogs of *p*-aminobenzoic acid (Table 1.1) that compete for the active sites of dihydropteroate synthetase (DHPS) and, as a result, block the synthesis of folic acid (Masters et al. 2003).

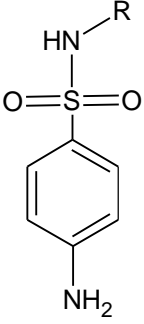
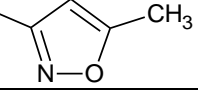
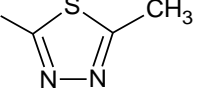
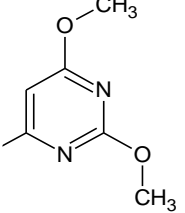
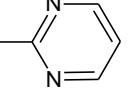
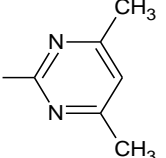
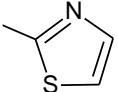
Since the discovery of sulfanilamide, more than 5,000 different molecules of this class of antibiotics have been developed (Rang et al. 2003). Currently, the most commonly used sulfonamide for human therapy is sulfamethoxazole (SMX) in combination with trimethoprim, known as co-trimoxazole. Trimethoprim is a diaminopyrimidine first introduced in 1962 (Huovinen 1987). Despite being structurally different from sulfonamides, trimethoprim shares most of the antibacterial spectrum and mechanism of action with the antibiotics of this class. It acts by inhibiting dihydrofolate reductase (DHFR), a downstream enzyme also involved in the synthesis of folic acid. Used separately, these drugs are bacteriostatic, but the synergistic combination of SMX and trimethoprim bears them bactericidal properties (Poe 1976; Huovinen 1987).

Co-trimoxazole is primarily used to treat urinary tract infections (targeting members of the family *Enterobacteriaceae*), respiratory tract infections (*Streptococcus pneumoniae*, *Haemophilus influenzae*, and *Moraxella catarrhalis*), gastrointestinal infections (*Salmonella* spp. and *Shigella* spp.), and skin-associated infections (*Staphylococcus aureus* and *S. epidermidis*). It is also the drug of choice for treatment and prophylaxis of *Pneumocystis jiroveci* pneumonia in HIV-infected patients (Masters et al. 2003). Furthermore, high doses of co-trimoxazole were shown to be effective against methicillin-resistant *Staphylococcus aureus* (MRSA) infections (Cassir et al. 2014).

Substantial use of other sulfonamide antibiotics in human therapy (i.e., sulfamethizole and sulfadimethoxine) has been reported only in a few European countries (Coenen et al. 2011; Gelband et al. 2015). Conversely, sulfadiazine, sulfamethazine, and sulfathiazole are mostly used for therapy and prophylaxis in veterinary medicine and animal husbandry

(Sarmah et al. 2006). Besides their therapeutic applications, sulfonamides are also often employed as growth promoters in animal husbandry (García-Galán et al. 2008).

Table 1.1. – General chemical structure of the most commonly used sulfonamide antibiotics, composed by an aniline moiety, a sulfonamide group and a heterocyclic moiety (R), adapted from Ingerslev and Halling-Sørensen (2000).

General structure	Sulfonamide	Heterocyclic moiety (R)
	Sulfanilamide	—H
	Sulfamethoxazole	
	Sulfamethizole	
	Sulfadimethoxine	
	Sulfadiazine	
	Sulfamethazine	
	Sulfathiazole	

Resistance against these antibiotics emerged not long after their introduction into clinical use (Huovinen et al. 1995), which is now restricting their use for human therapy (Sköld 2000). For both sulfonamides and trimethoprim, resistance occurs mainly by mutation of the chromosomally encoded DHPS (*folP* gene) and DHFR or by plasmid-mediated horizontal gene transfer (HGT) of insensitive versions of these enzymes (Sköld 2000; Sköld 2001; Perreten and Boerlin 2003). For sulfonamide antibiotics, several widespread genes encoding for mutated versions of *folP* have been described, namely, *sul1*, *sul2*, *sul3* and *sul4* (Sköld 2000; Perreten and Boerlin 2003; Razavi et al. 2017). Also, SmeDEF efflux

transporters were found to confer resistance to sulfonamides and trimethoprim alike (Sánchez and Martínez 2015).

Despite the high levels of resistance, these antibiotics are still widely used mainly in veterinary medicine. The applied amounts are close to those of tetracyclines and beta-lactams, which are the two most-consumed antibiotics in this sector (Sarmah et al. 2006; European Medicines Agency - EMA 2016). Due to their intensive use, persistence and inconsistent removal in conventional WWTP (Chen and Xie 2018), these drugs have become widespread micropollutants: they are frequently detected in surface water, groundwater and drinking water at 12 µg/l, 113 ng/l and 116 ng/l, respectively (Göbel et al. 2005; García-Galán et al. 2008; Zhang and Li 2011; Suzuki and Hoa 2012; Deng et al. 2018). Despite their limited adsorption to sediments, sulfonamides can also pollute soils through the use of antibiotic-contaminated manure (Deng et al. 2018). Indeed, sulfonamides are frequently detected in agricultural soils in concentrations up to 760 µg/kg (Deng et al. 2018).

In the next sections, we will focus on SMX since it is the model substance of sulfonamides and the main focus of this thesis. Firstly, we will discuss biotransformation reactions (section 1.3), and later, known biodegradation reactions entailing the cleavage of the sulfonamide bond (section 1.4.1) or the breakdown of the isoxazole ring (section 1.4.2). A similar underlying mechanism has been shown to mediate the transformation of several sulfonamide antibiotics. Hence, the transformation of other sulfonamides is discussed in section 1.5 and compared with SMX degradation.

1.3 Sulfamethoxazole biotransformation

The biotransformation of SMX (Fig. 1.2, Table 1.2) by pure cultures under aerobic conditions and in the presence of additional nutrients was first characterized by Gauthier et al. (2010) and Larcher and Yargeau (2011). For *Rhodococcus rhodochrous* (Gauthier et al. 2010), the authors observed a substitution of the primary amine in the aniline moiety

with a hydroxyl group. This yielded a product (SMX-1, Fig. 1.2) that could not be further metabolized by this strain. Later, for *Rhodococcus equi* and *Pseudomonas aeruginosa*, the same authors hypothesized the biotransformation of SMX into *N*⁴-acetylsulfamethoxazole (SMX-2, Fig. 1.2), which would be further transformed into an alcohol derivative (possibly *N*⁴-hydroxy-acetylsulfamethoxazole, SMX-2.1, Fig. 1.2) that accumulated at low amounts (Larcher and Yargeau 2011). Subsequently, Zhang et al. (2016) observed that a strain of *Alcaligenes faecalis* would also transform SMX into *N*⁴-acetylsulfamethoxazole (SMX-2, Fig. 1.2). Besides, the same strain also accumulated a second metabolite, hydroxylamine sulfamethoxazole (SMX-2.2, Fig. 1.2) (Zhang et al. 2016). Interestingly, both *N*⁴-acetylsulfamethoxazole and hydroxylamine sulfamethoxazole are one of the main human metabolites for this antibiotic (Cribb and Spielberg 1992; García-Galán et al. 2008).

A later study by Reis et al. (2018b) showed that the *N*⁴-acetylation of SMX was a fairly common microbial transformation process. In this study, the authors showed that multiple *Proteobacteria* strains isolated from mineral water (*Pseudomonas* spp., *Brevundimonas* spp. and *Stenotrophomonas* spp.) catalyzed the acetylation of SMX when grown in complex and rich medium, without accumulating other transformation products.

Noticeable, complex microbial communities in aerobic conditions were found to accumulate different products. For instance, incubations of soil amended with SMX led to the identification of an *N*¹-acetylated metabolite (SMX-3, Fig. 1.2) in addition to the *N*⁴-acetylated metabolite reported above for pure cultures (Koba et al. 2017).

SMX was also reported to be transformed into 4-nitro-sulfamethoxazole (SMX-4 Fig. 1.2) by activated sludge enriched for ammonia-oxidizing bacteria (AOB) under aerobic conditions with ammonium (NH₄⁺) as an energy source (Kassotaki et al., 2016). Indeed, the transformation of SMX on these environments was concomitant with nitrification. Besides, the addition of allylthiourea (ATU) completely suppressed this process, strongly

indicating that copper-containing enzymes, like ammonia-monooxygenase (AMO), may be responsible for the transformation of SMX.

Communities consisting of a mixture of river water and sediment under anoxic conditions with NO_3^- as an electron acceptor were observed to transform SMX into 4-nitro-sulfamethoxazole and desamino-sulfamethoxazole (SMX-4 and 4.1, Fig. 1.2) (Banzhaf et al. 2012; Nödler et al. 2012; Barbieri et al. 2012). Both these products were formed concomitantly with SMX degradation and nitrate reduction. Nevertheless, once the nitrite was fully consumed, 4-nitro-sulfamethoxazole reverted back to its original parental form, suggesting that SMX concentration in the environment may fluctuate depending on nitrate availability.

Particular consideration should be given to such biotransformation products when evaluating elimination rates. In some cases, only minor changes of the molecule occur, without elimination of the antibiotic activity or even resulting in an increased toxicity (e.g., 4-nitro-sulfamethoxazole) (Majewsky et al. 2014); in other cases, the metabolites can retransform back into the parental form. The latter process was also demonstrated by Radke et al. (2009) for *N*⁴-acetylsulfamethoxazole in microcosm experiments with river water and sediment at a 3:1 ratio incubated in the darkness at 20 °C, an initial pH of 8 during 64 days.

Hence, even though some SMX products may exhibit lower toxicity compared to their parental form, such as *N*⁴-acetylsulfamethoxazole (Majewsky et al. 2014), SMX transformation does not guarantee complete detoxification of the drug because the metabolites may be quickly reverted (Radke et al. 2009).

1.4 Sulfamethoxazole biodegradation

1.4.1 Cleavage of the sulfonamide bond

The earliest observations regarding the potential of aerobic heterotrophic bacteria to cleave SMX was first noted in activated sludge by Ingerslev and Halling-Sørensen (2000) and Pérez et al. (2005). In 2013, Müller and collaborators showed that activated sludge communities could degrade this antibiotic in either the presence or absence of additional carbon and nitrogen sources (Müller et al. 2013). Nevertheless, depending on nitrogen availability, two parallel metabolic pathways could occur. In the presence of additional carbon and nitrogen sources, SMX was fully converted into 3-amino-5-methylisoxazole (3A5MI, SMX-5, Fig. 1.2), which lacks antibiotic activity (Majewsky et al. 2014). These authors also observed that SMX degradation was faster in the absence of additional carbon and nitrogen sources. Nevertheless, continuous cultivation under these conditions caused a decrease in overall metabolic activity, but it remained unclear whether this happened because the drug is a poor carbon source for heterotrophic bacteria or because continuous exposure actively selected for degrader strains, decreasing the overall microbial diversity and activity of the sludge microbiota.

Studies with single bacterial strains further supported these findings. Very often, these strains were shown to cleave the sulfonamide bond resulting in the accumulation of the heterocyclic moiety as a dead-end product, while using the aniline moiety as carbon and energy source (Bouju et al. 2012; Topp et al. 2012; Ricken et al. 2013; Topp et al. 2016). Ricken et al. (2013) demonstrated that the degradation of SMX by *Microbacterium* sp. BR1 was initiated by *ipso*-hydroxylation of the aniline moiety, resulting in the cleavage of the S-N bond and accumulation of 3A5MI (SMX-5, Fig. 1.2). Concomitantly, sulfite and 4-aminophenol (SMX-6, Fig. 1.2) were transiently accumulated (Ricken et al. 2013), and the latter was further transformed into 1,2,4-trihydroxybenzene (THB, SMX-6.2) presumably via hydroquinone (HQ, SMX-6.1, Fig. 1.3) (Ricken et al., 2015a). Enzymes that cleave the

aromatic ring of trihydroxybenzene are widespread; therefore THB can be transformed into *cis-cis*-muconic acid before being channeled into the central metabolism via the citric acid cycle (Vaillancourt et al. 2006).

In 2017, a two-component flavin-dependent monooxygenase (SadA) was identified as the enzyme responsible for the initial *ipso*-hydroxylation of sulfonamide molecules resulting in the release of 4-aminophenol (SMX-6, Fig. 1.2) (Ricken et al. 2017). The gene that encodes SadA is contained in a cluster that also bears a second flavin-dependent monooxygenase (SadB) and an FMN reductase (SadC). *E. coli* cells expressing SadB were shown to transform 4-aminophenol into THB (SMX-6.2, Fig. 1.2), and SadC provided reduced FMN for both SadA and SadB.

More recently, Mulla et al. (2018) isolated three SMX-degrading strains from wastewater, activated sludge, and pig manure (Table 1.2) affiliated to *Actinobacteria* (*Gordonia* sp.) and *Proteobacteria* (*Ochrobactrum* sp. and *Labrys* sp.). The authors confirmed the presence of 4AP, 3A5MI, and HQ as main metabolites in cell-free supernatants. To date, no draft genomes were obtained for these bacterial strains, however the presence of the same metabolites accumulated by *Microbacterium* sp. BR1 suggests the same underlying mechanism for SMX transformation and possibly the presence of homologs encoding for the conserved sulfonamide monooxygenase (SadA).

Contrarily to the other *Proteobacteria* isolates, the cold-adapted *Pseudomonas psychrophila* HA-4 has been reported to degrade SMX through a different pathway (Jiang et al. 2014). In this study, sulfanilamide (SMX-7.2, Fig. 1.2) was detected instead of 4-aminophenol, suggesting that the cleavage occurs through hydrolysis of the N-C bond. This initial hydrolysis led to the formation of the unstable 4-amino-*N*-hydrobenzenesulfonamide (hypothetical, SMX-7) followed by deamination and desulfurization into aniline (SMX-7.1) and release of sulfanilamide (SMX-7.2) through an unknown pathway. However, 3A5MI (SMX-5) was also detected suggesting that SMX may be transformed by two independent

pathways in this strain: (i) the S-N cleavage, similar to *Microbacterium* sp. BR1 (Ricken et al. 2013), and (ii) the N-C hydrolysis resulting in the transient accumulation of aniline and sulfanilamide. 4-aminothiophenol (SMX-8) was also detected in this study; however, the underlying mechanism for this transformation could not be further elucidated and, to the best of our knowledge, no other isolates were shown to catalyze a similar reaction.

1.4.2 Cleavage of the isoxazole ring

Cleavage of the isoxazole ring has been first reported in anaerobic conditions. For instance, Mohatt et al. (2011), who investigated the transformation of SMX in soil under anaerobic Fe(III)-reducing conditions, found that the predominant reaction was the reductive cleavage of the N-O bond in the isoxazole group. This cleavage formed an unstable radical anion, which led to parallel reactions resulting in several stable dead-end products (SMX-9 to 9.3, Fig. 1.2), without cleavage of the S-N bond. However, the same reductive cleavage was observed in abiotic conditions with Fe(II) and goethite, suggesting that this reaction could be merely a by-product of the Fe(III) reduction carried out by soil microbiota and not the result of catalysis by specific enzymes. Similar dead-end products were reported by Jia et al. (2017) and by Alvarino et al. (2016), which observed the cleavage of the isoxazole moiety in sulfate-reducing conditions and in activated sludge under anaerobic conditions with a complex substrate mixture (skimmed milk and bicarbonate) (not shown). This finding suggests that the isoxazole moiety could be more easily degraded under reducing conditions, regardless of the nature of the electron acceptor. Alvarino et al. (2016) showed that despite the quick reduction of the isoxazole moiety, limited mineralization occurred (between 1.2% and 2.2%), implying that contrary to its behavior in aerobic conditions, the aniline moiety may remain intact.

Table 1.2. – Microbial communities and single bacterial strains able to degrade the antibiotic sulfamethoxazole.

Class	Order	Organism	Origin	Conditions	Identified metabolites	Reference
Complex microbial community			Activated sludge	Aerobic	3A5MI (SMX-5) and an additional uncharacterized metabolite	[1]
			Soil	Anaerobic (Fe ³⁺ reducing)	Cleavage of the N-O bond in the oxazole moiety (SMX-9 to 9.3)	[2]
			Water/ sediment	Anoxic (nitrate reducing)	4-nitro-sulfamethoxazole (SMX-4); desamino-sulfamethoxazole (SMX-4.1)	[3], [4]
			Anaerobic digester sludge	Anoxic (MFC)	Benzenesulfinic acid (SMX-10); 3A5MI (SMX-5) and isopropanol (SMX-5.1)	[5]
<i>Actinobacteria</i>	<i>Actinomycetales</i>	<i>Rhodococcus</i> sp. BR2	Membrane reactor	Aerobic	<i>N.d.</i>	[6]
		<i>Microbacterium</i> sp. BR1	Membrane reactor	Aerobic	4-aminophenol (SMX-6); HQ (SMX-6.1); THB (SMX-6.2); 3A5MI (SMX-5), sulfite and CO ₂	[6], [7], [8]
		<i>Rhodococcus rhodochrous</i> ATCC 13808	Culture collection	Aerobic	Hydroxyl- <i>N</i> -(5-methyl-1,2-oxazole-3-yl)benzene-1-sulfonamide (SMX-1)	[9]
		<i>Rhodococcus equi</i> ATCC 13557	Culture collection	Aerobic	<i>N</i> ⁴ -Hydroxy-acetylsulfamethoxazole (SMX-2.1)	[10]
		<i>Gordonia</i> sp. SMX-W2-SCD14	Activated sludge	Aerobic	4-aminophenol (SMX-6); HQ (SMX-6.1); 3A5MI (SMX-5)	[11]
<i>Alphaproteobacteria</i>	<i>Rhizobiales</i>	<i>Ochrobactrum</i> sp. SMX-PM1-SA1	Pig manure	Aerobic	4-aminophenol (SMX-6); HQ (SMX-6.1); 3A5MI (SMX-5)	[11]
		<i>Labrys</i> sp. SMX-W1-SC11	Wastewater			
<i>Betaproteobacteria</i>	<i>Burkholderiales</i>	<i>Alcaligenes faecalis</i> CGMCC 1.0767	Culture collection	Aerobic	<i>N</i> ⁴ -Acetylsulfamethoxazole (SMX-2); Sulfamethoxazole hydroxylamine (SMX-2.2)	[12]
		<i>Ralstonia</i> sp. HB1 and HB2	Membrane reactor	Aerobic	<i>N.d.</i>	[6]
		<i>Achromobacter</i> sp. BR3				
<i>Gammaproteobacteria</i>	<i>Pseudomonadales</i>	<i>Pseudomonas aeruginosa</i> PA01*	Culture collection	Aerobic	<i>N</i> ⁴ -Acetylsulfamethoxazole (SMX-2)	[10], [13]
		<i>P. psychrophila</i> HA-4	Activated sludge	Aerobic	3A5MI (SMX-5); 4-aminothiophenol (SMX-8); 4-amino- <i>N</i> -hydrobenzenesulfonamide (SMX-7); aniline (SMX-7.1); sulfanilamide (SMX-7.2)	[14]
		<i>P. mandelii</i> McBPA4 ^a	Mineral water	Aerobic	<i>N</i> ⁴ -Acetylsulfamethoxazole (SMX-2)	[15]

N.d. not determined. ^aSeveral other strains affiliated to *Proteobacteria* were shown to catalyze this transformation in this study; *Genome sequences are available for these strains. References: [1] Müller et al. (2013); [2] Mohatt et al. (2011); [3] Banzhaf et al. (2012); [4] Nödler et al. (2012); [5] Wang et al. (2016); [6] Bouju et al. (2012); [7] Ricken et al. (2013); [8] Ricken et al. (2015); [9] Gauthier et al. (2010); [10] Larcher and Yargeau (2011); [11] Mulla et al. (2018); [12] Zhang et al. (2016); [13] Stover et al. (2000); [14] Jiang et al. (2014); [15] Reis et al. (2018b).

This instability of the isoxazole moiety of SMX was also observed in anoxic conditions by Wang et al. (2016). In microbial fuel cells (MFCs) with potassium ferricyanide as an electrolyte in the cathode chamber, SMX could be cleaved with the accumulation of benzenesulfonic acid and 3A5MI (SMX-10 and SMX-5, respectively) (Wang et al. 2016). In contrast with aerobic degradation of SMX, 3A5MI could be effectively degraded in these conditions whereas the benzene ring was not cleaved and accumulated as a dead-end metabolite (Wang et al. 2016). The further degradation of 3A5MI was confirmed by feeding MFCs directly with this intermediate, which yielded isopropanol as a final product (SMX-5.1, Fig. 1.2).

Mulla et al. (2018) were the first authors reporting the degradation of 3A5MI under aerobic conditions, by bacterial isolates from *Actinobacteria* and *Proteobacteria* phyla. Unfortunately, no further products of 3A5MI transformation have been identified. However, these findings suggest that this moiety may not accumulate in the environment, even if it is released as a dead-end product of SMX degradation by some bacterial strains.

1.5 Biotransformation and biodegradation of other sulfonamides

Biotransformation of other sulfonamide antibiotics has not been so extensively studied. However, many sulfonamide antibiotics have been shown to undergo similar *N*⁴-acetylation and hydroxylation reactions as described extensively for SMX in section 1.3 (Ascalone 1981; Nouws et al. 1987; Lamshöft et al. 2007). However, to the best of our knowledge, these metabolites are yet to be detected in environmental samples. Conversely, in anaerobic conditions, only some sulfonamides were reported to undergo biotransformation. Mohring et al. (2009) and Mitchell et al. (2013), studied sulfadiazine and sulfamethazine degradation in anaerobic digesters inoculated with sludge and manure. These authors found that sulfadiazine was extensively transformed by hydroxylation of the pyrimidine ring, whereas sulfamethazine, with two methyl groups attached to the pyrimidine ring, was not transformed at all.

As for SMX, biodegradation of other sulfonamide antibiotics has been reported. Yang et al. (2015) studied on the degradation of sulfamethazine, a pyrimidine-substituted sulfonamide, by activated sludge from a municipal WWTP. The process was characterized by quick sorption to the sludge and a slow biodegradation process (Yang et al. 2015). Biodegradation yielded sulfanilic acid and sulfamethazine dimers as transient metabolites, but no metabolic pathway was proposed (Yang et al. 2015).

Liao et al. (2016) reported the degradation of sulfanilamide, a sulfonamide lacking heterocyclic moiety, by acclimatized biomass from a pilot-scale biological-activated-carbon filter system used to treat contaminated lake water. In this study, a slight increase in optical density occurred concomitantly with sulfanilamide degradation and led to the assumption that these microorganisms could use sulfanilamide as a source of carbon. The authors identified (i) benzene sulfonamide (loss of the primary amine, SML-1, Fig. 1.3) and (ii) hydroxylamine benzene sulfonamide (hydroxylation of the primary amine, SML-1.2, Fig. 1.3) as metabolic products. Another metabolite was found in this study, (iii) *p*-phenylenediamine (“extrusion” of the sulfonyl group, SML-1.3, Fig. 1.3); however, the reactions leading to its formation are difficult to explain from a mechanistic point of view. Besides, the authors studied the microbial diversity of the acclimatized microbial community, identifying *Bacillus* and *Chryseobacterium* as the dominant genera. These microorganisms were not explicitly linked to sulfonamide degradation, and it is unclear whether sulfanilamide was mineralized because CO₂ release was not assessed.

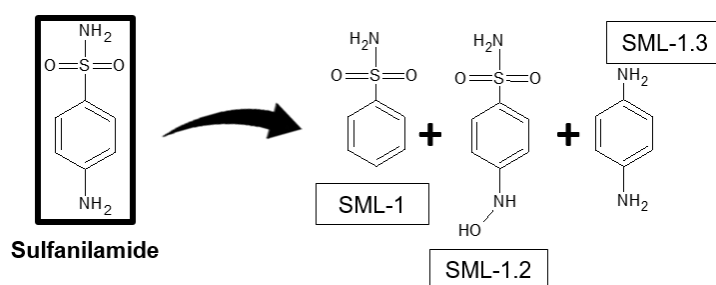


Figure 1.3 – Sulfanilamide degradation in biological-activated-carbon filter system described by Liao et al. (2016).

Biodegradation of other sulfonamide antibiotics was also reported by Ricken et al. (2013). These authors showed that *Microbacterium* sp. BR1 could degrade several sulfonamides (i.e., sulfadiazine, sulfadimethoxine, sulfamethazine, sulfamethizole) through the same underlying mechanism as the one observed for SMX transformation. Furthermore, for all investigated compounds, the corresponding heterocyclic moieties were released as dead-end products. However, the degradation rates were significantly different among the different sulfonamides (Ricken et al. 2013). These findings suggest that the nature and bulkiness of the heterocyclic group influence the affinity of each sulfonamide for the active site(s). From a mechanistic point of view, two features of the moiety bearing the heteroatom affect the kinetics of degradation. The first is its ability to accept the delocalized electron pair resulting from hydroxylation at the *ipso*-position, and the second is its ability to give rise to several resonance structures.

Further studies with single bacterial isolates frequently showed that sulfonamide degradation is often accompanied by the accumulation of their corresponding heterocyclic moieties. For example, 2-aminopyrimidine (SDZ-1, Fig. 1.4) has been detected in culture supernatants of the sulfadiazine degraders *Microbacterium lacus* sp. SDZm4 (Tappe et al. 2013) and *Arthrobacter* spp. strains D2 and D4, respectively (Deng et al. 2016), while 2-amino-3,4-dimethylpyridine (SMT-1, Fig. 1.4) is accumulated by sulfamethazine-degrading isolates from the genus of *Microbacterium* as described by Topp et al. (2012). The presence of these metabolites hinted that the same underlying mechanism could be involved in sulfonamide-degradation by these bacterial isolates and *Microbacterium* sp. BR1. Subsequently, the analysis of the draft genomes of these strains revealed that all these isolates shared a highly conserved sulfonamide monooxygenase (SadA) that was shown to *ipso*-hydroxylate the SMX molecule and released 3A5MI as a stable dead-end metabolite in *Microbacterium* sp. BR1 (Ricken et al. 2017).

Eventually, some of these dead-end products were also found to be susceptible to degradation. For instance, the two *Arthrobacter* sp. strains were found to only transiently

accumulate 2-aminopyrimidine and to further hydroxylate it (2-amino-hydroxypyrimidine, SDZ-1.1, Fig. 1.4) and presumably use it as a carbon source as well. Furthermore, even bacteria unable to degrade sulfonamides may degrade this dead-end product, as shown in a study by Tappe et al. (2015), which described a *Terrabacter* sp. strain isolated from a sulfadiazine-enriched sample able to hydroxylate 2-aminopyrimidine into 2-amino-hydroxypyrimidine (SDZ-1.1) and to further mineralize this aromatic molecule.

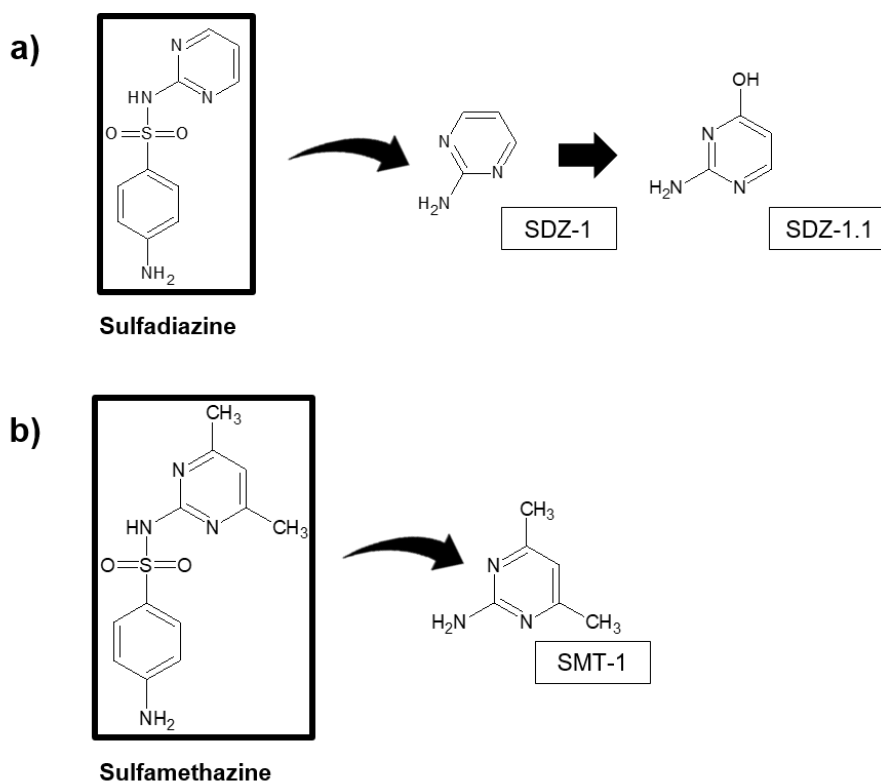


Figure 1.4 – Biodegradation of sulfadiazine and sulfamethazine by several bacterial strains under aerobic conditions.

1.6 Sulfonamide degradation by ligninolytic enzymes

Ligninolytic enzymes have also been shown to degrade sulfonamide antibiotics. Eibes et al. (2011) investigated the degradation of SMX by versatile peroxidase of the filamentous fungi *Bjerkandera adusta*. As observed in previous studies with heterotrophic bacteria, degradation by peroxidase yielded 3A5MI as the main stable metabolite. Carboxylic acids

(acetic and oxalic acid) and anions (nitrate, nitrite, and sulfate) were detected, suggesting that the aniline ring was effectively degraded by this enzyme, possibly through *ipso*-hydroxylation of the molecule as described by Ricken et al. (2013).

1.7 Feasibility of bioaugmentation and bioremediation to attenuate sulfonamides contamination

The research of Yang et al. (2016) explored the potential application of ligninolytic enzymes in bioremediation strategies. The authors applied spent mushroom compost (SMC, a potential source of ligninolytic enzymes) from *Pleurotus eryngii* to a soil-sludge mixture. On its own, SMC did not completely mineralize the sulfonamides. However, the unknown degradation products could be further mineralized easily.

Despite recent advances in the molecular characterization of bacterial sulfonamide degraders, few studies have assessed the feasibility of applying these degraders to attenuate sulfonamide degradation and resistance.

These strains may not perform well under environmental conditions, as Fenu et al. (2015) observed in membrane bioreactors spiked with *Microbacterium* sp. BR1 operating at temperatures below 20 °C and with 120-60 ng/l SMX. Compared to control experiments, this specialized strain did not improve SMX removal, because it was unable to thrive at low temperatures and to degrade the antibiotic at environmentally relevant concentrations.

Because some sulfonamide degraders were also shown to carry highly conserved sulfonamide resistance genes (Ricken et al. 2017), the direct application of these degraders may further promote an undesirable spread of resistance. A few studies have addressed this issue. For instance, Vila-Costa et al. (2017) investigated the correlation between SMX degradation and the spread of known resistance genes (*sul1* and *sul2*) in mesocosms with river water and biofilm from pristine and polluted environments. The authors observed an interesting effect, especially at high SMX concentrations (5 µg/l) in

waters from pristine environments: the quick degradation of the antibiotic lead to a reduced spread of the known resistance genes. These findings suggest that degradation may, in fact, decrease the horizontal gene transference of resistance genes and the proliferation of antibiotic-resistant bacteria. This study did not take into account a robust assessment of microbial diversity and overlooked the amount of mineralization. Nevertheless, it raised new and interesting questions regarding the role of these antibiotic degraders in achieving the equilibrium between antibiotic resistance and susceptibility in natural communities.

1.8 Microbial cooperation and pollutant degradation

As previously observed, the degradation of pollutants in the environment can result from metabolic cooperation between different members of a microbial community (Morris et al. 2013; Pande and Kost 2017). Perhaps the most compelling evidence of metabolic cooperation in the degradation of sulfonamides is the study of sulfadiazine degradation in lysimeter experiments by Tappe et al. (2013; 2015). Earlier studies with ¹⁴C labeled sulfadiazine in lysimeters indicated substantial degradation of both the aniline and the pyrimide moieties of this antibiotic (Tappe et al. 2013). Nevertheless, first isolation attempts led only to the purification of *Microbacterium lacus* SDZm4 (Tappe et al. 2013), that mineralized the aniline moiety and released 2-aminopyrimidine (SDZ-1, Fig. 1.4a) as a dead-end metabolite. This finding suggested that other members of the community could further transform the heterocyclic moiety of sulfadiazine.

Indeed, a posterior enrichment with 2-aminopyrimidine using lysimeter biomass as inoculum led to the isolation of a *Terrabacter* sp. strain. This strain was shown to hydroxylate 2-aminopyrimidine into 2-amino-hydroxypyrimidine (SDZ-1.1, Fig. 1.4a) and to further use it as a carbon source (Tappe et al. 2015). In this way, in the sulfadiazine-acclimatized lysimeters, this antibiotic appears to be initially cleaved by *M. lacus* that

mineralizes the aniline moiety and releases 2-aminopyrimidine as a dead-end metabolite that, in turn, serves as a carbon source for *Terrabacter* sp.

In this study, *M. lacus* and *Terrabacter* sp. could grow independently and appeared to cooperate only in the breakdown and mineralization of sulfadiazine. However, the evolution of environmental communities in heavily polluted environments is frequently driven by different selecting agents that often lead to niche-specialization and, consequently, to the onset of complex microbial cooperation strategies (Stewart 2012; Ponomarova and Patil 2015).

Many environmental microorganisms recurrently exchange metabolites or co-factors and often associate with xenobiotic-degraders to thrive in polluted environments (Schloss and Handelsman 2005; Merhej et al. 2009; Stewart 2012; Morris et al. 2013; Ponomarova and Patil 2015; Widder et al. 2016). These associations are commonly referred to as microbial syntrophy or cross-feeding, and they result from long-term and stable interactions between organisms within a given niche. This phenomenon has been extensively discussed by several authors; however, there is a lack of consensus in the literature regarding the best classification system (Estrela et al. 2012; Morris et al. 2013; Pande et al. 2015). From a microbial ecology perspective, perhaps the most appropriate approach has been outlined by Estrela et al. (2012). In this study the authors divide microbial syntrophy into several categories; however, they have also highlighted that the outcome of these associations is often hard to predict:

- i. **Mutualism (one-way or two-way):** when the benefits of the association outweigh the competitive costs. An example of this type of association has been reported in the mutualistic interaction between *Desulfovibrio vulgaris* (a sulfate-reducing bacterium) and *Methanococcus maripaludis* (a methanogenic archaeon) in anaerobic communities. These microorganisms were shown to exchange electrons

with the purpose of gaining energy in the degradation of lactate into acetate and methane (Stolyar et al. 2007);

- ii. **Competition:** when the effect of the interaction is detrimental for the members of the community. These type of associations are common in natural communities because most bacteria have to compete with their neighbors for limited space and resources. A prevalent example is that of antibiotic producers that excrete antimicrobial compounds to kill or inhibit other members of the community and, therefore, gain better access to resources (Hibbing et al. 2010);
- iii. **Exploitation:** when one member of the community benefits at the expense of other(s). Microorganisms may exploit public goods (metabolically expensive molecules that diffuse to the environment) or other microorganisms and thus become opportunistic. This behavior can be observed in co-culture experiments with *Pseudomonas aeruginosa* and a polymer-degrader *Aeromonas hydrophila* (Jagmann et al. 2010). When growing on chitin, *P. aeruginosa* would arrest the citric acid cycle in *A. hydrophila* by producing secondary metabolites (quorum sensing regulative molecules) and profit from the acetate released by this bacterium during the degradation of the polymeric resource.

These type of microbial interactions frequently lead to gene loss and, consequently, to “unculturability” under standard laboratory conditions (Stewart 2012; Morris et al. 2013; Pande and Kost 2017). This phenomenon in environmental microbial populations can be driven by nutrient availability and spatial distribution of microorganisms, and it is often illustrated by the “black queen hypothesis” (Morris et al. 2012). This hypothesis states that when a nutrient is abundant, auxotrophic mutants unable to synthesize it become favored and gain a fitness advantage when compared to prototrophs. Indeed, most studies on bacterial syntrophy report dependency on essential nutrients produced by prototrophs such as amino acids, vitamins, growth factors (e.g., siderophores) or proteins (Pande and Kost 2017). However, an increasing number of studies show that detoxification and

pollutant degradation can also drive microbial cooperation (Schloss and Handelsman 2005; Merhej et al. 2009; Stewart 2012; Widder et al. 2016). This type of cooperation has been previously reported in the degradation of terephthalate, an essential raw material used in the production of many plastics (Lykidis et al. 2011; Wu et al. 2013). These terephthalate-degrading organisms thrive in an intricate network formed between H₂-producing syntrophs and methanogenic archaea, with numerous other secondary interactions essential for the stability of the consortium (Lykidis et al. 2011; Wu et al. 2013).

Similarly, anammox bacteria which carry out the anaerobic removal of ammonium, are reported to form stable biofilm communities with ammonia-oxidizing (AOB) and nitrite-oxidizing bacteria (NOB) (Jetten et al. 2005a; Jetten et al. 2005b; Oshiki et al. 2013). Indeed, a delicate balance between these microbial populations is reported to be essential to guarantee optimal nitrogen removal efficiencies and to protect the sensitive anammox from atmospheric O₂ (Jetten et al. 2005a; Kindaichi et al. 2007; Oshiki et al. 2013; Ma et al. 2015).

Interestingly, none of these groups have pure culture representatives. To better understand detoxification and degradation in the environment high-throughput methodologies such as functional metagenomics should complement culture-dependent approaches. These approaches have proven to be successful for the discovery of new tetracycline oxidoreductases (Diaz-Torres et al. 2003; Forsberg et al. 2015). For instance, Diaz-Torres et al. (2003) isolated a novel tetracycline modifying enzyme, Tet37, using functional metagenomics with oral-microbiome samples from healthy individuals. This new gene carried out the NADPH-dependent transformation of this antibiotic conferring a high level of resistance to aerobically grown transformed *Escherichia coli*. More recently, Forsberg et al. (2015) investigated farm and grassland soil using functional metagenomics and a human pathogen (*Legionella longbeachae*) in search for enzymes that could cause resistance to tetracyclines. The study identified nine new flavoproteins able to oxidize

tetracyclines; these enzymes were found to be structural homologs to the initially described oxidoreductase TetX (Yang et al. 2004; Volkers et al. 2011), but shared little amino acid similarity with this gene.

1.9 Main objectives of this study

Sulfonamide consumption is still highly prevalent in animal farming and veterinary medicine leading to a dependency on these antibiotics and high levels of contamination and resistance. Recently, sulfonamide degradation has been reported in many heterotrophic bacteria and linked to the presence of a *sad* cluster consisting of a sulfonamide monooxygenase (*sadA*), 4-aminophenol monooxygenase (*sadB*) and an FMN-reductase (*sadC*). This cluster appears to be conserved in *Actinobacteria*; however, there is still a lack of knowledge regarding its dissemination among bacteria from different environments.

Recently, we have identified *Achromobacter denitrificans* strain PR1 as a sulfonamide degrader (Reis et al. 2014). However, further studies with this apparently axenic culture showed that this metabolic trait was spontaneously lost upon repeated sub-culturing of this strain in laboratory conditions. In this study, we aimed at understanding the reason behind this apparent metabolic instability in strain PR1. We also aimed at characterizing the metabolic pathway for SMX degradation by this strain and at identifying the genetic machinery linked to this trait. Moreover, we compared the genetic determinants with those of the previously described *sad* cluster. Finally, we analyzed the genetic vicinity of these genes in an attempt to assess the risk of dissemination through horizontal gene transference.

Chapter 2

Roadmap for the thesis

Sulfonamides were the first synthetic antibiotics successfully applied in therapy (Sköld 2000; Masters et al. 2003). Presently, these drugs are still among the most used in animal farming and veterinary medicine, and they are essential for a multitude of applications including the treatment of infections, prophylaxis and controversially used as growth promoters (Sarmah et al. 2006; García-Galán et al. 2008; European Medicines Agency - EMA 2016). However, due to increasing levels of resistance, sulfonamides are only sparsely used for human medicine (Masters et al. 2003; Cassir et al. 2014; Van Boeckel et al. 2014). Nevertheless, co-trimoxazole, containing trimethoprim and SMX in a one-to-five ratio as active substances, is still commonly used to treat a selected number of infections and as the drug of choice for the treatment of pneumonia in HIV-infected patients (Masters et al. 2003).

Current conventional treatments (WWTP) are often ineffective in the removal of these contaminants (Chen and Xie 2018). Conversely, some studies found that WWTP may even provide the ideal conditions (i.e., selective pressure and high cell density) for the proliferation and dissemination of ARB and ARG, thus aggravating the burden of resistance (Rizzo et al. 2013). Animal farming residues, such as manure, also contribute to the increase of resistance as they are often applied untreated to agricultural soils that may result in leaching and contamination of surface and ground waters with ARB and ARG alike (FAO 2014; Berendonk et al. 2015; Petrie et al. 2015). Hence, for these reasons, sulfonamides became widespread contaminants frequently detected at sub-inhibitory concentrations in many environmental compartments such as wastewaters, surface waters, ground waters and soils (Göbel et al. 2005; García-Galán et al. 2008; Zhang and Li 2011; Suzuki and Hoa 2012). The concentrations found in the environment are frequently insufficient to inhibit bacterial growth. However, they were shown to trigger the development of new antibiotic resistance mechanisms and to enhance the spread of pre-existing ARG (Martinez 2009; Gullberg et al. 2011). As the cost of new antibiotic discovery keeps rising and the research in this topic keeps dwelling (Welte 2016; Simpkin et al.

2017), it is crucial to develop strategies to contain the spread of resistance against existing antibiotics. Namely, by removing the antibiotic residues before the discharge of treated wastewater or agriculture residues in the environment.

Although a high number of studies have shown that sulfonamides can be removed from contaminated water by physicochemical processes, such as photo-Fenton, UV/H₂O₂ and TiO₂ photocatalysis (Hu et al. 2007; Batista et al. 2014), the implementation of these processes has a high cost (Baran et al. 2006). As referred to in the Introduction, in the past decades, many heterotrophic bacteria have developed the ability to transform and degrade these drugs. Hence, the feasibility of their application on biological treatment systems has been investigated. One of such studies was carried out by our research group. In this study, SMX-degraders were enriched from activated sludge collected from an urban WWTP (Reis et al. 2014). The enrichment culture was exposed to an increasing amount of SMX and decreasing amounts of yeast extract and was shown to degrade SMX with the stoichiometric accumulation of 3A5MI. The SMX-degrading culture was then serially diluted and spread according to Maltseva and Oriel (1997). This procedure resulted in the isolation of several bacterial strains, including *Achromobacter denitrificans* strain PR1 that was identified as an effective sulfonamide degrader (Reis et al. 2014). However, ongoing studies showed that this metabolic trait was spontaneously lost by some cells upon repeated sub-culturing in brain heart infusion agar (BHI) with SMX as a supplementary carbon source. This apparent metabolic instability prompted further functional and metabolic studies with this strain, which constitute the work of this thesis.

Initially, we had hypothesized that the enzyme responsible for the breakdown of sulfonamides could be encoded in a large catabolic plasmid. These plasmids are known to impose high metabolic burdens on their hosts and often produce plasmid-free progeny during replication (Lenski and Bouma 1987). In this way, we started by performing whole-genome sequencing (WGS) of strain PR1 with Illumina Miseq and MinION long-read sequencing (Oxford Nanopore Technologies, UK). The analysis of the complete genome of

strain PR1 revealed that it shared a high Average Nucleotide Identity (ANI) with the type strain of *A. denitrificans* (DSM 30026^T), further confirming its affiliation to this species. Furthermore, no potential plasmids were detected in its genome. The results of the sequencing and assembly of the complete genome of strain PR1 are presented in Chapter 3.

In an ongoing attempt to elucidate strain PR1 instability, we have discovered a low-abundance and slow-growing actinobacterium (strain GP) able to grow only in close contact with the *Proteobacteria* isolate after extended periods of incubation (≥ 10 days). In order to understand its role in sulfonamide degradation further studies were carried out with this consortium.

Although no pure cultures were obtained for strain GP, metagenomics and clone libraries of the 16S rRNA gene allowed the tentative identification of this strain as the representative member of a new species within the *Leucobacter* genus or potentially even of a new genus with the *Microbacteriaceae* family. Moreover, several experiments indicated that strain GP is the actual sulfonamide-degrader in this consortium and a putative degradation pathway could be proposed based on mass spectrometry studies (Ion Trap LC-MS and UPLC-QTOF-MS). These findings are discussed throughout Chapter 4.

Several experiments were devised in an attempt to isolate strain GP, and most of these findings are also discussed in Chapter 4. However, in an attempt to eliminate strain PR1 and purify strain GP, we isolated a bacteriophage able to infect strain PR1 and performed co-inoculation studies of this phage and the consortium. This study led to the discovery and characterization of a new polyvalent and virulent phage (vB_Ade_ART) able to infect multiple species of the *Achromobacter* genus. This characterization is presented in Chapter 5, as well as the implications of phage treatment for strain GP abundance and SMX-degradation activity.

At this point, the results suggested that direct contact with strain PR1 could be crucial for the growth of strain GP, both in liquid cultures and agar plates. In this way, we

reconstructed the draft genome of this bacterium from whole-metagenome sequencing of the consortium. We further analyzed the genome of this bacterium and compared it with the genomes of previously published *Leucobacter* spp. and with other fully sequenced sulfonamide-degraders. In this study, we set out to devise hypotheses that could explain the dependent phenotype of strain GP and further determine the genetic machinery linked to sulfonamide degradation in this strain. The results of this analysis are discussed in Chapter 6.

Chapter 3

Complete genome sequence of *Achromobacter denitrificans* PR1

Part of this chapter is published as:

A.C. Reis, K. Kroll, M. Gomila, B.A. Kolvenbach, P.F.X. Corvini, O.C. Nunes (2017). "Complete Genome Sequence of *Achromobacter denitrificans* PR1". *Genome Announcements*. 5(31), e00762-17, doi: 10.1128/genomeA.00762-17.

3.1 Abstract

Achromobacter denitrificans strain PR1 was isolated from an enrichment culture able to use sulfamethoxazole as an energy source. Here we describe the complete genome of this strain sequenced by Illumina Miseq and Oxford Nanopore MinION.

3.2 Genome Announcement

Achromobacter denitrificans are Gram-negative, rod-shaped bacteria commonly found in soil and occasionally in human infections (Kerstens and De Ley 1984; Coenye et al. 2003). Members of this species have been previously linked with xenobiotics degradation (Sałek et al. 2013; Pradeep et al. 2015; Mawad et al. 2016; Benjamin et al. 2016) highlighting their potential for bioremediation. Here we described the complete genome of *A. denitrificans* strain PR1, obtained originally from enriched activated sludge able to use sulfamethoxazole (SMX) as an energy source (Reis et al. 2014).

Strain PR1 was incubated overnight at 30°C in mineral medium B (Barreiros et al. 2003) with ammonium sulfate (0.54 g/l), succinate (0.83 g/l), yeast extract (0.2 g/l) and SMX (0.15 g/l). Genomic DNA extraction was performed with GenElute Bacterial Genomic DNA Kit (Sigma) and sequenced using Miseq (Illumina) and MinION (Oxford Nanopore). For Miseq paired-end sequencing (2 x 300 bp), two libraries were independently prepared from 1 µg DNA with TruSeq DNA LT Sample Prep Kit (lib1) from Illumina or KAPA HyperPrep Kit (lib2) from Kapa Biosystems. The MinION library was prepared from 1 µg DNA, sheared into 5 kb fragments with a g-TUBE (Covaris), subsequently prepared with Genomic DNA sequencing kit (SQK-MAP-103) and sequenced using flow cell with R7 chemistry (Oxford Nanopore). The library was loaded in the beginning and after 24 h to coincide with g1-to-g2 pore switch (Ip et al. 2015).

Miseq sequencing generated 2.5 million (lib1) and 0.3 million (lib2) paired-end raw reads. All reads were screened for PhiX contamination, adapter and quality-trimmed (>Q20) with BBDuk tool (<https://sourceforge.net/projects/bbmap/>). MinION sequencing generated

12,591 2D reads (>Q9) that were converted to fastq format with poretools v0.5.1 (Loman and Quinlan 2014). Hybrid *de novo* assembly was done with SPADES version 3.10.0 (Bankevich et al. 2012) with the options `-careful` and `-nanopore`. Contigs > 1 x coverage were removed from the assembly resulting in a single scaffold. Circularization was confirmed by designing primers to bridge the gap between the beginning and end of the single contig generated by *de novo* assembly with Primer-BLAST (Ye et al. 2012). The amplification of this region was performed with primers Gap_F and Gap_R (Table 3.1) in a 50 µl reaction containing 20 ng DNA, 0.5 µM of each primer (Eurofins), 1 x high fidelity buffer, 200 µM of dNTP mixture and 1 U of Phusion Polymerase (New England Biolabs). The PCR program was as follows: 98 °C for 3 min, 30 cycles of 98 °C for 10 sec, 67 °C for 15 sec and 72 °C for 30 sec, and a final extension at 72 °C for 5 min. Sanger sequencing (Eurofins) of the fragment generated a single circular chromosome of 6,929,205 bp with 46-fold average k-mer coverage and 67.4 % in G+C.

Table 3.1 – Sequences of the primers used to circularize the genome of *A. denitrificans* strain PR1.

Primer	Sequence (3' – 5')	Length (bp)
Gap_F	CTTGATCACCGAAGTAGCCG	20
Gap_R	GTGACGCTGCCTGCTTG	17

Analysis with Rapid Annotation using Subsystem Technology (RAST) server v2.0 (Overbeek et al. 2014) predicted 6,425 protein-coding sequences (CDS), 4 copies of the rRNA operon and 59 tRNA. Functional prediction of the CDS was further refined by aligning protein sequences against the Gene Ontology (GO) database (The Gene Ontology Consortium 2015) with InterProScan (Quevillon et al. 2005) and BLASTp (Altschul et al. 1997) in Blast2GO version 4.1 (Conesa et al. 2005) of the total CDS, 5,210 (81.1%) had a functional prediction and, from these, 2,939 (45.7%) had catalytic activity (891 hydrolases

and 746 oxidoreductases). ResFinder (Zankari et al. 2012) analysis identified multiple antibiotic resistance genes (*sul1*, *sul2*, *tetC*), with some (*cmlA1h*, *aadA2*) within the new class I integron In1410 (Moura et al. 2009). Average nucleotide identity (ANI) analysis (Rodriguez-R and Konstantinidis 2016) and *in silico* DNA-DNA hybridization (DDH) analysis (Clarke et al. 2002; Klenk et al. 2014) with *A. denitrificans* type strain genome (GenBank accession number BCTQ00000000) showed that strain PR1 belongs to the same species (ANI of 99.33%, DDH of 94.60% and a difference in G+C content of 0.19 %).

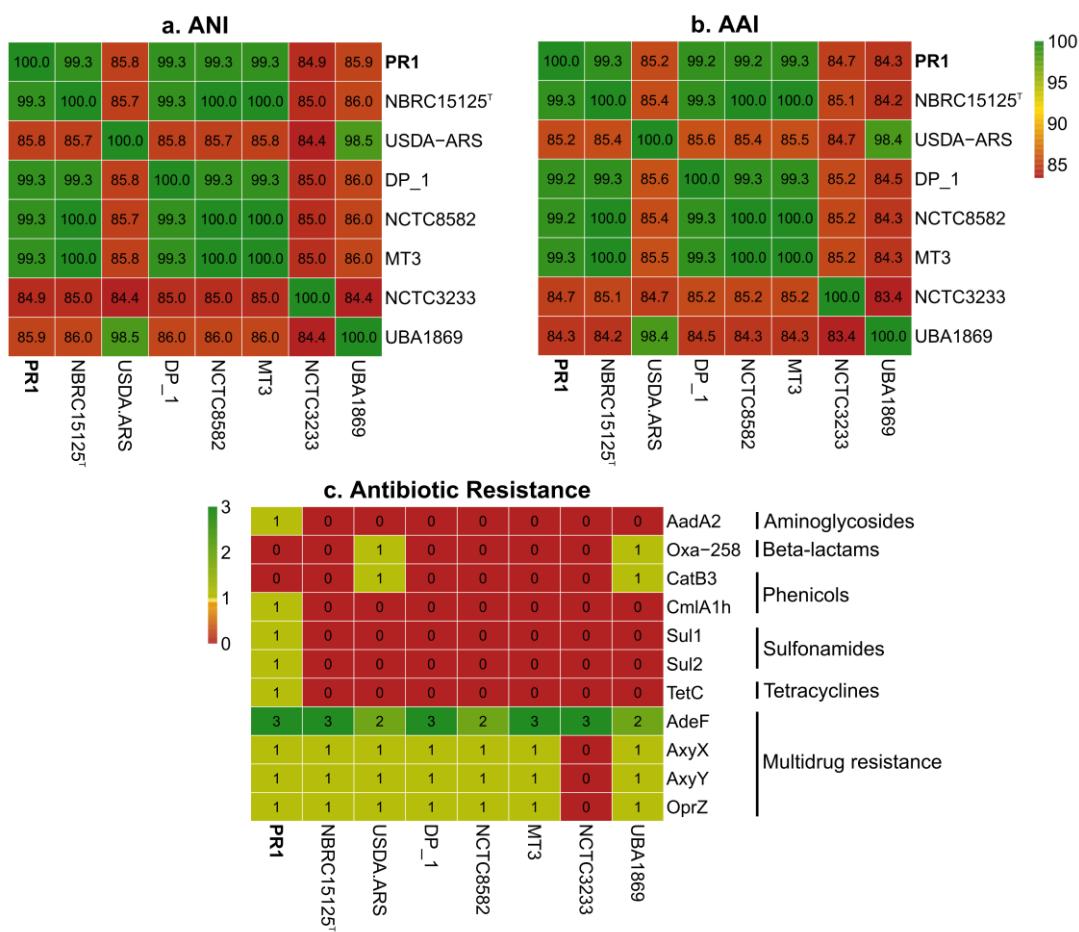


Figure 3.1 – ANI (a) and AAI (b) heatmaps comparing values between all fully sequenced strains of *A. denitrificans*: NBRC 15125^T (GCA_001571365); USDA-ARS-USMARC-56712 (GCA_001514355); DP_1 (GCA_002192685); NCTC8582 (GCA_900444675); MT3 (GCA_001945385); NCTC3233 (GCA_900444685) and UBA1869 (GCA_002338195). Presence/absence heatmap (c) for antibiotic resistance proteins found in each strain against aminoglycosides (AadA2), beta-lactams (Oxa-258), phenicols (CatB3 and CmlA1), sulfonamides (Sul1, Sul2), tetracyclines (TetC) and multidrug resistance efflux pumps (AdeF, AxyX, AxyY, OprZ).

The genome of strain PR1 was also compared with other *Achromobacter denitrificans* strains available in the National Center for Biotechnology Information (NCBI) (NCBI Resource Coordinators 2017) using BLAST Ring Image Generator (BRIG) (Alikhan et al. 2011). Furthermore, average nucleotide and average amino acid identity (ANI and AAI, respectively) were calculated AAI/ANI-matrix from the enveomics toolbox (<http://enve-omics.ce.gatech.edu/g-matrix>) (Rodriguez-R and Konstantinidis 2016). Antimicrobial resistance genes were analyzed in Comprehensive Antibiotic Resistance Database (CARD) with Resistance Gene Identifier for perfect and strict hits (Jia et al. 2017a).

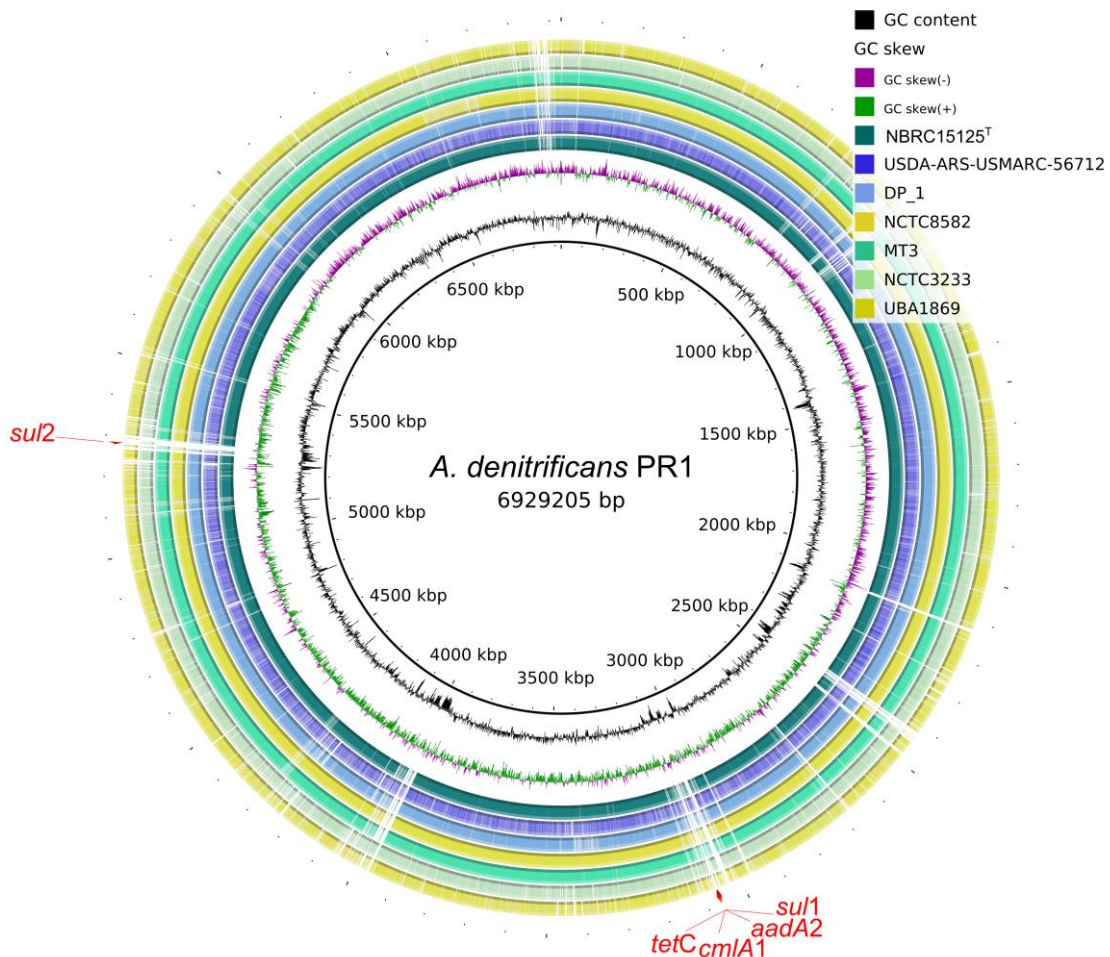


Figure 3.2 – Genome-wide nucleotide comparison (BLASTn) between fully sequenced strains of *A. denitrificans*. Strain PR1 genome is the innermost black circle and rings correspond, from inside out, to the draft/complete genome assemblies of strains: NBRC 15125^T (GCA_001571365); USDA-ARS-USMARC-56712 (GCA_001514355); DP_1 (GCA_002192685); NCTC8582 (GCA_900444675); MT3 (GCA_001945385); NCTC3233 (GCA_900444685) and UBA1869 (GCA_002338195). Within each ring, zones with higher transparency correspond to lower nucleotide identity. Gaps in the alignment correspond to the unique

regions found in the genome of strain PR1. Relevant antibiotic resistance genes of strain PR1 are indicated in red. The plot was generated with BRIG (Alikhan et al. 2011).

The analysis shows that strain PR1 is highly similar to the other strains of this species with ANI values ranging between 84.9 and 99.3 % and AAI values between 84.3 and 99.3 % (Fig. 3.1). Interestingly, alignment of the genomes with BRIG revealed that this strain possesses unique regions, most of these linked with antibiotic resistance (Fig. 3.1 and 3.2). Indeed, strain PR1 is the only strain within this group of *A. denitrificans* to harbor genes conferring resistance against aminoglycosides (*aadA2*) sulfonamides (*sul1*, *sul2*) and tetracyclines (*tetC*).

The genome of strain PR1 will provide further insights into SMX metabolism in this microbial consortium and into the species versatility and potential for xenobiotic degradation.

3.3 Nucleotide accession number

This complete genome sequence has been deposited in GenBank under the accession no. CP020917. The version described in this paper is the first version.

Chapter 4

Biodegradation of sulfamethoxazole by a bacterial consortium of *Achromobacter denitrificans* PR1 and *Leucobacter* sp. GP

Published as:

A.C. Reis, M. Čvančarová, Y. Liu, M. Lenz, T. Hettich, B.A. Kolvenbach, P.F.-X. Corvini, Olga C. Nunes (2018). "Biodegradation of sulfamethoxazole by a bacterial consortium of *Achromobacter denitrificans* PR1 and *Leucobacter* sp. GP". *Applied Microbiology and Biotechnology*. 102(23): 10299–10314. doi:10.1007/s00253-018-9411-9.

4.1 Abstract

In the last decade, biological degradation and mineralization of antibiotics have been increasingly reported feats of environmental bacteria. The most extensively described example is that of sulfonamides that can be degraded by several members of *Actinobacteria* and *Proteobacteria*. Previously we reported sulfamethoxazole (SMX) degradation and partial mineralization by *Achromobacter denitrificans* strain PR1, isolated from activated sludge. However, further studies revealed an apparent instability of this metabolic trait in this strain. Here we investigated this instability, and describe the finding of a low-abundance and slow-growing actinobacterium, thriving only in co-culture with strain PR1. This organism, named GP, shared highest 16S rRNA gene sequence similarity (94.6-96.9 %) with the type strains of validly described species of the genus *Leucobacter*. This microbial consortium was found to harbor a homolog to the sulfonamide monooxygenase gene (*sadA*) also found in other sulfonamide-degrading bacteria. This gene is overexpressed in the presence of the antibiotic and evidence suggest that it codes for a group D flavin monooxygenase responsible the *ipso*-hydroxylation of SMX. Additional side reactions were also detected comprising an NIH shift and a Baeyer-Villiger rearrangement, which indicate an inefficient biological transformation of these antibiotics in the environment. This work contributes to further our knowledge in the degradation of this ubiquitous micropollutant by environmental bacteria.

4.2 Introduction

Sulfonamides are synthetic drugs which were introduced into clinical use in the late 1930s, thus becoming the first selective antibiotics with application in human medicine. They are structural analogs of *p*-aminobenzoic acid, and, therefore, compete for the active sites of dihydropteroate synthetase (DHPS), blocking the synthesis of folic acid in bacteria (Masters et al. 2003). However, soon after their introduction, the intensive use of these drugs led to the onset and spread of antibiotic resistance, which occurs mainly through horizontal gene transference (HGT) of insensitive forms of DHPS encoded by the genes

sul1, *sul2*, *sul3*, and, the more recently described, *sul4* (Sköld 2000; Perreten and Boerlin 2003; Razavi et al. 2017). For this reason, the use of sulfonamides for human therapy has been steadily declining over the past decades. Currently, it is mostly limited to the combination of sulfamethoxazole (SMX) and trimethoprim, also known as co-trimoxazole (Sköld 2000; Masters et al. 2003; Van Boeckel et al. 2014). In contrast, due to their inexpensive synthesis, sulfonamides, such as sulfadiazine, sulfamethazine, and sulfathiazole are still heavily used in animal farming and agriculture, being amongst the most used antibiotic classes of this sector (Sarmah et al. 2006; EMA 2016). Consequently, these antibiotics and their corresponding resistance genes, are still considered ubiquitous micropollutants (Sköld 2000; García-Galán et al. 2008). They contaminate soils, river sediments and water bodies through the discharge of polluted effluents from Wastewater Treatments Plants (WWTP) or the use of contaminated manure or sewage sludge for soil fertilization (García-Galán et al. 2008; Heuer et al. 2011; Rizzo et al. 2013). SMX, for instance, has been consistently detected in WWTP effluents, surface water, and groundwater in concentrations ranging from 20 ng/l to 1 µg/l (Kümmerer 2009). While sulfamethazine and SMX have been reported in manure and soils up to 1 mg/kg (Martinez 2009; Chen et al. 2012), concentrations that were found to be mutagenic to microorganisms and bio-accumulate in some plant species, altering their growth (Martinez 2009). Moreover, these residual amounts of antibiotics are known to contribute to the propagation of resistance genes and the development of new mechanisms of resistance (Teuber 2001; Rizzo et al. 2013; Manaia et al. 2016).

The intensive use of these “miracle drugs” not only increased resistance but, as we saw in the last decade, contributed to the development of antibiotic degradation mechanisms in many heterotrophic bacteria (Larcher and Yargeau 2012; Ricken et al. 2017). This metabolic ability was initially reported in complex microbial communities, such as activated sludge (Ingerslev and Halling-Sørensen 2000; Pérez et al. 2005; Müller et al. 2013), and, more recently, in several phylogenetically distant bacteria. The biodegradation

of these drugs was shown to occur via three main routes: (i) co-metabolic transformation resulting in the introduction or cleavage of specific functional groups (e.g., hydroxylation, acetylation, hydrolysis, deamination, etc.); (ii) cleavage of the sulfonamide bond (S-N) followed by partial or near-complete mineralization of the benzene ring with or without accumulation of the heterocyclic moiety as a dead-end product; and, (iii) cleavage of the N-O bond present in sulfonamides with an isoxazole group (Larcher and Yargeau 2012; Deng et al. 2018; Reis et al. 2018b; Chen and Xie 2018).

The ability to mineralize sulfonamides has been increasingly reported in members of the phyla *Proteobacteria* and *Actinobacteria*, namely from the genera *Pseudomonas* (Jiang et al. 2014), *Ochrobactrum* (Mulla et al. 2018) and *Acinetobacter* (Wang et al. 2018), and *Microbacterium* (Bouju et al. 2012; Topp et al. 2012; Islas-Espinoza et al. 2012; Tappe et al. 2013), *Gordonia* (Mulla et al. 2018) and *Arthrobacter* (Deng et al. 2016), respectively. Most of these *Actinobacteria* members appear to harbor a conserved sulfonamide degradation cluster consisting of two monooxygenases (SadA and SadB) and one FMN-reductase (SadC), which allows them to hydroxylate the sulfonamide molecule at the sulfonyl group (Ricken et al. 2017). In *Microbacterium* sp. BR1 (Ricken et al. 2013; Ricken et al. 2015a; Ricken et al. 2017), in which this cluster has been described originally, the *ipso*-hydroxylation of SMX was shown to result in the accumulation of 3-amino-5-methylisoxazole (3A5MI) as a stable dead-end product and transient formation and subsequent mineralization of 4-aminophenol.

Although many studies have focused on the elucidation of the metabolic pathway for sulfonamide degradation in microbial isolates, few have attempted to characterize the metabolic associations and pathways in sulfonamide-degrading communities. Syntrophic relationships and interdependence has been previously described in xenobiotic-degrading communities for the degradation of simple and complex molecules. For instance, Sørensen et al. (2002) have previously described an herbicide-degrading *Sphingomonas* sp. strain that required amino acids produced by other soil bacteria to grow. Furthermore, the

degradation of several xenobiotic compounds has been shown to result from the metabolic cooperation within bacterial communities. This is the case of the degradation of 4-chlorosalicylate, an intermediate in the aerobic degradation of important organic pollutants (Pelz et al. 1999); the herbicide molinate (Barreiros et al. 2003); terephthalate, an essential raw material used in the production of many plastics (Lykidis et al. 2011; Wu et al. 2013).

In a previous study (Reis et al. 2014) we had concluded *Achromobacter denitrificans* strain PR1, a *Proteobacteria*, to be an effective sulfonamide degrader, assuming the same underlying mechanism of sulfonamide degradation as the one present in *Actinobacteria*. However, subsequent studies have shown this apparent metabolic trait to be unstable and subject to spontaneous loss upon repeated sub-culturing of this strain. In this study, we aimed at elucidating the reason for the presumed metabolic instability of strain PR1 and describe the finding of a lowly-abundant and slow-growing *Actinobacteria* present in apparently axenic cultures of strain PR1. We show that SMX degradation is carried out by the two-member consortium, with the *Actinobacteria* being the probable responsible for the initial cleavage of the molecule.

4.3 Materials and methods

4.3.1.1 Chemicals

¹⁴C-SMX ([¹⁴C]aniline [uniform]) with a specific radioactivity of 0.33 MBq mmol⁻¹ was from Hartmann Analytic, and ¹⁸O₂ (isotopic purity, 97%) was from Sigma (Switzerland). TiO₂ for photocatalytic experiments was AEROXIDE®P25 from Evonik (Germany). Unless stated otherwise, all other reagents were of analytical grade and purchased from Sigma.

4.3.2 Microorganisms and culture conditions

Achromobacter denitrificans strain PR1 (Reis et al. 2014) was recovered from a glycerol stock at -80°C and plated on 25% BHI with 0.6 mM SMX and 15 g/l agar (BHI-SMX-agar).

After 10 days of incubation in the dark at 30°C, two distinct morphotypes were visible (beige colonies and beige and yellow mixed colonies, respectively). In an attempt to purify all the organisms, each morphotype was successively streaked/spread onto several media and conditions (supplementary materials, section 1). This procedure only resulted in the purification of strain PR1, which formed beige colonies, and for which the complete genome was obtained (Reis et al. 2017). The colonies with the two morphotypes were successively re-purified onto BHI-SMX-agar 4 times and incubated for 3/4 weeks to ensure that only the organisms responsible for these morphotypes were present. This microbial consortium can be requested from the corresponding author. Axenic strain PR1 was deposited in public Bacterial Collection from the Belgian Co-ordinated Collections of Micro-organisms (BCCM/LMG) under the accession number LMG 30905.

Axenic cultures of strain PR1 and the microbial consortium were grown in either BHI-SMX-agar or in mineral medium B (Barreiros et al. 2003) with 0.6 mM SMX, 4 mM ammonium sulfate, 0.2 g/l yeast extract, and 7 mM succinate (MMSY-SMX). All incubations were carried out in the dark at 30°C, and liquid cultures were also continuously stirred at 120 rpm.

For resting cells assays, cells were prepared by growing either axenic cultures of *A. denitrificans* PR1 or the microbial consortium in MMSY-SMX for 36-38 h. At this point, near-complete degradation of SMX (> 80%) by the consortium was confirmed spectrophotometrically by modified Griess nitrate reaction (Ricken et al. 2015a), and the biomass was collected by centrifugation (9,000 *xg*) and washed twice with sterile phosphate buffer (PB, 50 mM, pH 7.2). Unless stated otherwise, all resting cells assays were performed at room temperature (RT, 22 °C) in 50 mM PB and under constant stirring at 120 rpm.

4.3.3 Attempts at purification of *Leucobacter* sp. strain GP

Several attempts were made to obtain pure cultures of strain GP on agar plates. Firstly, the consortium was diluted and spread on agar media with different compositions: BHI (100 or 25 % w/v), Tryptic Soy Agar (TSA), PY-BHI (Morais et al. 2006), Lysogeny Broth (LA) and R2A. For all media, the incubation was carried out in parallel under different atmospheric conditions: aerobic, microaerophilic (CampyGen sachets, Oxoid) or anaerobic (AnaeroGen sachets, Oxoid) atmosphere, respectively. The latter two conditions were incubated in a 2.5 l anaerobic jar.

Secondly, some modifications were introduced to 25% BHI plates: (i) Gellan Gum (Gelzan CM, Sigma), a less toxic solidifying agent, was used instead of agar as described elsewhere (Janssen et al. 2002); (ii) plates were supplemented with 1% (v/v) of crude cell extracts of *A. denitrificans* PR1; (iii) with 20% (v/v) of strain PR1 MMSY/BHI culture-spent supernatant or (iv) a mixture of supernatant and crude cell extracts. Crude cell extracts and culture-spent supernatant were obtained by growing axenic cultures of *A. denitrificans* PR1 for 15 h in MMSY or BHI with 0.6 mM SMX. The culture was centrifuged, and the supernatant filter-sterilized (cellulose acetate, 0.22 µm, Merck) and the remaining pellet was re-suspended in 10 ml of 50 mM PB (5.3 g_{cell dry weight}/L), passed 3 times through a high-pressure homogenizer (Emulsiflex-B15, Avestin) at 2,000 bar. The cell slurry was further centrifuged and sterilized by filtration (cellulose acetate, 0.22 µm, Merck) before incorporation into the agar plates.

According to the results obtained by Bhuiyan et al. (2015) some *Leucobacter* spp. may require exogenous porphyrins to grow on agar plates. Therefore, 25% BHI medium was also modified with 0.1-1 mg/l of heme (Sigma) or other commercially available porphyrin precursors, namely: coproporphyrin III (Lucerna-CHEM), coproporphyrin III tetramethylester (Sigma) and coproporphyrin I dihydrochloride (Sigma).

Considering that strain GP may require constant interaction with viable cells of strain PR1, a community culture approach was also tested (Pham and Kim 2012). Briefly, low binding membranes (0.22 µm, cellulose acetate, VWR) were used to filter several dilutions (10^{-3} to 10^{-8}) of the microbial consortium and placed on top of a strain PR1 lawn. After 3 weeks incubation, strain GP yellow colonies of strain GP grown on the upper surface of the membrane were re-suspended in sterile PB, diluted, and filtered and the membrane again placed on top of strain PR1 lawn.

4.3.4 16S rRNA metagenomics sequencing

The composition of the microbial consortium was assessed by 16S rRNA metagenomics using the MinION platform (Oxford Nanopore). The consortium was incubated in MMSY-SMX for 15 h. Genomic DNA was extracted from 10^9 cells with the GenElute Bacterial Genomic DNA Kit (Sigma) following the protocol for Gram-positive cells with a few modifications: digestion with 20 mg/ml lysozyme was increased to 2 h, the biomass was disrupted with 100 mg of glass beads (≤ 106 µm, acid-washed, Sigma) in a FastPrep-24 device (MP Biomedicals) at speed 6.0 for 60 s prior to incubation for 30 min in lysis solution. The complete 16S rRNA gene was amplified with universal primers 27f and 1391r (Lane 1991; Turner et al. 1999) with an annealing temperature of 47 °C and 30 cycles using HotStartTaq DNA Polymerase (Qiagen). DNA library was prepared from 700 ng using the Ligation Sequencing Kit 1D (SQK-LSK108, Oxford Nanopore) and omitting the End-repair and A-tailing steps since *Taq* DNA polymerase produces 3' adenine overhangs. The adapter-ligated library was further prepared with the Library Loading Bead Kit (EXP-LLB001, Oxford Nanopore) and loaded into a SpotON Flow Cell (R9.4, FLO-MIN106, Oxford Nanopore). 1D sequencing on the MinION was performed for a total of 24 h with live base calling.

1D raw reads were adapter trimmed with Porechop v0.2.3 (<https://github.com/rrwick/Porechop/>) and filtered with BBduk v38.05 from the BBDMap

package (<https://sourceforge.net/projects/bbmap/>) to the mean quality and size of $\geq Q9$ and 1200-1450 bp, respectively. Error correction was further performed with Canu v1.7 (Koren et al. 2017) with default settings. Error corrected reads were further clustered into operational taxonomic units (OTU) using CROP at 97% sequence identity threshold (Hao et al. 2011) with the following arguments: -s -r 0 -z 100. Clusters with only one sequence (singletons) were removed, and chimeric sequences were identified with DECIPHER (Wright et al. 2012). The taxonomic classification was performed with the RDP classifier trained with a 16S rRNA training set (TS16) at 80% confidence threshold (Wang et al. 2007) and further confirmed by aligning the sequences with Mega BLAST against the NCBI 16S ribosomal RNA database on the 10th of June of 2018 (Johnson et al. 2008). The long-reads of the 16S rRNA gene-based metagenome have been deposited into the NCBI Sequence Read Archive under the accession number SRP150172.

4.3.5 16S rRNA gene clone libraries

Biomass of the mixed colonies grown in MMSY-SMX for 15 h was used for genomic DNA extraction as described above. To decrease the relative abundance of strain PR1 some samples were pre-treated by alkaline lysis before extraction (Birnboim and Doly 1979). Briefly, the biomass was resuspended in TE solution (25 mM Tris-HCl at pH 8, 50 mM glucose, 10 mM EDTA) to a final cell density of 3×10^9 cells/ml, 2 volumes of alkaline lysis solution (0.2 M NaOH and 1% SDS) were added and the mixture was incubated for 10 min at RT to selectively lyse and digest the cells of the Gram-negative strain PR1 (Birnboim and Doly 1979; Wada et al. 2012). After incubation, the remaining cells were collected by centrifugation and washed four times with sterile PB.

The 16S rRNA gene was amplified from genomic DNA samples, pre-treated or not with alkaline lysis, as described above. PCR products were ligated into the p-GEM T-easy plasmid vector (Promega), with 3:1 ratio (insert:vector) and according to the manufacturer's instructions. Cloned fragments were further sequenced by Sanger

(Eurofins), and the 16S rRNA gene sequences were compared with others available in the EzBioCloud database (Yoon et al. 2017). To further classify strain GP, the 16S rRNA gene sequence of all validly described *Leucobacter* sp. type strains were retrieved from the LPSN database (Parte 2014), and inter-species pairwise similarity was determined based on the global alignment in the EzBioCloud webserver (Yoon et al. 2017). The near-complete 16S rRNA gene sequence (1382 bp) of strain GP was obtained and deposited in GenBank under the accession number MH094815.

4.3.6 Role of strain GP in the SMX-degrading consortium

Axenic cultures of strain PR1 and cultures of the consortium were grown in MMSY-SMX for 40 h, diluted in sterile PB and spread on BHI-SMX-agar. After 2 weeks of incubation, 10 beige colonies of *A. denitrificans* PR1 and 10 mixed colonies were picked and inoculated in 2 ml of MMSY-SMX. These cultures were incubated in parallel to an abiotic control and screened for their ability to degrade SMX.

To determine if the presence of signaling molecules produced by mixed colonies could induce SMX degradation in axenic cultures of strain PR1, culture-spent supernatant (40 h in MMSY-SMX) of the consortium was filtered-sterilized with a low binding membrane (cellulose acetate, 0.22 μ m, Merck) and replenished with nutrients of the MMSY medium. This modified medium (MMSY-CS) was reinoculated with axenic cultures of *A. denitrificans* PR1 and 0.6 mM SMX and was incubated for a total of 2 weeks and screened for SMX degradation activity.

4.3.7 Detection and sequencing of genes related to the metabolism of sulfonamides

The presence of the recently reported sulfonamide degradation gene cluster (Ricken et al. 2017) was investigated in the microbial consortium. Sulfonamide monooxygenase (encoded by *sadA*, GenBank accession number CDJ99310.1), 4-aminophenol

monooxygenase (encoded by *sadB*, GenBank accession number CDJ99309.1) and FMN reductase (encoded by *sadC*, GenBank accession number CDJ99306.1) were first aligned with BLASTp against the complete genome of *A. denitrificans* PR1 (Reis et al. 2017), with an e-value and amino acid identity cutoffs set to 1e-3 and 60%, respectively. Moreover, primers targeting *sadA*, *sadB*, and *sadC* were designed and their specificity tested with Primer-BLAST (Ye et al. 2012). End-point PCR was performed according to the conditions in Table 4.1 with total DNA extracted from overnight grown cultures of the microbial consortium in MMSY, with or without alkaline lysis pre-treatment. The DNA of axenic cultures of strain PR1 grown in the same medium was used as a negative control, and the DNA of *Microbacterium* sp. strain BR1 (Ricken et al. 2017) was used as a positive control. PCR products were sequenced by Sanger (Eurofins) and deposited in Genbank under the accession number MH253763. The *sadA* gene was then locally aligned to its homolog in *Microbacterium* sp. strain BR1 using the local similarity program in the ExPASy server (Gasteiger et al. 2003). The amino acid sequence of the *sadA* gene was further aligned to the conserved domain database in NCBI (Marchler-Bauer et al. 2017) and its structure was inferred by homology modeling using the SWISS-MODEL server (Waterhouse et al. 2018).

Table 4.1 - Primers and conditions used for the end-point amplification of *sadA*, *sadB* and *sadC* genes.

Target gene	Forward primer (5'-3')	Reverse primer (5'-3')	Amplicon size (bp)	Annealing
<i>sadA</i>	ATGAAATCTGTCCAATCGGCT	CTAAATCGGCATGACGAACTC	1242	62 °C
<i>sadB</i>	ATGGTCGATAGCAGTTTGCC	CTCAAACCAGAGGCGTAACG	1200	
<i>sadC</i>	ACATCGGTTCGCTCTATGAG	CGGTTGCTGATCGAGTTCTG	342	

4.3.8 Quantitative PCR (qPCR) and reverse transcriptase qPCR (RT-qPCR)

The absolute quantification of each of the strains during growth and degradation of SMX in MMSY was performed by qPCR with species-specific primers targeting the 16S rRNA gene. Total DNA was extracted from 1 to 4 ml culture as described in section 2.3 without the alkaline lysis pre-treatment. Standard curves were prepared using serial ten-fold dilutions

of the near-complete fragment of the 16S rRNA gene of each strain. DNA quantification and purity were measured with QuantiFluor (Promega) and spectrophotometrically with Nanodrop Spectrophotometer ND-1000 (NanoDrop Technologies). Gene copy numbers were calculated by the standard curve method as described elsewhere (Brankatschk et al. 2012).

For gene expression studies (RT-qPCR) the microbial consortium was grown in MMSY medium with (0.6 or 2 mM) or without SMX, and the cells were collected after 21 h of incubation and preserved in RNA later (Sigma) at -80 °C until RNA extraction. Total RNA was extracted using RNeasy Plus extraction Kit (Qiagen) with prior mechanical lysis of the cells by sonication (three-times: 0.5 s/s cycle and 100% amplitude for 30 s and 30 s rest on ice, Labsonic M, Sartorius). TURBO DNase Kit (Invitrogen) was used to eliminate genomic DNA from RNA preparations with and cDNA synthesis was performed with M-MLV reverse transcriptase, random primers, dNTPs and RNasin ribonuclease Inhibitor from Promega according to the manufacturer's instructions. Species-specific primers targeting the 16S rRNA gene of PR1 or GP and *sadA* were designed with Primer-BLAST (Table 4.2) (Ye et al. 2012).

To determine changes in gene expression during degradation of SMX by the microbial consortium the relative quantification, also known as the $\Delta\Delta\text{Ct}$ method was used (Livak and Schmittgen 2001). The fold-change in gene expression is calculated using the following formula:

$$\text{RQ} = \frac{E_{\text{target}}^{(\text{Ct}_{\text{test}} - \text{Ct}_{\text{control}})}}{E_{\text{reference}}^{(\text{Ct}_{\text{test}} - \text{Ct}_{\text{control}})}}$$

RQ represents relative quantification, E_{target} PCR efficiency of the target gene and $E_{\text{reference}}$ of the reference gene, Ct_{test} threshold cycle in the test condition and $\text{Ct}_{\text{control}}$ in the control

condition. Incubations without SMX were used as the control condition and the 16S rRNA gene of strain GP as the reference gene.

Table 4.2 – Primers, PCR conditions, and efficiency for the qPCR experiments.

Strains	Target	Primers (5' – 3')	Primers (µM)	Amplicon size (bp)	Efficiency	Annealing
PR1	16S rRNA	FW: AGTAGCGGGGATAACTACG RV: CTCAAACCAGCTACGGATCG	0.2	162	1.93	60 °C
GP	16S rRNA	FW: GGGACTCTTTGGACTGGT RV: AACATAGGACGAGGGTTGCC	0.2	105	1.87	60 °C
	<i>sadA</i>	FW: GAACGCGATTGACTGCAC RV: GATGGACTCTCGACATAGCAC	0.9	153	1.93	63 °C

qPCR reactions were performed with DNA (diluted 100 fold) or undiluted cDNA in a CFX Connect Real-Time system (Bio-rad). The reactions were carried out in 20 µl with 1x GoTaq qPCR Master Mix (Promega), and formamide (1.25%, v/v) was added as a PCR enhancer in *sadA* gene amplification reactions. Gene amplification was performed using the following program: 95 °C for 5 min and 40 cycles of 95 °C for 30 s followed by an annealing/extension step for 1 min. Additionally melting curves with increments of 0.5 °C from 65 to 95 °C were determined to assess the homogeneity of the amplification. The results were analyzed using the CFX software (Bio-rad). Specificity of the primers was confirmed visually by analyzing PCR fragments on an agarose gel and by including negative controls (DNA standard of the other strain) in each qPCR run.

4.3.9 Identification of metabolites

Elucidation of the metabolic pathway

The kinetics of SMX degradation and formation of 3A5MI, sulfite, sulfate, and ammonium ions were measured in resting cells experiments with the bacterial consortium and 0.3 mM SMX. 10-times diluted buffer (PB 5 mM, pH 7.2) was used for these assays to reduce the interference of phosphate ions and increase the sensitivity of the subsequent Ion

Chromatography (IC) analysis. Samples for IC and HPLC-UV/Vis were centrifuged and the supernatant filtered through 0.45 μm PVDF membrane filters prior to analysis. Sulfite and sulfate concentrations were quantified on an Ion Chromatography System (IS, Dionex 2100, Thermo Fisher Scientific) equipped with a self-regenerating suppressor (ASRS 300). An IonPac AS15 (2 x 250 mm, Dionex) analytical column and AG15 guard column (2 x 50 mm) were used for analysis at 35°C with a flow rate of 0.5 ml/min. The gradient of KOH (EGC III KOH eluent generator, Thermo Fisher Scientific) was as follows: for 4.5 min rising on a gradient from 40 to 45 mM, from 4.5-7 min further increase to 65 mM, from 7-9.9 min isocratic mode, 9.9-11 min decrease to 40 mM. Ammonium ion concentrations were quantified spectrophotometrically by a modified Berthelot reaction (Krom 1980; Laskov et al. 2007) using a microplate reader (Biotek) and recording absorbance at 660 nm.

Comparative kinetics experiments with SMX, 4-aminophenol (4AP) and sulfanilic acid (SA) were assessed by resting cells. To further assess if 4AP, hydroquinone (HQ) and 1,2,4-trihydroxybenzene (THB) are part of the metabolic pathway for SMX degradation, resting cells assays were also performed with 0.2 mM ^{14}C -SMX (0.36 $\mu\text{Ci/ml}$). Additionally, some replicates were spiked with an excess (1 mM) of non-labeled 4AP, HQ or THB, respectively, with the purpose of saturating the reaction and further allow the accumulation of ^{14}C -labeled metabolites. For assays spiked with an excess of 4AP, samples were collected over time to determine retro-inhibition of SMX degradation. Furthermore, due to the polarity of this metabolite and its tendency to auto-oxidate, part of each sample was acetylated with acetic anhydride (final concentration of 10% v/v, reaction time was 1 h at room temperature followed by immediate neutralization with 10M NaOH 10 M). The *N*-acetylation reaction of 4AP forms paracetamol that can be easily separated by reverse phase HPLC-UV/Vis. Assays carried out with an excess of HQ and THB were end-point assays aiming at determining the accumulation of their ^{14}C -labeled counterparts in the supernatant. All experiments were carried out in triplicate with the microbial consortium, axenic cultures of strain PR1 and abiotic controls.

SMX, 3A5MI, SA, *N*-acetyl-4AP (paracetamol), HQ and THB were quantified in a High-Performance Liquid Chromatography system (HPLC 1200 series, Agilent Technologies) using a Zorbax SB-C18 column (3.5 μm , 3.0 \times 150 mm) equipped with a Zorbax SB-C18 guard column (5 μm , 4.6 \times 12.5 mm) (Agilent Technologies). The compounds were separated using a gradient of formic acid (0.1% v/v) and methanol as previously described by Ricken et al. (2013). For detection and quantification of ^{14}C -SMX, ^{14}C -4AP, ^{14}C -HQ, and ^{14}C -THB, the HPLC-UV system was further coupled to a radioisotope detector 'Ramona Star' (Raytest) and the radioactivity of ^{14}C -labelled compounds were detected by adding Ultima-Flo M (PerkinElmer) cocktail at a flow 2.0 ml/min. Since ^{14}C -SMX is labeled exclusively in the aniline moiety, the molarity of subsequent aromatic metabolites could be estimated using a standard curve with ^{14}C -SMX standards, by plotting molarity against radioactivity. The final molarity of 4AP was finally corrected taking into account the reaction yield of the acetylation process.

Rates of degradation and metabolite formation were calculated assuming zero-order kinetics by linear regression of the data, and statistical analysis was performed as described elsewhere (Reis et al. 2014).

Ion Trap LC-MS analysis and $^{18}\text{O}_2$ experiments

Metabolic by-products were further investigated in cell-free supernatant of the microbial consortium, incubated in 50 mM PB with 0.2 mM SMX and an initial OD_{600} of 10 (5.3 $\text{g}_{\text{cell dry weight}}/\text{L}$). Samples were collected periodically and analyzed by LC-MS. Replicate assays were performed on subsequent days with freshly prepared whole cells of the consortium and in parallel to an abiotic (PB with SMX) and a biotic control (cell suspension in PB without SMX), to exclude abiotically formed products and unrelated metabolites produced by these strains.

To assess the incorporation of atmospheric oxygen in the metabolites, resting cell tests were performed in the same conditions in PTFE-sealed flasks, flushed with nitrogen and,

posteriorly filled with 20% (v/v) $^{18}\text{O}_2$. These assays were performed in triplicate and in parallel to controls in a $^{16}\text{O}_2$ atmosphere and to biotic and abiotic controls. The cell-free supernatant of the samples and controls were also analyzed by Ion Trap LC-MS.

The Ion Trap LC-MS system (1200 Series, Agilent) consisted of an Ion Trap Mass spectrometer (6320, Agilent) with electrospray ionization (ESI, Agilent). The samples were separated on a Nucleodur C18 Pyramid column (3.0 μm , 4.0 x 150 mm, Macherey-Nagel) equipped with a Nucleodur C18 Pyramid guard column (3.0 μm , 4.0 x 8.0 mm). The separation of parent compounds and metabolites was performed at room temperature, and the injection volume was 20 μl . Separation was achieved with a gradient program using (A) ammonium formate 20 mM and (B) acetonitrile at 0.6 ml/min. The elution program started with 0% (B) for 6 min, followed by a linear increase to 25% (B) in 20 min, and a further increase to 50% (B) in 3 min. The system was equilibrated to the initial conditions for 20 min before starting the next analysis. ESI operated in positive and negative modes, and ions were scanned within a mass range from 50 to 500 amu with a maximum accumulation time of 200 ms. Product ion scan mode (MS2) was used to elucidate the structure of target compounds. MS2 spectra were obtained at fragmentation amplitude 0.7. Capillary spray voltage was set to -1500 V, the nebulizer to 50 psi, drying gas to 10 l/min and drying temperature to 350°C.

Solid-Phase Extraction (SPE) and UHPLC-QTOF-MS

Metabolite M5 was further characterized by UHPLC-QTOF-MS to obtain its exact mass and product ion spectra. Briefly, M5 was produced by incubating the microbial consortium with 0.3 mM 4AP in resting cells conditions (see section 4.2). At least 10 ml of culture supernatant was injected and separated by Ion Trap LC-MS (see section 4.7.2) to collect the fraction eluting between 3.5 and 4.0 min. This fraction was then acidified to pH 1 with 1 M HCl and loaded into an SPE cartridge (Oasis HLB, 1 cm^3 x 30 mg, Waters) previously conditioned with 5 ml of methanol and 5 ml of acidified water (pH 1). After loading the

sample, the cartridge was dried under vacuum for 30 min, and the compound was eluted in 8 ml of acetonitrile. The eluted fraction was concentrated to 0.5 ml under gentle N₂ stream at 50°C.

Molecular structure characterization of the compound was performed on a UHPLC 1290 system combined with a 6540 quadrupole time-of-flight (Q-TOF) mass spectrometer (Agilent Technologies). The UHPLC system was used for flow injection analysis with a system flow of 0.4 ml/min. The mobile phase consisted of water/acetonitrile (40/60, v/v) plus five mM ammonium formate and the injection volume was set to 5 µl. The ESI source was operated in negative mode with the following settings: nebulizer pressure 35 psig, nozzle voltage 0 V, sheath gas flow 11 L/min, sheath gas temperature 375 °C, drying gas flow 8 l/min, drying gas temperature 250 °C, capillary voltage 3000 V, and fragmentor voltage 175 V. The mass spectrometer ran in targeted MS/MS mode with a predefined precursor list. The MS scan spectra were acquired over a range of 100 – 1000 m/z. For MS/MS experiment, the range was set from 50 – 150 m/z with an acquisition rate for both modes of one spectrum per second. The collision-induced dissociation experiment was performed with 22 V collision energy and nitrogen as collision gas with a collision cell flow of 18 psig. The instrument state mass range was set to 1700 m/z in high-resolution mode with 4 GHz analog-to-digital converter rate at a resolving power of 19 000 (measured at m/z 127). For internal reference mass correction two reference ions with exact masses of m/z 119.0363 and 966.0007 were used. The system control and data analysis were performed with MassHunter software (Agilent Technologies). The software feature “Generate Formulas” was used to calculate the sum formula of the metabolite based on mass accuracy, isotope abundance, and isotope spacing. Further, MetFrag Web tool was used with a database search against ChemSpider and with spectral similarity enabled (Wolf et al. 2010). The possible list of candidates was compared to the expected metabolite.

Synthesis of *ortho/meta* hydroxylated SMX by TiO₂/UV

Mono-hydroxylated SMX at *ortho/meta* position was synthesized by TiO₂/UV photocatalytic treatment of 0.3 mM SMX solutions prepared in ultrapure water. Briefly, 30 ml of SMX solution was treated with 1 g/l of TiO₂ (Degussa P25, Evonik) in a solar radiation simulator (ATLAS, model SUNTEST XLS+) at full irradiation (300-800 nm) for 40 min. The reaction was stopped by filtering the solution through a 0.45 µm syringe filter (PTFE).

4.4 Results

4.4.1 Identification of *Leucobacter* sp. strain GP

Previously, we have concluded *Achromobacter denitrificans* strain PR1 to be a sulfonamide degrader from activated sludge, able to cleave SMX and mineralize its aniline moiety, releasing 3A5MI as a stable dead-end product (Reis et al. 2014). However, subsequent studies revealed that this metabolic trait was highly unstable and irreversibly lost by the majority of strain PR1 colonies upon repeated sub-culturing on BHI-SMX-agar (data not shown). After prolonged incubation of initial stocks of this strain, small yellow colonies started to emerge on the surface of the beige colonies characteristic of this *Proteobacteria* (Fig. 4.1). The yellow colonies became visible only after more than 10 days of incubation, whereas the beige colonies formed after only 2 days. The Gram staining of these mixed colonies revealed the presence of both Gram-negative and Gram-positive organisms.

The beige colonies, composed only by Gram-negative staining cells, were readily purified from the original glycerol stocks of strain PR1 and grew in axenic conditions. The analysis of the complete genome of this organism confirmed its identification as *A. denitrificans* strain PR1 (Reis et al. 2017). In contrast, the Gram-positive yellow colonies grew only on the surface or in close contact with strain PR1 colonies. Moreover, the inclusion of diffusible and intracellular metabolites of strain PR1 in the culture media was insufficient to allow the purification of the Gram-positive morphotype.

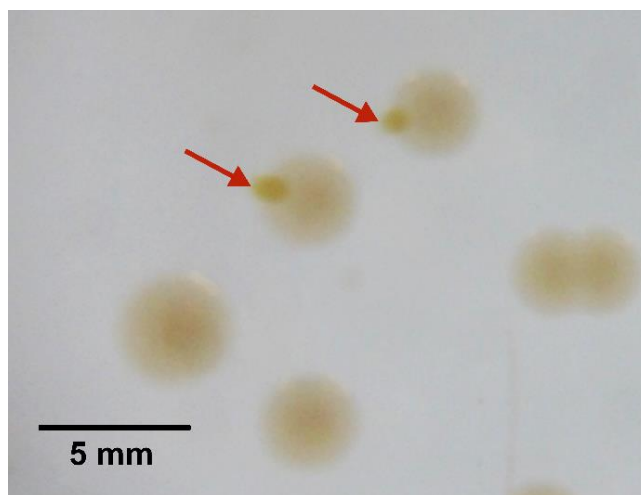


Figure 4.1 – Picture of the microbial consortium taken under a magnifying glass with bright field after 11 days of incubation on BHI-SMX-agar, yellow colonies of the *Leucobacter* sp. GP (red arrows) growing attached to the beige colonies of *A. denitrificans* PR1.

As none of the tested conditions allowed the isolation of the yellow colonies (see supplementary material, section 1) in axenic cultures, to identify this new strain the 16S rRNA gene-based metagenome of the mixed colonies was obtained. Sequencing resulted in 283,310 1D raw reads that were filtered, and error corrected resulting in 10,927 high-quality sequences. These sequences were clustered into 9 representative non-chimeric OTU. Classification with the RDP Classifier and NCBI Blast against 16S rRNA gene database revealed that 6 of these OTU were affiliated either to *Leucobacter* or *Achromobacter* genera (Table 4.3), with the latter being the most abundant genus in the consortium (98.9%). The 3 remaining OTU, which constituted approximately 0.15 % of the total reads, could not be affiliated to any validly described genus but could be affiliated to the family level, sharing highest sequence similarity with organisms from *Microbacteriaceae* and *Alcaligenaceae* families (87-91%). The alignment of these clusters to the 16S rRNA gene sequence of representative strains revealed a high percentage of indels (4-5% gaps in the alignment), a standard error associated with 1D sequencing on the MinION platform.

Table 4.3 – Taxonomic classification of representative OTU in the SMX-degrading consortium obtained with RDP classifier and confirmed with NCBI BLAST against the 16S ribosomal RNA database, and pairwise sequence similarity of each representative OTU with the 16S rRNA gene sequence of strains PR1 or GP retrieved from the clone libraries.

Taxonomic classification	Number OTU	Relative abundance (%)	Identity of clusters to strains PR1/GP
<i>Bacteria; Proteobacteria; Betaproteobacteria; Burkholderiales; Alcaligenaceae; Achromobacter</i>	3	98.88	97-99% to PR1
<i>Bacteria; Actinobacteria; Actinobacteria; Actinomycetales; Microbacteriaceae; Leucobacter</i>	3	0.97	98-99% to GP
<i>Bacteria; Proteobacteria; Betaproteobacteria; Burkholderiales; Alcaligenaceae</i>	2	0.10	87-91% to PR1
<i>Bacteria; Actinobacteria; Actinobacteria; Actinomycetales; Microbacteriaceae</i>	1	0.05	91% to GP

To further confirm the identity of the consortium members, 16S rRNA clone libraries were performed. The DNA of the consortium was extracted with and without the alkaline lysis pre-treatment, to reduce the highly dominant and easily lysed *Proteobacteria*. The libraries originated from non-treated biomass yielded sequences 100% identical to strain PR1 (data not shown), while the sequences found in clones derived from pre-treated biomass, which could not be identified as strain PR1, were identical among themselves and shared highest sequence similarity with members of the *Leucobacter* genus. This new microorganism, designated strain GP, showed low pairwise similarities with other type strains of validly described species of *Leucobacter* (94.6 - 96.9 %) suggesting that it probably represents a new species within this genus (supplementary material, Table 4.4).

Table 4.4 - Inter-species pairwise similarity between *Leucobacter* sp. GP and other, validly described, *Leucobacter* spp. was determined based on the global alignment in the EzBioCloud webserver (Yoon et al. 2017).

	1	2	3	4	5	6	7	8	9	10	11	12	13	14	15	16	17	18	19	20	21	22	23	
	<i>L. aerolatus</i> Sj 10 ^T	<i>L. albus</i> IAM 14851 ^T	<i>L. alluvii</i> RB10 ^T	<i>L. aridicollis</i> L-9 ^T	<i>L. celer</i> subsp. <i>astrifaciens</i> CBX151 ^T	<i>L. celer</i> subsp. <i>celer</i> NAL101 ^T	<i>L. chironomi</i> MM2LB ^T	<i>L. chromiireducens</i> subsp. <i>chromiireducens</i> L-1 ^T	<i>L. chromiireducens</i> subsp. <i>solipictus</i> TAN 31504 ^T	<i>L. chromiireducens</i> subsp. <i>chromiireducens</i> JG 31 ^T	<i>L. denitrificans</i> M1T8B10 ^T	<i>L. exalbidus</i> K-540B ^T	<i>L. holotrichiae</i> T14 ^T	<i>L. iarius</i> 40 ^T	<i>L. komagatae</i> JCM 9414 ^T	<i>L. luti</i> Rf6 ^T	<i>L. musarum</i> subsp. <i>musarum</i> CBX152 ^T	<i>L. musarum</i> subsp. <i>japonicus</i> CBX130 ^T	<i>L. populi</i> 06C10-3-11 ^T	<i>L. salsicius</i> M1-8 ^T	<i>L. tardus</i> DSM 19811 ^T	<i>L. zeae</i> CC-MF41 ^T	<i>Leucobacter</i> sp. GP	
1		96.5%	95.8%	96.3%	97.3%	96.3%	96.1%	97.9%	97.8%	96.3%	97.0%	98.7%	95.5%	96.6%	97.0%	97.4%	98.1%	98.1%	95.2%	99.4%	97.4%	96.5%	95.6%	
2			96.8%	98.8%	97.2%	96.1%	96.4%	96.6%	96.3%	97.1%	97.5%	96.7%	94.9%	97.6%	98.6%	97.6%	98.1%	98.1%	95.2%	96.8%	95.7%	96.6%	95.5%	
3				97.8%	98.2%	97.0%	96.6%	97.2%	96.8%	99.4%	97.6%	95.7%	95.5%	98.1%	97.1%	97.0%	98.2%	98.2%	95.3%	96.1%	96.3%	96.2%	95.6%	
4					98.0%	96.9%	97.1%	97.6%	97.4%	98.1%	98.5%	96.5%	95.2%	98.7%	98.5%	97.6%	97.9%	97.9%	95.9%	96.5%	96.2%	96.5%	96.1%	
5						100.0%	99.3%	99.1%	98.9%	98.7%	98.3%	97.9%	97.0%	98.2%	97.7%	98.0%	97.8%	97.8%	97.3%	97.8%	97.8%	97.5%	96.7%	
6							97.7%	97.3%	97.2%	97.6%	97.2%	96.5%	96.3%	97.2%	96.5%	96.9%	97.8%	97.8%	96.2%	96.5%	96.7%	96.7%	95.7%	
7								96.8%	96.4%	97.4%	97.1%	96.7%	95.4%	96.8%	96.9%	96.5%	97.8%	97.8%	96.0%	96.5%	96.7%	97.1%	95.3%	
8									99.5%	97.4%	97.7%	98.1%	94.9%	97.8%	97.0%	98.3%	98.2%	98.2%	95.2%	98.1%	97.1%	96.3%	96.0%	
9										97.1%	97.6%	97.7%	94.6%	97.6%	96.8%	98.3%	98.1%	98.1%	95.2%	97.9%	97.0%	96.3%	96.0%	
10											97.9%	96.3%	95.9%	98.4%	97.5%	97.4%	98.4%	98.4%	95.9%	96.4%	96.4%	96.4%	96.2%	
11												96.7%	96.1%	98.2%	97.8%	97.6%	98.0%	98.0%	96.1%	97.1%	96.2%	96.8%	96.2%	
12													94.5%	96.3%	97.1%	97.5%	98.2%	98.2%	94.6%	99.1%	97.7%	96.5%	95.3%	
13														95.4%	94.9%	95.3%	95.8%	95.8%	95.9%	94.8%	94.9%	95.7%	94.6%	
14															97.6%	97.9%	98.1%	98.1%	95.2%	96.5%	96.5%	96.5%	96.0%	
15																98.1%	98.8%	98.8%	95.5%	97.2%	96.2%	96.9%	96.2%	
16																	99.5%	99.5%	95.4%	97.6%	96.8%	96.9%	96.7%	
17																		100.0%	95.9%	98.2%	97.8%	97.9%	96.9%	
18																			95.9%	98.2%	97.8%	97.9%	96.9%	
19																				95.0%	94.9%	95.7%	95.1%	
20																					97.4%	96.6%	95.7%	
21																						97.2%	95.5%	
22																							96.0%	
23																								

Although we cannot completely rule out the presence of other very low-abundant bacteria, the analysis of the 16S rRNA gene of the consortium through clone libraries and long read sequencing suggests that *A. denitrificans* strain PR1 and *Leucobacter* sp. strain GP compose the consortium.

4.4.2 Role of the members of the sulfamethoxazole-degrading consortium

As observed before (Reis et al. 2014), SMX degradation in mineral medium with succinate and yeast extract (MMSY) resulted in the accumulation of 3A5MI (Fig. 4.2a). qPCR targeting the 16S rRNA gene of *A. denitrificans* strain PR1 or *Leucobacter* sp. strain GP revealed that these organisms grow simultaneously in this medium (Fig. 4.2a), maintaining a stable relative proportion throughout all phases of growth. Strain PR1 remained highly dominant in comparison to *Leucobacter* sp. strain GP (> 96%). Despite its low abundance, strain GP appears to carry out a crucial role in SMX degradation, as the degradation of this sulfonamide was only achieved by cultures obtained from mixed colonies (Fig. 4.1, red arrows) but never in *A. denitrificans* PR1 axenic cultures.

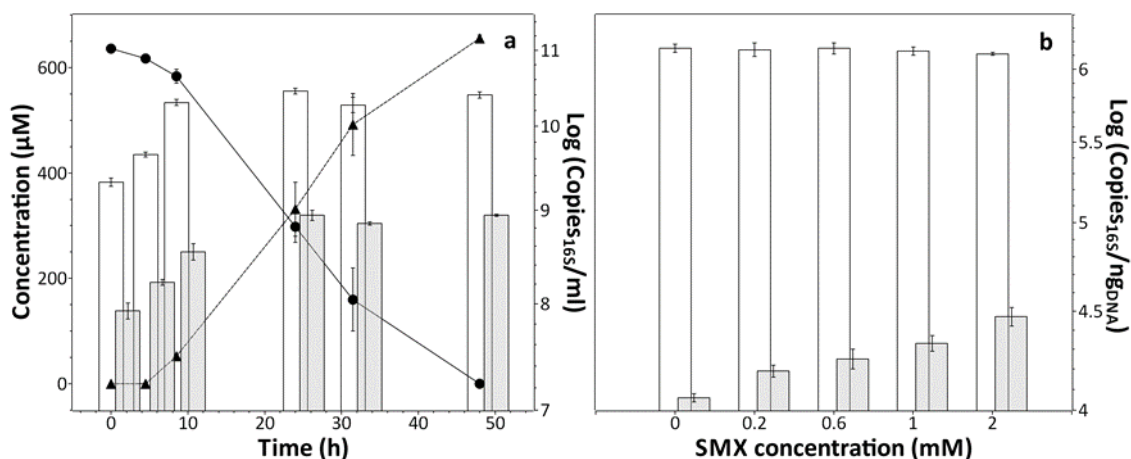


Figure 4.2 - Abundance of strains PR1 and GP, respectively, during growth of the consortium in MMSY medium with SMX as a supplementary carbon source. a: growth of both strains over time in MMSY with 0.6 mM of SMX. b: abundance of both strains after 7 h incubation with different SMX concentrations. SMX concentration (●); 3A5MI concentration (▲); 16S rRNA gene copy number of strain PR1 per ml of culture or ng of DNA (white bars); 16S rRNA gene copy number of strain GP per ml of culture or ng of DNA (grey bars). Values are the mean of triplicates and error bars represent standard deviation.

This result also held true for PR1 cultures supplemented with culture spent-supernatant of the consortium (MMSY-CS), pointing out that strain GP or other low abundance strain of this consortium do not produce signaling molecules able to induce degradation of SMX in strain PR1. Additionally, increasing SMX concentrations in MMSY medium significantly favored the growth of strain GP ($p < 0.05$, Fig. 4.2b), while the abundance of strain PR1 was not affected. In this way, these results point out that SMX degradation occurs only in the consortium and that strain PR1 may not participate in the initial cleavage of the molecule.

4.4.3 Elucidation of the metabolic pathway

In diluted phosphate buffer (PB, 5 mM) the degradation of SMX by the consortium ($1.62 \pm 0.05 \mu\text{mol/g}_{\text{cell dry weight min}}$) was accompanied by the concomitant release of near equimolar amounts of 3A5MI ($1.52 \pm 0.03 \mu\text{mol/g}_{\text{cell dry weight min}}$), sulfur-species (sulfite + sulfate, $1.21 \pm 0.05 \mu\text{mol/g}_{\text{cell dry weight min}}$) and ammonium ions ($1.22 \pm 0.11 \mu\text{mol/g}_{\text{cell dry weight min}}$) (Fig. 4.3).

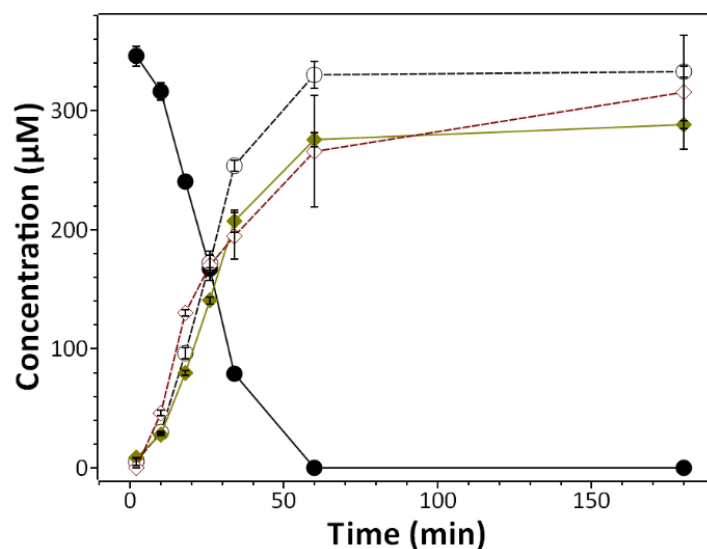


Figure 4.3 - Degradation of SMX (●) by the microbial consortium in resting cells assays with the concomitant release of the dead-end product 3A5MI (▲), sulfur species (sulfite and sulfate, dark yellow ◆) and ammonium ions (dark red ◇). Values are the mean of triplicates and error bars represent standard deviation.

Mass spectrometry analysis (Ion Trap LC-MS) of cell-free supernatants from resting cells assays was further used to identify additional metabolites. Total ion chromatograms of resting cells incubated with SMX were compared to the respective abiotic (buffer with SMX without cells) and biotic controls (buffer with cells without SMX). Respective standard and fragmentation confirmed the identity of the previously reported 3A5MI in the positive mode (Fig. 4.4). In addition to 3A5MI, six other potential metabolites were detected (M1-M6, Table 4.5, Fig. 4.5). To elucidate the structure of these metabolites, protonated molecular ions $[M+H]^+$ or deprotonated molecular ions $[M-H]^-$ were further fragmented in subsequent analyses, product ion mass spectra were recorded, and the structure of each metabolite was proposed (Table 4.5).

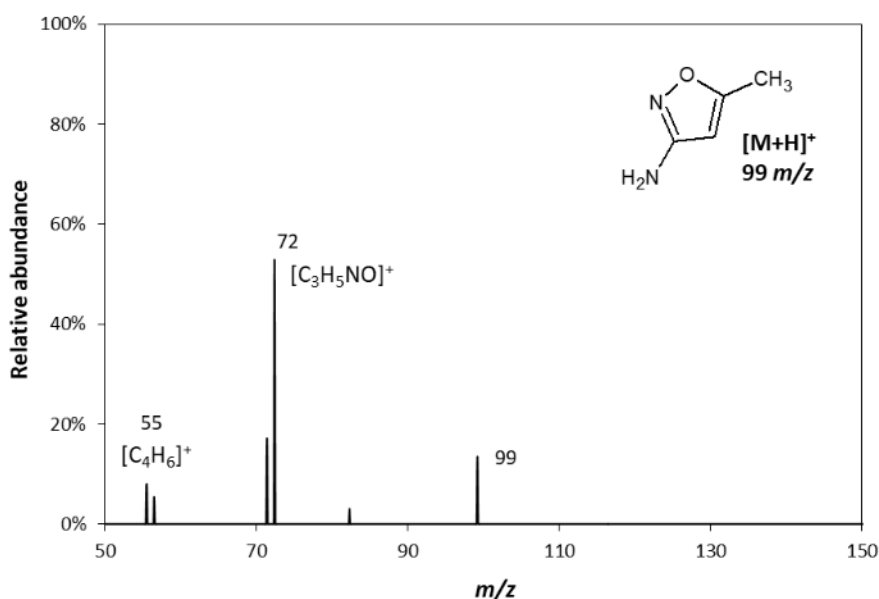


Figure 4.4 – Mass spectrum of 3-amino-5-methylisoxazole product ion recorded in positive mode with possible sum formula annotation.

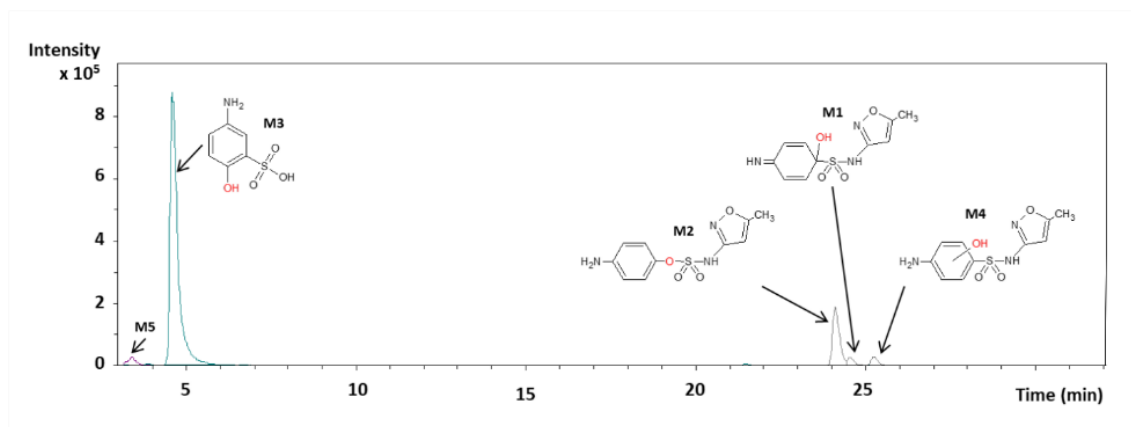


Figure 4.5 - Extracted ion chromatogram (EIC) of some of the main metabolites identified throughout this study recorded in negative mode (-ESI).

SMX, with protonated molecular ion $[M+H]^+$ at m/z 254, was fragmented in positive mode creating specific product ions at m/z 92, 99, 108, 156, 160 and 188, respectively (Fig. 4.6). The difference between SMX and metabolites M1, M2, and M3 (Fig. 4.7, 4.8 and 4.9, respectively) with protonated molecular ions $[M+H]^+$ at m/z 270 is 16 Da, indicating the incorporation of an oxygen atom into each of these molecules. The incorporation of molecular oxygen was further confirmed by analyses of cells incubated with SMX in ¹⁸O₂-atmosphere, which resulted in a mass shift of 2 Da (m/z 272) of the molecular ions $[M+H]^+$ for all three metabolites. This shift indicates that all three metabolites were formed by the incorporation of one atmospheric oxygen atom (Table 4.5). Since SMX degradation results in the accumulation of equimolar amounts of the methylisoxazole moiety of the antibiotic, the hydroxylation in M1, M2, and M3 most probably occurs in the aniline moiety (Reis et al. 2014). For metabolites M2 and M3, the hydroxylation of the benzene ring was further confirmed by a typical fragment of the MS2 spectra at m/z 99 corresponding to the methylisoxazole ion (Fig. 4.8 and 4.9).

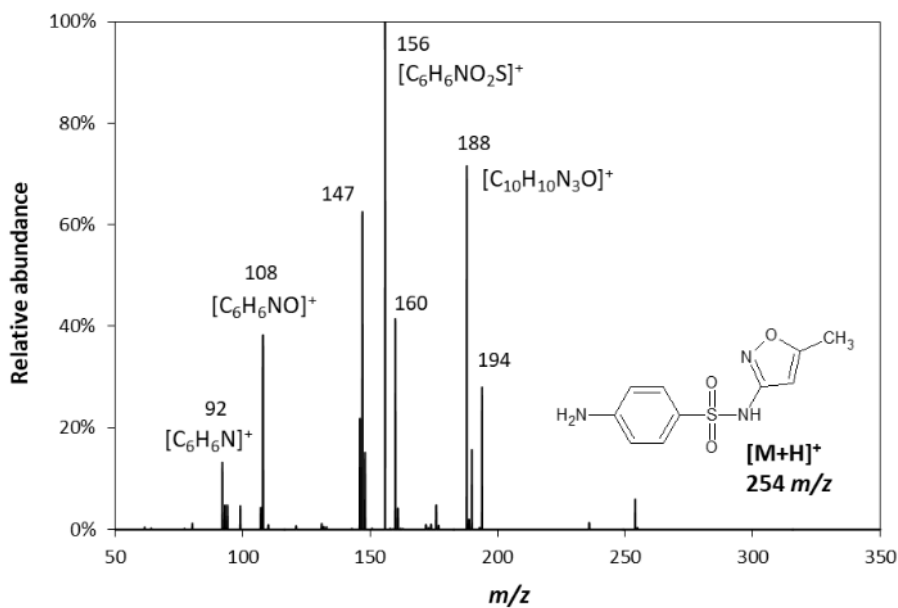


Figure 4.6 – Mass spectrum of sulfamethoxazole product ion recorded in positive mode with possible sum formula annotation.

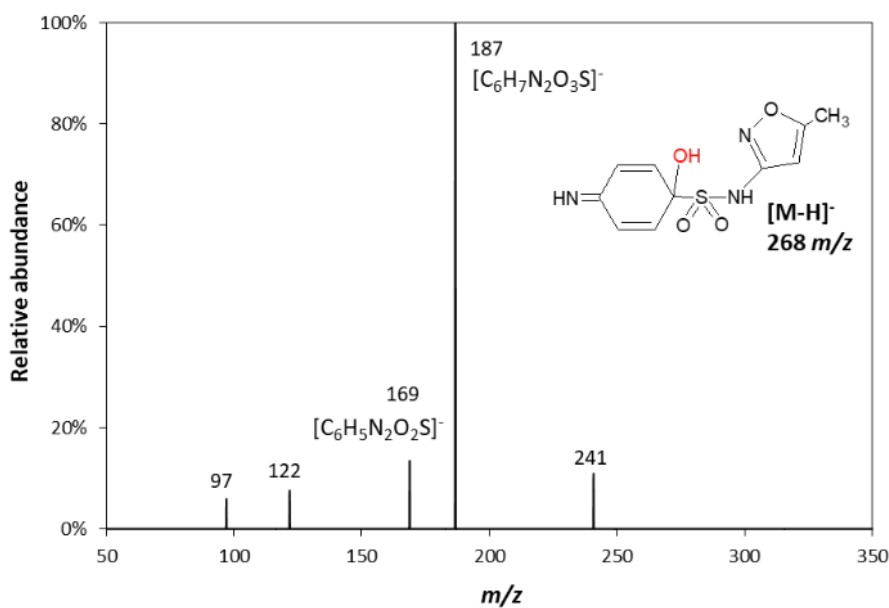


Figure 4.7 – Mass spectrum of M1 product ion recorded in negative mode with possible sum formula annotation.

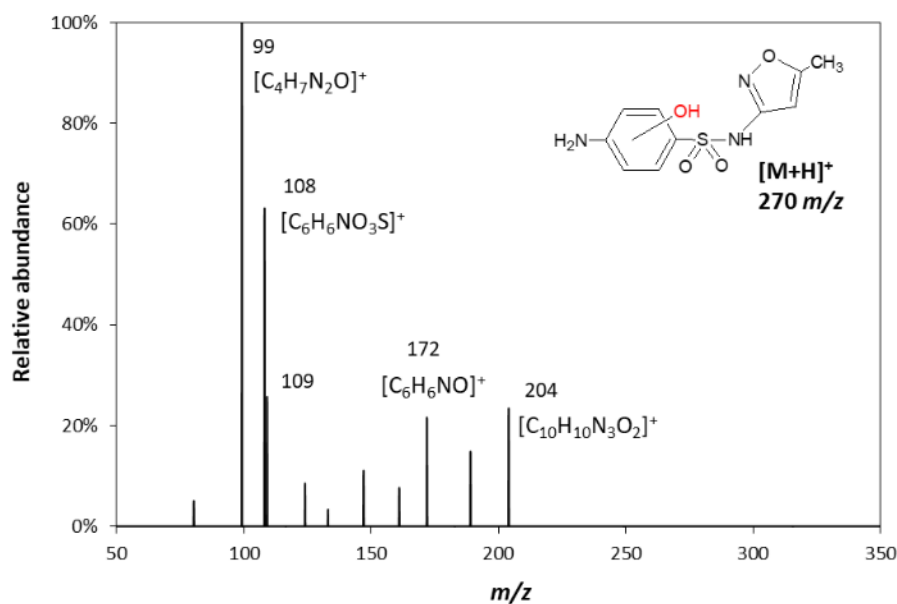


Figure 4.8 – Mass spectrum of M2 product ion recorded in positive mode with possible sum formula annotation.

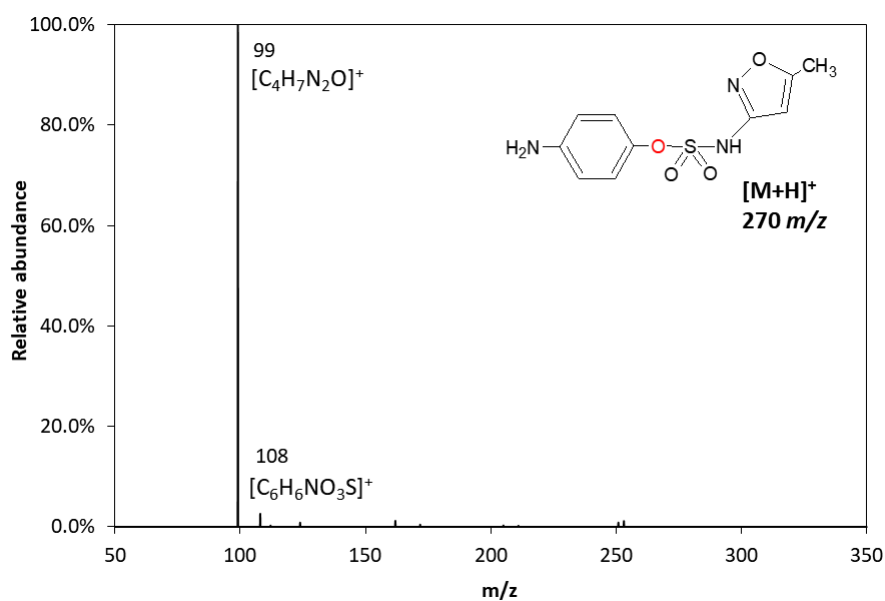


Figure 4.9 – Mass spectrum of M3 product ion recorded in positive mode with possible sum formula annotation.

Hydroxylamine-SMX, with [M+H]⁺ at *m/z* 270, was observed before as a metabolite of SMX transformation in bacteria (Zhang et al. 2016) and humans (Cribb and Spielberg 1992). Nevertheless, it was ruled out as a potential metabolite since its retention time, and fragmentation pattern did not fit with any of the mono hydroxylated SMX metabolites

(data not shown). Due to the inexistence of other commercially available standards, hydroxylation of the SMX molecule was achieved by TiO₂/UV treatment as this method has been previously shown to produce several hydroxy derivatives of the antibiotic (García-Galán et al. 2008) (supplementary material, section 3). Indeed, one of the most significant photo-transformation products was found to have a molecular ion [M+H]⁺ at *m/z* 270. This transformation, representing a hydroxylation in the benzene ring in *ortho* or *meta* position, has been previously reported as one of the most prominent products of TiO₂/UV treatment by several authors (Hu et al. 2007; Su et al. 2016). These authors found it to have the same molecular ion and an MS₂ spectrum identical to that of metabolite M2 (Fig. 4.8). Although the specific position of this substitution in M2 was not experimentally confirmed, it can be predicted based on the resonance and the steric hindrance of the molecule. The primary amine substituent donates a pair of electrons to the benzene ring while the sulfonyl group delocalizes the electron density of the ring towards itself. This conformation leaves the carbons near the amine group more exposed and vulnerable to electrophilic attacks. In this way, providing that the reaction does not result from intracellular radical attacks, the substitution is more likely to occur in the carbon adjacent to the amine group, forming a *meta*-hydroxylated SMX.

Since no additional standards were available, structures of metabolites M1 and M3 were further deduced from their MS₂ spectra. Hydroxylation at the *ipso* position was considered as a candidate mechanism. *Ips*o-hydroxylation is a common mechanism which has been reported for many different enzyme families (Ricken et al. 2015b). Previously it has been found to be the mechanism of SMX degradation by *Microbacterium* sp. BR1 (Ricken et al. 2013) and three other isolates from *Actinobacteria* and *Alphaproteobacteria* (Mulla et al. 2018). Based on the analysis of the MS₂ spectra, metabolite M1 can be assumed to result from an *ipso*-hydroxylation of SMX.

Table 4.5 – Metabolites detected by LC-MS (Ion Trap) during SMX degradation in resting cells of the microbial consortium. Oxygen atoms in red represent probable atoms originated from the incorporation of atmospheric O₂. N.d., not determined; (*) metabolite confirmed with a standard; (!) M1 could not be fragmented in positive mode (ESI+), therefore, the product ions correspond to fragmentation in negative mode (ESI-).

Compound	Precursor ion m/z ¹⁶ O ₂	¹⁸ O ₂	Molecular formula	t_R (min)	Main product ions ESI+/ESI-	Proposed structure
Sulfamethoxazole	[M+H] ⁺ 254	254	C ₁₀ H ₁₁ N ₃ O ₃ S	26.9	ESI+: 194, 188, 160, <u>156</u> , 147, 108, 92	
3-amino-5-methylisoxazole*	[M+H] ⁺ 99	99	C ₄ H ₆ N ₂ O	12.5	ESI+: <u>72</u> , 71, 55	
M1 [!]	[M+H] ⁺ 270	272	C ₁₀ H ₁₁ N ₃ O ₄ S	24.1	ESI-: 241, <u>187</u> , 169, 122, 97	
M2*	[M+H] ⁺ 270	272	C ₁₀ H ₁₁ N ₃ O ₄ S	24.7	ESI+: 204, 172, 109, 108, <u>99</u>	
M3	[M+H] ⁺ 270	272	C ₁₀ H ₁₁ N ₃ O ₄ S	23.7	ESI+: <u>99</u> , 108	
5-amino-2-hydroxybenzenesulfonic acid (M4)*	[M+H] ⁺ 190	192	C ₆ H ₇ NO ₄ S	5.0	ESI+: <u>172</u> , 124	
(Z)-6-Oxohex-3-enoic acid (M5)	[M-H] ⁻ 127	131	C ₆ H ₈ O ₃	3.7	N.d.	
M6	[M-H] ⁻ 138	144	N.d.	4.5	N.d.	N.d.

This metabolite was fragmented in negative mode, and significant product ions at m/z 187 and 169 were created (Fig. 4.7). Nevertheless, unlike the other mono-hydroxylated metabolites (M2 and M3), M1, when fragmented in positive mode, did yield detectable fragments. This observation partially confirms the *ipso*-hydroxylation hypothesis, because to create the typical positive ion at m/z 99, a neutral loss of 171 Da ($C_6H_5NO_3S$) is necessary. *Ips*o hydroxylation prevents the formation of a double bond between the sulfur and benzene ring, and thus the neutral loss of 171 Da is not released, and the typical positive ion at m/z 99 is not created.

Metabolite M3 was probably formed from a spontaneous rearrangement of metabolite M1 by migration of sulfo-methylisoxazole moiety to the oxygen atom of the hydroxyl group, a mechanism known as Baeyer-Villiger rearrangement (Baeyer and Villiger 1899). This mechanism is an expected consequence of *ipso*-hydroxylation of aromatic molecules as nonylphenols and bisphenol A (Gabriel et al. 2005; Kolvenbach et al. 2007). This molecular rearrangement enables the neutral loss of 171 Da; thus an intensive signal at m/z 99 was detected after fragmentation in positive mode (Fig. 4.9).

Metabolite M4 was identified as 5-amino-2-hydroxybenzenesulfonic acid by comparison to an authentic standard (Table 4.5). The retention time of both the metabolite M4 and the standard was 5.0 min, and both compounds shared similar product ion spectra (Fig. 4.10). Assays in $^{18}O_2$ -atmosphere increased the mass of the molecular ion by 2 Da, pointing out the incorporation of a single oxygen atom. 4-amino-2-hydroxybenzenesulfonic acid and 4-amino-3-hydroxybenzenesulfonic acid were also analyzed as standards. While they had the same molecular ion as metabolite M4 ($[M+H]^+$ m/z 190), their retention times (3.5 and 3.1 min, respectively) and product ion spectra (data not shown) were considerably different from those of M4.

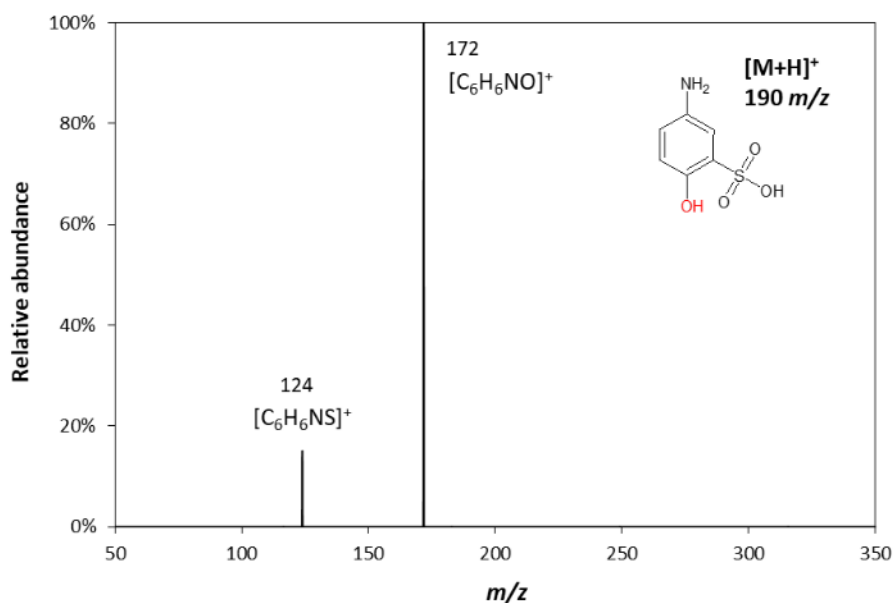


Figure 4.10 – Mass spectrum of 5-amino-2-hydroxybenzenesulfonic acid (M4) product ion recorded in positive mode with possible sum formula annotation.

Further downstream metabolites were detected, namely metabolites M5 and M6, featuring molecular ions $[M-H]^-$ of m/z 127 and 138, respectively. In assays with $^{18}O_2$ -atmosphere, these metabolites showed a shift of 4 Da and 6 Da, indicating the incorporation of two and three atmospheric oxygen atoms, respectively. However, only M5 accumulated in amounts sufficient for further characterization. This metabolite was partially purified by preparative HPLC, concentrated by solid-phase extraction (SPE) and analyzed by UHPLC-QTOF-MS to determine its exact mass and possible molecular formula. Product ion spectra (Fig. 4.11) resulted in no significant hits against the MassBank database (Wolf et al. 2010) and, therefore, the molecular formula and structure were proposed by *in silico* fragmentation using MetFrag (Wolf et al. 2010). Due to the high polarity, low concentration and unavailability of commercial standards for this compound the molecular formula could not be further confirmed.

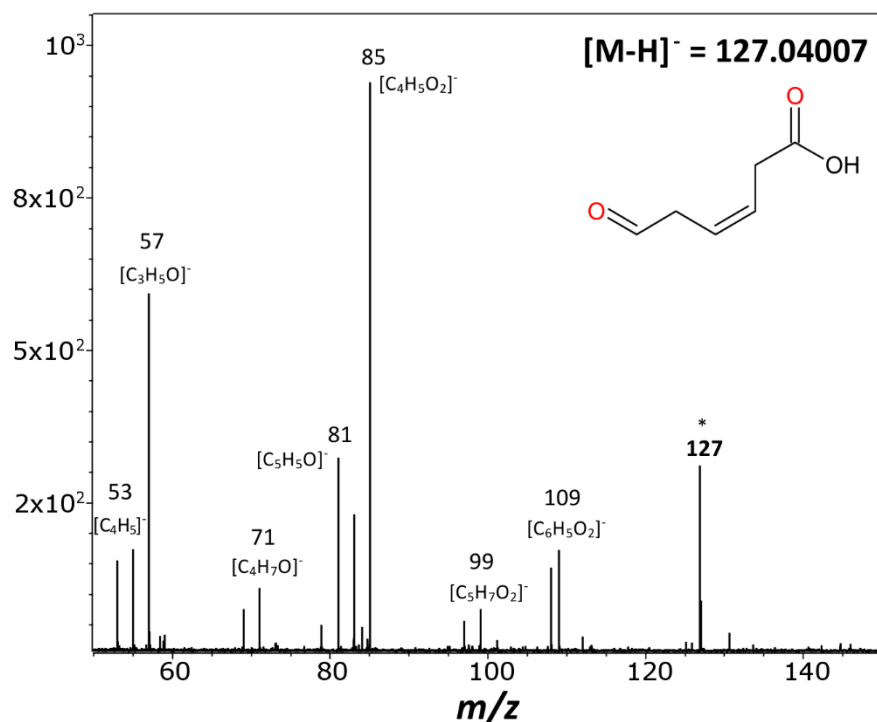


Figure 4.11 – Product ion (QTOF) mass spectra of $[M - H]^-$ of metabolite M5 and possible molecular structure.

Neither 4-aminophenol (AP) nor sulfanilic acid (SA), two commonly reported metabolites resulting from bacterial degradation of sulfonamide antibiotics (Ricken et al. 2013; Yang et al. 2015; Mulla et al. 2018), could be identified as metabolites produced by the consortium. However, since SMX appears to be hydroxylated at *ipso* position, 4AP was the most plausible candidate. Indeed, comparative resting cells assays showed that the microbial consortium could readily degrade 4AP, but not SA, while axenic suspensions of strain PR1 degraded neither of these substrates (Fig. 4.12).

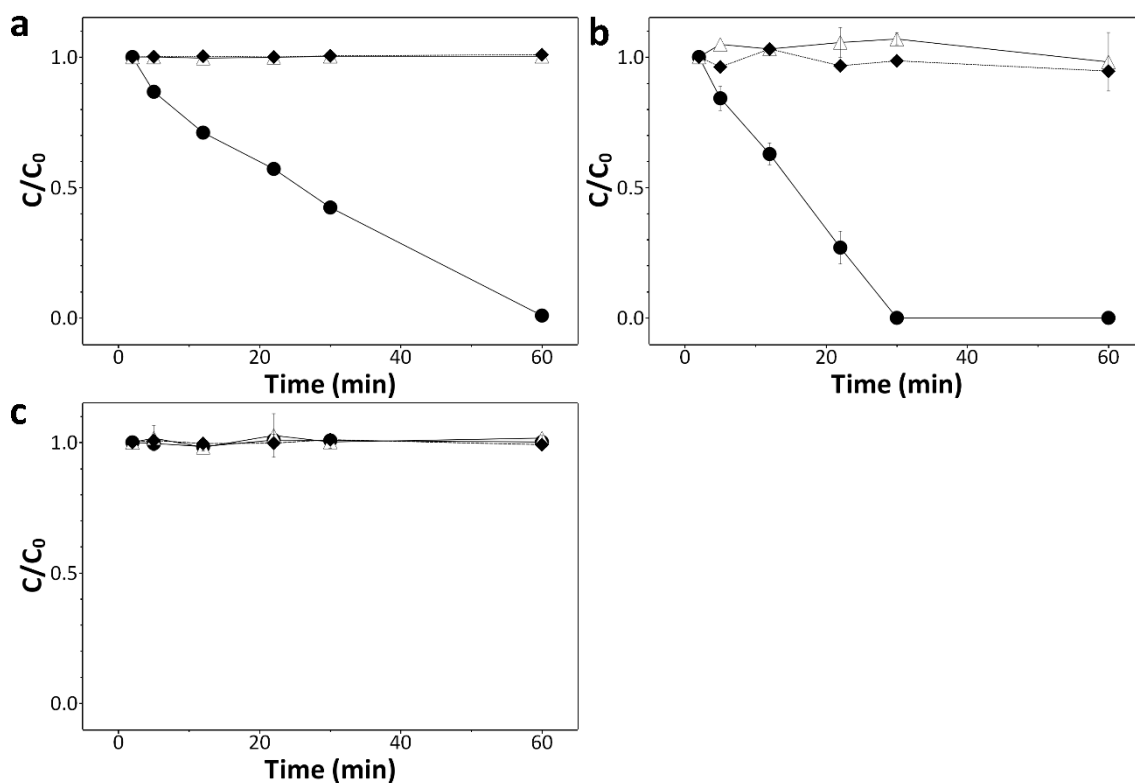


Figure 4.12 - Degradation of sulfamethoxazole (a), 4-aminophenol (b) and sulfanilic acid (c) in resting cells conditions by the microbial consortium (●), axenic cultures of strain PR1 (△) and in abiotic controls (◆). Values are the mean of triplicates and error bars represent standard deviation.

Moreover, the degradation of 4AP by the consortium occurred at a significantly higher rate ($p < 0.05$) when compared to SMX controls (1.81 ± 0.15 and $1.04 \pm 0.03 \mu\text{mol}/\text{g}_{\text{cell dry weight}} \text{ min}$, respectively), further indicating that this metabolite is immediately transformed without accumulation. To support these observations, we investigated the degradation of ^{14}C -SMX in the presence and absence of 1 mM non-labeled 4AP. The excess of non-labeled 4AP led to an accumulation of ^{14}C -4AP (Fig. 4.13). Furthermore, it resulted in a decreased rate of SMX degradation when compared to non-spiked controls (0.65 ± 0.01 and $1.35 \pm 0.02 \mu\text{mol}/\text{g}_{\text{cell dry weight}} \text{ min}$, for spiked and non-spiked assays respectively). This apparent retro-inhibition effect further indicates that SMX degradation occurs via 4AP.

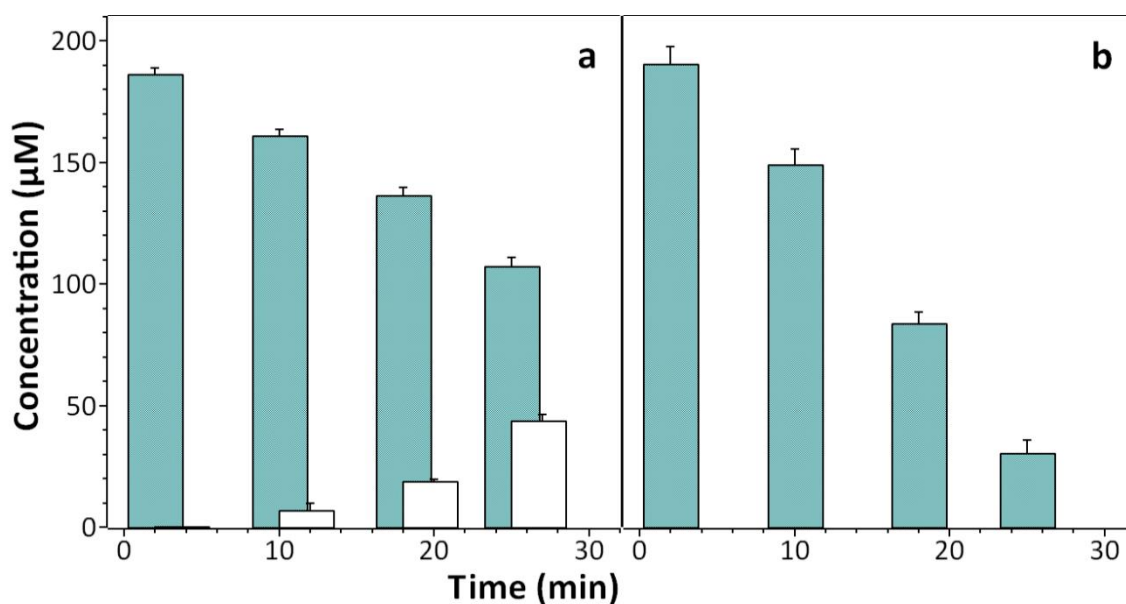


Figure 4.13 - Release of ¹⁴C-4AP (white bars) during the consumption of ¹⁴C-SMX (green bars) in assays spiked (a) and non-spiked (b) with 1 mM of non-labelled 4AP. Values are the mean of triplicates and error bars represent standard deviation.

In *Microbacterium* sp. BR1, the further transformation of 4AP is suspected to occur through its successive oxidation into hydroquinone (HQ), and 1,2,4-trihydroxybenzene (THB) (Ricken et al. 2015a; Ricken et al. 2017). However, none of these two metabolites were detected in the supernatant during SMX, ¹⁴C-SMX or 4AP degradation, even when assays with the ¹⁴C labeled substrate were saturated with an excess of unlabeled HQ or THB. Only the metabolites M5 and M6 were further detected in the supernatant of the consortium during 4AP degradation.

4.4.4 Detection and expression of the *sadABC* cluster in the consortium

As pointed out before, *Microbacterium* sp. BR1 (Ricken et al. 2017) harbors a gene cluster consisting of two genes coding for monooxygenases (*sadA* and *sadB*, respectively) and one coding for a flavin reductase (*sadC*). The two monooxygenases, *sadA*, and *sadB*, code for the enzymes that carry out the specific hydroxylation of SMX and 4AP, respectively, whereas the product of *sadC* provides reduced FMN required by both monooxygenases.

However, it was shown that the lack of *sadC* could be compensated by a related FMN reductase present in *Escherichia coli* (Ricken et al. 2017).

The possible involvement of these enzymes and their coding genes in SMX oxidation by the consortium was assessed first *in silico* and, posteriorly, through end-point PCR and RT-qPCR. BLASTp searches showed that no homologs to *sadA*, *sadB* or *sadC* genes were found in the genome of strain PR1 (Reis et al. 2017). Using PCR primers targeting the three genes, DNA samples of the consortium, pre-treated or not with alkaline lysis, only yielded PCR products with primers apt to amplify *sadA* (Fig. 4.14) while the DNA from axenic PR1 cultures did not yield any product for any of these genes. The near-complete gene sequence of the *sadA* homolog found in the consortium shares 93.8 % amino acid identity to the *sadA* gene carried by *Microbacterium* sp. BR1. Furthermore, gene expressions studies by RT-qPCR revealed that *sadA* transcripts were significantly enriched in the consortium during degradation of SMX in MMSY with a higher amount of transcripts detected in incubations with 2 mM in comparison to those with 0.6 mM SMX ($p < 0.05$), 2.9 ± 0.2 versus 2.3 ± 0.1 fold increase, respectively.

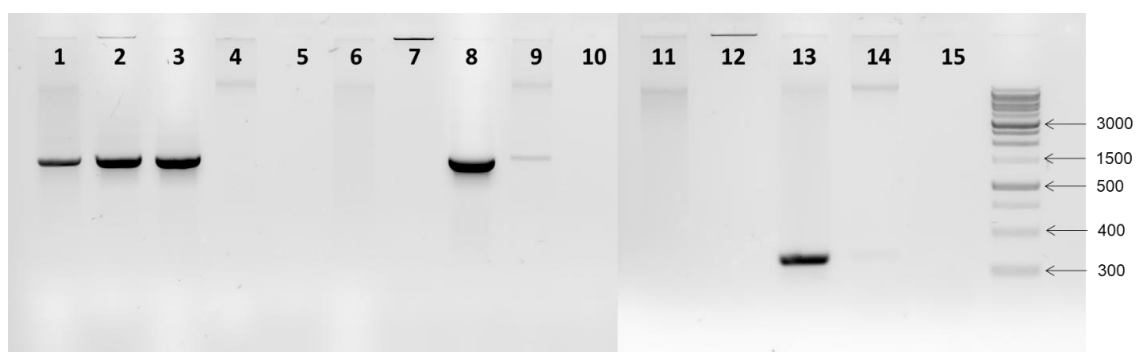


Figure 4.14 - Agarose gel electrophoresis of the PCR products obtained from the amplification of *sad* cluster. *sadA* (1-5), *sadB* (6-10) and *sadC* (11-15). 1/6/11: Consortium. 2/7/12: Consortium after alkaline lysis. 3/8/13: *Microbacterium* sp. BR1 (positive control). 4/9/14: *A. denitrificans* PR1 (negative control). 5/10/15: Blank.

4.4.5 Functional classification of the sulfonamide monooxygenase SadA

The alignment of the amino acid sequence of SadA to the conserved domain database in NCBI (Marchler-Bauer et al. 2017) revealed the presence of an acyl-CoA dehydrogenase domain, indicating that this enzyme is a Group D flavoprotein monooxygenase according

to the most recent classification by Huijbers et al. (2014). Furthermore, homology modeling with SWISS-MODEL (Waterhouse et al. 2018) showed the highest homology to XiaF protein from *Streptomyces* sp. (PDB: 5LVU), 4-hydroxyphenylacetate hydroxylase from *Acinetobacter baumannii* (PDB: 2JBR) and HsaA monooxygenase from *Mycobacterium tuberculosis* and *Rhodococcus* sp., respectively (PDB: 3AFE and 2RFQ). Up to now, Group D enzymes were only shown to catalyze aromatic hydroxylation and *N*-hydroxylation reactions, however, SadA appears to catalyze the *ipso*-hydroxylation of SMX, a reaction that, so far, has been restricted to Group A enzymes (alkylphenol monooxygenases), suggesting that it could be the first Group D enzyme able to catalyze such reactions.

4.5 Discussion

Previously, we described *A. denitrificans* PR1 as a sulfonamide degrading bacterium (Reis et al. 2014). However, after prolonged incubation (≥ 10 d) some colonies of strain PR1 were found to consist of a heterogeneous mixture of two distinct morphotypes. Metagenomic sequencing and clone library of the 16S rRNA gene revealed the presence of a bacterium of low-abundance, designated strain GP. Despite forming a stable association in agar plates, strain PR1 could be readily purified and grown in axenic conditions.

In contrast, the growth of the actinobacterium was found to be confined to the surface of the colonies of strain PR1, a limitation that was independent of the tested medium and culture conditions, suggesting that strain GP requires constant interaction with strain PR1 for growth. It is not the first time that syntrophic behavior has been reported in a *Leucobacter* sp. strain. Bhuiyan et al. (2015) described a *Leucobacter* sp. strain dependent on diffusible growth factors produced by *Sphingopyxis* sp. GF9, a member of the phylum *Proteobacteria*. However, in this study, we found that neither diffusible nor intracellular growth factors produced by strain PR1 allowed the isolation of strain GP on agar plates. The dependence of a helper strain to form colonies was also reported before, namely by Vartoukian et al. (2016). These authors observed that some bacteria from the oral

microbiome would grow only on the surface of a helper strain, averting further attempts to purify some strains. Moreover, the authors suggested that this behavior could result from a specific and unknown genetic adaptation to a biofilm lifestyle (Vartoukian et al. 2016).

The results herein obtained suggest that strain PR1 may either carry out the typical role of a helper strain, supplying essential and possibly unstable or insoluble growth factors to strain GP, or that both strains may interact through cross-feeding, typically observed in biofilm and other natural communities (Pelz et al. 1999; Schink 2002; Wintermute and Silver 2010). These studies point out the challenges of understanding the intricate metabolic networks formed by natural communities. Furthermore, they also show that the microbiome may have evolved to be more interdependent than initially anticipated. Therefore, it can be shortsighted to attempt to isolate independent organisms without first understanding their environment and interaction with other members of the microbiota (Lykidis et al. 2011; Hays et al. 2015).

Despite our inability to purify strain GP and to further determine the nature of the metabolic cooperation within this consortium, several observations strongly suggest that strain GP is solely responsible for the initial cleavage of the SMX molecule and subsequent hydroxylation of the 4AP intermediate. Indeed, axenic cultures of PR1 were unable to degrade SMX or 4AP. Furthermore, a higher relative abundance of strain GP was observed in incubations with increasing SMX concentrations, and a *sadA* homolog was present and overexpressed by the consortium. This gene, which has been previously linked to sulfonamide metabolism in another *Actinobacteria* (Ricken et al. 2017), is significantly overexpressed during degradation of SMX (2.3 to 2.9-fold increase) but is absent in the genome of *A. denitrificans* PR1 (Reis et al. 2017).

An in-depth study of the metabolic pathway in this consortium revealed that SMX degradation is initiated by *ipso*-hydroxylation of the molecule at the sulfonyl group,

resulting in the transient accumulation of an *ipso*-substituted SMX (M1, Fig. 4.15). This mechanism was initially proposed by Ricken et al. (2013) for *Microbacterium* sp. BR1 and for several other isolates by Mulla et al. (2018), but these authors only detected 4AP and not the *ipso*-substituted SMX metabolite, which is reported in this study for the first time. Evidence gathered in this, and previous studies (Ricken et al. 2017) suggest that this reaction is mediated by the SadA sulfonamide monooxygenase, which is present and overexpressed in the microbial consortium. Moreover, homology modeling revealed that SadA is a Group D flavin monooxygenase due to the presence of an acyl-CoA dehydrogenase domain, becoming the first described enzyme able to catalyze an *ipso*-hydroxylation reaction, a reaction that was thought to be restricted to Group A enzymes.

The *ipso*-substituted SMX is quickly converted into sulfite and 4AP (Fig. 4.3 and 4.13). In opposition to Mulla et al. (2018) and Ricken et al. (2013), no evidence of the further degradation of 4AP to HQ or THB before further channeling of intermediates into the Krebs cycle were gathered. The additional downstream metabolites detected in this study, namely M5 and M6, accumulated in negligible amounts, which averted further structural confirmation. Nevertheless, the structure of M5 could be proposed by *in silico* analysis of the product ion spectra generated by fragmentation with QTOF. The proposed structure for M5 suggests that it may result from the reduction of maleylacetate, a known metabolite formed during degradation of several aromatic compounds, including 4AP (Takenaka et al. 2003; Kolvenbach et al. 2012).

Contrary to previous studies (Ricken et al. 2013; Mulla et al. 2018), we found that the hydroxylation at the *ipso* position caused additional molecular rearrangements consisting of a NIH shift of the sulfonyl group (Guroff et al. 1967), from the C1 to the C2 position (M4) and a Baeyer-Villiger rearrangement (M3, side reaction II, Fig. 4.15), inserting the oxygen between the aromatic moiety and the sulfonyl group. These two side reactions are well stabilized and were previously described for the *ipso*-hydroxylation of nonylphenols, bisphenol A, 4-hydroxyarylaldehydes and fluorinated benzenes (Gabriel et al. 2005;

Kolvenbach et al. 2007; Ricken et al. 2015b). However, unexpectedly, NIH shift is usually reported for hydrogen, deuterium, halogens, acyl, aryl, alkyl and methyl groups (Yagi et al. 1972; Owens 2012). An NIH shift involving the migration of a sulfur-species has only been reported before for the degradation of 1-naphthalene sulfonic acid by *Scenedesmus obliquus* (Kneifel et al. 1997). This green alga accumulates high amounts of an NIH shifted metabolite during the ineffective desulfonation of the molecule. In the microbial consortium of strain PR1 and GP, both M4 and M3 also appear to be dead-end metabolites of SMX degradation since they were still detected in the supernatant of resting cells after overnight incubation. Also, directly feeding the mixed culture with M4 resulted in no appreciable degradation after 20 min of incubation (data not shown).

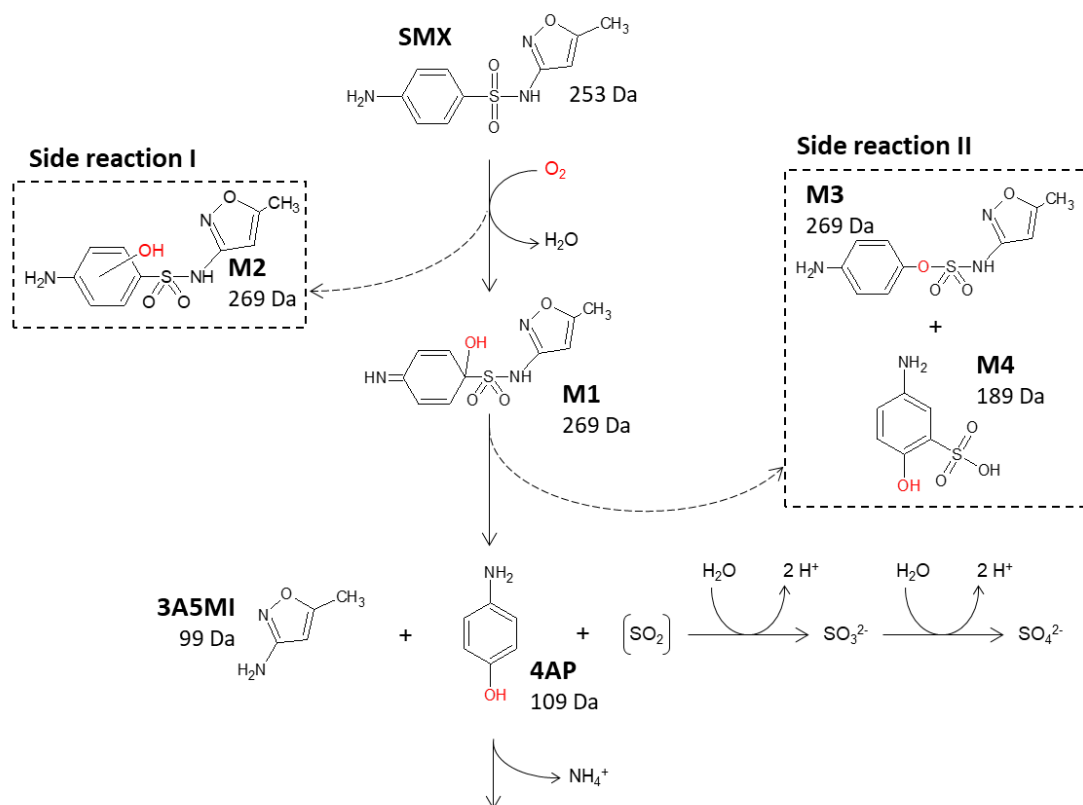


Figure 4.15 – Proposed metabolic pathway for sulfamethoxazole degradation in microbial consortium between *Leucobacter* sp. strain GP and *Achromobacter denitrificans* PR1, oxygen atoms marked in red represent atoms originating from atmospheric O_2 , as confirmed in assays with $^{18}O_2$.

In parallel to the *ipso*-hydroxylation and molecular rearrangement reactions, we detected the accumulation of another hydroxylated SMX, metabolite M2 (side reaction I, Fig. 4.15). This metabolite possessed similar product ion spectra to the mono-hydroxylated SMX produced by photocatalysis with TiO₂/UV, corresponding to the insertion of a hydroxyl group in *ortho* or *meta* position. Similar parallel hydroxylation reactions were observed before in other biological systems (Zakharieva et al. 1998; Taupp et al. 2006; Ullrich and Hofrichter 2007; El-Awaad et al. 2016), and, as shown by multiple authors, it can be a feature of monooxygenases when acting on substrates other than their original substrate (Gorsky et al. 1984; Hillas and Fitzpatrick 1996). However, this reaction could also be non-enzymatic, as it has already been described for SMX degradation in boiled human liver microsomes by Sanderson et al. (2008). None of the dead-end metabolites detected in this study (M2 to M4) accumulated in sufficient amounts to further assess their toxicity or antimicrobial activity.

In this study, we describe a new microbial consortium between a cultivable *Proteobacteria* and a new organism affiliated to the *Leucobacter* genus. Although we have previously identified *A. denitrificans* strain PR1 as a sulfonamide degrader, the results presented here show that the initial cleavage of SMX and transformation of the downstream metabolite 4AP is carried out only by the consortium. Metagenomics and RT-qPCR studies indicate that the *Leucobacter* strain GP is the probably responsible for the initial *ipso*-hydroxylation of the parent molecule through a sulfonamide monooxygenase encoded by a gene homolog to *sadA*.

The metabolic relationship between these two phylogenetically distant strains could not be further elucidated. However, further research is being carried out in an attempt to fully characterize this consortium using metagenomics and metatranscriptomics approaches. These studies will be vital to increase our knowledge and further our understanding of the degradation of these environmental micropollutants.

Chapter 5

Isolation and characterization of *Achromobacter* phage vB_Ade_ART, a novel phage with potential medical and environmental application

Manuscript submitted:

A. Tskhvediani², A.C. Reis¹, M. Chami, P. Vandamme, B.A. Kolvenbach, O.C. Nunes, M. Tediashvili, P.F.-X. Corvini. "Isolation and characterization of *Achromobacter* phage vB_Ade_ART, a novel phage with potential medical and environmental application".

Manuscript in preparation..

² These authors contributed equally to this work.

5.1 Abstract

Bacteria of the genus *Achromobacter* are increasingly recognized as emergent opportunistic pathogens but also as versatile xenobiotic degraders with potential application for bioremediation. Therefore, the isolation of phages able to infect members of this ubiquitous and diverse genus is increasingly important. In this study we isolated and characterized a phage active against *A. denitrificans* strain PR1. This phage, named vB_Ade_ART, is a new member of the *Siphoviridae* family possibly affiliated to the genus *Jwrvirus*. It has a linear dsDNA genome with 95,343 bp and a polyvalent nature, propagating in members of *A. denitrificans*, *A. mucicolens*, and *A. insolitus*.

Its broad host range is possibly linked to the mosaic nature of this phage, which may result from the presence of gene clusters linked to the queuosine biosynthetic pathway and DNA recombination. When applied to a microbial consortium consisting of strain PR1 and the PR1-dependent and sulfonamide-degrader strain GP, phage ART was able to increase the abundance of the slow-growing strain GP and, therefore, enhance the overall degradation efficiency of sulfamethoxazole. These preliminary results suggest that besides therapy, phages have potential application to increase the success of bioremediation strategies by shaping the dynamics of bacterial communities.

5.2 Introduction

In natural communities, bacteriophages have been considered as key players in the biology of microbes, shaping dynamics and even long-term evolution of microbial populations (Clokier et al. 2011). Besides, due to their ability to lyse microbes, they have also been regarded as suitable alternatives to antibiotics for the treatment of infections in humans, animals, and plants (Borysowski et al. 2011; Pirnay et al. 2012; Chan et al. 2013; Silva et al. 2016).

Despite the potential of phage therapy, their application as antibacterial agents has been restricted to the former Soviet Union and Eastern European countries (Kutateladze and

Adamia 2010; Chanishvili 2012), where phages have been continuously and extensively used in clinic for the past decades. Presently, the increased prevalence of multi-drug resistant infections has stirred the interest in phage therapy (Chan et al. 2013; Bragg et al. 2014).

In addition, phages have been drawing the attention of the scientific community due to their potential application in agriculture and aquaculture (Dy et al. 2018; Kering et al. 2019). Their ability to control pests and infections, provide a highly selective way to increase the productivity of these industries. However, their potential to enhance or suppress several environmental processes has often been overlooked.

The genus *Achromobacter*, a highly diverse group of the class *Betaproteobacteria*, comprises Gram-negative rod-shaped bacteria with a ubiquitous distribution among different environments including soil and surface waters (Kersters and De Ley 1984; Coenye et al. 2003; Amoureux et al. 2013). It is unclear whether these organisms are part of the normal human microbiota. However, they are increasingly reported as opportunistic and shown to cause severe infections in immunocompromised individuals, such as in persons with cystic fibrosis (Ridderberg et al. 2012), cancer (Aisenberg et al. 2004), and HIV (Tatro et al. 2014). This opportunistic behavior is predominantly found in isolates from *A. xylosoxidans* and *A. denitrificans* species, which also have high levels of intrinsic and acquired antibiotic resistance (Li et al. 2013). Also, several strains of these two species have been previously reported to degrade xenobiotics (Sałek et al. 2013; Pradeep et al. 2015; Mawad et al. 2016; Benjamin et al. 2016) highlighting their potential for bioremediation.

Table 5.1 – List of *Achromobacter* spp. strains used in this study. Sequence type (ST) was retrieved from sequences publicly available at the *Achromobacter* pubMLST database (www.pubmlst.org/achromobacter; Jolley and Maiden, 2010). N.A. means not available.

Species	Strain	Culture collection no.	Sequence type (ST)	Origin	16S rRNA accession no.
<i>Achromobacter anxifer</i>	Type strain	LMG 26857	100	Human sputum, cystic fibrosis patient	HF586508
<i>Achromobacter deleyi</i>	Type strain	LMG 3458	133	Mouse, lung autopsy sample	HG324053
<i>Achromobacter denitrificans</i>	Type strain	LMG 1231	102	Soil	AJ278451
<i>Achromobacter denitrificans</i>	PR1	LMG 30905	419	Activated sludge	KJ124851
<i>Achromobacter insolitus</i>	Type strain	LMG 6003	99	Leg wound	AY170847
<i>Achromobacter kerstersii</i>	Type strain	LMG 3441	138	Soil	HG324052
<i>Achromobacter mucicolens</i>	Type strain	LMG 26685	106	Human sputum, non-cystic fibrosis patient	HE613446
<i>Achromobacter piechaudii</i>	Type strain	LMG 1873	167	Pharyngeal swab	AB010841
<i>Achromobacter ruhlandii</i>	Type strain	LMG 1866	30	Soil	AB010840
<i>Achromobacter xylosoxidans</i>	Type strain	LMG 1863	20	Ear discharge	Y14908
<i>Achromobacter xylosoxidans</i>	T7	DSM 11852	N.A.	Soil	MH656843
<i>Achromobacter xylosoxidans</i>	CCUG 48386	DSM 26073	N.A.	Human sputum, cystic fibrosis patient	MH656900

Strain PR1 was isolated from activated sludge and identified as *Achromobacter denitrificans* (Reis et al. 2017). Furthermore, it represents a new sequence type (ST, Table 5.1) within this species, as confirmed by multilocus sequence analysis of *nusA*, *eno*, *rpoB*, *gltB*, *lepA*, *nuoL* and *nrdA* gene fragments (www.pubmlst.org/achromobacter) (Jolley and Maiden 2010; Spilker et al. 2012). Strain PR1 was also initially identified as a sulfonamide degrader (Reis et al. 2014; Nguyen et al. 2017). Nevertheless, further studies have shown that, what initially appeared to be an axenic culture, was, in fact, a consortium between strain PR1 and a slow-growing *Leucobacter* sp. This strain, named strain GP, is unable to grow independently from *A. denitrificans* and, interestingly, it was shown to be the probable responsible for the initial cleavage of the sulfonamide bond (Reis et al. 2018a). Despite its importance in this sulfonamide degrading consortium, strain GP remains a stable minority throughout all phases of growth and cannot be further purified due to the fast-growing and multi-drug resistant phenotype of strain PR1.

In this study, we aimed at isolating and characterizing phages able to infect *A. denitrificans* strain PR1 and to assess the feasibility of using phage treatment to influence the cooperation of the two strains in the sulfonamide-degrading consortium. Furthermore, since many *Achromobacter* spp. isolates have been increasingly reported as opportunistic we tested this phage's ability to infect other species within this genus, assessing the feasibility of using this phage as an alternative to antibiotic therapy.

5.3 Materials and methods

5.3.1 Bacterial strains and culture conditions

Axenic cultures of *Achromobacter denitrificans* strain PR1 and the microbial consortium consisting of this strain and *Leucobacter* sp. strain GP (Reis et al. 2017; Reis et al. 2018a) were grown with 0.6 mM sulfamethoxazole (SMX) either in 25% Brain Heart Infusion Broth (BHI) with 15 g/l agar (BHI-SMX-agar) or in mineral medium B (Barreiros et al. 2003) with 4 mM ammonium sulfate, 0.2 g/l yeast extract, and 7 mM succinate (MMSY-

SMX). All incubations were carried out in the dark at 30°C, and liquid cultures were also continuously stirred at 120 rpm.

Eleven additional *Achromobacter* spp. strains (Table 5.1) were obtained either from BCCM/LMG (Belgium) or DMSZ (Germany) and cultured in Tryptic Soy Agar (TSA, Sigma) at 30°C for 48 h.

5.3.2 Determination of antibiotic resistance phenotypes for *Achromobacter* spp.

Antibiotic resistance phenotypes were determined using the agar diffusion method (CLSI 2018) on Mueller-Hinton agar (Oxoid). The antibiotics tested were: erythromycin (ERY, 15 µg); gentamicin (GEN, 10 µg); sulfamethoxazole (SMX, 100 µg); ciprofloxacin (CIP, 5 µg); chloramphenicol (CHL, 30 µg); doxycycline (DOX, 30 µg) and ampicillin (AMP, 10 µg). Filter paper disks impregnated with a specific amount of SMX were prepared as recommended in the guidelines (CLSI 2018); the remaining disks were purchased from Bio-rad. The plates with bacterial lawns and antibiotic discs were incubated for 48 h at 30 °C before the determination of the inhibition diameters. The concentration of SMX tested in this study was not included in the CLSI list, in this way, the phenotype was determined according to the following the criteria: $S \geq 17/R < 12$. Inhibition zone diameters between 13 and 16 mm were referred to as intermediary.

5.3.3 Bacteriophage isolation, propagation and culturing conditions

For phage isolation, 50 ml of activated sludge were collected after secondary treatment in an urban wastewater treatment plant (WWTP, Basel, Switzerland). The sludge was filtered through a 0.2 µm pore-size membrane (Millex-GS), mixed with Tryptic Soy Broth (TSB) and the host strain PR1 (10^8 CFU/ml) in a ratio of 10:10:1, and incubated overnight at 37 °C.

The obtained lysate was centrifuged and tested for lytic activity on the host strain, followed by titration using the double layer agar method (Adams, 1959; Gratia, 1936).

Single plaques were further purified by repeated single plaque isolation. The phage was propagated in TSB medium and concentrated by high-speed centrifugation (at 20,000 xg for 3 h). This phage was named following the nomenclature of viruses of *Bacteria* and *Archaea* (Kropinski et al. 2009).

5.3.4 Efficiency of plating (EOP)

Phage with an initial concentration of 10^7 PFU/ml was tittered on the host strain by double layer agar and incubated at 4 °C, 22 °C, 30 °C or 37 °C for 24 h. The efficiency of plating (EOP) was assessed relative to the optimal temperature (with the highest number of negative plaques), and the temperature displaying the highest efficiency of infection was selected for subsequent studies.

5.3.5 Infection parameters

Adsorption

The mixture of exponentially grown bacteria and phage at a multiplicity of infection (MOI) of 0.1 was incubated at 37°C. Samples were taken every 5 min, filtered through 0.2 μm pore size filters (Millex-GS) and tittered to determine the number of non-adsorbed phages. One-step growth curve analysis was performed according to the method of Ellis and Delbrück (1939). Phage-bacteria mixture at an MOI 0.01 was incubated for 10 min at 37°C to allow adsorption. After removal of the excess phage by centrifugation, the cell pellet was resuspended in fresh TSB medium and incubated shaking at 37°C. Samples at different time points were immediately serially diluted and plated for phage titration.

The latent period was defined as the interval between adsorption of the phages to the bacterial cells and the release of phage progeny. The ratio between the final number of released phage particles and the number of infected bacterial cells during the latent period was considered as a burst size (Adams, 1959).

Host Range Analysis

The host range of the bacteriophage was tested on the 11 environmental and clinical *Achromobacter* spp. isolates. Phage lysate was diluted in liquid TSB medium to 10^7 PFU/ml, and 10 μ l aliquots were spotted on the bacterial lawns containing 10^8 log phase cells of *Achromobacter* spp. Plates were incubated at 30°C for 24 h. Lysis of strains was further confirmed by the development of single plaques by double-layer agar technique upon appropriate dilution of the phages.

Phage stability

The phage diluted in phosphate buffer (50 mM) with an initial concentration of 10^7 PFU/ml was used for stability tests. The residual infectivity was determined by double layer agar method.

Sensitivity to five different temperatures (-20, 4, 22, 60, and 70 °C; 37 °C as control) and four pH values (pH 2, 4, 8 and 10; pH 7 as control) were tested by incubating the phage for 1 h under these conditions. For the stability test at -20 °C, 50% (v/v) glycerol was also added to the storage buffer. To test sensitivity to UV radiation, the phage was exposed at short wavelengths (254 nm) for up to 5 min. Its resistance to osmotic shock was tested by incubating in phosphate buffer with sodium chloride (final concentration 4.5 M) for 15 min, followed by transference to the same buffer without NaCl. Sensitivity to detergents was assessed by incubating in 0.1% SDS (w/v, sodium dodecyl sulfate) for 20 min at 45 °C, 0.1% Sarkosyl (w/v, sodium lauroyl sarcosinate) and 0.1% CTAB (w/v, cetyltrimethylammonium bromide) at 22 °C for 10 and 1 min respectively. The effect of organic solvents was studied in 63% (v/v) ethanol and 90% (v/v) acetone after 1 h of incubation; and also in 90% (v/v) chloroform and 50% (v/v) DMSO at 4 °C for 24 h.

5.3.6 Electron microscopy

Virion morphology was studied by Transmission Electron Microscopy (TEM) and Cryogenic electron microscopy (Cryo-TEM).

For TEM analyses, 4 µl aliquot of the sample was adsorbed onto a glow-discharged carbon film-coated copper grid, and subsequently negatively stained with 2% uranyl acetate. Images were recorded using Philips FEI Spirit Electron Microscope operating at 80 kV on a Veleta CCD camera (Olympus, Germany).

For Cryo-TEM, 4 µl aliquot of the sample was adsorbed onto the holey carbon-coated grid (Lacey, Tedpella), blotted with Whatman 1 filter paper and vitrified into liquid ethane at -180 °C using a vitrobot (FEI, Netherlands) (Dubochet et al. 1988). Frozen grids were transferred onto a Talos Electron microscope (FEI, USA) using a Gatan 626 cryo-holder (GATAN, USA). Electron micrographs were recorded at an accelerating voltage of 200 KV using a low-dose system (30 e-/Å²) and keeping the sample at -175°C. Defocus values were -3 to 6 µm. Micrographs were recorded on 4K x 4K Ceta CMOS camera.

5.3.7 Bacteriophage DNA extraction, genome sequencing and assembly

DNA extraction was performed from concentrated cell lysates of *A. denitrificans* PR1 after pre-treatment with DNase I (New England Biolabs) at 37 °C for 30 min to minimize host DNA contamination. Viral genomic DNA was extracted with Dneasy Blood & Tissue DNA Extraction Kit (Qiagen) according to the manufacturers' instructions. High-quality DNA was used for paired-end sequencing (2 x 150 bp) with the Hiseq platform (Illumina) by GATC Biotech (Germany). Paired-end reads were adapter and quality trimmed (≥Q20) with the BBDuk tool (<https://sourceforge.net/projects/bbmap>). To avoid chimeric assemblies between phage and host DNA, the resulting data was further screened to remove reads with high sequence identity (≥ 98%) to the host DNA using BBMap version 38 (<https://sourceforge.net/projects/bbmap>). A subset of reads (1%) was used for assembly with SPAdes version 3.11.1 (Bankevich et al. 2012) with the option -careful. Reads were mapped to scaffolds with BWA-MEM (Li 2013) and used for further scaffolding with BESST version 2.2.8 (Sahlin et al. 2014). The final assembly was polished with several iterations with Pilon version 1.22 (Walker et al. 2014), and the final genome

coverage was calculated with Qualimap version 2.2.1 (Okonechnikov et al. 2015). The complete linear genome of this bacteriophage has been deposited in GenBank under the accession number MH746817.

5.3.8 Genome annotation and phylogenetic analysis

Open-reading frames (OFR) were predicted and annotated with Prokka (Seemann 2014) using the virus and prophage database from August 3, 2017, available on PHASTER (<http://phaster.ca/databases>) (Arndt et al. 2016) and the Prokaryotic Virus Orthologous Groups (pVOGs) (Grazziotin et al. 2017). The 15 closest relatives to phage ART were determined using the PAirwise Sequence Comparison (PASC) web tool (Bao et al. 2014). Amino acid and nucleotide similarity values between the closest relatives were calculated using the web-based tool AAI/ANI matrix calculator (<http://enve-omics.ce.gatech.edu/g-matrix/>) (Saitou and Nei 1987; Rodriguez-R and Konstantinidis 2016). Furthermore, amino acid sequences were compared using the Genome-BLAST Distance Phylogeny (GBDP) method under settings recommended for prokaryotic viruses (Meier-Kolthoff et al. 2013; Meier-Kolthoff et al. 2017). The resulting intergenomic distances were used to infer a balanced minimum evolution tree with branch support via FASTME including SPR post-processing (Lefort et al. 2015) for each of the formulas D0, D4, and D6, respectively. Branch support was inferred from 100 pseudo-bootstrap replicates. Taxon boundaries at the species, genus, and family level were estimated with the OPTSIL program (Göker et al. 2009), the recommended clustering thresholds and an F value (fraction of links required for cluster fusion) of 0.5 (Meier-Kolthoff et al. 2014; Meier-Kolthoff et al. 2017). The resulting tree was visualized with FigTree version 1.4.3 (<http://tree.bio.ed.ac.uk/software/figtree/>). Comparative genomic analysis between phage vB_Ade_ART and others from the same genus was performed with Roary with a BLASTp identity threshold set to 70 % (Page et al. 2015) to determine the core genes of this genus and the accessory genes present in the novel phage isolate.

5.3.9 Bacterial consortium DNA extraction and quantitative PCR (qPCR)

The genomic DNA of the bacterial consortium was extracted from 1 ml of culture medium with the GenElute Bacterial Genomic DNA Kit (Sigma) as described previously (Reis et al. 2018a). The absolute quantification of strains PR1 and GP was performed by qPCR with species-specific primers targeting the 16S rRNA gene as described by Reis et al. (2018).

5.3.10 Effect of the bacteriophage in a sulfonamide-degrading consortium

The feasibility of using the test phage for strain PR1 population control in the sulfonamide degrading consortium was assessed in batch experiments at different MOI. Firstly, the impact of *Leucobacter* sp. GP on phage infection and propagation were studied by assessing the efficiency of plating at a different multiplicity of infection (MOI) on strain PR1 axenic cultures and the consortium. Both axenic cultures and the consortium were incubated overnight before measuring the efficiency of plating.

Furthermore, the effect of the phage infection on the activity of the dependent *Leucobacter* sp. was tested by measuring the ability of the consortium to degrade SMX under different MOI. This experiment was performed in triplicate and parallel to a non-infected control, and the flasks were incubated at 30 °C with constant stirring (120 rpm) for 48 h. The abundance of each bacterial strain was measured by qPCR as previously described (Reis et al. 2018a), and the quantification of SMX was performed by HPLC as previously described by Ricken et al. (2013). Significant differences ($p < 0.05$) between the overall abundance of strain GP were determined by one-way ANOVA (using the ratio of the 16S rRNA copies/ml of strains GP and PR1) and Tukey's tests in R (de Mendiburu, 2013; R Core Team, 2015).

5.4 Results and discussion

5.4.1 Isolation of the bacteriophage

The bacteriophage was isolated from an activated sludge sample taken in 2017 from an urban WWTP in Basel, Switzerland. After checking lytic activity, the primary lysate was

tittered on *A. denitrificans* PR1. From three different phage clones, one with a clear plaque and the highest titer on the host strain was selected for further studies and named vB_Ade_ART.

5.4.2 Morphological analysis

Phage vB_Ade_ART forms clear plaques typical for lytic (virulent) phages, 1-2 mm in size, indicating larger virions, presumably because of slow diffusion through the top agar (Park et al, 2000).

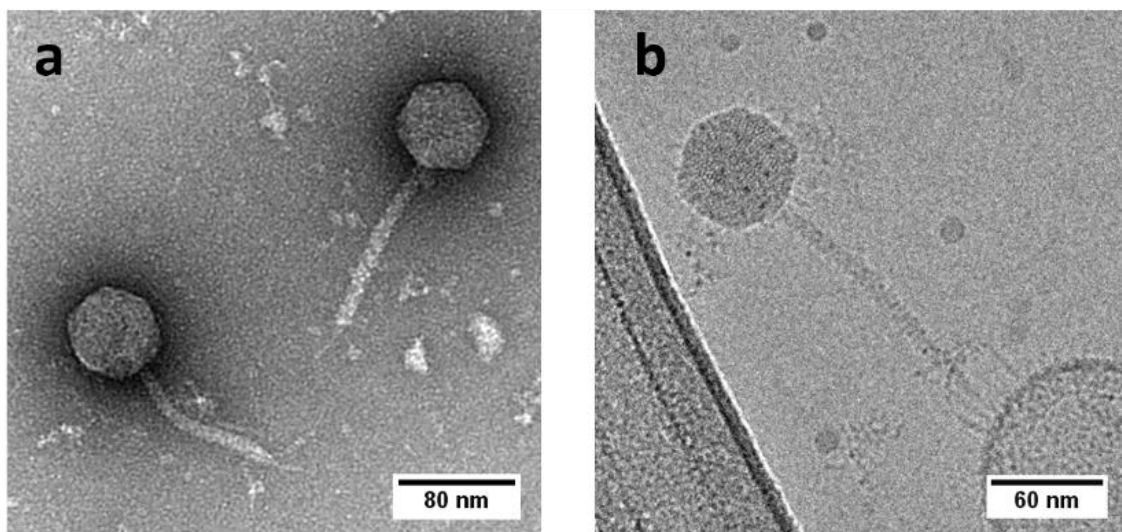


Figure 5.1 – Electron micrographs of the bacteriophage vB_Ade_ART negatively stained in (a) and frozen hydrated in (b). The magnification in (a) is 17500 and in (b) is 24000x.

Virion morphology examined by transmission electron microscopy (TEM and Cryo-TEM) revealed that phage vB_Ade_ART belongs to the order of tailed phages- *Caudovirales*, family *Siphoviridae* (long non-contractile tail), the most abundant and well-described phage family. The following parameters were determined: head diameter (67 ± 1 nm); tail width (11 ± 1 nm); and tail length (123 ± 1 nm) (Fig. 5.1). Virion size and morphology corresponds to the phage genomic and physiological properties. In particular, head size fits the large size genome, while the tail tip complex consisted of central spike and 3 fibers, resulting in high efficiency of infection (Shao and Wang 2008).

5.4.3 Infection parameters

The studies on phage adsorption and single-step growth processes provided general information of the phage infection cycle, including the adsorption velocity, the latent period and the burst sizes. After 5 min, 67.5% of the phage particles were already adsorbed, while the maximal adsorption was achieved within 20 min (> 90 %) (Fig. 5.2). Adsorption velocity (constant) of this phage into its host was of 1.2×10^{-10} ml/min. Furthermore, this phage showed a latent period of approximately 20 min and a burst size of 130 new phage particles per infected cell.

The efficient adsorption, short latent period, and a high number of newly produced phage particles (titer 3×10^{11} in 2 hours), characterize this phage as highly infective (Fig. 5.2).

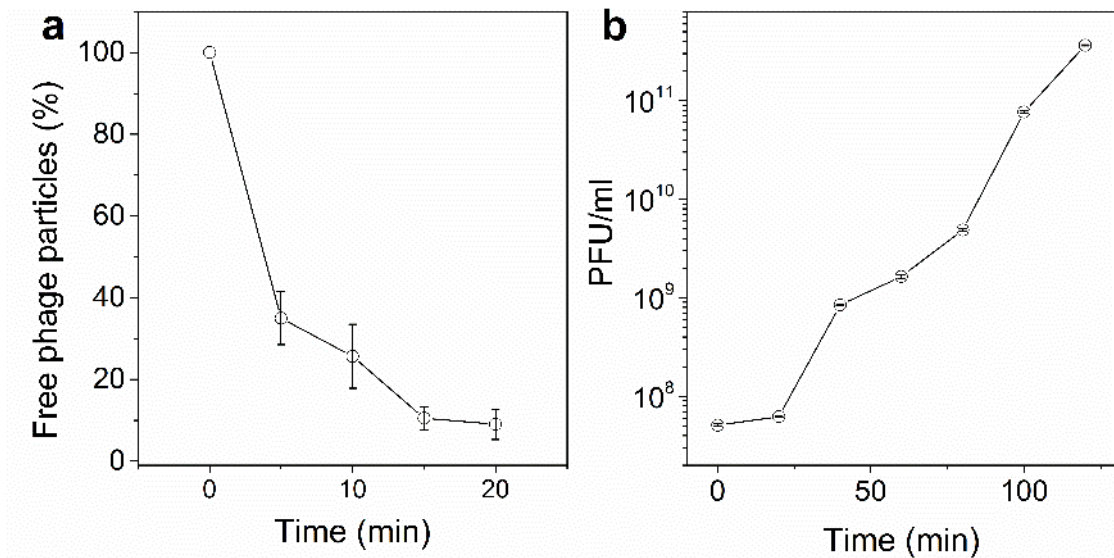


Figure 5.2 – Adsorption (a) and one-step growth cycle (b) of *Achromobacter* phage vB_Ade_ART. Values for adsorption are plotted as percentage of free PFU and one-step growth cycle (PFU/ml) is plotted in logarithmic scale. All values are the mean of triplicates, and the error bars represent the standard deviation.

5.4.4 Phage host range determination

Bacteriophages are essentially genus-specific and even species-specific in replication (Ackermann et al. 1978). However, some lytic phages have been reported to have a broad host range, crossing the boundaries of different taxa (Evans et al. 2010). These phages are

also referred to as polyvalent bacteriophages. To investigate the specificity of phage vB_Ade_ART, 11 clinical and environmental *Achromobacter* spp. isolates were tested for phage sensitivity by spot test. The phage was additionally tittered on different strains to distinguish infection from a phenomenon of “lysis from without” (Adriaenssens et al. 2012).

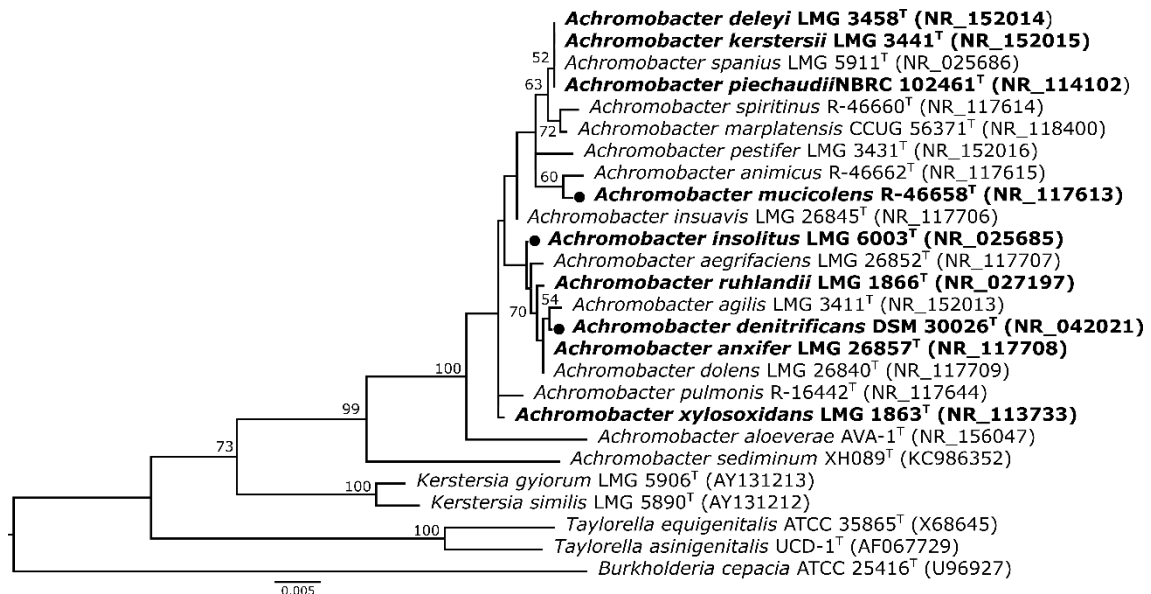


Figure 5.3 – Phylogenetic tree derived from 16S rRNA gene sequence analysis, showing the relationship between all type strains of the genus *Achromobacter*. Type strains of *Kerstersia*, *Taylorella* and *Burkholderia* genera were used as outgroups. The maximum likelihood phylogenetic tree based on the 16S rRNA gene was inferred with the Jukes–Cantor model from 1000 bootstrap replicates in MEGA6 software (Tamura et al. 2013). Bootstrap values at or above 50%, are indicated at branch points. The scale bar indicates the number of substitutions per site. Strain names in bold indicate the species used in this study, strains with a circle next to the tip of the branch indicate the species that could be infected by *Achromobacter* phage vB_Ade_ART.

To the best of our knowledge, all of the previously described *Achromobacter* phages were found to be specific to *A. xylooxidans* (Wittmann et al. 2014a; Wittmann et al. 2014b; Li et al. 2016; Dreiseikelmänn et al. 2017). Phage vB_Ade_ART is, therefore, the first described phage able to infect strains of *A. denitrificans*. Furthermore, contrary to the previously described phages, phage vB_Ade_ART showed a broader host range, showing interspecies infectivity and propagating in strains from distinct species (Fig. 5.3), namely the type strains of *A. mucicolens* and *A. insolitus*, noticeably, both opportunistic human pathogens (Fig. 5.4) (Li et al. 2017). Furthermore, all infected strains exhibited a multi-drug resistant

phenotype, highlighting the potential use of phage vB_Ade_ART as an alternative to antibiotics for the treatment of opportunistic infections in immunocompromised individuals (Aisenberg et al. 2004; Ridderberg et al. 2012; Tatro et al. 2014). However unlike previously isolated phages for *Achromobacter* spp., phage vB_Ade_ART was unable to infect any of the *A. xylosoxidans* strains, since all the three strains of this species herein tested were found to be phage - insensitive or showed “lysis from without” at phage concentrations of 10^6 PFU/ml (data not shown).

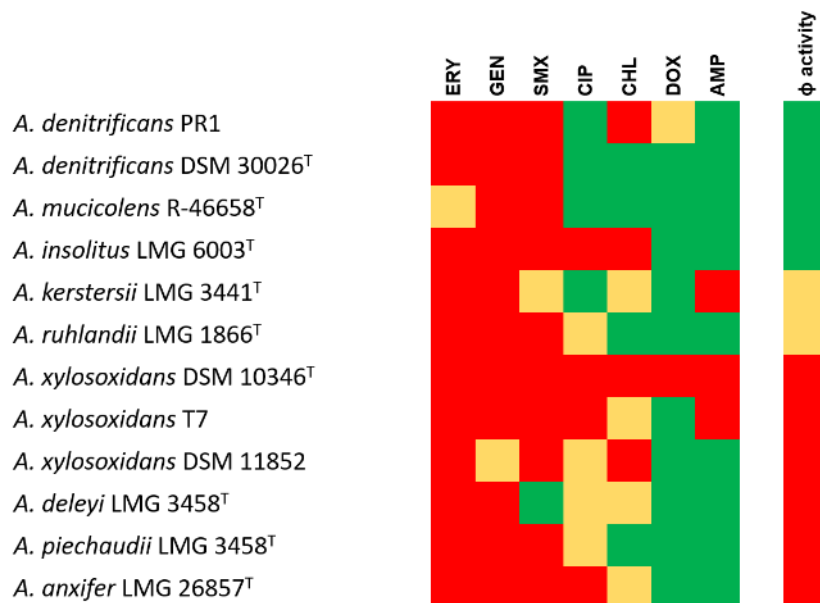


Figure 5.4 – Antibiotic resistance pattern and bacteriophage host range for different strains of the genus *Achromobacter*. For both antibiotics and phage red represents resistant, yellow intermediate and green susceptible phenotypes.

5.4.5 Phage stability

Phages are quite resistant to natural and anthropogenic stressors. They are more stable than their hosts in particular environments without the loss of their infectious capabilities. In sensitivity assays at different temperatures, phage titer was shown to be stable at -20, 4, 22°C and 37°C – the range of temperature required for phages used as biocontrol agents (Rombouts et al. 2016) (Fig. 5.5). This stability has been reported before and is a well-known characteristic of tailed phages (Ackermann et al. 2004). Moreover, phages of the

Siphoviridae family show long-term survivability when kept lyophilized with 50% glycerol. Although EOP analysis revealed that incubation at low temperature (4 °C) completely inhibits the infection process, while the phage successfully infects the host when grown at temperatures of 22 °C, 30 °C and 37 °C with the highest effectiveness at 37 °C. It is known that lower than optimal temperatures decreases penetration efficiency and, therefore, fewer phages get involved in the multiplication phase (Jończyk et al. 2011). According to the previously suggested grouping of phages based on the effect of temperature on the efficiency of plating (Kaliniene et al. 2010), this phage belongs to mid-temperature phage, plating in the range of 15–42 °C.

At high temperature, phage titer did not decrease significantly, with a reduction of 0.62 ± 0.2 log PFU/ml or 2.19 ± 0.07 log PFU/ml at 60°C and 70°C, respectively (Fig. 5.5). Thus, the phage can be considered as quite thermostable. Based on previous studies, the formation of disulfide cross-links within phage capsid proteins could play a role in the stabilization of the phage against thermal denaturation (Caldeira and Peabody 2007).

Another important factor influencing phage stability is the acidity of the environment. In the stability test with low and high pH, reduction in phage titer was negligible at pH ranging from pH = 4 – 10; at pH 8 there was even a minor increase of some PFU/ml (Fig. 5.5). In opposite, the viability of phage particles dramatically dropped at pH 2. Stability at alkaline rather than in acidic pH is a general feature of *Siphoviridae* family phages (Hamdi et al. 2017). Sharp and Hook (1946) suggest irreversible coagulation and precipitation might be the factors limiting phage activity in a highly acidic environment.

UV irradiation for 5 min does not cause any considerable damage to the bacteriophage capsid, as shown by a minor decrease in phage titer (decrease of 0.35 ± 0.07 PFU/ml). This feature is also described in different phages, presumably related to the phage morphology (Lee and Sobsey 2011). Tailed phages and especially phages from *Siphoviridae* family are the most resistant to UV radiation (Ackermann et al. 2004; Lee and Sobsey 2011). Consequently, one can expect a high efficiency of infection by phage vB_Ade_ART not only

in habitats devoid of UV, like in human or animal guts but also in other environments, outside of the mammalian organism. This stability in different conditions may enable phage to persist for a long time in natural environments and thus, becoming a good candidate for biotechnological applications.

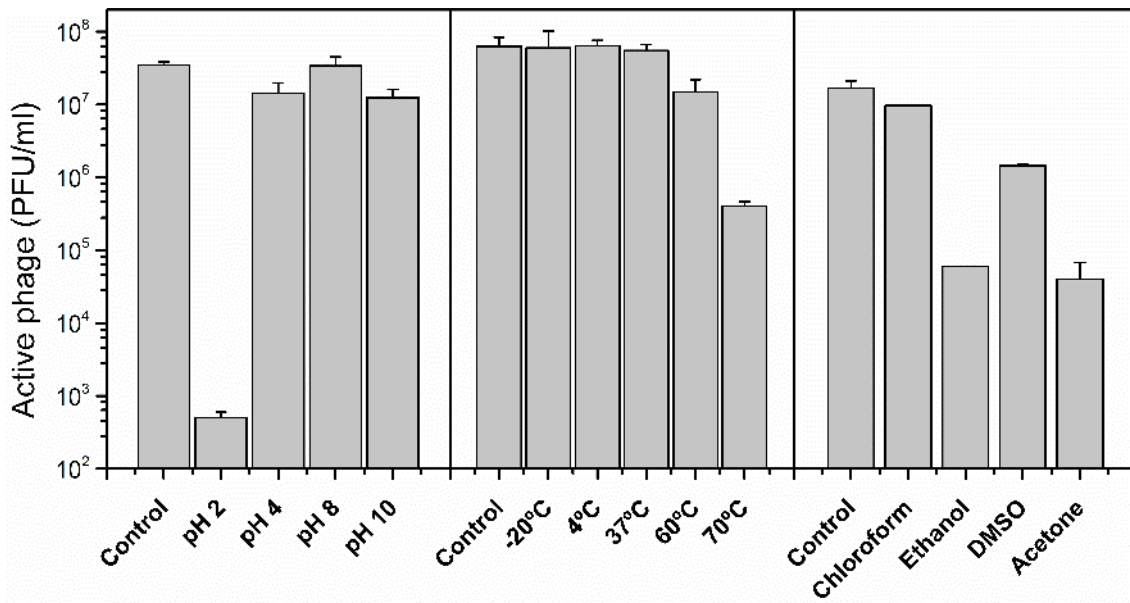


Figure 5.5 – Active phage particles after incubation under different pH values (a), temperature (b) and the presence of organic solvents (c). Control conditions correspond to pH 7 at 22 °C in the absence of organic solvents. Values for PFU/ml are in logarithmic scale and represent the mean of three replicates and error bars represent the standard deviation.

On the contrary, organic solvents such as ethanol and acetone caused a significant decrease in phage titer, though the virions were more stable in DMSO and relatively resistant to chloroform (Fig. 5.5). This acute sensitivity to organic solvents might be explained by the possible presence of a lipid-rich membrane. The same sensitivity has been described in some membrane –containing phages (Poranen et al. 2015). The factors influencing the phagecidal activity of alcohol solutions was explained by the difference between the hydrophobicity-hydrophilicity balance of these solutions, and the hydrophobicity-hydrophilicity balance of the phage surface proteins (Yamashita et al. 2000).

Phage vB_Ade_ART showed a high sensitivity to detergents. For instance, sarcosyl and CTAB were able to inactivate all phage particles in a short period (10 and 1 min, respectively), while only a few phage particles remained active after incubation with SDS (reduction of 6.16 ± 0.06 log PFU/ml after 20 min). Inhibition of infectivity by detergents has been described for some phages (Jurczak-Kurek et al. 2016), perhaps indicating enzymatic interference with phage adsorption (Srinivasan and Ramasamy 2017).

5.4.6 Taxonomic classification and genomic analysis

Genome sequencing generated 13 million paired-end reads that were trimmed and quality filtered resulting in 12.3 million paired-end reads. *De novo* assembly resulted in a double-stranded DNA sequence of 95,343 bp with 128 putative open reading frames (ORFs) and 55 % of GC content.

Amino acid and nucleotide sequence comparison revealed that *Achromobacter* phage vB_Ade_ART probably represents a new member of the genus *Jwrvirus*, with only two other representative phages described to date (Fig. 5.6). Comparative genomic analysis revealed that these three members have an AAI value of 72-73%, ANI value of 77-82% and share at least 30 core genes, the majority of these with unknown function (Table 5.2). Beside early genes which are linked to essential functions such as DNA metabolism and packaging, host interaction, transcription, replication, structure and lysis (Wittmann et al. 2014b), these three members all share a tRNA for Proline (TGG) (locus tag ART_00058) and an integrase gene (locus tag ART_00043) (Table 5.2). The presence of tRNA is an expected characteristic of virulent phages since it ensures optimal translation and, therefore, faster replication which results in higher infectivity (De Paepe and Taddei 2006; Bailly-Bechet et al. 2007).

Furthermore, the comparative analysis revealed that phage vB_Ade_ART possesses unique genes with no close homologs in the genomes of *Achromobacter* phage 83-24 (accession NC_028834) and *Achromobacter* phage JWX (NC_028768), the other two representative members from the same genus (amino acid identity cutoff of 70%) (Fig. 5.7, Table 5.3).

Table 5.2 – Core genes of the *Jwrvirus* genus as determined by core/pangenomic analysis. *, these genes are not annotated in GenBank, the nucleotide position of the coding sequence is presented instead.

Annotation/function	Locus tag		
	<i>Achromobacter</i> phage vB_Ade_ART	<i>Achromobacter</i> phage 83-24	<i>Achromobacter</i> phage JWX
Bifunctional 3'-5' exonuclease/DNA polymerase	ART_00001	AVV27_gp46	AVV28_gp48
Hypothetical protein	ART_00003	AVV27_gp44	AVV28_gp46
Helicase	ART_00004	AVV27_gp43	AVV28_gp45
Hypothetical protein	ART_00005	AVV27_gp42	AVV28_gp44
Hypothetical protein	ART_00007	AVV27_gp40	AVV28_gp42
Thymidylate synthase	ART_00010	AVV27_gp36	AVV28_gp39
Deoxycytidylate deaminase	ART_00011	AVV27_gp35	AVV28_gp38
Hypothetical protein	ART_00012	AVV27_gp34	AVV28_gp37
Hypothetical protein	ART_00013	27005..27259*	AVV28_gp36
Endolysin	ART_00014	AVV27_gp33	AVV28_gp35
Hypothetical protein	ART_00017	25556..25846*	AVV28_gp32
Hypothetical protein	ART_00019	AVV27_gp28	AVV28_gp30
Tail component protein	ART_00022	AVV27_gp25	AVV28_gp27
Hypothetical protein	ART_00024	AVV27_gp23	AVV28_gp25
Tape measure domain protein	ART_00030	AVV27_gp19	AVV28_gp21
Putative tail protein	ART_00033	AVV27_gp16	AVV28_gp18
Major structural phage protein	ART_00034	AVV27_gp15	AVV28_gp17
PD-(D/E)XK nuclease superfamily protein	ART_00037	AVV27_gp56	AVV28_gp61
Hypothetical protein	ART_00042	AVV27_gp52	AVV28_gp56
Integrase	ART_00043	AVV27_gp51	AVV28_gp55
Hypothetical protein	ART_00044	AVV27_gp50	AVV28_gp54
Hypothetical protein	ART_00045	AVV27_gp49	AVV28_gp53
Hypothetical protein	ART_00047	AVV27_gp03	AVV28_gp04
Putative terminase small subunit	ART_00049	AVV27_gp05	AVV28_gp07
Terminase large subunit	ART_00050	AVV27_gp06	AVV28_gp08
Portal protein	ART_00051	AVV27_gp07	AVV28_gp09
Scaffold protein	ART_00052	AVV27_gp08	AVV28_gp10
Putative major capsid protein	ART_00053	AVV27_gp09	AVV28_gp11
Virion structural protein	ART_00056	AVV27_gp12	AVV28_gp14
Virion structural protein	ART_00057	AVV27_gp61	AVV28_gp67

Table 5.3 – Genes unique to *Achromobacter* phage vB_Ade_ART within the *Jwrvirus* genus as determined by core/pangenomic analysis and manual curation of the results.

Annotation/function	Gene length (bp)	Locus tag
Phosphoribosyl-ATP pyrophosphohydrolase	464	ART_00008
Structural protein	290	ART_00026
Minor tail protein	1862	ART_00027
Putative tail chaperonin protein	344	ART_00032
Bifunctional 3'-5' exonuclease/DNA polymerase	1964	ART_00059
Tail component protein	3467	ART_00062
MazG nucleotide pyrophosphohydrolase	698	ART_00067
DNA polymerase	2069	ART_00068
DNA polymerase beta subunit	995	ART_00069
Putative cysteine dioxygenase type 1	500	ART_00074
Queuosine tRNA-ribosyltransferase	920	ART_00075
GTP cyclohydrolase FolE	677	ART_00078
putative 6-pyruvoyl tetrahydropterin synthetase protein QueD	446	ART_00079
Putative queuosine biosynthesis protein QueC	860	ART_00080
Organic radical activating enzyme QueE	716	ART_00081
Helicase	1709	ART_00086
Exonuclease	908	ART_00087
Putative ATPase AAA	683	ART_00089
Putative DNA binding protein	461	ART_00092
Chaperone protein DnaJ	263	ART_00095
Replicative primase helicase	2363	ART_00100
Endonuclease	449	ART_00101
Putative D-alanyl-D-alanine carboxypeptidase	572	ART_00107
Terminase small subunit	731	ART_00111
Terminase large subunit	1535	ART_00112
Putative structural protein	1634	ART_00113
Putative scaffold protein	707	ART_00114
Putative major capsid protein	1034	ART_00115
Structural protein	518	ART_00118
Structural protein	377	ART_00119
Structural protein	473	ART_00120
Major structural phage protein	1325	ART_00121
Putative structural protein	470	ART_00122
Putative tail chaperonin protein	293	ART_00123
Putative tail completion protein	434	ART_00124
Tape measure domain protein	2555	ART_00125
Tail fiber protein	1319	ART_00128

However, the majority of these unique genes are closely related to other phylogenetically distant phages suggesting that they may have been acquired through homolog recombination between different phages and between the phage and different hosts (Hendrix 2002). This recombination resulted in a highly mosaic phage which may explain its broader host range in comparison to other phages for *Achromobacter* spp previously described.

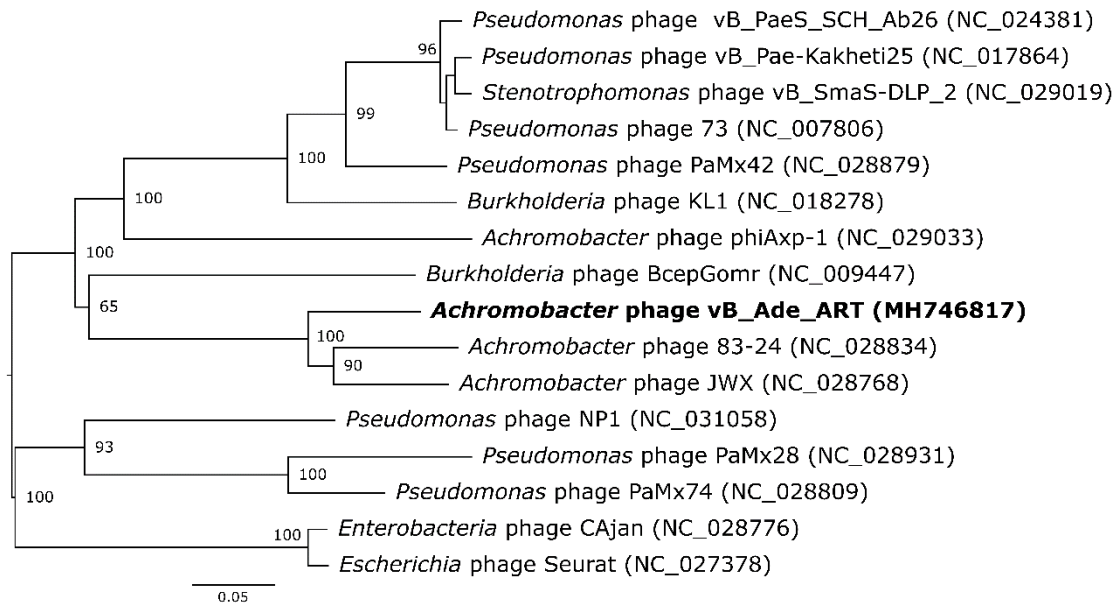


Figure 5.6 – Phylogenomic GBDP tree from representative phages from the *Siphoviridae* family inferred using the balanced minimum evolution method based on the D4 formula (Meier-Kolthoff et al. 2017). Pseudo-bootstrap support values were generated from 100 replications, values above 50% are indicated at branch points. Tree was rooted at the midpoint and visualized with FigTree. Scale bar represents the number of substitutions per site.

However, interestingly, it also resulted in a highly incongruent phylogenetic nature, since, among other genes, phage vB_Ade_ART appears to have acquired additional terminase subunits (ART_00111 and ART_00112) similar to the ones found in *Burkholderia* phage BcepGomr (accession number YP_001210221.1 and YP_001210224.1, respectively). This incongruence is a well-described characteristic among other phages, particularly in the extremely versatile bacteriophage lambda (Hendrix 2002; Hillyar 2012). Although, to the best of our knowledge, this is the first described phage harboring two phylogenetically distant copies of both large and small terminase subunits.

Phage mosaicism is a well-studied characteristic, and particularly well described for lambda phage (accession number J02459.1). In this phage, strong genetic mosaicism is commonly linked to the recombination machinery consisting of a cluster of three genes: exonuclease Exo (AAA96569.1), ssDNA-binding protein Bet (AAA96570.1) and host nuclease inhibitor protein Gam (AAA96571.1) (Hillyar 2012).

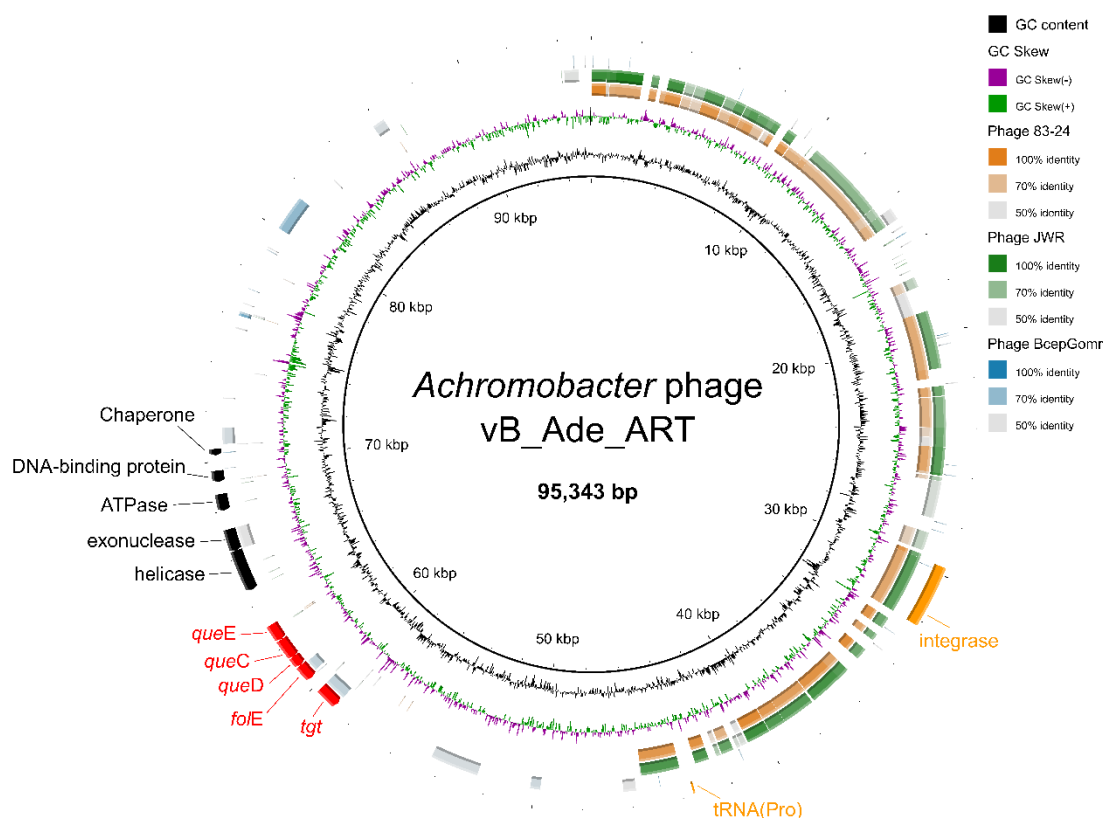


Figure 5.7 – Circular representation of the genome of *Achromobacter* phage vB_Ade_ART obtained with BRIG (Alikhan et al. 2011). The beginning of the genome is placed on the leftmost side of the virion DNA.

The genomes of the closest relatives were aligned with BLAST+ and are represented as follows: *Achromobacter* phage 83-24 (orange), *Achromobacter* phage JWR (green) and *Burkholderia* phage BcepGomr (blue). Genes from the queuosine biosynthetic cluster are represented in red; genes possibly involved in recombination are represented in black.

However, phage vB_Ade_ART has no close homologs to any of these genes in its genome. Despite the lack of closely related genes, the functional annotation of phage ART genome revealed the presence of a gene cluster in the intermediate region linked with DNA replication, recombination and repair. These genes consist of a helicase (ART_00086), exonuclease (ART_00087), ATPase AAA (ART_00089), putative DNA-binding protein (ART_00092) and a chaperone protein DnaJ (ART_00095). Furthermore, phage

vB_Ade_ART harbors part of the non-essential queuosine biosynthetic pathway, a rare nucleoside which may protect phage DNA against host endonucleases (Nikolskaya et al. 1976; Kulikov et al. 2014; Thiaville et al. 2016).

In contrast to phage lambda, which relies on protein Gam for protection, phage vB_Ade_ART harbors several genes of the queuosine pathway, including *tgt*, *queC*, *queD*, *queE* and *foIE* (locus tag ART_00075 and ART_00078 to ART_00081, respectively), which may carry out a similar function. The presence of this cluster has been reported in other phages from the *Siphoviridae* family namely in several members of the genus *Seuratvirus* and well characterized in *Escherichia coli* phage 9g (Kulikov et al. 2014; Sazinas et al. 2018).

5.4.7 Effect of phage in the sulfonamide-degrading consortium

The highest burst size of the phage was obtained at the multiplicity of infection MOI= 10. The efficiency of plating was slightly higher (with minor differences in titer) when propagating *Achromobacter* PR1 alone, rather than in the consortium of this strain and the low-abundance *Leucobacter* sp. GP. Although, at some multiplicities, phage infection was more successful in the presence of this actinobacterium (Fig. 5.8). As a result, the inhibition of phage infection by this dependent strain was excluded. Moreover, co-inoculation of the phage and the consortium resulted in a significantly higher abundance of *Leucobacter* sp. strain GP after 48 h of incubation at all MOI ($p > 0.05$) when compared with the control (Fig. 5.9).

This effect was slightly enhanced at high MOI values, suggesting that a higher amount of phage particles in comparison to PR1 cells favors the propagation of this phage in the culture and enhances the abundance of the slow-growing actinobacterium.

Interestingly, SMX degradation was more efficient at lower MOI values ($p > 0.05$). This result was expected based on our previous observations that the growth of strain GP may be linked to the viability of its helper – strain PR1 (Reis et al. 2018a). In this way, optimal

SMX degradation efficiency is achieved with a specific ratio between the two strains, and not only correlated with the overall abundance of strain GP.

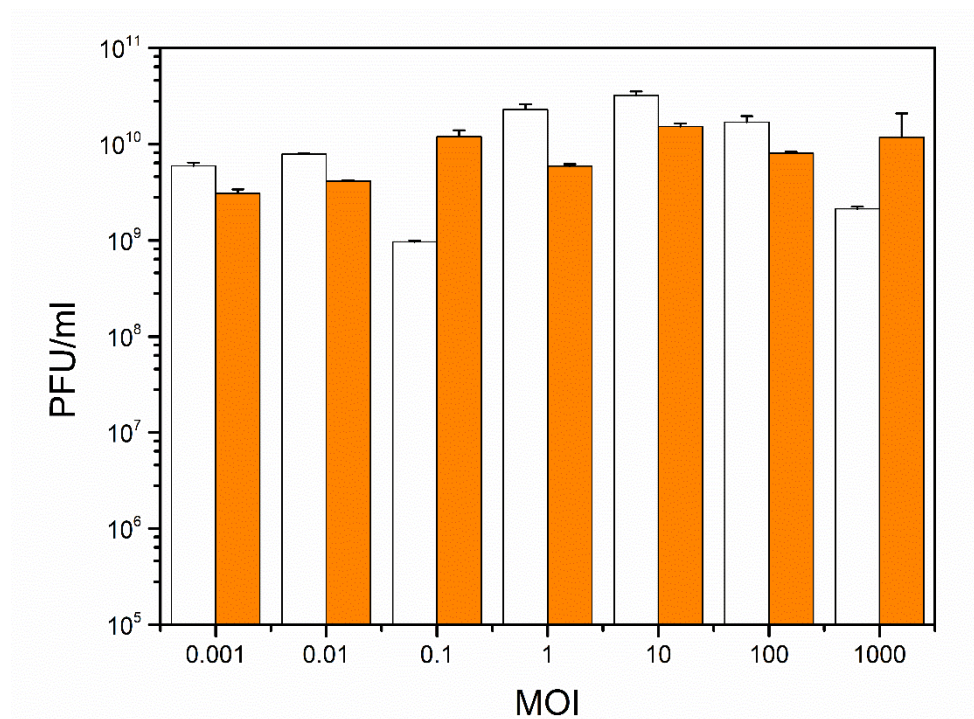


Figure 5.8 – Phage titer at different multiplicity of infection (MOI) in *Achromobacter denitrificans* PR1 and in the consortium between this strain and *Leucobacter* sp. GP. Values for phage titer in PFU/ml in strain PR1 (white bars) and in the microbial consortium (orange bars) are in logarithmic scale and represent the mean of triplicates and error bars the standard deviation.

Specifically, at high MOI, plating efficiency showed a considerable decrease in the viability of strain PR1 (Table 5.4). Nevertheless, we observed no considerable decrease in the 16S rRNA gene copy number for strain PR1. These results suggest that either the pellet used for extraction contained lysed and non-viable PR1 cells or it may point out to incomplete or inefficient lysis of this strain. This result agrees with previously published observations (Wittmann et al. 2014a) whereas the efficiency of the lysis was always low when a single bacteriophage was applied as a biocontrol tool. In this way, for effective biocontrol of a specific bacterial strain, the application of a phage cocktail of two or more phages would be a more suitable approach (Chan et al. 2013).

Table 5.4 – Viability (log CFU/ml) of strain PR1 determined by plating after 90 min incubation in mineral medium (MMSY – SMX) at different MOI.

Multiplicity of infection (MOI)	Strain PR1 viable cells (log CFU/ml)	
	Initial	90 min incubation
Control without phage	8.18 ± 0.04	8.90 ± 0.08
10	7.27 ± 0.03	4.90 ± 0.08
1	7.63 ± 0.21	7.26 ± 0.26

The enhanced degradation efficiency and increased abundance of strain GP obtained in this study indicate that phages could be used as useful biocontrol tools to engineer microbial communities and increase the efficiency of specific biological functions.

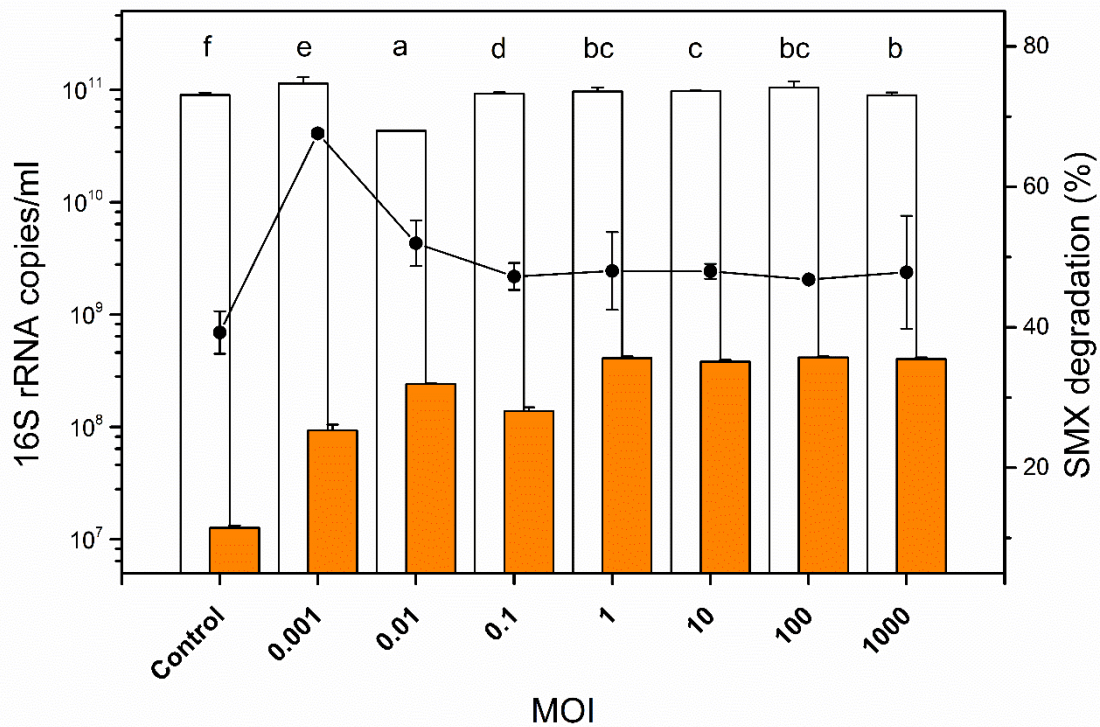


Figure 5.9 – Effect of phage vB_Ade_ART in the abundance of *Leucobacter* sp. strain GP in the consortium with *A. denitrificans* strain PR1 after 48 h of incubation in MMSY with 0.6 mM SMX. Values for 16S rRNA gene copies per ml for strain PR1 (white bars) and strain GP (orange bars) are in logarithmic scale. Degradation of SMX (●) is represented as the percentage of antibiotic concentration decrease. Abiotic controls present negligible degradation of SMX. At all MOI, phage titer after 48 h is of 9.85 ± 0.30 log PFU/ml. All values are the mean of triplicates and error bars represent the standard deviation. Significant differences in strain GP / strain PR1 ratio are indicated by a, b, c, d, e and f (from higher to lower values of the mean) as determined by one-way ANOVA and the Tukey test at $p < 0.05$.

5.5 Conclusions

In conclusion, in this study we isolated a new polyvalent phage able to infect multiple species of the *Achromobacter* genus. Genomic analysis of the phage revealed a highly mosaic nature, suggesting that this phage underwent extensive recombination. The findings obtained in this study provide new insights into the nature of environmental *Achromobacter* phages. Further studies suggested that this phage could influence the stability and evolution of a sulfonamide-degrading consortium, slightly enhancing its efficiency, however, more studies are necessary to understand the effectiveness of this phage in contaminated natural systems.

Chapter 6

Comparative genomics reveals a novel genetic organization of the sad cluster in the sulfonamide-degrader '*Candidatus* Leucobacter sulfamidivorax' strain GP

Manuscript under revision:

A.C. Reis, B.A. Kolvenbach, P.F.-X. Corvini, M. Chami, L. Gales, C. Egas, O.C. Nunes.

"Comparative genomics reveals a novel genetic organization of the sad cluster in the sulfonamide-degrader '*Candidatus* Leucobacter sulfamidivorax' strain GP". BMC Genomics.

Under revision.

6.1 Abstract

Background: Microbial communities recurrently establish metabolic associations resulting in increased fitness and ability to perform complex tasks, such as xenobiotic degradation. In a previous study, we have described a sulfonamide-degrading consortium consisting of a novel low-abundant actinobacterium, named strain GP, and *Achromobacter denitrificans* PR1. However, we found that strain GP was unable to grow independently and could not be further purified.

Results: Previous studies suggested that strain GP might represent a new putative species within the *Leucobacter* genus (16S rRNA gene similarity < 97 %). In this study, we found that average nucleotide identity (ANI) with other *Leucobacter* spp. ranged between 76.8 and 82.1 %, further corroborating the affiliation of strain GP to a new provisional species. The average amino acid identity (AAI) and percentage of conserved genes (POCP) values were near the lower edge of the genus delimitation thresholds (65 and 55 %, respectively). Phylogenetic analysis of core genes between strain GP and *Leucobacter* spp. corroborated these findings.

Comparative genomic analysis indicates that strain GP may have lost genes related to tetrapyrrole biosynthesis and thiol transporters, both crucial for the correct assembly of cytochromes and aerobic growth. However, supplying exogenous heme and catalase was insufficient to abolish the dependent phenotype. The actinobacterium harbors at least two copies of a novel genetic element containing a sulfonamide monooxygenase (*sadA*) flanked by a single IS1380 family transposase. Additionally, two homologs of *sadB* (4-aminophenol monooxygenase) were identified in the metagenome-assembled draft genome of strain GP, but these were not located in the vicinity of *sadA* nor of mobile or integrative elements.

Conclusions: Comparative genomics of the genus *Leucobacter* suggested the absence of some genes encoding for important metabolic traits in strain GP. Nevertheless, although media and culture conditions were tailored to supply its potential metabolic needs, these

conditions were insufficient to isolate the PR1-dependent actinobacterium further. This study gives important insights regarding strain GP metabolism; however, gene expression and functional studies are necessary to characterize and further isolate strain GP.

Based on our data, we propose to classify strain GP in a provisional new species within the genus *Leucobacter*, '*Candidatus Leucobacter sulfamidivorax*'.

6.2 Background

Microbial communities are known to establish sophisticated metabolic interactions in order to achieve complex and energy-expensive tasks (Jetten et al. 2005a; Lykidis et al. 2011; Oshiki et al. 2013; Wu et al. 2013; Ponomarova and Patil 2015). These syntrophic relationships are frequently studied in bacterial pathogens and symbiotic bacteria, where the interaction with the host often drives progressive adaptation, mutation, and subsequently, gene loss. These phenomena may render the bacteria “unculturable” or difficult to grow under standard laboratory conditions (Silva et al. 2001; Moran 2003; Stewart 2012; Pham and Kim 2012; Bryant et al. 2012; Vartoukian et al. 2016).

On the contrary, the phenomena underlying metabolic cooperation and competition within environmental communities are often more complex, and their implications for microbial ecology are still poorly understood (Stewart 2012; Ponomarova and Patil 2015). These communities recurrently exchange metabolites or co-factors and are often associated with xenobiotic-degraders thriving in polluted environments (Schloss and Handelsman 2005; Merhej et al. 2009; Stewart 2012; Morris et al. 2013; Ponomarova and Patil 2015; Widder et al. 2016). This syntrophy has been previously observed in terephthalate-degrading communities (Lykidis et al. 2011; Wu et al. 2013), anammox (Jetten et al. 2005a; Jetten et al. 2005b; Oshiki et al. 2013), in the dichloromethane-degrader '*Candidatus Dichloromethanomonas elyunquensis*' (Kleindienst et al. 2017), and in members of the candidate phylum '*Candidatus Latescibacteria*', that thrive in hydrocarbon-impacted environments (Youssef et al. 2015; Farag et al. 2017). However, to

date, no representatives of these groups could be isolated as pure cultures and their metabolic needs are difficult to assess.

Terephthalate-degraders, for instance, thrive in an intricate network formed between H₂-producing syntrophs and methanogenic archaea, with numerous other secondary interactions essential for the stability of the consortium (Lykidis et al. 2011; Wu et al. 2013). Anammox bacteria were shown to form stable biofilm communities with ammonia-oxidizing bacteria (AOB), that appear to be essential to protect the sensitive anammox species from atmospheric O₂ (Jetten et al. 2005a; Kindaichi et al. 2007; Oshiki et al. 2013; Ma et al. 2015).

The evolution of these communities is driven by selective pressure and stress and may result in complex syntrophic relationships that may lead to niche-specialization and dependency on other members of the community. In order to characterize the members of these communities, cell-sorting and metagenomics approaches are being used to circumvent the need for cultivation (Schloss and Handelsman 2005). Furthermore, these studies are frequently complemented with comparative genomics which has emerged as a valuable tool to determine the evolution and functional prediction between even distantly related bacteria (Makarova et al. 2006; Lee et al. 2008; Merhej et al. 2009). The cultivation of several members of the ubiquitous SAR11 aquatic bacteria, with no closely related culturable relatives, has been made possible by *in silico* metabolic studies and next-generation sequencing approaches (Tripp 2013). Furthermore, the evolution of this abundant group of *Alphaproteobacteria* and their ecological importance has been further elucidated using comparative genomic approaches (Thrash et al. 2014).

In a previous study, we have described a microbial consortium between *Achromobacter denitrificans* strain PR1 and strain GP that depends on strain PR1's presence for growth (Reis et al. 2018a). Strain GP showed the highest pairwise similarity of its 16S rRNA gene sequence to members of the genus *Leucobacter*. Independently of the tested culture media,

cofactors and culture conditions no pure cultures were obtained for strain GP (Reis et al. 2018a). To characterize strain GP, we have sequenced the two-member consortium and reconstructed its draft genome. Also, we performed comparative genomic studies in order to understand its phylogenetic relationship with other members of the *Leucobacter* genus and propose the hypothesis that may allow us to understand why this strain has eluded isolation in previous studies.

6.3 Results and discussion

6.3.1 Morphological and physiological characterization of the consortium

The microbial consortium between strain *A. denitrificans* and the low-abundant strain GP was visualized by Cryo-TEM during mid-stationary phase (Fig. 6.1), as well as by FISH (Fig. 6.2). As expected, strain PR1 showed the typical morphology of Gram-negative rods with an average cell size of 801.3 ± 40.2 nm (width), 1332 ± 98.7 nm (length) and 38.2 ± 6.5 nm (periplasmic space) (Fig. 6.1a). Moreover, peritrichous flagella were observed by negative stain electron microscopy (FG, Fig. 6.1c and d). Although flagella have not been previously reported for the type strain of *A. denitrificans*, their presence has been repeatedly observed in other strains from this species (Glupczynski et al. 1988) and other species of the *Achromobacter* genus (Igra-Siegman et al. 1980; Nejidat et al. 2008). Conversely, strain GP displayed the typical morphology of Gram-positive rods. Its cells showed an average size of 506.6 ± 30.1 nm (width) and 1341.0 ± 29.7 nm (length) (Fig. 6.1b), and the rigid cell wall of this organism had an average thickness of 20.6 ± 2.2 nm. No flagella were observed for this bacterium, suggesting that it is non-motile, like previously reported for other members of the *Leucobacter* genus (Morais et al. 2006; Sturm et al. 2011).

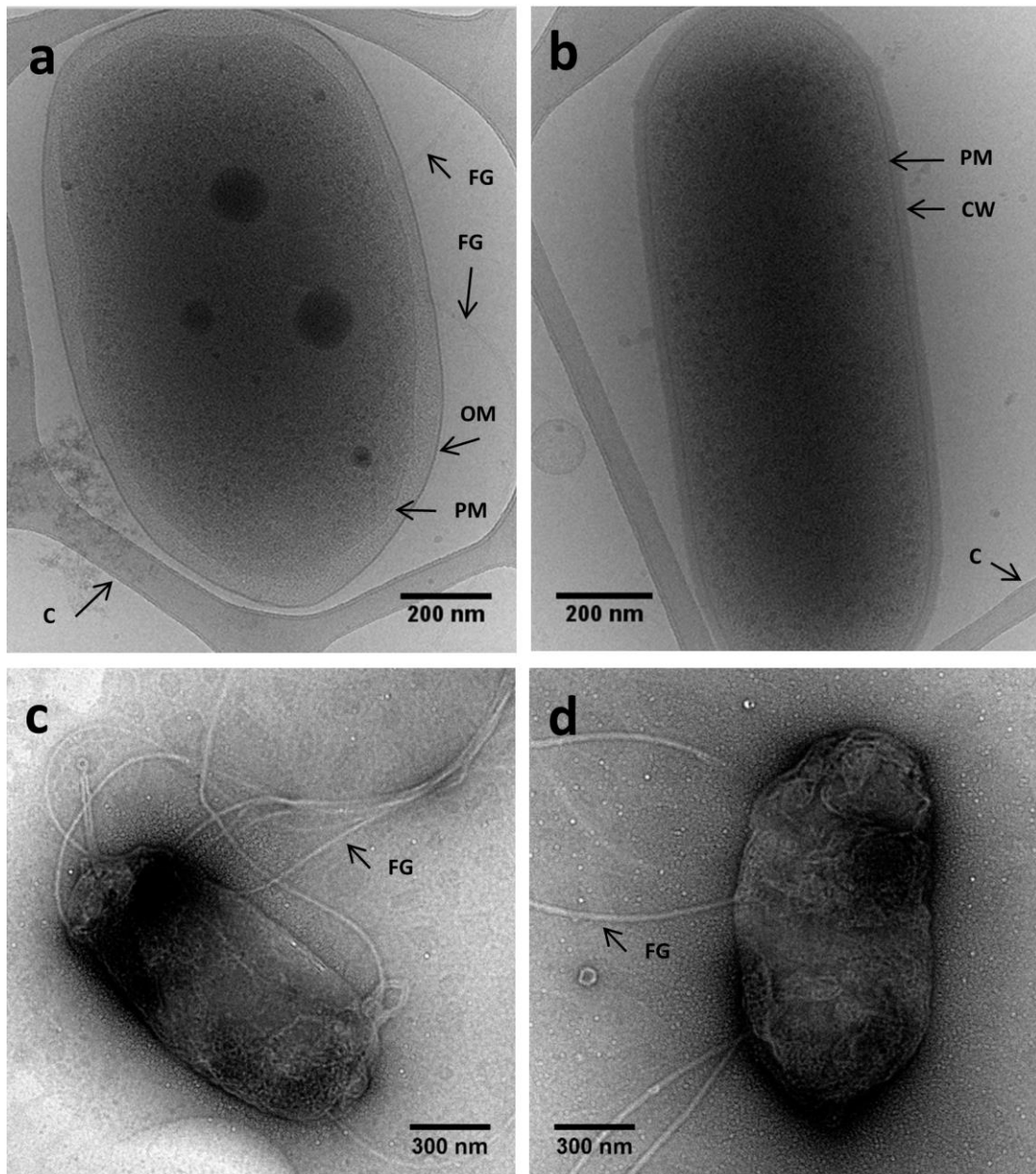


Figure 6.1 - Electron micrographs of frozen hydrated *Achromobacter denitrificans* strain PR1 (a) and strain GP (b). Micrographs of negatively stained *A. denitrificans* PR1 showing the presence of peritrichous flagella (c and d). PM - Plasma membrane; OM - Outer membrane; FG - Flagellum; CW - Cell wall; C - Carbon support grid.

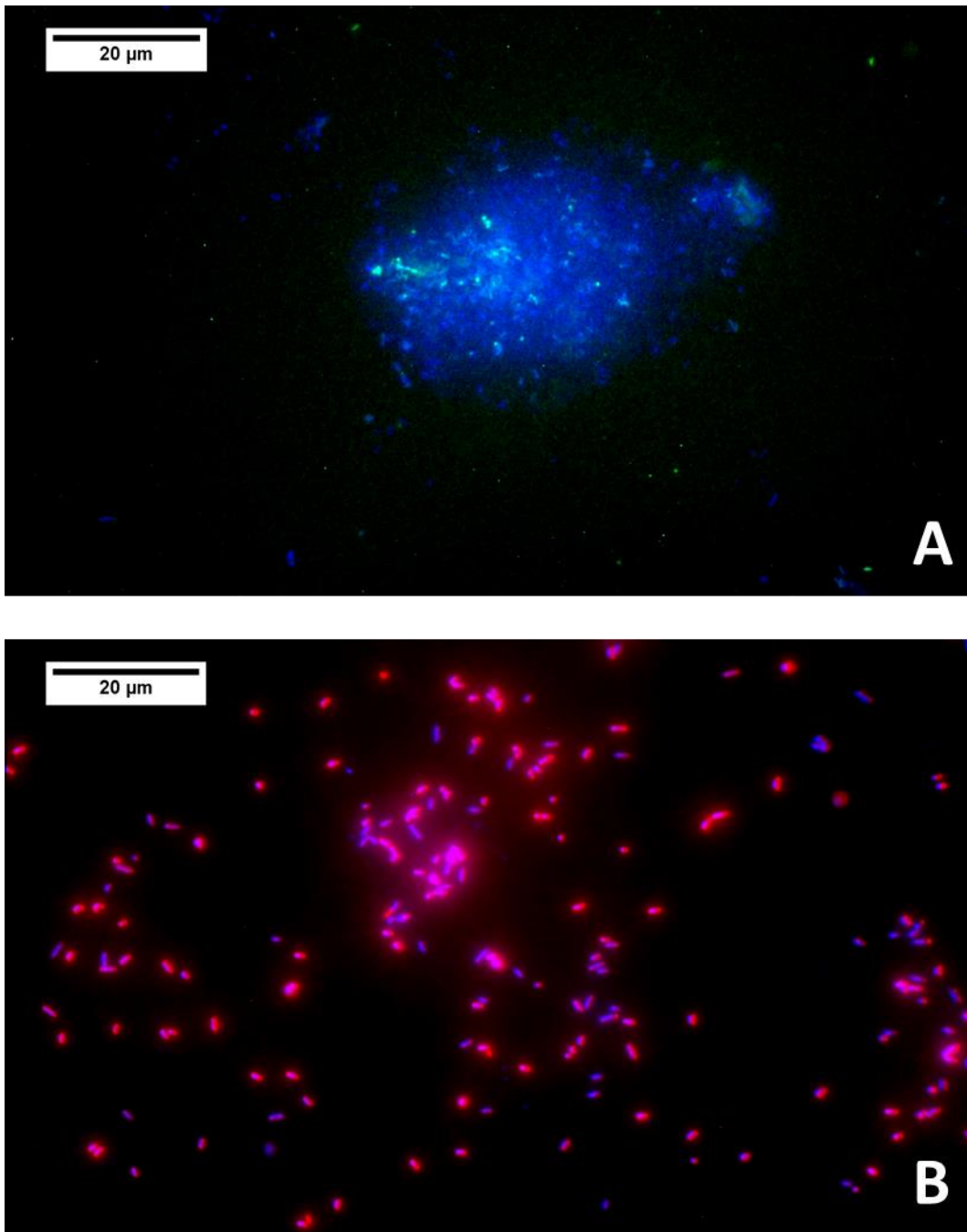


Figure 6.2 – Fluorescence microscopy composite images of DAPI-stained cells of the microbial consortium (blue) and (A) cells hybridized with the modified ActORD1 FISH probe (stains strain GP, 5' fluorophore: FAM, green) or with (B) cells hybridized with Alca2 FISH probe (stains strain PR1; 5' fluorophore: Cy3, orange/red).

The two members of the consortium revealed significant differences regarding their respective tolerances toward temperature, pH and salinity (Fig. 6.3). While the abundance of strain PR1 was constant when incubating at 22, 30 and 37 °C, respectively, strain GP abundance was significantly reduced at 37 °C ($p < 0.05$) when compared to the other tested temperatures. Strain GP also showed a lower abundance when incubated at pH 5.5,

in comparison to cultures incubated in media at neutral (pH 7.2) and basic (pH 9.5) pH values (Fig. 6.3). As it is typically observed for members of the *Achromobacter* genus (Vandamme et al. 2016), NaCl concentrations up to 4 % (w/v) did not influence the abundance of strain PR1; however, its abundance was significantly reduced above this value (Fig. 6.3). Although the absolute amount of strain GP 16S rRNA copy numbers also decreased above 4 % NaCl (w/v), the relative abundance of this strain in the consortium was significantly higher (ranging from 0.24 % at 0 % NaCl, to a maximum of 4.26 % at 8 % NaCl). Interestingly, the abundance of strain GP was significantly lower in complex media (TSA, BHI, and R2A) than in mineral media with defined carbon sources (MMSY, Fig. 6.4).

These results suggest that strain GP is possibly oligotrophic, unlike previously described for members of the *Leucobacter* genus, which thrive in complex media, such as BHI enriched with peptone and yeast extract, as observed for *L. luti* RF6^T (Morais et al. 2006).

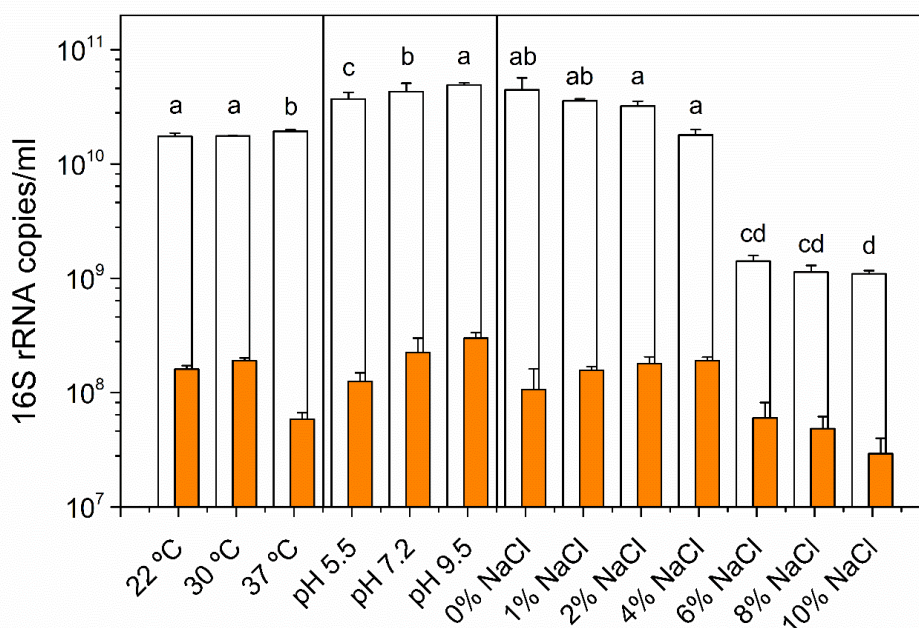


Figure 6.3 – Abundance of strain PR1 and strain GP after 15 h incubation at different pH and salinity in DLB and at different temperatures in MMSY. The values for copies of the 16S rRNA gene per ml are plotted in logarithmic scale for strains PR1 (white) and GP (orange). Values are the mean values of triplicates and the error bars represent the standard deviation. Significant differences in strain GP abundance are indicated by a, b, c and d (from higher to lower values of the mean) as determined by two-way ANOVA and the Tukey test at $p < 0.05$ within each tested condition (pH, temperature and salinity) (R Core Team 2015).

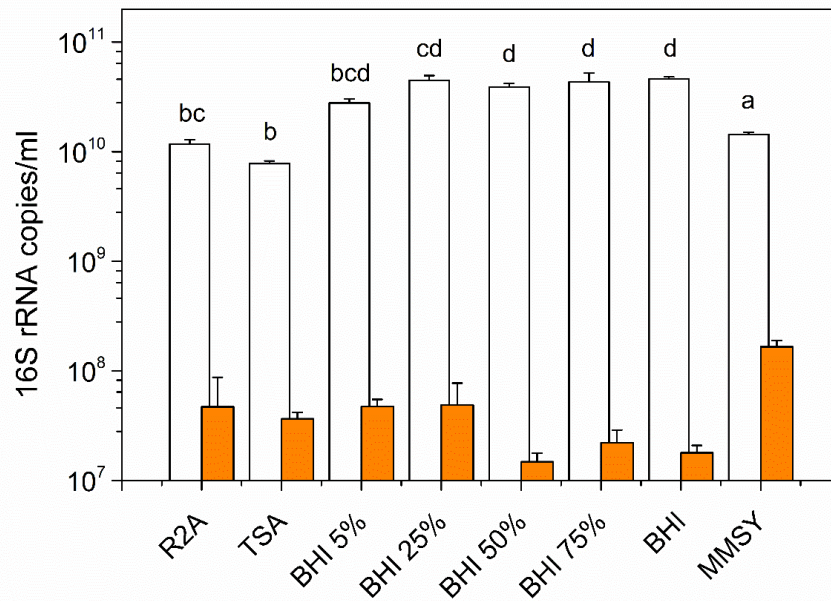


Figure 6.4 - Abundance of strain PR1 and strain GP after 15 h incubation in different media. The values for copies of the 16S rRNA gene per ml are plotted in logarithmic scale for strains PR1 (white) and GP (orange). Values are the mean values of triplicates, and the error bars the standard deviation. Significant differences in strain GP abundance (16S rRNA copy numbers of strain GP divided by those of PR1) are indicated by a, b, c and d (from higher to lower values of the mean) as determined by one-way ANOVA and the Tukey test at $p < 0.05$ among all tested media (R Core Team 2015).

6.3.2 Analysis of the metagenome-assembled genome of strain GP

The analysis of the metagenomic contigs with SSU finder (rRNA small subunit) from CheckM (Parks et al. 2015) revealed the presence of only two phylogenetic distinct organisms: one identified as *A. denitrificans* PR1 and the other as strain GP. The reconstruction of strain GP's genome from whole-consortium sequencing generated a MAG consisting of 11 contigs, with 3.84 Mb, 3,621 CDS, 69.68 % in G+C and a total mapped coverage of 61x (Table 6.1). In spite of an enrichment step with 2-phenylethanol, only 18.5% of the total of reads obtained with Oxford Nanopore (ONT) and Illumina technologies were mapped to strain's GP MAG, while the remaining reads mapped to the complete genome of *A. denitrificans* PR1 (Table 6.2), previously determined (Reis et al. 2017).

Table 6.1 – List of named species of the *Leucobacter* genus used in the phylogenetic and comparative studies. Assembly quality was calculated using QUAST (Konstantinidis and Tiedje 2005) with a minimum contig size set to 200 bp. Completeness and contamination were computed with CheckM (Parks et al. 2015). 16S rRNA pairwise similarity was computed with the global alignment tool in the EzBioCloud web server (Yoon et al. 2017). Strains sequenced in this study are shown in bold.

Strain	16S rRNA pairwise similarity to GP	Genome*/ assembly accession no.	Completeness (%)	Contamination (%)	Number contigs/ scaffolds	Genome size (Mb)	Contig N50	G+C content (%)	Number of CDS	Reference
'Candidatus Leucobacter sulfamidivorax' GP	-	QZLF00000000	95.91	0.58	11	3.84	956,104	69.68	3,621	This study
<i>L. aridicollis</i> L-9^T	96.23 %	QYAE00000000	99.27	0.58	8	3.56	888,847	67.3	3,212	This study
<i>L. celer</i> subsp. <i>astrifaciens</i> CBX151 ^T	95.87 %	GCA_001273835.1	98.83	0.00	235	4.14	349,813	69.1	3,661	Clark and Hodgkin (2015)
<i>L. chironomi</i> MM2LB ^T	95.43 %	GCA_000421845.1	100.00	0.88	27	2.96	268,438	69.9	2,662	Laviad et al. (2015)
<i>L. chromiireducens</i> subsp. <i>chromiireducens</i> L-1^T	96.23 %	QYAD00000000	100.00	0.58	6	3.22	623,960	67.0	2,843	This study
<i>L. chromiireducens</i> subsp. <i>solipictus</i> TAN 31504^T	96.15 %	QYAC00000000	99.42	2.05	11	3.54	451,461	68.9	3,096	This study
<i>L. chromiiresistens</i> J31 ^T	96.23 %	GCA_000231305.1	100.00	0.00	2	3.21	2,823,343	70.3	2,895	Sturm et al. (2011)
<i>L. chromiiresistens</i> NS354	96.37 %	GCA_001477055.1	95.03	0.00	194	2.79	35,220	70.8	2,423	Midha et al. (2016)
<i>L. komagatae</i> DSM 8803 ^T	96.79	GCA_006716085.1	98.54	1.75	2	3.75	3,292,530	66.6	3,253	Unpublished
<i>L. luti</i> RF6 ^T	96.81 %	QYAG00000000	100.00	0.58	5	3.62	1,858,864	69.4	3,088	This study
<i>L. massiliensis</i> 122RC15 ^T	96.52 %	GCA_002982315.1	100.00	1.75	24	3.14	232,656	71.0	2,789	Leangapichart et al. (2018)
<i>L. musarum</i> subsp. <i>japonicus</i> CBX130 ^T	95.87 %	GCA_001273855.1	99.56	0.58	144	3.59	248,155	66.8	3,311	Clark and Hodgkin (2015)
<i>L. musarum</i> subsp. <i>musarum</i> CBX152 ^T	95.87 %	GCA_001273845.1	99.85	0.58	125	3.44	200,785	66.8	3,147	Clark and Hodgkin (2015)
<i>L. salsicius</i> M1-8 ^T	95.94 %	GCA_000350525.1	99.42	0.00	28	3.18	197,637	64.5	2,741	Yun et al. (2014)
<i>L. triazinivorans</i> JW-1 ^T	96.4	GCA_004208635.1	100.00	0.88	1	3.48	-	69.37	2,978	(Sun et al. 2018)
<i>L. zeae</i> CC-MF41^T	95.88 %	QYAB00000000	99.85	0.58	6	3.47	2,226,772	70.6	3,042	This study

The MAG of strain GP encoded a complete rRNA operon and harbored two copies of the 5S and one copy of the 16S and 23S rRNA subunits, respectively. Moreover, analysis with tRNAscan-SE (Lowe and Chan 2016) identified 44 tRNA encoding for all 20 amino acids. Analysis with CheckM (Parks et al. 2015) showed high completeness and low contamination values for this assembly as only 7 marker genes were not detected in the draft genome and 3 markers had 2 copies in the assembly (95.9 % completeness and 0.6 % contamination, respectively). Therefore, according to Bowers et al. (2017), these findings indicate that this methodology allowed the reconstruction of a high-quality MAG for strain GP.

Table 6.2 - Mean coverage and GC content per strain and contig in the metagenome assembly of the consortium consisting of *Achromobacter denitrificans* PR1 and '*Candidatus* *Leucobacter sulfamidivorax*'

Strain/Contig	CDS	Size (bp)	Mapped coverage (x)			G+C (%)
			Illumina	ONT	Total	
PR1 / Genome	6,357	6,929,205	58.8	89.6	148.4	67.40
GP / 1	1,415	1,477,215	13.6	42.2	61.0	70.09
GP / 2	861	956,104	13.6	41.9		70.26
GP / 3	796	867,453	14.4	43.3		68.92
GP / 4	347	329,436	14.0	42.8		69.85
GP / 5	80	74,101	42.2	109.1		63.24
GP / 6	59	65,197	12.9	39.7		71.71
GP / 7	25	22,555	128.5	357.5		62.64
GP / 8	13	15,023	12.8	45.9		70.20
GP / 9	8	11,854	44.3	133.4		64.29
GP / 10	11	11,114	16.5	45.5		67.51
GP / 11	6	7,813	13.4	38.5		70.79

6.3.3 Analysis of mobile and conjugative elements

The identification of potential plasmids and other mobilizable elements in the genome of strain GP was performed *in silico* by measuring differences in coverage and G+C content between the contigs of the draft assembly. Compared to the average values for all contigs, for at least three (5, 7 and 9) showed a significantly higher coverage, and lower G+C content (Table 6.2). The differential coverage among contigs was observed consistently

with both Illumina and ONT libraries, which were prepared from different biological replicates of the consortium. Therefore, these differences are unlikely to arise from library preparation and sequencing bias. The differences encountered suggest that these contigs may represent potential plasmids with an average copy number per cell of approximately 2-3 (contigs 5 and 9) and 9 (contig 7), respectively. Furthermore, conserved domain search and CONJscan revealed the presence of several elements linked to plasmid replication, stability, partitioning, conjugation, and mobility (Table 6.3).

Out of these three contigs, only contig 9 (11.8 kb) was marked as circular by Circlator (Hunt et al. 2015); however, it had no relevant hits to other plasmids available in the National Center for Biotechnology Information (NCBI) database. Contrarily, contig 7 (22.5 kb) featured residual homology to a new plasmid found in *Cnuibacter physcomitrellae* XA^T (accession number CP020716.1, 4,285 bp alignment with 99 % identity to this plasmid), and the plasmid pKpn-35963cz from *Klebsiella pneumoniae* Kpn-35963cz (accession number MG252894.1, 2,030 bp alignment with 99 % identity to this plasmid). The respective homologous regions contained genes encoding for transposases and mercury resistance. Both contigs 7 and 9 carry a gene encoding for a putative relaxase (locus tag: D3X82_18105, D3X82_18250, respectively) with a TrwC family domain (accession no. pfam08751; E-value: 3.7e-28 and 7.6e-25, respectively), commonly observed in proteins from the MOB_F (mobility) family (e.g., TraA from *Arthrobacter* sp. Chr15, accession no. ABR67091.1 (Garcillán-Barcia et al. 2009)). This classification was further confirmed by CONJscan (Guglielmini et al. 2014; Mareuil et al. 2017; Afgan et al. 2018), which found that both D3X82_18105 (contig 7) and D3X82_18250 (contig 9) possess a highly conserved MOB_F domain (E-values of 5.3e-105 and 4.1e-106, respectively). Additional mobility elements were only found in contig 7. This contig was found to harbor a putative plasmid replication protein (locus tag: D3X82_18090; Family: RepA_C; accession no: pfam04796; E-value: 9.0e-07).

Table 6.3 – Genes and corresponding conserved domains linked to integrative, conjugative and resistance elements found in contigs 5, 7 and 9 from the draft assembly of strain GP. Families and E-values in bold indicate the best hits obtained with CONJscan (Abby et al. 2014). n.a., not applicable.

System	Contig	Locus tag	Description	Family	Accession	E-value
Replication, stabilization and partitioning	5	D3X82_17420	Toxin protein from a toxin/antitoxin system	Zeta_toxin	pfam06414	1.6e-19
	5	D3X82_17550	Plasmid partition protein A	BcsQ	COG1192	2.2e-43
	5	D3X82_17555	Single-stranded DNA-binding protein	SSB_OBF	cd04496	8.5e-12
	7	D3X82_18090	Plasmid replication protein	RepA_C	pfam04796	9.0e-07
Mobilization and conjugative elements	5	D3X82_17410	Plasmid mobilization relaxosome protein MobC	MobC	pfam05713	5.7e-05
	5	D3X82_17470	Conjugal transfer protein	TrwC	pfam08751	9.0e-97
	5	D3X82_17385	Type IV secretion protein (T4SS)	MOB_F	n.a.	1.3e-85
	5	D3X82_17390	Coupling protein (T4CP)	VirB4	n.a.	1.40e-25
	5	D3X82_17390	Coupling protein (T4CP)	VirD4	COG3505	4.2e-16
	5	D3X82_17405	Relaxase	T4CP2	n.a.	5.7e-40
	5	D3X82_17405	Relaxase	Relaxase	pfam03432	9.8e-10
	5	D3X82_17405	Relaxase	MOB_{P1}	n.a.	4.20e-40
Multi-drug and heavy metal resistance	7	D3X82_18105	Conjugal transfer protein	TrwC	pfam08751	3.7e-28
	7	D3X82_18105	Conjugal transfer protein	MOB_F	n.a.	5.3e-105
	9	D3X82_18250	Conjugal transfer protein	TrwC	pfam08751	7.6e-25
	9	D3X82_18250	Conjugal transfer protein	MOB_F	n.a.	4.1e-106
	5	D3X82_17365	Sulfonamide monooxygenase	NcnH	cd01159	1.52e-84
	5	D3X82_17695	SadA	CaiA	COG1960	1.93e-30
	5	D3X82_17695	SadA	Acyl-CoA_dh_2	pfam08028	5.8e-20
	5	D3X82_17485	Tet(A)/Tet(B)/Tet(C) family tetracycline efflux MFS transporter	MFS_TetA	cd17388	2.4e-145
	5	D3X82_17505	ANT(3'')-Ia family aminoglycoside nucleotidyltransferase AadA1	PRK13746	PRK13746	0e+00
	5	D3X82_17505	ANT(3'')-Ia family aminoglycoside nucleotidyltransferase AadA1	DUF4111	pfam13427	1.31e-41
5	D3X82_17510	Quaternary ammonium compound efflux SMR transporter QacE delta 1	Multi_Drug_Res	pfam00893	1.75e-28	
5	D3X82_17515	Sulfonamide-resistant dihydropteroate synthase Sul1	Pterin_bind	pfam00809	1.8e-87	
5	D3X82_17685	Mercury(II) reductase	MerA	TIGR02053	1.2e-171	

In this way, according to Guglielmini et al. (Guglielmini et al. 2014) and Smillie et al. (Smillie et al. 2010), the presence of a MOB element in contigs 7 and 9 suggests these putative elements are mobilizable but non-conjugative. Contig 5, with 74 kb, was found to contain various integrative and conjugative elements (Table 6.3) (Martini et al. 2016). Besides, this contig contained all antimicrobial resistance genes found in the genome of strain GP (*sul1*, *tet(33)*, *aadA1*, *qacE*), as well as two copies of the *sadA* gene encoding for the previously described sulfonamide monooxygenase (Reis et al. 2018a).

Homology searches for contig 5 against the NCBI database (NCBI Resource Coordinators 2017) revealed residual homology to *Enterobacter cloacae* strain EclC2185's genomic island (accession number MH545561.1, 5,187 bp alignment with 99 % identity to the genomic island of this strain) containing a class I integron with multi-drug resistance genes (*aadA1*, *sul1*, and *qacE*). Other significant alignments included regions conferring mercury resistance (*Cnuibacter physcomitrella* XA^T plasmid, accession number CP020716.1, 5,928 bp alignment with 99 % identity to this plasmid) and intergenic regions of the new plasmid pOAD2 from *Flavobacterium* sp. KI723TI (accession number D26094.1, 14,820bp alignment with 94 % to this plasmid).

According to conserved domain search and CONJscan analyses, two putative MOB elements were found in contig 5: (i) D3X82_17470, a relaxase from the MOB_F family with a TwrC conserved domain (CONJscan domain search: E-value 1.3e-85); (ii) D3X82_17405, a relaxase from the MOB_{P1} family (CONJscan domain search: E-value 4.2e-40). Other essential mobilizable elements detected include a type IV coupling protein (T4CP, locus tag D3X82_17390) with a conserved VirD4 domain (CONJscan domain search: E-value 5.7e-40) and a type IV secretion protein (T4SS, locus tag D3X82_17385) with a VirB4 domain (CONJscan domain search: E-value 1.4e-25). According to Smillie et al. (Smillie et al. 2010), these three elements are at the core of plasmid conjugation, however, no other known accessory proteins were detected in our analysis, presumably due to incomplete assembly and/or low identity to previously characterized proteins from the mating-pair

formation (MPF) system. In this way, no complete type IV secretion systems were detected in contig 5 suggesting this element may be mobile but possibly not conjugative.

6.3.4 Phylogenetic analysis

As reported previously, strain GP shares the highest 16S rRNA gene sequence similarity with members of the genus *Leucobacter* (94.6-96.9 %, Table 6.4), below the 98.7 % threshold currently used to define a new species (Chun et al. 2018; Reis et al. 2018a) and the close to 97 % threshold used to define a new genus (Stackebrandt and Goebel 1994). The phylogenetic analysis inferred from the alignment of the near-complete 16S rRNA gene between all the type strains of the *Microbacteriaceae* family and all fully sequenced *Leucobacter* spp. showed that strain GP indeed clusters with *Leucobacter* spp. (Fig. 6.5).

Nevertheless, the ANI values between strain GP and the type strains of the validly named species of this genus ranged between 80.0 and 82.1 % (Fig. 6.6a), well below the general species delimitation thresholds (94-96 %) (Konstantinidis and Tiedje 2005; Richter and Rosselló-Móra 2009), indicating that strain GP could not be affiliated to any of these species. Average amino acid identity (AAI) comparisons between this strain and the type strains of the validly named species of this genus ranged between 64.2 and 69.1 % (Fig. 6.6b). These values are near the lower edge of the typical genus delimitation boundaries (approximately 65 %) (Konstantinidis and Tiedje 2005), and the specific interspecies boundaries found between the analyzed type strains of *Leucobacter* spp. (51.0 – 87.3 %). This result was further supported by the percentage of conserved genes (POCP) (Qin et al. 2014). POCP values ranged between 46.7 and 56.5 % (Fig. 6.6c), which is also on the lower edge of the interspecies boundaries found for this genus (42.0 – 81.3 %) and the value suggested by Qin et al. (Qin et al. 2014) for new genus delimitation (55 %).

Table 6.4 – List of all bacterial strain used for comparative genomics. (T) type strain; (*) sulfonamide degraders; N.A. not available; (bold) strains sequenced in this study; (1) available on Github ; * the 16S rRNA gene sequence of this strain has a gap between positions 706 and 761; ** no rRNA was annotated in this sequence; cells highlighted in orange indicate strain for which the genome sequence became available after November 2018, and, therefore were not included in the comparative genomics studies to assess gene loss in strain GP.

Organism	Genbank accession no.	16S rRNA accession no. or locus tag	%G+C	16S rRNA	ANI	AAI	POCP	Free-living	Origin
<i>Agromyces aureus</i> AR33 ^T	GCA_001660485.1	NZ_CP013979.1	70.39	92.32	78	55.41	40.35	Yes	Mining site
<i>Arthrobacter</i> sp. D2*	GCA_001742015.1	NZ_LUKB01000087.1	63.42	92.74	82.25	50.81	34.12	Yes	Activated sludge (AS)
<i>Arthrobacter</i> sp. D4*	GCA_001742005.1	NZ_LUKC01000100.1	63.41	92.74	79.38	50.61	33.86	Yes	Activated sludge (AS)
<i>Gulosibacter molinativorax</i> ON4 ^T	GCA_003010915.1	NZ_PXVE01000103.1	64.28	93.92	82.59	54.21	42.12	Yes	Molinate-contaminated soil
<i>Leifsonia aquatica</i> ATCC 14665 ^T	GCA_000469485.1	NZ_AULS01000007.1	70.17	92.78	78.4	55.41	38.47	Yes	Distilled water
<i>Leucobacter aridicollis</i> L-9^T	N.A.	D3229_13785	67.3	96.23	80.47	64.44	48.41	Yes	Activated sludge (AS)
<i>Leucobacter celer</i> subsp. <i>astrifaciens</i> CBX151 ^T	GCA_001273835.1	NZ_JHEI01000141.1	69.1	95.87	81.37	68.44	54.19	No	<i>Caenorhabditis elegans</i> (nematode)
<i>Leucobacter chironomi</i> MM2LB ^T	GCA_000421845.1	NZ_ATXU01000012.1	69.9	95.43	81.71	68.51	56.49	No	<i>Chironomidae</i> (arthropod)
<i>Leucobacter chromiireducens</i> LYC-2	GCA_003917135.1	not included in the phylogenetic trees	69.85	n.a. **	80.55	67.24	51.19	Yes	Tannery wastewater
<i>Leucobacter chromiireducens</i> subsp. <i>chromiireducens</i> L-1^T	N.A.	D3226_06110	67	96.23	80.17	67.44	52.46	Yes	Activated sludge (AS)
<i>Leucobacter chromiireducens</i> subsp. <i>solipictus</i> TAN 31504^T	N.A.	D3230_15760	68.9	96.15	79.99	67.11	53.64	No	<i>Caenorhabditis elegans</i> (nematode)
<i>Leucobacter chromiireducens</i> JG 31 ^T	GCA_000231305.1	NZ_JH370379.1	70.3	96.23	81.23	66.98	51.65	Yes	Activated sludge (AS)
<i>Leucobacter chromiireducens</i> NS354	GCA_001477055.1	NZ_LDRK01000056.1	70.8	96.37	80.97	67.21	49.06	No	<i>Oryza sativa</i> (plant)
<i>Leucobacter komagatae</i> DSM 8803 ^T	GCA_006716085.1	NZ_VFON01000001.1	66.63	96.79	80	64.19	46.73	Yes	Culture contaminant
<i>Leucobacter komagatae</i> VKM ST2845	GCA_000834055.1	not included in the phylogenetic trees	65.3	n.a. **	79.8	63.75	46.56	Yes	Environment
<i>Leucobacter luti</i> BIGb0106	GCA_004339635.1	NZ_SMGC01000003.1	64.67	96.92	79.4	66.97	49.9	No	<i>Caenorhabditis elegans</i> (nematode)
<i>Leucobacter luti</i> JUb18	GCA_004362775.1	NZ_SNYA01000014.1	64.42	96.92	79.66	66.95	49.84	No	<i>Caenorhabditis elegans</i> (nematode)
<i>Leucobacter luti</i> RF6^T	N.A.	NR_042425.1	69.4	96.81	80.66	67.66	54.63	Yes	Activated sludge (AS)

<i>Leucobacter massiliensis</i> 122RC15 ^T	GCA_002982315.1	NZ_MWZD01000014.1	71	96.52	81.77	68.43	51.8	No	Pharynx (human)
<i>Leucobacter musarum</i> subsp. <i>japonicus</i> CBX130 ^T	GCA_001273855.1	NZ_JHBX01000111.1	66.8	95.87	80.44	65.76	49.75	No	<i>Caenorhabditis elegans</i> (nematode)
<i>Leucobacter musarum</i> subsp. <i>musarum</i> CBX152 ^T	GCA_001273845.1	NZ_JHBW01000088.1	66.8	95.87	80.52	65.55	48.52	No	<i>Caenorhabditis elegans</i> (nematode)
<i>Leucobacter salsicium</i> M1-8 ^T	GCA_000350525.1	NZ_AOCN01000008.1	64.5	95.94	79.99	65.99	52.9	Yes	Jeotgal (food)
<i>Leucobacter</i> sp. 4J7B1	GCA_001373475.1	NZ_CDWJ01000013.1	67.44	96.16	80.43	66.93	49.39	No	Rhizosphere (<i>Nerium</i> sp.)
<i>Leucobacter</i> sp. 7(1)	GCA_900163635.1	NZ_FUID01000098.1	65.83	96.01	79.9	66.61	53.04	Yes	Soft smear-ripened cheese
<i>Leucobacter</i> sp. AEAR ¹	N.A.	N.A.	70.25	96.3	81.7	66.7	44.52	No	<i>Caenorhabditis angaria</i> and <i>C. remanei</i> (nematode)
<i>Leucobacter</i> sp. Ag1	GCA_000980875.1	NZ_LAY001000034.1	70.27	96.08	81.21	65.87	49.99	No	<i>Anophelesgambiae</i> (arthropod)
<i>Leucobacter</i> sp. DSM 101948	GCA_004028235.1	NZ_CP035037.1	70.47	95.49	81.89	67.93	49.56	No	<i>Mus musculus</i>
<i>Leucobacter</i> sp. G161	GCA_001482305.1	NZ_LOHP01000073.1	65.32	95.86	80.1	63.73	47.16	Yes	Chromate-contaminated soil
<i>Leucobacter</i> sp. OAML11	GCA_002763835.1	NZ_MTCJ01000069.1	70.3	96.3	81.22	67.44	50.89	No	<i>Orius laevigatus</i> (arthropod)
<i>Leucobacter</i> sp. OAMSW11	GCA_002752515.1	NZ_MTCK01000097.1	70.32	96.3	81.2	67.45	50.68	No	<i>Orius laevigatus</i> (arthropod)
<i>Leucobacter</i> sp. OH1287	GCA_003859945.1	NZ_RQYM01000028.1	58.87	95.16	77.32	58.65	37.95	No	<i>Canis lupus familiaris</i>
<i>Leucobacter</i> sp. OH2974_COT-288	GCA_003858425.1	NZ_RQYU01000008.1	56.66	94.93	76.83	58.19	35.86	No	<i>Canis lupus familiaris</i>
<i>Leucobacter</i> sp. OLAS13	GCA_002752375.1	NZ_MRAR01000001.1	70.49	96.3	81.3	67.44	51.28	No	<i>Orius laevigatus</i> (arthropod)
<i>Leucobacter</i> sp. OLCALW19	GCA_002752215.1	NZ_MPIM01000021.1	70.48	96.3	81.31	67.43	51.31	No	<i>Orius laevigatus</i> (arthropod)
<i>Leucobacter</i> sp. OLC4	GCA_002752325.1	NZ_MRAS01000099.1	70.49	96.3	81.24	67.48	51.29	No	<i>Orius laevigatus</i> (arthropod)
<i>Leucobacter</i> sp. OLDS2	GCA_002752395.1	NZ_MRAT01000024.1	70.5	96.3	81.26	67.47	51.33	No	<i>Orius laevigatus</i> (arthropod)
<i>Leucobacter</i> sp. OLES1	GCA_002752315.1	MRAU01000032.1	70.15	96.72	81.57	66.97	44.75	No	<i>Orius laevigatus</i> (arthropod)
<i>Leucobacter</i> sp. OLIS6	GCA_002752355.1	NZ_MRAV01000007.1	70.49	96.3	81.24	67.46	51.36	No	<i>Orius laevigatus</i> (arthropod)
<i>Leucobacter</i> sp. OLS4	GCA_002752415.1	NZ_MRAW01000114.1	70.5	96.3	81.28	67.5	51.16	No	<i>Orius laevigatus</i>

										(arthropod)
<i>Leucobacter</i> sp. OLTW20	GCA_002752295.1	NZ_MRAQ01000065.1	70.27	96.3	81.22	67.45	50.83	No	<i>Orius laevigatus</i> (arthropod)	
<i>Leucobacter</i> sp. PH1c	GCA_000633415.1	NZ_AYMV01000048.1	71.32	96.08	81.34	67.85	51.51	No	<i>Phytotelma</i> sp. (plant)	
<i>Leucobacter</i> sp. UBA1945	GCA_002336855.1	N.A.	64.78	48.35 *	79.95	68.06	47.94	Yes	Wastewater	
<i>Leucobacter</i> sp. UCD-THU	GCA_000349545.1	NZ_KB714599.1	70.34	95.37	81.73	68.38	51.51	Yes	Residential toilet	
<i>Leucobacter</i> sp. wl10	GCA_003569785.1	NZ_KZ984022.1	69.86	95.44	81.53	67.7	53.8	Yes	Wastewater	
<i>Leucobacter triazinivorans</i> JW-1 ^T	GCA_004208635.1	NZ_CP035806.1	69.37	96.4	82.09	69.07	55.62	Yes	Activated sludge (AS)	
<i>Leucobacter zeae</i> CC-MF41^T	N.A.	D3248_15480	70.6	95.88	81.4	67.31	51.66	No	Rhizosphere of maize	
<i>Microbacterium lacus</i> SDZm4*	GCA_002812805.1	NZ_NMUM01000037.1	67.27	92.37	82.11	56.12	44.67	Yes	Lysimeters	
<i>Microbacterium luticocti</i> DSM 19459 ^T	GCA_000422405.1	NZ_ATXU01000010.1	70.69	91.73	77.64	55.45	41.63	Yes	Sewage sludge compost	
<i>Microbacterium paraoxydans</i> DSM 15019 ^T	GCA_900105335.1	NZ_LT629770.1	70.02	93.26	77.79	55.47	42.04	No	Blood (human)	
<i>Microbacterium</i> sp. BR1*	GCA_002812725.1	NZ_NMUN01000004.1	68.08	92.16	81.5	55.64	44.35	Yes	Membrane bioreactor (AS)	
<i>Microbacterium</i> sp. C448*	GCA_000582705.1	NZ_KI271991.1	67.39	92.16	78.73	55.54	43.12	Yes	Agricultural soil	
<i>Microbacterium</i> sp. CJ77*	GCA_002911615.1	NZ_PQBR01000006.1	68.27	92.23	81.5	55.72	44.54	Yes	Sulfonamide- contaminated sediments	

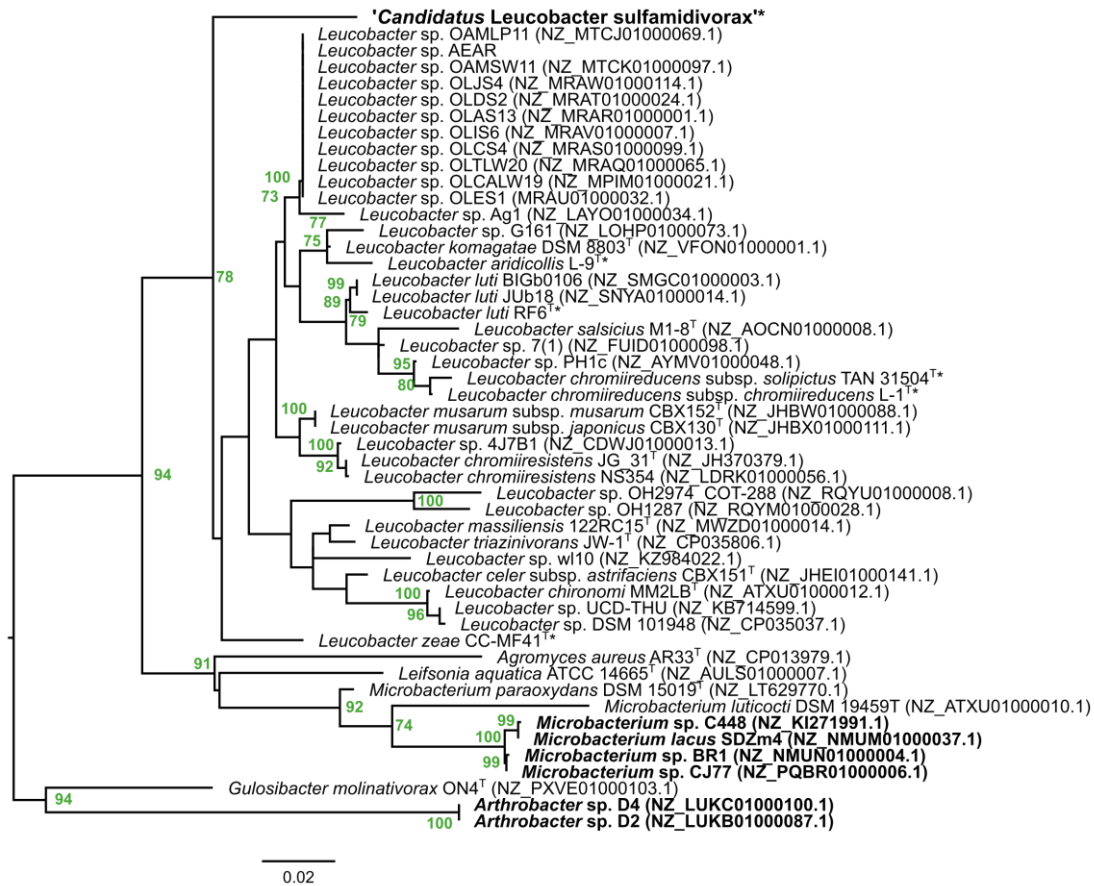


Figure 6.5 - Cladogram of the 16S rRNA gene inferred from maximum likelihood estimation with MEGA6 with the best-fitting model: TN93+G+I (Tamura et al. 2013). *Leucobacter* spp. strains sequenced in this study are marked with an asterisk, and sulfonamide degraders are shown in bold. The tree was rooted at the outgroup and visualized with FigTree. The scale bar represents the number of expected substitutions per site. Bootstrap values were inferred from 1000 replicates, values above 70% are shown at the corresponding nodes.

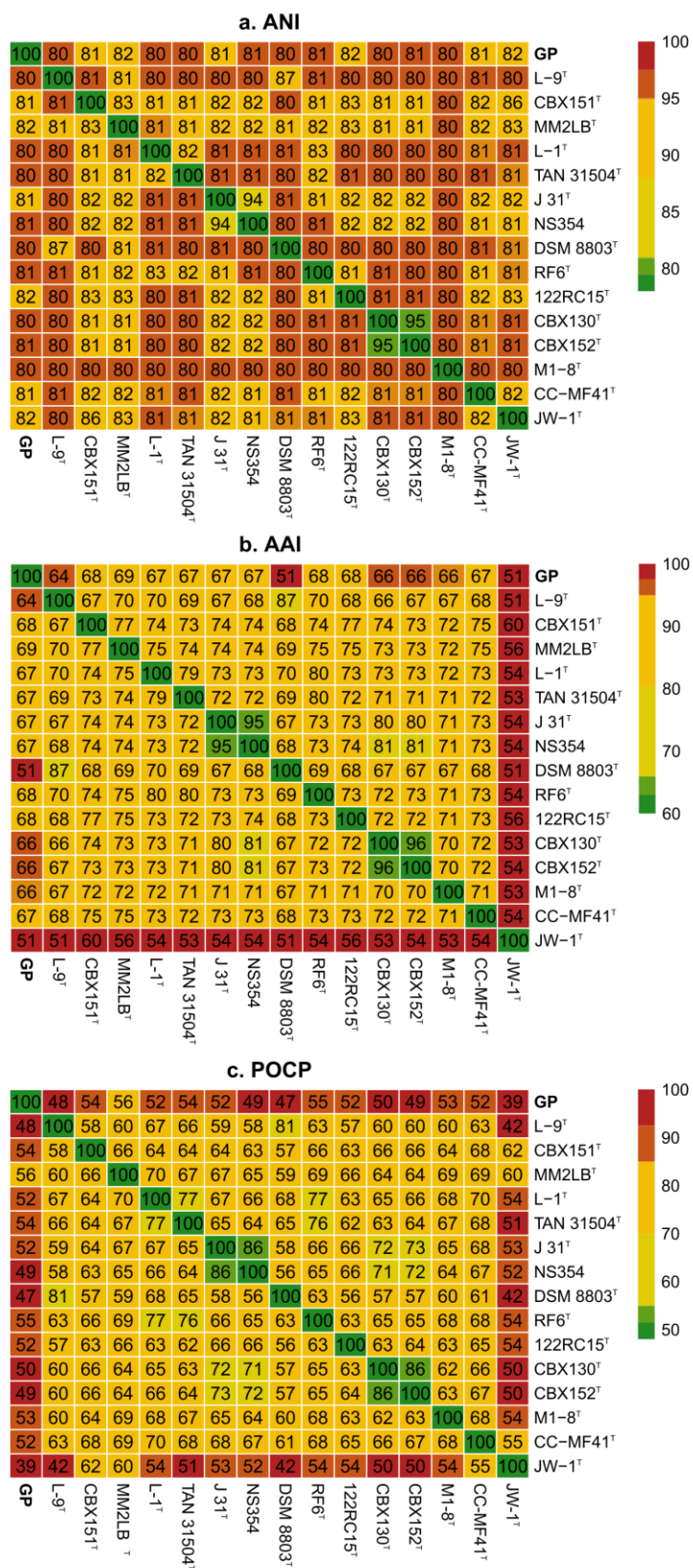


Figure 6.6 – ANI (a), AAI (b) and POCP (c) heatmaps comparing values between strain GP and validly named species of the *Leucobacter* genus at the time of the analysis.

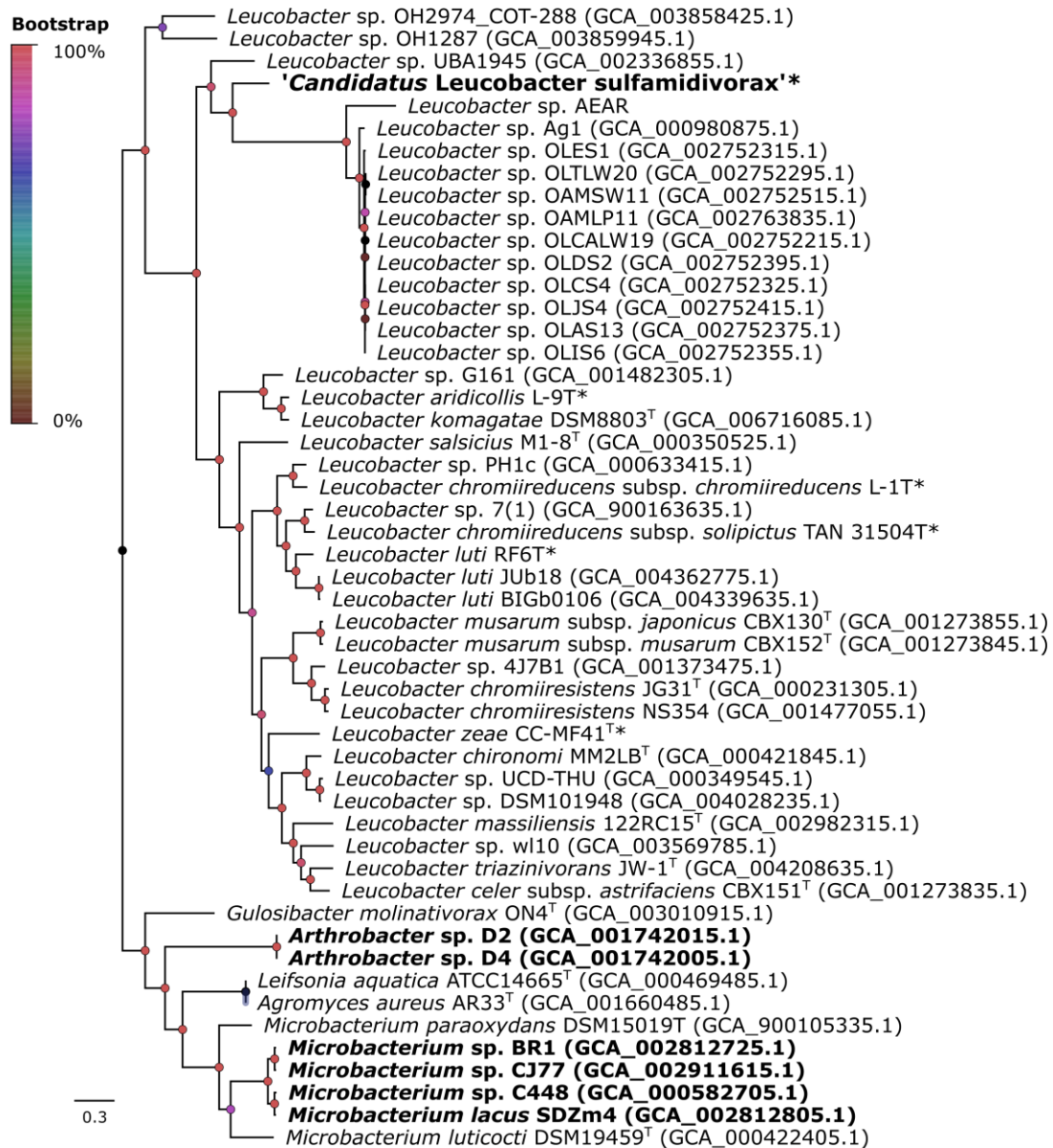


Figure 6.7 – Phylogenomic relationships between the *Leucobacter* genus and strain GP inferred from concatenated amino acid alignments of 400 universal proteins obtained with PhyloPhlAn (Segata et al. 2013). Representative members of genera *Microbacterium*, *Leifsonia*, *Gulosibacter*, *Agromyces* and *Arthrobacter* were included as the outgroup. *Leucobacter* spp. strains sequenced in this study are marked with an asterisk, and sulfonamide degraders are shown in bold. Node labels indicate local support values obtained with FastTree using the Shimodaira-Hasegawa test (Shimodaira 2002). The scale bar represents the number of expected substitutions per site. The tree was rooted at the outgroup node and visualized with FigTree.

The G+C content of strain GP was of 69.7 % (Table 6.1), which, according to previous studies (Goodfellow and O'Donnell 1993) is within the expected G+C interval (10 %) for organisms of the same genus. In fact, for the type strains of all validly named species of the *Leucobacter* genus, G+C content ranged between 64.5 and 71.0 % (Table 6.4). Moreover,

the phylogenetic analysis of 400 conserved proteins of *Leucobacter* spp. using the PhyloPhlAn pipeline (Segata et al. 2013) revealed that although strain GP appears to share a common origin with the other isolates of *Leucobacter* spp. (Fig. 6.7), it also does not cluster with any of the analyzed strains.

6.3.5 Core and softcore genome of *Leucobacter* spp.

Orthologs gene cluster analysis with GET_HOMOLOGUES (Contreras-Moreira and Vinuesa 2013) revealed that *Leucobacter* spp. and strain GP core and softcore genome contain 456 and 885 orthologs gene clusters, respectively (Fig. 6.8). However, only a fraction of these (approximately 50 %) could be functionally annotated with eggNOG-Mapper and BlastKOALA (Kanehisa et al. 2016; Huerta-Cepas et al. 2017). This analysis revealed that most of these clusters are related to central metabolic pathways (Koonin and Galperin 2003), including nucleotide and amino acid metabolism (118 clusters), and carbohydrate and lipid metabolism (16 clusters) (Table 6.5), respectively. Furthermore, these strains lack orthologs linked to antimicrobial resistance, quorum sensing, and biofilm formation, suggesting that they form a diverse and versatile genus with specific adaptations to different environments.

Only a few of the fully sequenced *Leucobacter* spp. analyzed in this study are free-living organisms isolated from wastewater or soil. These free-living strains did not form a clade. The majority of the strains form facultative symbiotic associations with arthropods, nematodes, and plants (Table 6.4). While *Leucobacter* sp. AEAR (Percudani 2013), whose genome has been directly reconstructed from whole genome sequences of the nematodes *Caenorhabditis angaria* and *Caenorhabditis remanei*, could not be isolated, all *Leucobacter* spp. symbionts were able to grow independently from their hosts. Nevertheless, the analysis of strain AEAR genome revealed that it should be able to grow independently as all essential pathways seem to be present in its draft genome (Percudani 2013). This observation is further supported by the analysis of the phylogenomic tree (Fig. 6.7), which

shows that strain AEAR forms a monophyletic clade with *Leucobacter* sp. Ag1 (accession no. GCA_000980875.1) and other 9 strains, which are all facultative symbionts from arthropod species (Chen et al. 2017). These results suggest that the living style does not correlate with the phylogeny of the strains.

Interestingly, strain GP appears to share many conserved genes with *L. chironomi* DSM 19883^T (Laviad et al. 2015), a facultative symbiotic bacterium isolated from a member of the *Chironomidae* family (56.49 % POCP, Fig. 6.5c). Bidirectional best-hits (BDBH) analysis with GET_HOMOLOGUES of these two strains showed that they share 1,372 orthologs gene clusters, amounting to 38.6 % of the total CDS of strain GP. Most of these genes are linked to central metabolic pathways. As strain GP, *L. chironomi* also carries iron-heme acquisition operons *hmuTUV* (accessions no. WP_024357741.1, WP_024357742.1 and WP_029747012.1, respectively) and *efeUOB* (accessions no. WP_024356012.1, WP_024356011.1 and WP_024356010.1, respectively), and a homolog of heme oxygenase (*hmuO*, accession no. WP_024356032.1). However, unlike in strain GP, *L. chironomi* does not bear these operons *efeUOB* and *hmuTUV* adjacently in its genome. The *efeUOB* operon and *hmuO* are absent from the softcore genome of *Leucobacter* spp. but are shared between several members of this genus (data not shown). Furthermore, strain GP also carries a chromate transport protein A (locus tag D3X82_06990) which was demonstrated to be linked to chromate resistance, and a common feature shared between several members of the *Leucobacter* genus (Yun et al. 2014).

Table 6.5 – Complete and near-complete (1 block missing = 1 ortholog gene missing) modules of the softcore genome of *Leucobacter* spp. and strain GP reconstructed *in silico* with KEGG Mapper (Kanehisa et al. 2017).

Pathway	Module	Paths	No. of KEGG orthologs	Coverage
Carbon fixation	M00167 Reductive pentose phosphate cycle	map00710 map01200 map01100 map01120	8	Complete
	M00168 CAM (Crassulacean acid metabolism) dark	map00710 map01200 map01100 map01120	1	1 block missing
Methane metabolism	M00345 Formaldehyde assimilation	map00680 map01200 map01120	2	1 block missing
Central carbohydrate metabolism	M00002 Glycolysis	map00010 map01200 map01230 map01100	5	1 block missing
	M00003 Gluconeogenesis	map00010 map00020 map01100	8	1 block missing
	M00307 Pyruvate oxidation	map00010 map00020 map00620 map01200 map01100	3	1 block missing
	M00009 Citrate cycle (TCA cycle Krebs cycle)	map00020 map01200 map01100	13	1 block missing
	M00010 Citrate cycle, first carbon oxidation	map00020 map01200 map01210 map01230 map01100	3	Complete
	M00011 Citrate cycle, second carbon oxidation	map00020 map01200 map01100	10	1 block missing
	M00007 Pentose phosphate pathway, non-oxidative phase	map00030 map01200 map01230 map01100 map01120	4	1 block missing
Other carbohydrate metabolism	M00012 Glyoxylate cycle	map00630 map01200 map01100 map01110	4	1 block missing
	M00549 Nucleotide sugar biosynthesis	map00520 map01100	2	1 block missing
Fatty acid metabolism	M00082 Fatty acid biosynthesis, initiation	map00061 map01212 map01100	4	Complete
	M00083 Fatty acid biosynthesis, elongation	map00061 map01212 map01100	3	1 block missing
	M00086 beta-Oxidation, acyl-CoA synthesis	map00071 map01212 map01100	1	Complete
	M00087 beta-Oxidation	map00071 map01212 map01100	4	1 block missing
Lipid metabolism	M00093 Phosphatidylethanolamine (PE) biosynthesis	map00564 map01100	2	1 block missing
Purine metabolism	M00048 Inosine monophosphate biosynthesis	map00230 map01100	10	Complete
	M00049 Adenine ribonucleotide biosynthesis	map00230 map01100	5	Complete
	M00050 Guanine ribonucleotide biosynthesis	map00230 map01100	5	Complete
Pyrimidine metabolism	M00051 Uridine monophosphate biosynthesis	map00240 map01100	9	1 block missing
	M00052 Pyrimidine ribonucleotide biosynthesis	map00240 map01100	4	Complete
	M00053 Pyrimidine deoxyribonucleotide biosynthesis	map00240 map01100	8	1 block missing
Serine and threonine metabolism	M00020 Serine biosynthesis	map00260 map01200 map01230 map01100	3	Complete
	M00018 Threonine biosynthesis	map00260 map01230 map01100 map01110	6	Complete

Cysteine and methionine metabolism	M00021 Cysteine biosynthesis	map00270 map01200 map01230 map01100 map01110	2	Complete
Branched-chain amino acid metabolism	M00019 Valine/isoleucine biosynthesis	map00290 map01210 map01230 map01100 map01110	5	Complete
	M00535 Isoleucine biosynthesis	map00290 map01210 map01230 map01100	3	1 block missing
	M00570 Isoleucine biosynthesis	map00290 map01230 map01100	6	Complete
Arginine and proline metabolism	M00432 Leucine biosynthesis	map00290 map01210 map01230 map01100 map01110	3	1 block missing
	M00015 Proline biosynthesis	map00330 map01230 map01100	3	Complete
	M00844 Arginine biosynthesis	map00220 map01230 map01100	3	Complete
Aromatic amino acid metabolism	M00029 Urea cycle	map00220 map01230 map01100	4	1 block missing
	M00022 Shikimate pathway	map00400 map01230 map01100 map01110 map01130	8	Complete
	M00023 Tryptophan biosynthesis	map00400 map01230 map01100 map01110	8	1 block missing
	M00025 Tyrosine biosynthesis	map00400 map01230 map01100	3	1 block missing
Other amino acid metabolism	M00040 Tyrosine biosynthesis	map00400 map01230 map01100 map01110	2	1 block missing
	M00027 GABA (gamma-Aminobutyrate) shunt	map00250 map01100	4	1 block missing
Cofactor and vitamin biosynthesis	M00115 NAD biosynthesis	map00760 map01100	5	1 block missing
	M00120 Coenzyme A biosynthesis	map00770 map01100	6	Complete
	M00140 C1-unit interconversion, prokaryotes	map00670 map01100	2	1 block missing
	M00141 C1-unit interconversion, eukaryotes	map00670 map01100	1	1 block missing
Polyamine biosynthesis	M00134 Polyamine biosynthesis	map00330 map01100	1	1 block missing
	M00135 GABA biosynthesis eukaryotes	map00330 map01100	2	1 block missing

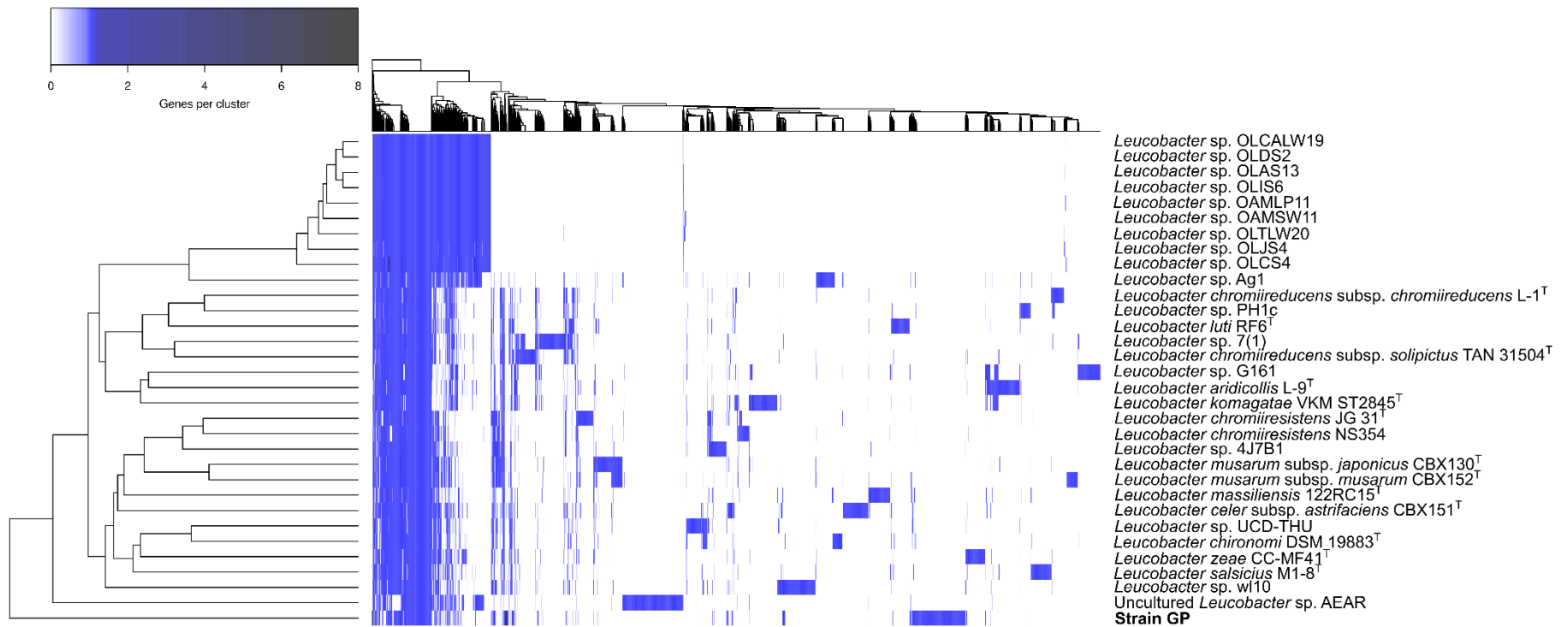


Figure 6.8 – Presence/absence heatmap representation and dendrograms of the 12,998 orthologs gene clusters found in the pangenome of *Leucobacter* spp. and strain GP obtained with the GET_HOMOLOGUES package (Contreras-Moreira and Vinuesa 2013). Each column represents a different gene cluster which can be absent (white) or present (blue) in each strain. As paralogs were included in the analysis, some clusters have more than one homolog per genome, and these are shown in darker blue.

6.3.6 Estimation of gene loss in strain GP

Prior studies suggested that strain GP was obligatorily dependent on *A. denitrificans* PR1 for growth, as no isolated colonies of this organism were recovered after incubation in several conditions (Reis et al. 2018a). Surprisingly, despite its dependent phenotype, strain GP did not show significant genome reduction as it is commonly reported in symbiotic bacteria (Table 6.1) (McCutcheon and Moran 2012). In fact, the number of genes and the genome size of this strain was similar to the ones found in other members of the *Leucobacter* genus (Table 6.4). These results suggest that, despite the PR1-dependent phenotype, strain GP differs from obligate parasites that, in the process of adapting to their hosts, undergo a process called reductive genome evolution, which results in relatively small genomes (often < 1 Mb) (Andersson and Kurland 1998; Wernegreen 2015).

Comparative genomic analysis of the *Leucobacter* genus revealed that the pangenome consists of 12,998 unique clusters. The clusters present in at least 90 % of the *Leucobacter* spp. (28 of 31 genomes) were used as reference to determine potentially missing genes in the draft genome of strain GP. These results were carefully analyzed and manually curated, due to the high frequency of annotation errors associated with draft assemblies (Denton et al. 2014; Salzberg 2019). In this way, of all these clusters, only 141 were present in 90 % of the *Leucobacter* spp. and were apparently absent from the draft genome of strain GP.

From these 141 clusters, only 9 clusters were non hypothetical genes and no alternative pathways were found in the draft genome of strain GP (Table 3).

Strain GP may have lost genes linked with amino acid metabolism, specifically genes linked to the metabolism of methionine, arginine, and ornithine (accession no. WP_042543310.1 and WP_024355584.1). MtnA (WP_024355584.1), for instance, catalyzes the first step of the methionine salvage pathway and is absent from the genome

of both strains PR1 and GP (Reis et al. 2017; Reis et al. 2018a). This pathway allows the recovery of methionine and, consequently sulfur, from 5'-methylthioadenosine (MTA), a byproduct of polyamine biosynthesis (Albers 2009). Nevertheless, even though strain GP may be unable to recycle this metabolite, it should be capable of regenerating L-methionine from L-homocysteine since it encodes for a homolog of methionine synthase (locus tag D3X82_09525). However, as no alternative pathways for MTA degradation are present, its accumulation may become detrimental to the cells since this metabolite was found to be cytotoxic (Parveen and Cornell 2011; Sauter et al. 2013).

Table 6.6 – Essential genes missing from the draft genome of strain GP identified by core/pangenome analysis with GET_HOMOLOGUES (Contreras-Moreira and Vinuesa 2013).

Representative accession no.		KO identifiers	Description	Pathway/System
<i>Leucobacter</i>	Strain PR1			
WP_042543310.1	ASC67664.1	K01476	Arginase RocF	L-arginine biosynthesis/ Urea cycle
WP_024355584.1	Absent	K08963, K08964	S-methyl-5-thioribose-1-phosphate isomerase MtnA	Methionine salvage pathway
WP_024357159.1	ASC65015.1	K06147, K06148, K16013, K16014	Thiol reductant ABC exporter subunit CydD	Glutathione / L-cysteine ABC transporter
WP_042544611.1	ASC65016.1	K06148, K16012	Thiol reductant ABC exporter subunit CydC	
WP_084766924.1	ASC65168.1	K02492	Glutamyl-tRNA reductase HemA	
WP_042543805.1	ASC64797.1	K01698	Porphobilinogen synthase HemB	Porphyrin and chlorophyll metabolism
WP_084766919.1	ASC63016	K01749	Porphobilinogen deaminase HemC	
WP_042543807.1	ASC64317.1	K01599	Uroporphyrinogen decarboxylase HemE	
WP_042545361.1	ASC67862.1	K02083, K06016	Allantoate deiminase AllC	Purine metabolism

Arginase, an enzyme catalyzing the hydrolysis of L-arginine into L-ornithine and urea (Solomon et al. 2010), is also absent in strain GP yet present in the genome of strain PR1 (accession no. ASC67664). Although strain GP seems to carry alternative pathways for the synthesis of L-ornithine (*argJ*, locus tag D3X82_05235, L-arginine biosynthesis II – acetyl

cycle), the lack of RocF may prevent from storing an excess of nitrogen in the form of urea. However, the urea cycle is facultative in bacteria. Hence, a defective cycle has only been linked to a decreased fitness in pathogenic acid-sensitive *Helicobacter pylori*, which relies on urease activity for protection against acidic conditions (McGee et al. 1999).

The draft genome of strain GP shows the loss of a homolog of allantoate deiminase (*allC*), an inducible enzyme from the (S)-allantoin degradation pathway which allows bacteria to recover the nitrogen from purine compounds, such as allantoin (Huerta-Cepas et al. 2017). However, despite the presence of homologs of *allC* in other *Leucobacter* spp., the remaining enzymes of this pathway appear to be missing from the softcore genome. Nevertheless, this is a facultative metabolic pathway; therefore, its absence is unlikely to be detrimental to the growth of strain GP.

Noticeably, several essential genes linked to the porphyrin and chlorophyll pathway (*hemABCE*) and thiol transport (*cydDC*) seem to be missing. Both essential systems for the synthesis and correct assembly of cytochromes (Georgiou et al. 1987; Poole et al. 1994; Goldman et al. 1996; Dailey et al. 2017). The CydDC complex performs the transport of glutathione and L-cysteine and is responsible for maintaining an optimal redox balance in the periplasm (Pittman et al. 2002; Pittman et al. 2005). This balance is crucial for the correct assembly of cytochromes in the plasma membrane, and its loss is usually associated with increased sensitivity to high temperature and oxidative stress, respectively (Georgiou et al. 1987; Poole et al. 1994; Goldman et al. 1996). *HemABCE* encodes the proteins involved in the synthesis of tetrapyrroles and, subsequently, heme which acts as a prosthetic group in many respiratory and non-respiratory cytochromes (Dailey et al. 2017).

To the best of our knowledge, only a few bacterial strains have been found to be incapable of *de novo* heme biosynthesis (Choby and Skaar 2016). These strains are mainly pathogenic and affiliated to *Haemophilus influenza*, except the recently described

environmental isolate *Leucobacter* sp. strain ASN212 which requires exogenous heme for growth (Bhuiyan et al. 2015; Choby and Skaar 2016; Takai et al. 2017). As well as many pathogenic bacteria, these organisms rely on complex heme-acquisition systems to thrive in iron-deficient environments and to synthesize essential heme-containing proteins.

Functional analysis of the draft genome of strain GP revealed the presence of a heme ABC transport operon (*hmuTUV*) that encodes for a hemin-binding periplasmic protein HmuT (locus tag D3X82_13650), a permease protein HmuU (D3X82_13655) and an ATP-binding protein HmuV (D3X82_13660), respectively. This system has been extensively described and found to be highly conserved in the Gram-positive *Corynebacterium diphtheria* (Choby and Skaar 2016). However, in this organism, additional heme-binding genes (*htaABC*) and a heme oxygenase *hmuO* were found to be essential for successful heme and iron-heme acquisition (Choby and Skaar 2016). A homolog to *hmuO* was found in the genome of strain GP (locus tag D3X82_07630). However, the conserved *htaABC* operon, essential for exogenous heme-binding, appeared to be missing. Instead of this operon, strain GP possesses a different adjacent gene cluster encoding for a deferriochelatase/peroxidase EfeB (D3X82_13665), an iron uptake system component EfeO (D3X82_13670) and a ferrous iron permease EfeU (D3X82_13675). These enzymes have been previously linked to ferrous/ferric iron acquisition in *Bacillus subtilis* (Miethke et al. 2013) and to intact heme transport in *Escherichia coli* (Létoffé et al. 2009). However, to the best of our knowledge, the EfeUOB system has not been directly linked to intact heme-acquisition in Gram-positive bacteria.

In previous studies (Reis et al. 2018a) we have supplied the consortium with exogenous heme and known heme precursors such as coproporphyrin III, coproporphyrin III tetramethylester and coproporphyrin I dihydrochloride, replicating the conditions that allowed the isolation of the heme-dependent *Leucobacter* sp. ASN212 (Bhuiyan et al. 2015; Reis et al. 2018a). However, adding these metabolites to agar plates did not abolish the dependent phenotype of strain GP. This result was unexpected as strain GP possesses

several downstream genes of the porphyrin pathway; therefore, it should at least be able to use coproporphyrin III as a heme precursor. This finding suggests that either the heme transport system of strain GP is insufficient for intact heme transport across the thick peptidoglycan cell wall or that other essential cofactors or conditions are missing. Unfortunately, the genome of strain ASN212 is not publicly available, which hinders further efforts to characterize the transport of intact heme and heme precursors across the cell wall of this heme-dependent actinobacterium.

Considering that strain GP may also lack homologs to thiol ABC transporters (accession numbers WP_024357159.1 and WP_042544611.1), it may be vulnerable to oxidative stress and unable to correctly assemble cytochromes (Georgiou et al. 1987; Poole et al. 1994; Goldman et al. 1996). In other sensitive organisms, the absence of this redox regulating system has been compensated by growing deficient strains in catalase-containing media and even in co-culture with catalase-producing bacteria (Goldman et al. 1996; Morris et al. 2011). However, none of these strategies allowed the independent growth of strain GP.

Furthermore, the accumulation of the toxic MTA metabolite during polyamine synthesis in strain GP may affect the growth of this actinobacterium. Although polyamines (e.g. putrescine and spermidine) are not mandatory for growth, mutant strains lacking this pathway were found to have increased susceptibility to oxidative stress (Jung et al. 2003). In this way, we attempted supplying the strain with exogenous putrescine to decrease the intracellular accumulation of MTA. Nevertheless, this also did not abolish the strain's dependent phenotype. Furthermore, a combination of exogenous heme, catalase and putrescine were insufficient to allow the independent growth of strain GP.

Genomic studies are inherently limited because they rely on gene homology for functional annotation and prediction (Silva et al. 2001). Furthermore, draft genomes are known to present extensive annotation errors (Denton et al. 2014), and the presence of a given gene

may not even be translated into a particular phenotype. Indeed, genes can be silenced by mutations in the coding region or their promoters, a common phenomenon in the evolution of dependent and pathogenic bacteria which suffer progressive phenotypic and genetic changes due to the interaction with their hosts and environment (Beacham 1987; Laskos et al. 1998; Silva et al. 2001). Therefore, these preliminary results require further functional studies in order to understand gene expression and activity in both strains from the microbial consortium.

6.3.7 Unique genes shared between sulfonamide degraders

Genetic synteny

As previously discussed, strain GP was shown to be responsible for the breakdown of sulfonamides in the two-member consortium (Reis et al. 2018a). Some members of the *Microbacterium* genus able to degrade sulfonamides carried a conserved gene cluster encoding for two monooxygenases (SadA and SadB, accession no. WP_100812327.1 and WP_036299419.1, respectively) and one FMN-reductase (SadC, WP_100812326.1). SadA is known to catalyze the *ipso*-hydroxylation of SMX releasing 4-aminophenol, while SadB appears to be responsible for the further oxidation of this unstable and transient metabolite (Ricken et al. 2017; Reis et al. 2018a). Although the former enzymes appear to be highly specific for these substrates, the role of SadC can easily be fulfilled by other enzymes with similar activity. This has previously been demonstrated in assays with transformed *E. coli* that contained an incomplete cluster encoding for SadA and SadB alone (Ricken et al. 2017). The genetic synteny in *Microbacterium* spp. (Fig. 6.9) appears to be highly conserved (Ricken et al. 2017). Indeed, all strains of this genus harbor a cluster consisting of a *trwC* relaxase (WP_100812428.1), a polyisoprenoid-binding protein *yceI* (WP_100812427.1), a *sadA* monooxygenase (WP_100812327.1), a *sadB* monooxygenase (WP_036299419.1) and a *sadC* flavin monooxygenase (WP_100812326.1).

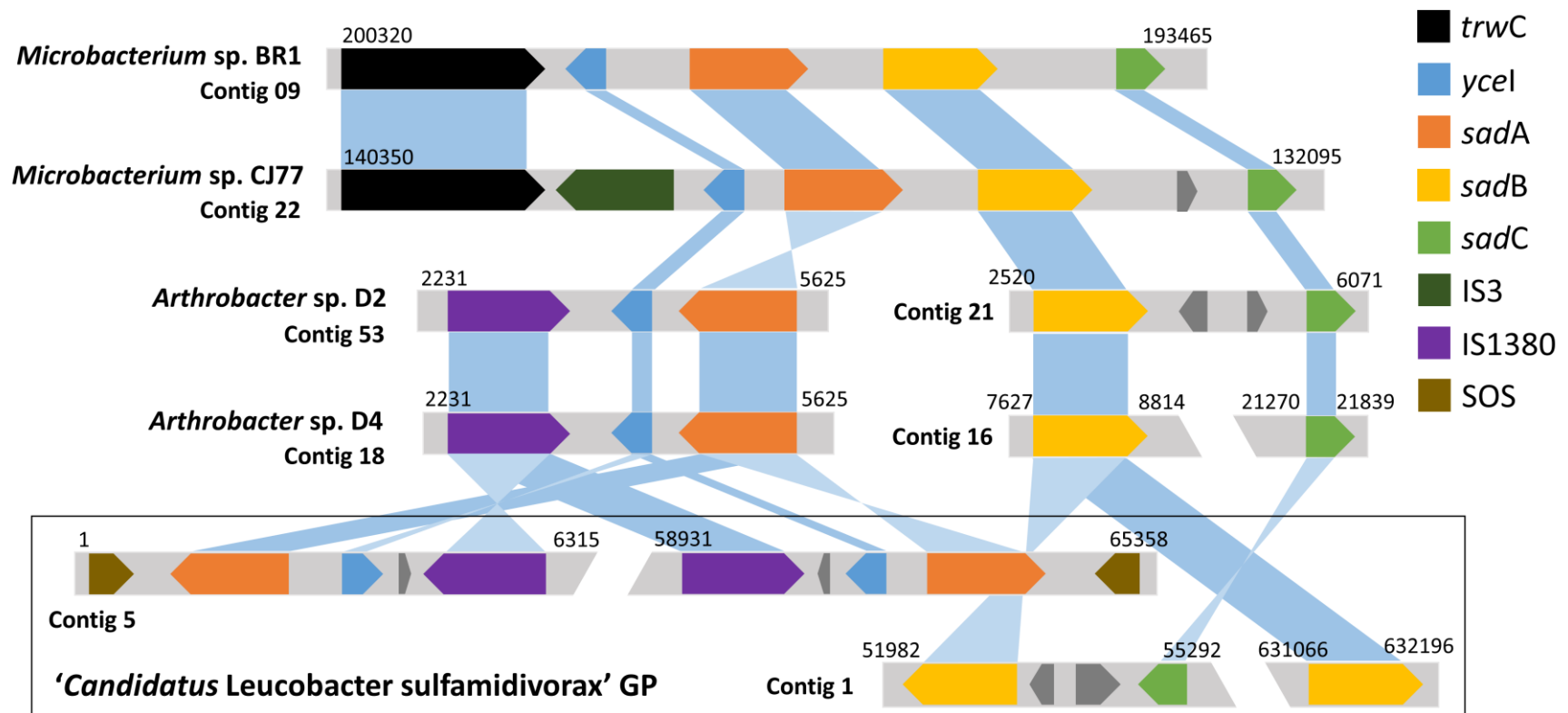


Figure 6.9 – Representation of the genetic organization of the *sad* cluster in sulfonamide degraders: *Microbacterium* sp. strains BR1 and CJ77, *Arthrobacter* sp. strains D2 and D4 and strain GP. Scaffolds or contig numbers and locus are shown next to the DNA backbone.

Except for the putative sulfonamide degrader, *Microbacterium* sp. CJ77 that carries an additional gene within the *sad* cluster encoding for an IS3 family transposase (WP_103663393.1), located between *trwC* and *yceI* (Fig. 6.9).

Likewise, strain GP carries homologs for most of these genes, albeit with a different synteny. This strain harbors at least two identical copies of a transposon containing a homolog of *sadA* (locus tag D3X82_17695 and D3X82_17365) in contig 5 (Fig. 6.8). Both copies of *sadA* are flanked downstream by a gene encoding for an SOS response-associated peptidase (D3X82_17690 and D3X82_17360, respectively), and upstream by a single IS1380 family transposase (D3X82_17710 and D3X82_17380, respectively) and a polyisoprenoid-binding protein *yceI* (D3X82_17700 and D3X82_17370, respectively) (Fig. 6.9).

Except for the SOS response peptidase, a similar genetic organization was found in the draft genome of the two sulfonamide-degraders from the *Arthrobacter* genus – strains D2 and D4 (Fig. 6.9). Interestingly, *Arthrobacter* spp. and strain GP have a truncated *sad* cluster with the genes coding for the SadB monooxygenase and the SadC reductase found in different regions of the genome (Fig. 6.9). However, in contrast to all other sulfonamide-degrading isolates, strain GP appears to carry two similar copies of the SadB homolog (locus tag D3X82_00235 and D3X82_03160, 93 % amino acid identity against each other), one of these near SadC reductase (locus tag D3X82_00250).

One of the copies of the *sadA*-cluster of strain GP (contig 5, locus 1 to 4909 bp, Fig. 6.9) is flanked by a T4CP (locus tag D3X82_17390), T4SS (locus tag D3X82_17385), two recombinases from different families (D3X82_17355 and D3X82_17350 from Ser_Recombinase and Zn_ribbon_recom superfamilies, respectively) and a class I integron with multiple resistance genes (*aadA1*, *sul1* and *qacE*), as described above (Table 6.3).

Notably, *Microbacterium* sp. BR1 was also shown to harbor a homolog of the IS1380 transposase (WP_100810554.1) identical to the transposase found in the *sadA*-containing

transposon of strain GP. However, contrarily to strain GP, this transposase did not cluster with the *sad* genes and was found in a different region of *Microbacterium* sp. BR1's genome (contig 4, instead of contig 9).

Phylogenetic analysis

The analysis of proteins associated with sulfonamide degradation showed that the SadA and YceI homologs shared a high percentage of amino acid identity between *Microbacterium* sp. and strain GP, while the two *Arthrobacter* sp. isolates were more similar among themselves (Fig. 6.10).

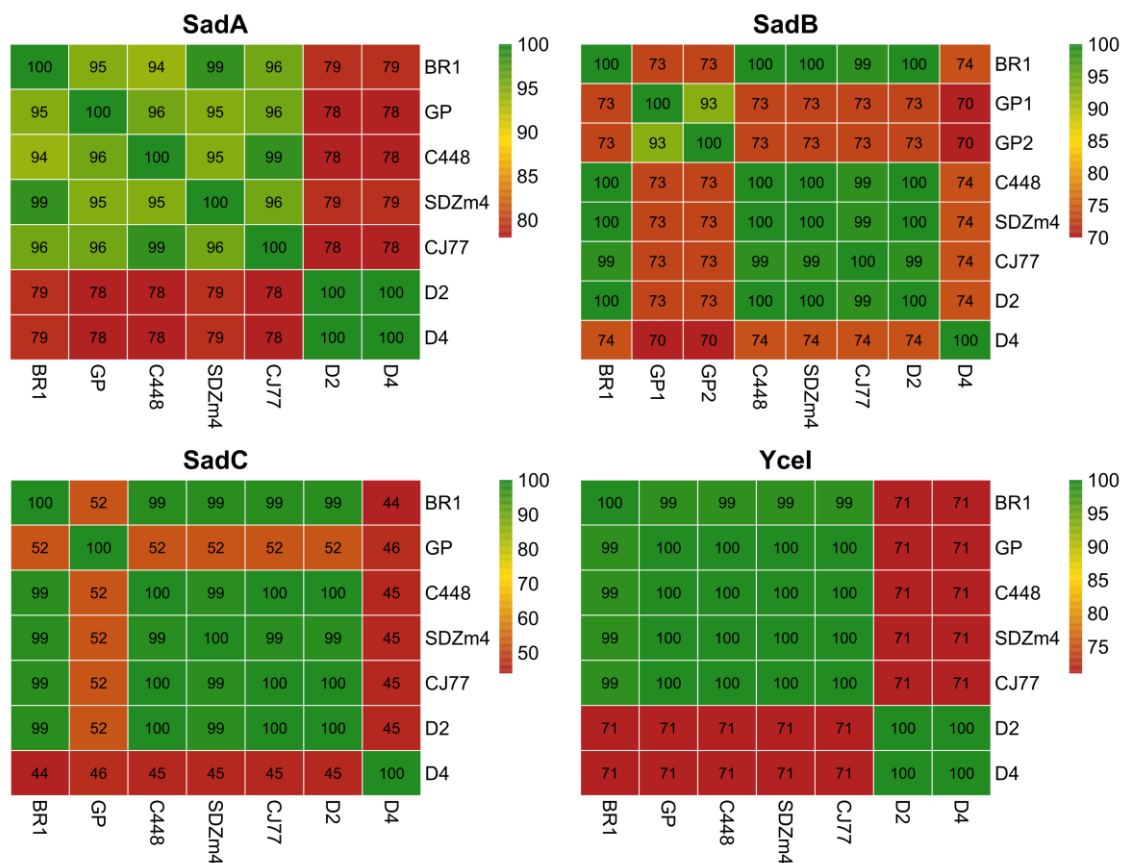


Figure 6.10 – Heatmaps representing amino acid identity (BLASTp) of the SadABC complex and YceI transporter among isolates from the *Microbacterium* genus (strains BR1, C448, SDZm4 and CJ77), *Arthrobacter* genus (strains D2 and D4) and strain GP.

The high identity between these homologs among strains affiliated to different bacterial species suggests that these genetic determinants may share a common ancestor. This

hypothesis was further supported by phylogenetic studies of these proteins. For instance, the Maximum Likelihood (ML) phylogenetic tree shows that all SadA and YceI homologs form a conserved clade with high support values (Figure 6.11), also obtained when using both cladistic (Bayesian inference) and distance-based (Neighbor Joining, NJ) methods. Furthermore, the co-existence of both the SadA monooxygenase and the YceI transporter in all the genomes suggests that the YceI binding-protein may play a complementary role in the sulfonamides degradation by enhancing the uptake of these molecules, as previously described for other systems (Bosdriesz et al. 2015).

In contrast, SadB and SadC homologs were highly identical in all *Microbacterium* sp. isolates and *Arthrobacter* sp. D2 (Fig. 6.10). And the phylogenetic analysis revealed that these proteins form a highly conserved clade (Fig. 6.11).

Despite the lower identity between the SadB homologs in *Arthrobacter* sp. D4 and strain GP, in comparison to the other sulfonamide-degraders (Fig. 6.10), these proteins also appear to share a common ancestor with their homologs in *Microbacterium* spp. (Figure 6.11b). Conversely, the SadC homologs found in these two strains do not appear to share a common ancestor between themselves nor with the other sulfonamide-degrading strains. This result is in agreement with previous studies with the recombinant SadABC complex from *Microbacterium* sp. BR1 (Ricken et al. 2017). This study showed that SadA and SadB are sufficient to carry out complete SMX degradation in recombinant *E. coli*, suggesting that the role of SadC could be fulfilled by other flavin reductases present in the genome of the host strain (Ricken et al. 2017).

Noticeable, the IS1380 transposase flanking SadA in strain GP is identical to a homolog in *Microbacterium* sp. BR1 (WP_100810554.1, amino acid identity of 100 %), and these two proteins form a highly conserved clade in the phylogenetic tree (Figure 6.11). Interestingly, the IS1380 family transposase is located far from the *sad* cluster in *Microbacterium* sp. BR1 (contig 4, instead of contig 9), suggesting that this transposase

may be involved in gene mobility in different species and genera of the *Actinobacteria* phylum.

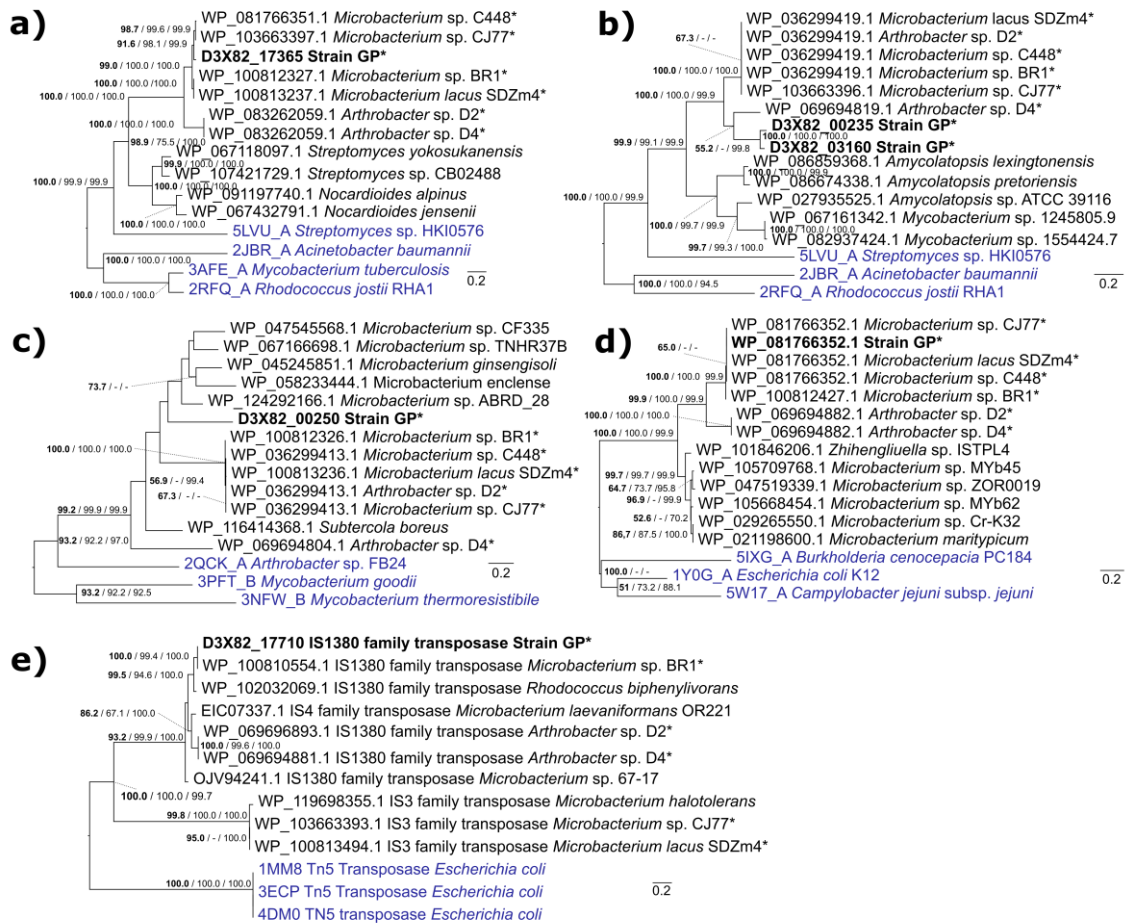


Figure 6.11 – Maximum likelihood phylogenetic trees inferred from amino acid alignments with MEGA6 (Tamura et al. 2013) of (a) SadA, (b) SadB, (c) SadC, (d) Ycel transporter and (e) IS1380/IS3/IS4 transposases shared between sulfonamide degraders. Strain GP is shown in bold; sulfonamide degraders are marked with an asterisk (*); and structural homologs to these enzymes obtained with SWISS-MODEL (Waterhouse et al. 2018) are shown in bright blue. Node labels indicate ML bootstrap support above 50% (in bold) / NJ bootstrap support values above 50% / Bayesian posterior probabilities above 70%. The scale bar represents the number of expected substitutions per site. The tree was rooted at the midpoint and visualized with FigTree.

Structural analysis of SadA and SadB

Structurally, all SadA and SadB homologs contain an acyl-CoA dehydrogenase domain (Fig. 6.12), classifying them as Group D flavoprotein monooxygenases (Huijbers et al. 2014; Reis et al. 2018a)..

(a) Acyl-CoA dehydrogenase, N-terminal (Pfam Acyl-CoA_dh_N)

SadA [Strain GP]	50	HEHAPDSDRDRRVS	EVVIDALEELDLFQVCT	PRRYGGFQSNFRTLFE	ELTA	99
SadA [<i>Microbacterium</i> sp. BR1]	50	HEHAPDSDRDRRVS	EVVIDGLEELDLFQVCT	PRRYGGFQSNFRTLFE	ELTA	99
SadA [<i>Arthrobacter</i> sp. D2]	41	REHALDSDRDRRVS	QVVIDKMEELDLFQVCT	PRRYGGFQANFRTLFD	LTA	90
SadA [<i>Arthrobacter</i> sp. D4]	41	REHALDSDRDRRVS	QVVIDKMEELDLFQVCT	PRRYGGFQANFRTLFD	LTA	90
SadB1 [Strain GP]	20	EANGAQGETDRRVLQDS	IDALEAIGA FRVTQPKKYGGF	QGGLSQDHVDVA	R	69
SadB2 [Strain GP]	3	EANGAKGEADRRAVES	IDALEAIGA FRVTQPKKYGGF	QGGLSQDHVDVA	R	52
SadB [<i>Microbacterium</i> sp. BR1]	25	EKNAAQGEAERRVVS	QESIDALEAIGA FRVTQPAKYGGY	EGDSRAQVDVGA		74
SadB [<i>Arthrobacter</i> sp. D2]	25	EKNAAQGEAERRVVS	QESIDALEAIGA FRVTQPAKYGGY	EGDSRAQVDVGA		74
SadB [<i>Arthrobacter</i> sp. D4]	21	RANGEQGEQNRRAVES	IEALEAVGA FRVTQPSRFGGF	QGGLSQDHVDVA	R	70
SadA [Strain GP]	100	EIARGDGGTAWAFA	LLNSNAWGVGTYSRE	AQ	130	
SadA [<i>Microbacterium</i> sp. BR1]	100	EIARGDGGTAWAFA	LLNSNAWGVGTYSRE	AQ	130	
SadA [<i>Arthrobacter</i> sp. D2]	91	EIARGDGGTAWAFA	GLLNSNAWGVGTYSR	QAQ	121	
SadA [<i>Arthrobacter</i> sp. D4]	91	EIARGDGGTAWAFA	GLLNSNAWGVGTYSR	QAQ	121	
SadB1 [Strain GP]	70	AVGRGDGGTGWITALI	NMA GWLTA LL PDQAQ		100	
SadB2 [Strain GP]	53	AVGRGDGGTGWITALI	NMA GWLTA LL PEQAQ		83	
SadB [<i>Microbacterium</i> sp. BR1]	75	AVGKGDGGTAWVVALT	NIANWLTA LLYPEKAQ		105	
SadB [<i>Arthrobacter</i> sp. D2]	75	AVGKGDGGTAWVVALT	NIANWLTA LLYPEKAQ		105	
SadB [<i>Arthrobacter</i> sp. D4]	71	AIGKADGGTAWVVALI	NIISNWLTSLYPRQAQ		101	

(b) Acyl-CoA dehydrogenase, middle domain (Pfam Acyl-CoA_dh_M)

SadA [Strain GP]	149	AAGSTASARKVDGGYV	ISGRWPYASGSLHAQWV	NLGF	.VEIDGAPVRMM	197
SadA [<i>Microbacterium</i> sp. BR1]	149	PAGPTASARKVDGGYV	ISGRWPYASGSLHAQWA	ELGFV	.VEIDGAPVRMM	197
SadA [<i>Arthrobacter</i> sp. D2]	140	AAGPTASARRVDGGYL	ISGRWPYASGSLHAQWA	ELGFD	.VEIDGETVWMM	188
SadA [<i>Arthrobacter</i> sp. D4]	140	AAGPTASARRVDGGYL	ISGRWPYASGSLHAQWA	ELGFD	.VEIDGETVWMM	188
SadB1 [Strain GP]	116	. . ATNGKTRRVPGGYI	VSGEWGYASGSWHA	EW SFLGAE	LVDENGDFDDA	163
SadB2 [Strain GP]	99	. . ATNGKTKRVPGGYI	VSGEWGYASGSWHA	EW SFLGAE	LVDENGDFDDA	146
SadB [<i>Microbacterium</i> sp. BR1]	121	. . ATNGKTKRVDGGYL	VSGEWSYNSASWHT	QWALGAE	LVDENGDFVDTA	168
SadB [<i>Arthrobacter</i> sp. D2]	121	. . ATNGKTKRVDGGYL	VSGEWSYNSASWHT	QWALGAE	LVDENGDFVDTA	168
SadB [<i>Arthrobacter</i> sp. D4]	117	. . ATSGKTRRVDGGYV	VSGEWPYASGSLHS	DWALV	GANLVDENGDFDDA	164
SadA [Strain GP]	198	S . LVPMDDEVTL	EDTWYVAGMRSGSNT	VVGT		227
SadA [<i>Microbacterium</i> sp. BR1]	198	T . LVPMDDEVTL	EDTWYVAGMRSGSNT	VVGT		227
SadA [<i>Arthrobacter</i> sp. D2]	189	T . LLLPINEVTVE	EDTWYVAGMRSGSNT	IVGR		218
SadA [<i>Arthrobacter</i> sp. D4]	189	T . LLLPINEVTVE	EDTWYVAGMRSGSNT	IVGR		218
SadB1 [Strain GP]	164	QLLIPKSDLG YQDTWY	VAGMRSSGSNTWT	AD		194
SadB2 [Strain GP]	147	QLLIPKTDLG YKDTWY	VAGMRSSGSNTWV	AE		177
SadB [<i>Microbacterium</i> sp. BR1]	169	QLLIPRSDLGFKDI	WHVAGMRSSGSNALS	AT		199
SadB [<i>Arthrobacter</i> sp. D2]	169	QLLIPRSDLGFKDI	WHVAGMRSSGSNALS	AT		199
SadB [<i>Arthrobacter</i> sp. D4]	165	QLLIPRSEFAYKDTWY	VAGMRSSGSNTLI	AN		195

(c) Acyl-CoA dehydrogenase, C-terminal (Pfam Acyl-CoA_dh_2)

SadA [Strain GP]	268	VLVGAQIGLAQAALDY	ALEKLPTRGVTYTKY	AKGSDAPT	NQIAVAEANA	317
SadA [<i>Microbacterium</i> sp. BR1]	268	VLVGAQVGLAQAALDY	ALEKLPTRGVTNTKY	AKGSDAPT	NQIAVAEANA	317
SadA [<i>Arthrobacter</i> sp. D2]	259	ILVAAQIGLAQAALDF	ALEILPQRGVTKTKY	RKGS EAPS	NQIAVAEANA	308
SadA [<i>Arthrobacter</i> sp. D4]	259	ILVAAQIGLAQAALDF	ALEILPQRGVTKTKY	RKGS EAPS	NQIAVAEANA	308
SadB1 [Strain GP]	237	ILAGAQLGIGRAVL	DKVIAGA . SKPIAYTS	IAHKSDSVA	FQLDIAKAALT	285
SadB2 [Strain GP]	220	ILAGAQLGIGRAVL	DKVIAGA . AKPIAYTS	IAHKSDSVA	FQLDIAKAALT	267
SadB [<i>Microbacterium</i> sp. BR1]	242	ILVGPQLGMGRAV	LVERVISKADSKA	IAYTS FERQSDS	IAFQLDIAKAALL	291
SadB [<i>Arthrobacter</i> sp. D2]	242	ILVGPQLGMGRAV	LVERVISKADSKA	IAYTS FERQSDS	IAFQLDIAKAALL	291
SadB [<i>Arthrobacter</i> sp. D4]	238	ILTGAQLGIGRGV	LELVAEKANKKS	IAYTS FERQSDS	IAFQLDIAKAALL	287
SadA [Strain GP]	318	IDTARMLGRRAC	YDIDAAVVTNRGQ	IDWATRARI	RMDLATIAVLCRESID	367
SadA [<i>Microbacterium</i> sp. BR1]	318	IDTARMLGRRAS	YDIDAAVVTNRGQ	IDWATRARI	RMDAATIAVLCRESID	367
SadA [<i>Arthrobacter</i> sp. D2]	309	IDVARMLAKRAC	YDIDAAVFNNGA	IDLPTRARIR	MDTASIAVQCREAIE	358
SadA [<i>Arthrobacter</i> sp. D4]	309	IDVARMLAKRAC	YDIDAAVFNNGA	IDLPTRARIR	MDTASIAVQCREAIE	358
SadB1 [Strain GP]	286	LDSADLMIERACRE	IDEPA . AAGVY	PDYLT	RARNRAYVGVAAETVSKAIE	334
SadB2 [Strain GP]	268	LDSADLMIERACRE	IDEPA . AAGEY	PDYLT	RARNRAYVGVAAETVSKAIE	316
SadB [<i>Microbacterium</i> sp. BR1]	292	LEAAEGFAHRAT	DEIDIPA . AAGVY	PDYLT	RARNRAYVGVWIV EHTARAIE	340
SadB [<i>Arthrobacter</i> sp. D2]	292	LEAAEGFAHRAT	DEIDIPA . AAGVY	PDYLT	RARNRAYVGVWIV EHTARAIE	340
SadB [<i>Arthrobacter</i> sp. D4]	288	LDAADMVFAHRAC	KEIDLPA . EAGEY	PGYLV	RARNRAYVGVSWVEHISR AIE	336
SadA [Strain GP]	368	KMLTAIGSAAFA	SVNPLQQVWRD	SETASR	HAMVN	401
SadA [<i>Microbacterium</i> sp. BR1]	368	KMLTAIGSAAFA	SVNPLQQVWRD	SETASR	HALVN	401
SadA [<i>Arthrobacter</i> sp. D2]	359	RLLTAVGSAAF	ASTSPLQQIWRD	AGTASR	HAMVN	392
SadA [<i>Arthrobacter</i> sp. D4]	359	RLLTAVGSAAF	ASTSPLQQIWRD	AGTASR	HAMVN	392
SadB1 [Strain GP]	335	MLLTAHGS	GGFAEVNAIQR	FWRDQAV	ARHAFIL	368
SadB2 [Strain GP]	317	TLLTAHGS	GGFAEVNAIQR	FWRDQAV	ARHAFIL	351
SadB [<i>Microbacterium</i> sp. BR1]	341	MLLTAHGS	GAFAEVNP	LQR	LWRDQAVASR HAFV L	374
SadB [<i>Arthrobacter</i> sp. D2]	341	MLLTAHGS	GAFAEVNP	LQR	LWRDQAVASR HAFV L	374
SadB [<i>Arthrobacter</i> sp. D4]	337	MLLTSAGS	GAFAEVNP	LQRMWR	DQAVASR HAFV L	370

Figure 6.12 –Amino acid alignment with MUSCLE (Edgar 2004) of Acyl-CoA domains: N-terminal (a), middle (b) and C-terminal (c); between SadA and SadB homologs in *Microbacterium* sp. BR1, *Arthrobacter* sp. D2 and D4 and strain GP (SadB1: D3X82_00235; SadB2: D3X82_03160). Conserved regions within SadA and SadB and highlighted in green and conserved regions shared between all proteins are marked with an asterisk.

Furthermore, structural homology search with SWISS-MODEL (Waterhouse et al. 2018) resulted in highest similarity with XiaF (FADH₂) from *Streptomyces* sp. HKI0576 (PDB: 5LVW), 4-hydroxyphenylacetate hydroxylase (4-HPA) from *Acinetobacter baumannii* (PDB: 2JBR), HsaA monooxygenase from *Mycobacterium tuberculosis* and *Rhodococcus jostii* RHA1 (PDB: 3AFE and 2RFQ, respectively). All of these monooxygenases are known to hydroxylate aromatic compounds

For instance, XiaF is likely involved in terpenoid biosynthesis in *Streptomyces* sp., it is tetrameric and acts in a two-component system together with a flavin reductase (Kugel et al. 2017). Furthermore, this monooxygenase can use indole as a surrogate substrate and form indigo and indirubin, as previously described by Kugel et al. (2017) while 4-HPA (EC 1.14.14.9) and HsaA monooxygenases (EC 1.14.14.12) catalyze the insertion of oxygen in the benzene ring of 4-hydroxyphenylacetate or 3-hydroxy-9,10-seconandrost-1,3,5(10)-triene-9,17-dione, respectively.

The similarities between XiaF and SadA (32 % amino acid identity, 51 % similarity, 4 % gaps and E-value of 8e-66), SadB1 (locus tag: D3X82_00235, 33 % identity, 51 % similarity, 2 % gaps and E-value of 8e-68), and SadB2 (locus tag: D3X82_03160, 35 % identity, 52 % similarity, 1 % gaps and E-value of 9e-69) are sufficient to suggest a high degree of confidence on the homologous relationship between these proteins (Sander and Schneider 1991; Pearson 2013). The use of XiaF as a template for modelling resulted in a robust structural prediction of these proteins with quality scores above -4 (QMEAN, Qualitative Model Energy ANalysis) (Benkert et al. 2011): -2.45, -1.48 and -1.52, for SadA, SadB1 and SadB2, respectively. These results suggest that the comparison with XiaF is suitable to perform preliminary structural analysis of these monooxygenases.

Phylogenetic analysis revealed that XiaF shares a common ancestor with other xenobiotic-degrading enzymes (Kugel et al. 2017), suggesting that both monooxygenases of the SadABC complex likely share ancestry with similar enzymes. However, pairwise sequence

alignment revealed a low degree of similarity within the substrate binding pocket of XiaF and homologs regions of SadA and SadB. For instance, the presence of isoleucine I237 in an alpha-helix of XiaF (Fig. 6.13a) constricts the size of the substrate binding pocket of this monooxygenase. However, alanine residues neighboring I237 are substituted in strains GP, *Microbacterium* sp. BR1 and *Arthrobacter* sp. D2 and D4 by proline residues (P261 and P264 in strain GP) that may induce its structural change to a loop. This conformation probably creates a wider pocket in SadA and may allow easier access to the active site of this monooxygenase.

Additional substitutions in the active site of all SadA homologs further support this hypothesis. Specifically, the serine residue (S121, Fig. 6.12a and 6.13) of XiaF is substituted by an alanine in strain GP (A145) and threonine in *Microbacterium* sp. BR1 (T144) and both *Arthrobacter* sp. (T135). The serine residue has a hydroxymethyl and side chain, while alanine and threonine have a methyl and 1-hydroxyethyl groups, respectively. Serine and threonine are both polar amino acids and likely make the active site of these enzymes amenable for polar cyclic substrates while SadA of strain GP may prefer aromatic substituted substrates.

a

	XiaF	134	K L A . S V F A	140	251	*	T A A I A A M	257
	SadA [Strain GP]	141	R I T W A T N P	149	260		T P M A P H F	266
	XiaF	134	K L A S V . . .	138	251	*	T A A I A A M	257
	SadA [<i>Microbacterium</i> sp. BR1]	141	R I T T V T N P	148	260		T P M V P N H	266
	XiaF	134	K L A S V F . A	140	251	*	T A A I A A M	257
	SadA [<i>Arthrobacter</i> sp. D2]	132	R I T T A T R P	139	250		T P L A P N H	256
	SadA [<i>Arthrobacter</i> sp. D4]	132	R I T T A T R P	139	250		T P L A P N H	256

b

	XiaF	134	* K L A S V F A A	141	251	*	T A A I A A M	257
	SadB1 [Strain GP]	112	K V T V V L A T	119	229		A G W I P W L	235
	SadB2 [Strain GP]	95	K V T V V L A T	102	212		A G W I P W L	218
	SadB [<i>Microbacterium</i> sp. BR1]	117	K V S V V L A T	124	234		A G W I P V L	240
	SadB [<i>Arthrobacter</i> sp. D2]	117	K V S V V L A T	124	234		A G W I P V L	240
	SadB [<i>Arthrobacter</i> sp. D4]	113	K V S V V L A T	120	229		A G W I P V L	235

Figure 6.13 – Pairwise alignment with BLASTp of the regions of the substrate binding pocket of XiaF (accession number 5LVW) and each homolog of SadA (a) and SadB (b) in strains GP, *Microbacterium* sp. BR1 and *Arthrobacter* sp. D2 and D4. Conserved regions between the different SadA and SadB homologs are highlighted in green, non-conserved residues are highlighted in red. Residues shared by all sequences are marked with an asterisk. The diagrams were designed with Excel 2013.

Furthermore, the alanine residue (A145) in the SadA of strain GP would make the active site of this enzyme slightly larger than the active sites of SadA of *Microbacterium* sp. BR1 and XiaF. These findings may explain the differences in SMX degradation rate found between the consortium of strain GP and *A. denitrificans* PR1 and axenic cultures of *Microbacterium* sp. BR1 (Ricken et al. 2013; Reis et al. 2014). For instance, in resting cells conditions the specific degradation rates of the axenic cultures and the consortium were similar (approximately $2 \mu\text{mol}/\text{g}_{\text{cell dry weight}} \times \text{min}$) (Ricken et al. 2013; Reis et al. 2014), however, considering that the abundance of strain GP is significantly low (1-4 % relative abundance, Reis et al. 2018a), this strain appears to be more efficient than *Microbacterium* sp. BR1. Furthermore, in the consortium, 4-aminophenol never accumulated in sufficient amounts to be detected and was only observed in incubations with ^{14}C -SMX saturated with an excess of the unlabeled 4-aminophenol (Reis et al. 2018a).

Conversely, the substitutions and subsequent changes in the structure of SadB are harder to predict. For instance, in all SadB homologs, the XiaF S121 is substituted by a valine (isopropyl side chain, Fig. 6.13b). Furthermore, the A236 of XiaF is substituted by tryptophan in all SadB homologs (W231 in SadB1 of strain GP) suggesting that SadB's binding pocket could be significantly smaller than XiaF's and thus accommodate smaller substrates. Despite the low amino acid identity between some of the SadB homologs (Fig. 6.10), the analysis of the conserved domains indicates that the active site could be highly conserved among these enzymes.

In this way, although none of the expected metabolites were detected during 4AP degradation in strain GP (Reis et al. 2018a), the presence of homologs of SadB in the genome of this strain suggests that it might catalyze 4AP hydroxylation as previously described for *Microbacterium* sp. BR1 (Ricken et al. 2015a).

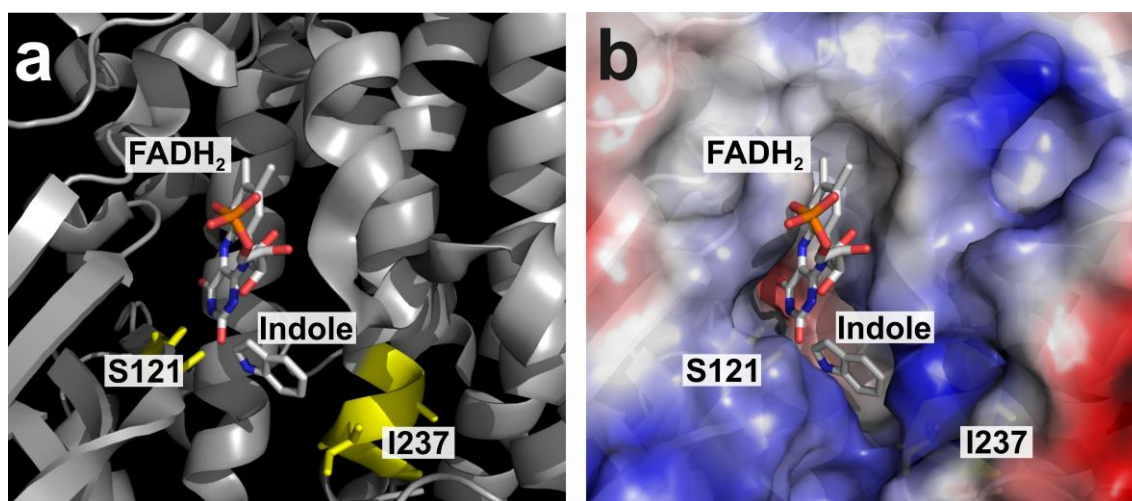


Figure 6.14 – Close-up of the substrate-binding pocket of XiaF (PDB: 5LVW) bound to FADH₂ and indole obtained by Kugel et al. (2017). FADH₂ is the co-factor, indole the substrate and S121 and I237 are the residues that are modified in SadA of *Microbacterium* sp. BR1 and strain GP. The ribbon (a) and electrostatic surface potential (b) diagrams have been prepared with PyMol (Schrödinger 2002). In b negative potential is shown in red and positive potential in blue.

6.3.8 Taxonomic classification of strain GP

The total dependency of strain GP on strain PR1 and the lack of similar organisms hinder further efforts for accurate taxonomic classification. Nevertheless, according to the

recommendations of the International Committee on Systematic Bacteriology, organisms unable to grow in pure culture can have a provisional taxonomic status (*Candidatus*) (Murray and Stackebrandt 1995).

When comparing our data with the standards proposed by Konstantinidis et al. (Konstantinidis et al. 2017) to describe uncultivated prokaryotes and/or those forming microbial consortia, we propose to classify strain GP in a provisional new species within the genus *Leucobacter*, '*Candidatus* *Leucobacter* sulfamidivorax'.

6.3.9 Description of '*Candidatus* *Leucobacter* sulfamidivorax'

'*Candidatus* *Leucobacter* sulfamidivorax' [sul.fa.mi.di.vo'rax N.L. n. *sulfamidum*, sulfonamide; L. adj. *vorax* devouring, ravenous, voracious; N.L. masc. adj. *sulfamidivorax*, sulfonamide-degrading].

Forms a bacterial consortium with *A. denitrificans* strain PR1 and can only be cultured in association with this *Proteobacteria*. Cells stain Gram-positive, present a rod-shaped morphology (1.3 ± 0.03 μm long and 0.5 ± 0.03 μm wide), and are probably non-motile. It produces light yellow-colored colonies with less than 1 mm in diameter on top of the colonies of *A. denitrificans* strain PR1 after 10 d of incubation on 25% (w/v) BHI plates at 30 °C. In liquid medium, it constitutes between 1 and 4% of the total cells. In medium MMSY, the aerobic growth is significantly impaired at 37°C when compared to that at 22 and 30°C. Grows well at neutral (pH 7.2) and basic (pH 9.5) pH values when compared to that at pH 5.5. Grows better in oligotrophic media (e.g., MMSY), in comparison to complex and rich medium (e.g., BHI and TSA). Tolerates up to 8 % (w/v) NaCl. The DNA G+C content is 69.68 mol%. The representative strain, GP, which degrades sulfonamides, was obtained from a sulfamethoxazole enrichment culture produced from activated sludge from an urban WWTP, in North Portugal, in 2011.

6.4 Conclusions

The genomic analysis showed that strain GP carries at least two copies of *sadA* encoding for the previously described sulfonamide monooxygenase. Both copies are flanked by a single IS1380 family transposase and were found in contig 5 that represents a potential plasmid carried by strain GP. Noticeably, a highly similar *sadA*-containing cluster was also found in the genomes of *Arthrobacter* sp. D2 and D4.

All sulfonamide-degrading *Actinobacteria* harbored homologs to *sadB* and *sadC*, nevertheless, in strains GP and *Arthrobacter* sp. D2 and D4 these genes were not in the vicinity of *sadA* and were not associated neither with mobile nor integrative elements.

Functional analysis of strain GP genome revealed that this strain may have lost some essential genes, mainly of genes linked to tetrapyrrole biosynthesis and thiol transporters. These results strongly suggest that strain GP may be unable of synthesizing respiratory and non-respiratory cytochromes, essential for aerobic growth, and may need a helper strain to provide exogenous heme and help maintain an optimal redox balance. However, supplying strain GP with exogenous heme and catalase did not abolish this strain's dependent phenotype. Additional studies are necessary to evaluate the gene expression in strain GP and the mechanisms of intact heme acquisition in this Gram-positive bacterium.

Our data suggests that strain GP should be considered as the representative strain of a putatively new species within the *Leucobacter* genus, '*Candidatus* *Leucobacter* sulfamidivorax'.

6.5 Methods

6.5.1 Culture conditions and DNA extraction

Five type strains of the genus *Leucobacter* were selected for comparative studies based on 16S rRNA gene pairwise similarity to strain GP (Table 6.1) (Reis et al. 2018a) and purchased from DMSZ (Germany). These strains were grown in Brain-Heart Infusion (BHI,

Sigma) for 15 h. All incubations were carried out in the dark at 30°C under continuous shaking at 120 rpm.

The two-member consortium (Reis et al. 2018a) consisting of *Achromobacter denitrificans* PR1 (LMG 30905) and strain GP was incubated for 7 d in mineral medium with 0.2 g/l yeast extract, 700 mM succinate, 0.6 mM SMX, and 2.5 g/L 2-phenylethanol (Sigma) as an inhibitor of Gram-negative cells (MMSY-SMX-PE). Further attempts to isolate strain GP were performed by incubating the consortium in 25% BHI agar plates (v/v) with 0.6 mM SMX, heme or heme precursors (10 µg/l, coproporphyrin III, coproporphyrin III tetramethylester, coproporphyrin I dihydrochloride) (Reis et al. 2018a), putrescine (9 µg/l) and catalase (500 U) from Sigma, respectively.

Genomic DNA extraction of the *Leucobacter* spp. type strains and the two-member consortium was performed from 2×10^{10} cells with GenElute Bacterial Genomic DNA Kit (Sigma) as previously described (Reis et al. 2018a).

6.5.2 Physiological characterization of the consortium

The effect of environmental parameters on the abundance of each strain of the consortium was investigated. The effect of temperature was examined by incubating the culture in MMSY at 22°C, 30°C and 37°C. The influence of pH was tested at 30°C in diluted LB medium (DLB, 25% w/v) with 12 mM of MES (pH 5.5), 12 mM phosphate buffer (pH 7.2) or 12 mM of CAPS (pH 9.5) at 30°C. The tolerance to NaCl was examined in DLB supplemented with NaCl at final concentrations of 2, 4, 6, 8 or 10% (w/v) at 30°C. To determine the influence of different standard media in the growth of strain GP, the consortium was incubated in unbuffered R2A, TSA and different dilutions of BHI (5, 25, 50, 75 and 100%). Cultures under all these conditions were incubated at 30 °C for 15 h and carried out in triplicate and in parallel to an abiotic control. The abundance of each strain in the consortium was assessed by quantitative PCR with primers targeting the 16S rRNA gene as previously described (Reis et al. 2018a). Significant differences ($p < 0.05$) between

overall abundance of strain GP were determined either by two-way ANOVA (to compare 16S rRNA copies/ml of GP and PR1 at different pH, temperature and salinity) or one-way ANOVA (to compare the ratio of the 16S rRNA copies/ml of strains GP and PR1 across different media) and Tukey's tests using RStudio v 1.1.463 running with R v3.5.2 (de Mendiburu 2013; Team 2015a; Team 2015b).

6.5.3 Microscopy

The consortium was visualized in mid-stationary phase (12 h incubation, MMSY, 0.6 mM SMX) by Cryo-Transmission Electron Microscopy (Cryo-TEM) for morphological characterization. Briefly, a 4 μ l aliquot of the overnight grown liquid culture was adsorbed onto a holey carbon-coated grid (Lacey, Tedpella, USA), blotted with Whatman 1 filter paper and vitrified into liquid ethane at -180 °C using a vitrobot (FEI, USA). Frozen grids were transferred onto a Talos Electron microscope (FEI, USA) using a Gatan 626 cryo-holder (GATAN, USA). Electron micrographs were recorded at an accelerating voltage of 200 kV using a low-dose system (20 to 40 e-/Å²) and keeping the sample at -175°C. Defocus values were -3 to 6 μ m. Micrographs were recorded on 4K x 4K Ceta CMOS camera. The cell size, and periplasmic and cell wall thickness were measured with Fiji from the ImageJ platform (Schindelin et al. 2012).

For TEM analyses, 4 μ l aliquot of the sample was adsorbed onto a glow-discharged carbon film-coated copper grid, and subsequently negatively stained with 2% uranyl acetate. Images were recorded using Philips CM200FEG electron microscope operating at 200 kV on TemCam-F416 CMOS camera (TVIPS, Germany).

Fluorescence in situ hybridization (FISH) was performed as previously described (Pernthaler et al. 2001) with a few modifications. To analyze strain GP (A) the cells of the microbial consortium were fixed with ethanol for 16 h at 4 °C. Prior to hybridization the cells were pre-treated with achromopeptidase (Sigma) at 60 U/ml for 60 seconds at 37 °C. While, to analyze *Achromobacter denitrificans* PR1 cells (B) the microbial consortium was

fixed with 4 % (v/v) formaldehyde (Sigma) for 3 h at 4 °C and no pre-treatment was performed. Probe concentration was 3 or 10 ng/μl for strain PR1 and GP, respectively. Formamide (Sigma) concentration was 25 or 50% (v/v) for PR1 and GP, respectively.

To visualize strain GP the modified ActORD1 FISH probe was used: 5' fluorophore: FAM, green; sequence: 5'- CACCAGGAATTCCAATCTCC-3'; original probe accession number: pB-1931 (Kyselková et al. 2008). To visualize strain PR1, cells hybridized with the Alca2 FISH probe: 5' fluorophore: Cy3; orange/red; sequence: 5'- CATCTTTCTTTCCGAACCGC-3'; probe accession number: pB-2127 (Sanguin et al. 2006).

6.5.4 *Leucobacter* spp. type strains whole-genome sequencing and assembly

High-quality DNA of the selected *Leucobacter* spp. type strains (Table 6.1) was used for paired-end sequencing (2 x 150 bp) with the Hiseq 2500 platform (Illumina) by GATC Biotech (Germany). Paired-end reads were adapter and quality trimmed ($\geq Q20$) with the BBDuk from the BBMap package v35.74 (<https://sourceforge.net/projects/bbmap>). High-quality reads were used for *de novo* assembly with SPAdes version v3.11.1 (Bankevich et al. 2012) with the option `-careful`. Contigs longer than 500 bp were used a further extension with SSPACE v3.0 (Boetzer et al. 2011) with recommended settings.

6.5.5 Whole consortium sequencing

The metagenome of the consortium was sequenced in the Miseq (Illumina) and MinION (Oxford Nanopore Technologies, ONT) platforms. The paired-end Miseq library was prepared from 1 μg of high-quality DNA with KAPA HyperPrep Kit (Kapa Biosystems) and TruSeq DNA PCR-free LT Kit library adaptors (Illumina) with a few modifications. Briefly, enzymatic fragmentation of the genomic DNA was increased to 25 min, and ligation was performed for 2 h at 20°C. 8 cycles of enrichment PCR and size selection for fragments with approximately 500-700 bp was carried out with NucleoMag magnetic beads

(Macherey Nagel). Paired-end sequencing (2 x 250 bp) was performed in an Illumina Miseq system (Illumina) with a V2 MiSeq Reagent Kit (500 cycles).

Two independent libraries were prepared for MinION long-read sequencing. Both libraries were prepared from 1.5 µg high-quality DNA sheared with a g-TUBE (Covaris) to approximately 8 kb fragments. The libraries were then prepared with the 1D genomic DNA sequencing kit (SQK-LSK108), pooled, loaded with the Library Loading Bead Kit (EXP-LLB001) and sequenced using a flow cell with R9.4 chemistry (FLO-MIN 106, Oxford Nanopore).

6.5.6 Metagenome-assembled genome (MAG) of strain GP

ONT long reads were adapter trimmed with Porechop v0.2.3 (<https://github.com/rrwick/Porechop>). Illumina paired-end reads were adapter and quality trimmed ($\geq Q20$) with BBDuk from the BBMap package v35.74 (<https://sourceforge.net/projects/bbmap/>). The high-quality paired-end reads were used for hybrid error correction of ONT reads with LoRDEC v0.9 (Salmela and Rivals 2014). The resulting long reads were subsequently used for whole-metagenome assembly with Canu v1.7 (Koren et al. 2017).

Metagenomics contigs were analyzed with SSU finder from CheckM v1.0.11, to determine the amount and affiliation of taxonomic bins present in the metagenome (Parks et al. 2015). The metagenome was aligned to the complete genome of strain PR1 (Genbank accession no. CP020917) (Reis et al. 2017) with BLASTn v2.7.1+ to remove contigs affiliated to the proteobacterium (Zhang et al. 2000) (e-value, identity and hit length threshold cutoffs set to $1e-10$, 80% and 30%, respectively). Contigs without significant hits were retrieved from the metagenome and used to construct the new taxonomic bin corresponding to strain GP.

Both ONT Illumina-corrected and Illumina reads were used for read binning between strain PR1 and GP with GraphMap v0.5.2 (Sović et al. 2016) and BWA v0.7.12 (Li 2013), respectively. Reads mapping uniquely to strain GP bin were used for re-assembly with SPAdes v3.7.1 (Bankevich et al. 2012). High-coverage contigs ($\geq 1\times$ k-mer coverage) obtained with hybrid assembly were used for further scaffolding and polishing with Circlator v1.5.5 (Hunt et al. 2015) and four iterations with Pilon v1.22 (Walker et al. 2014). All data has been deposited in NCBI under the Bioproject accession number PRJNA490017.

6.5.7 Genome annotation, completeness, and mobile genetic elements

Quality scores of draft assemblies were assessed with QUAST v4.6.3 (Konstantinidis and Tiedje 2005). Genome contamination and completeness were determined with CheckM v1.0.11 (Parks et al. 2015), and tRNA were identified with tRNAscan-SE v2.0 (Lowe and Chan 2016). Open-reading frames (ORFs) were predicted and annotated with NCBI Prokaryotic Genome Annotation Pipeline (PGAP) v4.7 (Tatusova et al. 2016) and with RASTtk on the RAST webserver v2.0 (Brettin et al. 2015). Antibiotic resistance genes were confirmed by aligning amino-acid sequences with BLASTp v2.7.1+ against the Antibiotic Resistance Database (ARDB) v1.1 from July, 2009 (Liu and Pop 2009) and by analyzing the draft genome with the Resistance Gene Identifier (RGI) against the CARD database v3.0.1 (Jia et al. 2017a). Functional annotation and KEGG Orthology (KO) assignment was further performed with eggNOG-Mapper v4.5.1 (Huerta-Cepas et al. 2017) and BlastKOALA v2.1 (Huerta-Cepas et al. 2017).

The presence of plasmids in the genome of strain GP was investigated by assessing differences in coverage and G+C content between contigs, and by further searching for similarities with other plasmids using NCBI Blast to search against the non-redundant (*nr*) database on November, 2018 (Johnson et al. 2008). The differences in coverage were identified by mapping both Illumina and ONT reads against the metagenome of the

consortium (concatenated draft assembly of strain GP and complete genome of strain PR1) with BWA v0.7.12 (Li 2013) or Graphmap v0.5.2 (Sović et al. 2016), respectively. The coverage of sorted bam files was evaluated with Qualimap v2.2.1 (Okonechnikov et al. 2015).

Genes typically associated with plasmids (Martini et al. 2016) were identified by aligning amino-acid sequences against the CDD database (v3.17) using the NCBI conserved domain search with default settings on November, 2018 (Finn et al. 2014; Marchler-Bauer et al. 2015; Finn et al. 2016). Conjugative elements associated with the type VI secretion systems and possible origins of replication were analyzed with CONJscan v1.0.2 using the Galaxy platform at Pasteur (Guglielmini et al. 2014; Mareuil et al. 2017; Afgan et al. 2018).

6.5.8 Phylogenetic analysis of strain GP

The full genome and the 16S rRNA gene of all fully sequenced *Leucobacter* spp. isolates and MAGs were used for phylogenetic analysis (Table 6.4). Sequences were retrieved from the NCBI database (last accessed on November, 2018) (NCBI Resource Coordinators 2017), except for *Leucobacter* sp. AEAR which was available in GitHub (<https://github.com/Percud/Leucobacter>). Moreover, representative genomes of *Microbacterium*, *Leifsonia*, *Agromyces* and *Arthrobacter* genera, were further included to serve as outgroup (Table 6.4).

16S rRNA sequences were used for multiple sequence alignment with MUSCLE in MEGA6 (Edgar 2004; Tamura et al. 2013). The phylogenetic tree was inferred from maximum likelihood analyses using MEGA6 (Tamura et al. 2013) with the best-fitting model: Tamura-Nei (Tamura and Nei 1993) substitution model with gamma distribution and invariant sites (TN93+G+I). Bootstrap support values inferred from 1000 replicates.

The PhyloPhlAn pipeline v0.99 (Segata et al. 2013) was used to infer phylogenomic relationships among all fully sequenced members of the *Leucobacter* genus and strain GP

(data available on July 2019, Table 6.4). 400 universal proteins were identified and extracted with USEARCH v5.2.32 (Shimodaira 2002) and used for amino acid alignments with MUSCLE v3.8.31 (Edgar 2004). The concatenated alignments were used for approximately-maximum-likelihood analysis with FastTree v2.1.8 (Price et al. 2010) and for the computation of local support values was performed using the Shimodaira-Hasegawa test (Shimodaira 2002). Both the 16S rRNA phylogenetic tree and the PhyloPhlAn phylogenomic tree were visualized with FigTree v1.4.3 (<http://tree.bio.ed.ac.uk/software/figtree>) and rooted at the midpoint or the outgroup, respectively.

16S rRNA gene pairwise sequence similarity, Average Nucleotide Identity (ANI), Average Amino-acid Identity (AAI), and Percentage of Conserved Proteins (POCP) (Qin et al. 2014) between strain GP and all validly named and fully sequenced strains of the *Leucobacter* genus on July 2019 (Table 6.1) were determined using the pairwise similarity tool and 16S-based ID app available on the EzBioCloud platform (Yoon et al. 2017), AAI/ANI-matrix from the enveomics toolbox (<http://enve-omics.ce.gatech.edu/g-matrix>) (Rodriguez-R and Konstantinidis 2016) and the POCP.sh script provided by Harris et al. (Harris et al. 2017) (<https://doi.org/10.6084/m9.figshare.4577953.v1>).

6.5.9 *Leucobacter* spp. core and pangenome analysis

Gene search between *Leucobacter* spp. genomes (last accessed on November 2018) and strain GP (Table 6.4) was computed with GET_HOMOLOGUES package v3.1.4 (Contreras-Moreira and Vinuesa 2013) using all-against-all BLASTp with default settings and Pfam-domain scanning. Clustering was performed with COGtriangles v2.1 (-G -t 0 -D), orthoMCL v1.4 (-M -t 0 -D) and BDBH (-D -e) algorithms. For comparison between two genomes only BDBH was used. For the pangenome analysis, the clusters were generated from the intersection of COGtriangles and orthoMCL using the compare_clusters.pl script (-t 0) from the GET_HOMOLOGUES pipeline (Contreras-Moreira and Vinuesa 2013). Orthologs gene

clusters present in the core and softcore genome (present in 95% of the genomes) (Kaas et al. 2012) were used for functional annotation with eggNOG-Mapper (Huerta-Cepas et al. 2017) and BlastKOALA (Huerta-Cepas et al. 2017). The list of KO identifiers was used to visualize and analyze core metabolic pathways in KEGG (Kanehisa et al. 2017) and compared to the metabolic reconstruction obtained with Pathway Tools v22.0 (Karp et al. 2016).

To evaluate possible gene loss, clusters present in at least 90% (28 of 31 genomes) of *Leucobacter* spp. genes but absent in the genome of strain GP were found by analyzing all clusters with the `parse_pangenome_matrix.pl` script from the GET_HOMOLOGUES pipeline (Contreras-Moreira and Vinuesa 2013). To exclude annotation errors, clusters marked as missing were further curated by aligning representative sequences of each cluster to the draft genome of strain GP with tBLASTn (Johnson et al. 2008).

6.5.10 Whole genome comparisons and evolution of the SadABC complex

Whole genome comparison between strain GP and other sulfonamide degraders (Table 6.4), was performed with the GET_HOMOLOGUES package as described above (Contreras-Moreira and Vinuesa 2013). The core and softcore genes shared between these strains were obtained by computing the intersection of clusters generated by COGtriangles and orthoMCL using the `compare_clusters.pl` script (-t 7; -t 6, respectively). Relevant gene clusters (i.e., SadA, SadB, SadC, YceI, and IS1380/IS3/IS4 transposases) were further used for homology searches with BLASTp against the NCBI non-redundant database (Johnson et al. 2008), structural modelling in SWISS-MODEL (Waterhouse et al. 2018) and conserved domain searches in NCBI database (Marchler-Bauer et al. 2017). The phylogeny and evolution of these proteins and their corresponding homologs were inferred from amino acid alignments with MUSCLE in MEGA6 (Edgar 2004; Tamura et al. 2013). The phylogeny was estimated from combination of three methods: Maximum Likelihood (ML), Bayesian optimization and Neighbor Joining (NJ). For the ML method, the amino acid alignments

were first evaluated with ProtTest v3.4.2 (Darriba et al. 2011) to find the best-fitting model of protein substitution. For SadA and SadB phylogeny the LG substitution model was used (Le and Gascuel 2008) with gamma plus invariant sites heterogeneity model (G+I); for SadC and YceI the WAG model (Whelan and Goldman 2001) was used with G or G+I, respectively; and for the transposase the JTT model (Jones et al. 1992) was used with the G heterogeneity model. The ML trees with bootstrap support values from 1,000 replicates were constructed with MEGA6 (Tamura et al. 2013). Bayesian optimization was calculated with BEAST v1.10.4 (Suchard et al. 2018). Markov chain Monte Carlo (MCMC) were run using one million iterations and trees were sampled every 100 generations. The results of triplicate runs were combined with LogCombiner from the BEAST package (Suchard et al. 2018), and the combined output was analyzed with Tracer v1.7.1 to assess the overall quality of the estimation (Rambaut et al. 2018). Posterior probability support values and consensus tree was calculated from 10 % of the total number of iterations (300,000). For the NJ method, the phylogenetic trees were constructed in MEGA6 using the JTT model (Jones et al. 1992) with uniform rates and bootstrap support values were inferred from 1,000 replicates. The ML trees were rooted at midpoint and visualized with FigTree v1.4.3 (<http://tree.bio.ed.ac.uk/software/figtree/>), Bayesian posterior probability values, and ML and NJ bootstrap support values were included in the final tree.

Functional comparison between strain GP and its helper strain, *A. denitrificans* PR1, was performed by submitting both genomes for annotation with RASTtk (Brettin et al. 2015). Furthermore, the metabolic reconstruction and comparison between these distantly related strains were achieved with the function based comparison tool in the SEED viewer version 2.0 (Overbeek et al. 2014).

Chapter 7

General Discussion

Antibiotic resistance is considered an ancient phenomenon that has spread to unprecedented levels due to the intensive and sometimes imprudent and inappropriate use of these drugs over the past decades (Andersson and Hughes 2010; Gullberg et al. 2011). Many resistance mechanisms are thought to have evolved by mutation and transference of genes conferring protection to antibiotic-producing bacteria (Martin and Liras 1989; Hopwood 2007; Van Goethem et al. 2018). Presently, resistance is reported to occur through three primary mechanisms: (i) target modification, (ii) efflux and (iii) enzymatic inactivation (Wright 2005; Blair et al. 2015). Overall, the widespread dissemination of these mechanisms has led to the loss of efficiency of current antibiotics and plunge the world into crisis (Ventola 2015; Welte 2016; Simpkin et al. 2017). In this way, new strategies need to be developed in order to attenuate the burden of resistance.

7.1 Antibiotic degraders: a threat or an opportunity?

In this framework, many researchers are investigating antibiotic degradation by microorganisms as a way to control the propagation of resistance. However, in light of the most recent knowledge, we should consider the following question: do antibiotic degraders present a threat or an opportunity?

Antibiotics are especially hard to remove. They are micropollutants that exert important changes in environmental communities, especially at concentrations well below their minimum inhibitory limits (Martinez 2009; Gullberg et al. 2011; Nicoloff and Andersson 2016). This phenomenon is recurrent in stressful environments with high cell densities typically found in WWTP and animal farms. In these environments, the presence of these micropollutants may promote the development of resistance, instead of reducing it (Rizzo et al. 2013). Furthermore, these niches can often act as resistance hotspots and have most likely aided in the widespread dissemination of these traits among pathogenic and commensal bacteria (Rizzo et al. 2013; Lood et al. 2017; Sabri et al. 2018). In this way, antibiotic contamination cannot be dealt in the same way as contamination with persistent pollutants. Therefore, typical bioaugmentation and bioremediation strategies need to be

revised before being further considered. Instead, a more heuristic approach should integrate the knowledge on the development and spread of resistance with the knowledge on strategies for xenobiotic decontamination.

Naturally occurring antibiotics, perhaps due to the more prolonged exposure of the microbiota, are expected to be more susceptible to degradation in comparison to their synthetic counterparts. An example of this phenomenon is the enzymatic hydrolysis of beta-lactams. The prolonged and extensive use of these natural and semi-synthetic antibiotics has intensified the development of an ever-increasing amount of hydrolytic enzymes able to cleave the beta-lactam ring (Naas et al. 2017). These beta-lactamases can cleave the beta-lactam ring of penicillins and semi-synthetic beta-lactams such as carbapenems, leading to the complete loss of antimicrobial susceptibility (Bush and Jacoby 2010; Amador and Prude 2013; Naas et al. 2017). Noticeably, enzymes with beta-lactamase activity are thought to be ancient and have recently been identified in microorganisms isolated from a pristine four-million-year-old cave (Bhullar et al. 2012).

However, researchers have suspected that microbiota in stressful conditions would eventually evolve to degrade even synthetic antibiotics, as it has been continuously described for other xenobiotic compounds (Timmis and Pieper 1999; Rieger et al. 2002). Indeed, transformation and consequent inactivation of antibiotics have been extensively described for antibiotics of almost all classes (Wright 2005; Larcher and Yargeau 2012; Woappi et al. 2014; Caracciolo et al. 2015), including sulfonamides, the first fully synthetic antibiotics with application in therapy.

The ability to degrade antibiotics presents an opportunity to decontaminate the environment and mitigate the burden of resistance. However, many antibiotic transformations serve only as a mean of detoxification and, thus are often reversible (see Introduction section 1.3). Nevertheless, an increasing minority of microorganisms has been shown to use antibiotics as carbon and energy sources (Woappi et al. 2014; Deng et

al. 2018). These reactions often involve the cleavage of important bonds within the antibiotic molecule. Hence, they are expected to be irreversible and to form metabolites devoid of antimicrobial activity (see Introduction section 1.4).

Therefore, this ability could be exploited for bioremediation and bioaugmentation, but, far from an opportunity, it is increasingly regarded as a public health concern. Indeed, the ability to degrade antibiotics may also confer resistance to the host strain. This resistance phenotype has been observed in many bacterial strains carrying beta-lactamase-encoding genes (Bush 1989; Paterson and Bonomo 2005; Amador and Prude 2013). Also, sulfonamide resistance was significantly enhanced in recombinant *Escherichia coli* transformed with an arylamine *N*-acetyltransferase (BanatC) from *Bacillus anthracis* (Pluvinage et al. 2007); and, more recently, in an imipenem-susceptible *Escherichia coli* transformed with a Baeyer-Villiger monooxygenase (Ar-BVMO) from *Acinetobacter radioresistens* (Minerdi et al. 2016). Furthermore, as shown for the tetracycline monooxygenase encoded by *tetX* (Yang et al. 2004; Leski et al. 2013; Ghosh et al. 2015) and for tetracycline destructases (Forsberg et al. 2015), these elements may be highly mobile and transfer from environmental into commensal and even pathogenic bacteria with aggravated risks to human and animal health.

Many studies subsequently showed that these antibiotic degraders might also cause indirect resistance by inadvertently conferring protection to susceptible pathogenic bacteria and leading to treatment failures (Leski et al. 2013; Forsberg et al. 2015; Nicoloff and Andersson 2016). For these reasons, strategies aiming to harness microorganisms' ability to degrade antibiotics to mitigate antibiotic resistance should take into account the risks of HGT.

7.2 A sulfonamide-degrading two-member consortium and dependency of strain GP

Motivated by the need to understand antibiotic degraders further, our group had previously carried out enrichment cultures that lead to the isolation of *A. denitrificans*

strain PR1, which seemed to catalyze the partial mineralization of SMX with concomitant accumulation of its corresponding heterocyclic moiety (3A5MI) (Reis et al. 2014). Even during the earlier studies, the isolation of this degrader from the original enriched culture proved to be difficult. The degrader appeared to be a minority in this mixed culture and, as we later discovered, it also irreversibly lost the ability to degrade sulfonamides after repeated sub-culturing in laboratory conditions. It was only when incubation time was increased to more than 10 d (Chapter 4) that an additional morphotype became visible on agar plates. The additional morphotype, named strain GP, was identified as representing a new species and potentially a new genus within the *Microbacteriaceae* family (Chapter 4 and 6). Curiously, it was also found to be unable to grow independently from *A. denitrificans* PR1, suggesting that a syntrophic relationship may form between the two members of this sulfonamide-degrading consortium.

Metabolic syntrophy or dependency on community members is increasingly recognized as a generalized behavior in natural communities. Relevant examples of important syntrophs are terephthalate-degrading communities (Lykidis et al. 2011; Wu et al. 2013), anammox (Jetten et al. 2005a; Jetten et al. 2005b; Oshiki et al. 2013), dichloromethane-degrader '*Candidatus* Dichloromethanomonas elyunquensis' (Kleindienst et al. 2017), and members of the candidate phylum "*Latescibacteria*", which thrive in hydrocarbon-impacted environments (Youssef et al. 2015; Farag et al. 2017). Interestingly, to date, no culturable representatives were obtained for these microorganisms.

To the best of our knowledge, the only other description of a sulfonamide-degrading consortium has been made by Levine (2016). These authors enriched soil from a cattle feedlot with sulfadiazine. This procedure resulted in the recovery of a sulfadiazine-degrading consortium. The main culturable members of this culture were isolated and identified as *Brevibacterium epidermidis* and *Castellaniella* sp. However, neither axenic cultures of each isolate nor the co-culture of the two were able to catabolize the

sulfonamide molecule (Levine 2016), suggesting that the sulfonamide-degrader may be an unculturable member of the consortium.

Syntrophic relationships, like the ones described above, are hard to characterize when one or several members of the consortium cannot be grown in axenic cultures. Hence, in order to elucidate the type of syntrophic relationship between the members of our sulfonamide-degrading consortium several attempts were made to isolate strain GP. These attempts started by testing different media, co-factors and culture conditions (Chapter 4). However, these approaches failed to produce axenic cultures, further suggesting that strain GP may need PR1 to provide non-diffusible or unstable growth factors or to prevent the accumulation of toxic metabolites.

Later, comparative studies between the draft genome of strain GP and its closest relatives (*Leucobacter* spp.) revealed a moderate gene loss in this sulfonamide degrader (Chapter 6). This analysis showed that strain GP might be unable to synthesize heme and other tetrapyrrole compounds and lacked thiol transporters. Noticeably, the inability of *de novo* tetrapyrrole and heme biosynthesis appears to be rare and it has only been reported in strains of the pathogen *Haemophilus influenza* and a single environmental isolate affiliated to *Leucobacter* spp. (Bhuiyan et al. 2015; Choby and Skaar 2016; Takai et al. 2017). However, in these strains, the supplementation of the growth medium with exogenous heme sources was sufficient to allow them to grow independently. Furthermore, the inclusion of catalase, which has been previously shown to compensate the lack of thiol transporters in deficient strains (Goldman et al. 1996; Morris et al. 2011), was also insufficient to abolish the dependent phenotype. Additionally, the enrichment of the growth medium with a combination of exogenous heme, porphyrins, and catalase did not allow the further isolation of this slow-growing *Actinobacteria*.

Surprisingly, 3-month-long incubations of the consortium and axenic cultures of *A. denitrificans* PR1 with 5 mM SMX as sole carbon source revealed that the *Proteobacteria*'s abundance and viability were not significantly affected by the presence or absence of

strain GP (data not shown). These findings revealed that the presence of strain GP does not inhibit or enhance the survival of *A. denitrificans* PR1. In this way, a one-way mutualistic interaction between strain GP and strain PR1 is the most probable type of association between these two bacteria. In sum, the results herein obtained allowed the generation of hypotheses and, subsequently, will enable the design of further studies to evaluate the co-factors exchanged by the members of this consortium.

7.3 Pathway and genes involved in sulfamethoxazole degradation

In metabolic studies carried out with the two-member consortium (Chapter 4 and 6), we found that strain GP carried a sulfonamide monooxygenase gene (*sadA*) initially described in *Microbacterium* sp. BR1 (Ricken et al. 2017), and that its expression was significantly enhanced in the presence of high amounts of SMX (Chapter 4, section 4.4.4). Furthermore, studies with ¹⁴C-SMX allowed the identification of 4-aminophenol as the main transient metabolite, as previously described for *Microbacterium* sp. B1 (Fig. 4.12 and 4.13, Chapter 4). Surprisingly, despite the high similarity between SadA in strain GP and its homolog in *Microbacterium* sp. BR1 (94% amino acid identity), additional new products arose from the *ipso*-hydroxylation of this antibiotic in strain GP. Two additional side-reactions were detected and resulted in the accumulation of dead-end metabolites at residual amounts. These dead-end metabolites derived mainly from abiotic rearrangements of the SMX molecule and included: (i) hydroxylated SMX (M2, *ortho* or *meta* position in the benzene ring), (ii) NIH shift of the sulfonyl group (Guroff et al. 1967), from the C1 to the C2 position (M4) and a Baeyer-Villiger rearrangement (M3, Fig. 4.15, Chapter 4), inserting the oxygen between the aromatic moiety and the sulfonyl group.

Studies with *Microbacterium* sp. BR1 and multiple strains from *Actinobacteria* (*Gordonia* sp.) and *Proteobacteria* (*Ochrobactrum* sp. and *Labrys* sp.) phyla (Mulla et al. 2018) show that either THB or HQ, respectively, can be released during 4AP degradation. However, these products have yet to be detected in the two-member consortium. Indeed, in supernatants collected during SMX degradation by the two-member consortium, only two

lower-mass metabolites were detected (M5 and M6, Table 4.5, Chapter 4). However, only M5 structure could be proposed (Fig. 4.11, Chapter 4). This metabolite could result from the reduction of maleylacetate, a known metabolite formed during degradation and ring opening of several aromatic compounds, including 4AP (Takenaka et al. 2003; Kolvenbach et al. 2012).

Antibiotic degradation by hydroxylases is quite rare. To the best of our knowledge, the first antibiotics reported to be susceptible to hydroxylation were tetracyclines which could be transformed by the flavoprotein TetX (tetracycline monooxygenase) (Yang et al. 2004). This protein subsequently led to the discovery of structurally similar hydroxylases, able of extensive tetracycline transformation in a functional metagenomic study by Forsberg et al. (2015). More recently Minerdi et al. (2016) reported increased resistance to imipenem, a carbapenem, mediated by a Baeyer-Villiger monooxygenase (Ar-BVMO). Among these enzymes, Ar-BVMO was found to have the broader substrate range as it was shown to oxidize two anticancer drugs (i.e., danusertib and tozasertib) besides imipenem. Including SadA, all of these enzymes are flavin-containing monooxygenases.

Unlike the previous transformations which reduced toxicity and antimicrobial activity of the parent compound, sulfonamide transformation by SadA alone may be a double-edged sword, because, this reaction releases 4AP as a toxic and mutagenic intermediate (Yoshida et al. 1998). In *Microbacterium* sp. BR1, this potential shortcoming seems to be compensated by the presence of a gene encoding for a 4-aminophenol monooxygenase (SadB) in the same genetic cluster as *sadA*. However, as seen in comparative genomic studies between all available genomes of sulfonamide degraders (Chapter 6), these two genes may not be co-acquired. Indeed, the sulfonamide degraders affiliated to the genus *Microbacterium* carry a highly conserved cluster (*sadABC*).

In contrast, in strains *Arthrobacter* sp. D4 and GP, the homologs of these genes, do not form a cluster. Instead, these strains share a novel transposable element containing *sadA*

and flanked by a single copy of an IS1380 family transposase (Fig. 6.7, Chapter 6). The synteny between this distantly related *Actinobacteria* suggests that at least the *sadA* gene may have been acquired through HGT.

7.4 Potential application for bioaugmentation

The presence of mobile genetic elements in the vicinity of *sadA* or the *sadABC* complex (i.e., transposase and relaxase, respectively) indicates that HGT may mediate the spread and acquisition of these genes. This finding suggests that the burden of resistance may be aggravated by the direct use of these strains for bioremediation and bioaugmentation in antibiotic-polluted environments.

Despite these concerns, there is a lack of knowledge regarding the application of these sulfonamide degraders and potential risks of HGT and indirect resistance. The few studies that tackled this research questions focused on the optimization of degradation efficiency. For instance, Fenu et al. (2015) studied the performance of membrane bioreactors spiked with *Microbacterium* sp. BR1. In this study, the bioaugmentation strategy did not influence the overall SMX degradation efficiency of the bioreactor. However, studies by Nguyen et al. (2017; 2019) showed more promising results. These studies were carried out with sulfonamide-degrading cultures of *A. denitrificans* PR1, before the detection of the low-abundance and slow-growing strain GP in the consortium (Nguyen et al. 2017; 2019).

Preliminary studies showed that the *A. denitrificans* PR1 and strain GP consortium was able to degrade SMX at environmentally relevant concentrations (down to 600 ng/l) (Nguyen et al. 2017). Additional bioaugmentation studies in membrane bioreactors treating pre-clarified wastewater effluent collected from a municipal WWTP showed only a slight enhancement of the overall SMX degradation efficiency, but only when the antibiotic concentration was 10 µg/l SMX (Nguyen et al. 2019). Indeed, experiments with 10 µg/l SMX, 4 mM acetate and 6 h hydraulic retention time (HRT) resulted in a specific elimination rate of $6.4 \pm 3.4 \mu\text{g}_{\text{SMX}}/(\text{g}_{\text{SS}} \times \text{d})$ and $4.9 \pm 1.7 \mu\text{g}_{\text{SMX}}/(\text{g}_{\text{SS}} \times \text{d})$ for the

bioaugmented and non-bioaugmented reactors, respectively. In contrast, when the SMX was closer to environmental values (1 µg/l), specific elimination rates did not differ significantly between bioaugmented and non-bioaugmented reactors and were approximately $1.9 \pm 0.2 \mu\text{g}_{\text{SMX}}/(\text{g}_{\text{SS}} \times \text{d})$ at an HRT of 6 h and 4 mM acetate (Nguyen et al. 2019).

Nevertheless, the authors also showed that the abundance of *A. denitrificans* PR1, as well as the overall degradation efficiency, decreased over time, indicating that both members of the consortium may be easily out-competed by the autochthonous microbiota. These findings are a promising step; however, further studies are needed to assess the risk of dissemination of genes linked to sulfonamide resistance (*sul1*, *sul2*) and degradation (*sadA*, *sadB*) carried by this microbial consortium.

Chapter 8

Main Conclusions

The main conclusions of this work can be summarized as follows:

- *A. denitrificans* strain PR1, initially described as an effective sulfonamide degrader, was only part of a two-member consortium established between this strain and a slow-growing and low-abundance actinobacterium, named strain GP;
- Comparative genomics and phylogenetic studies using the draft genome of strain GP showed that it could represent a new genus within the *Microbacteriaceae* family closely related to the *Leucobacter* genus;
- Genomic analysis showed that strain GP carries at least two copies of a novel transposable element containing a copy of an highly conserved sulfonamide monooxygenase (*sadA*), previously described in *Microbacterium* sp. BR1, a *yceI* binding protein and a single copy of an IS1380 family transposase. This element was also detected in the previously described sulfadiazine degraders, *Arthrobacter* sp. D2 and D4;
- In strain GP, one of these transposons was located near a class I integron with multi-drug resistance genes (*aadA1*, *sul1*, and *qacE*), recombinases and an enzyme affiliated to the type IV secretion system, indicating it may be prone to potential HGT;
- Studies with SMX and its downstream metabolite 4AP showed that *A. denitrificans* PR1 was unable to degrade either of these compounds. Furthermore, the *sadA* gene carried by strain GP was significantly overexpressed in the presence of this antibiotic. These findings indicate that both the initial cleavage of the sulfonamide bond and subsequent degradation of 4AP, are probably catalyzed by strain GP alone;
- Degradation of SMX by strain GP resulted in additional metabolites not observed in other SMX degraders. These side reactions consisted of the accumulation of

residual amounts of: (i) *ortho/meta* hydroxylated SMX, (ii) an NIH shift and an (iii) putative Baeyer-Villiger molecular rearrangement. These differences may be explained by a substitution of threonine by an alanine in strain GP, in comparison to its homolog in *Microbacterium* sp. BR1. This mutation may increase the size of the enzyme's active site in strain GP making it more efficient, but also, enhance abiotic rearrangements of the molecule;

- Although strain PR1 was shown to grow independently, no pure cultures were obtained for strain GP. Furthermore, co-inoculation of this consortium with phage vB_Ade_ART showed that a decrease in strain PR1 viability resulted in a slight increase of strain GP abundance. However, a higher MOI did not linearly correlate with a significant enhancement in SMX degradation. These findings suggest that an ideal ratio between the two strains may be essential for optimal SMX degradation;
- Comparative genetic studies allowed the identification of missing essential genes in the genome of strain GP related to cytochrome synthesis and assembly. Namely, this strain lacked several genes from the upstream pathway of tetrapyrrole biosynthesis and thiol transporters, which were shown to be essential to maintain a good redox balance in the periplasm. However, the inclusion of these essential metabolites and catalase did not allow further purification of strain GP.

In summary, this study led to the identification of a novel specialized syntroph able to catalyze the *ipso*-hydroxylation of sulfonamide antibiotics. The results suggest that other sulfonamide degraders may have acquired homologs of *sadA* through HGT and that *sadB* and, consequently, 4AP degradation may be transferred independently. Moreover, these findings raise important questions about bacterial syntrophy and the role of these syntrophs in the degradation of xenobiotics and antimicrobials in contaminated environments.

Chapter 9

Proposal for additional and future work

The present work has shed light into sulfonamide degradation in the microbial consortium between the high-abundance and fast-growing *A. denitrificans* PR1 and the slow-growing actinobacterium strain GP. In concrete, it led to the description of a putative sulfonamide degradation pathway and the identification of a sulfonamide monooxygenase homolog (*sadA*) in the genome of strain GP. A highly conserved gene shared with other fully sequenced *Actinobacteria* able to degrade sulfonamides. Moreover, we found that in strain GP the *sad* cluster was fragmented with *sadA* being flanked by a single transposon and homologs to *sadB* present in other regions of the genome, far from the gene encoding the enzyme responsible for the initial breakdown of SMX. Notwithstanding, multiple observations made during this study led to other research questions:

- In Chapter 6, the analysis of strain GP genome suggested that *sadA* could be encoded within a plasmid, due to differences in coverage, G+C content, and enrichment of integrative elements in this scaffold. In this way, the presence of this plasmid could be confirmed by electrophoresis techniques (e.g., total DNA separation by PFGE) and by attempting to extract plasmid DNA from the consortium using established techniques relying in alkaline lysis (Birnboim and Doly 1979), proven to be effective in the isolation of multiple environmental plasmids (Burton et al. 1982; Delaney et al. 2018). This work is undergoing.
- What is the nature of the syntrophic relationship between strain GP and its helper, strain PR1? Although multiple growth conditions were tested, strain GP could not be further isolated and always grew in tight association with strain PR1. Furthermore, the media tailored to supplement strain GP metabolic needs (with heme, catalase, and putrescine) was also insufficient to stimulate the development of independent colonies. Additional research is necessary to determine gene expression in this consortium (e.g., RNA-seq), and further functional studies (e.g., knock-outs of missing genes in similar strains or producing strain GP clones

containing these genes) are crucial to understanding heme transport and synthesis in this *Actinobacteria*.

- Although a homolog to *sadA* was found in the genome of strain GP, this gene was not within a cluster with *sadB* and *sadC* as previously described for other sulfonamide degraders. Two *sadB* homologs were found in other regions of the genome of strain GP. Unlike *sadA*, which seemed to be acquired through horizontal gene transference in the strain, the *sadB* homologs had a lower amino acid similarity to the original gene described for *Microbacterium* sp. BR1 (73 %). In this way, further functional studies should be carried to determine the role of these homologs in 4AP degradation in strain GP.
- Because the homolog of *sadA* in strain GP appears to be highly conserved, it is essential to understand how widespread this gene is and study its frequency in important ARG and ARB reservoirs, such as hospital and urban wastewaters and soils using qPCR and metagenomics sequencing approaches.
- Moreover, is it the *sadA* sufficient to confer sulfonamide resistance to a sensitive strain? Can this gene alone be considered a true antibiotic resistance gene? Alternatively, does the host carrying *sadA* requires additional genes in order to degrade the toxic intermediate, 4AP, further? Also, what is the role of these degraders in the proliferation of sulfonamide resistance in natural communities? Preliminary work by Vila-Costa et al. (2017) showed that these degraders could attenuate the development of resistance in natural communities; however, further studies are necessary to assess the real implications of these findings.

References

- Abby SS, Néron B, Ménager H, Touchon M, Rocha EPC (2014) MacSyFinder: A Program to Mine Genomes for Molecular Systems with an Application to CRISPR-Cas Systems. *PLoS One* 9:e110726 . doi: 10.1371/journal.pone.0110726
- Ackermann H-W, Audurier A, Berthiaume L, Jones LA, Mayo JA, Vidaver AK (1978) Guidelines for bacteriophage characterization. In: Lauffer MA, Bang FB, Maramorosch K, Smith KM (eds) *Advances in Virus Research*. Academic Press, New York, pp 1–24
- Ackermann H, Tremblay D, Moineau S (2004) Long-term bacteriophage preservation. *WFCC Newsl.* 35:35–40
- Adams MH (1959) *Bacteriophages*. Interscience Publishers, New York
- Adriaenssens EM, Van Vaerenbergh J, Vandenhoevel D, Dunon V, Ceysens P-J, De Proft M, Kropinski AM, Noben J-P, Maes M, Lavigne R (2012) T4-related bacteriophage LIMEstone isolates for the control of soft rot on potato caused by *Dickeya solani*. *PLoS One* 7:e33227 . doi: 10.1371/journal.pone.0033227
- Afgan E, Baker D, Batut B, van den Beek M, Bouvier D, Čech M, Chilton J, Clements D, Coraor N, Grüning BA, Guerler A, Hillman-Jackson J, Hiltemann S, Jalili V, Rasche H, Soranzo N, Goecks J, Taylor J, Nekrutenko A, Blankenberg D (2018) The Galaxy platform for accessible, reproducible and collaborative biomedical analyses: 2018 update. *Nucleic Acids Res* 46:W537–W544 . doi: 10.1093/nar/gky379
- Aisenberg G, Rolston K V., Safdar A (2004) Bacteremia caused by *Achromobacter* and *Alcaligenes* species in 46 patients with cancer (1989-2003). *Cancer* 101:2134–2140 . doi: 10.1002/cncr.20604
- Albers E (2009) Metabolic characteristics and importance of the universal methionine salvage pathway recycling methionine from 5'-methylthioadenosine. *IUBMB Life* 61:1132–1142 . doi: 10.1002/iub.278
- Alikhan N-F, Petty NK, Ben Zakour NL, Beatson SA (2011) BLAST Ring Image Generator (BRIG): simple prokaryote genome comparisons. *BMC Genomics* 12:402 . doi: 10.1186/1471-2164-12-402
- Altschul SF, Madden TL, Schäffer AA, Zhang J, Zhang Z, Miller W, Lipmann DJ (1997) Gapped BLAST and PSI-BLAST: a new generation of protein database search programs. *Nucleic Acids Res* 25:3389–3402 . doi: 10.1093/nar/25.17.3389
- Alvarino T, Nastold P, Suarez S, Omil F, Corvini PFX, Bouju H (2016) Role of biotransformation, sorption and mineralization of ¹⁴C-labelled sulfamethoxazole under different redox conditions. *Sci Total Environ* 542:706–715 . doi: 10.1016/j.scitotenv.2015.10.140
- Amador P, Prude C (2013) Beta-lactams : chemical structure , mode of action and mechanisms of resistance. *Rev Med Microbiol* 24:7–17 . doi: 10.1097/mrm.0b013e3283587727
- Aminov RI (2010) A brief history of the antibiotic era: lessons learned and challenges for the future. *Front Microbiol* 1:134 . doi: 10.3389/fmicb.2010.00134
- Amoureux L, Bador J, Fardeheb S, Mabilie C, Couchot C, Massip C, Salignon A-L, Berlie G, Varin V, Neuwirth C (2013) Detection of *Achromobacter xylosoxidans* in hospital, domestic, and outdoor environmental samples and comparison with human clinical isolates. *Appl Environ Microbiol* 79:7142–7149 . doi: 10.1128/aem.02293-13
- Andersson DI, Hughes D (2010) Antibiotic resistance and its cost: is it possible to reverse resistance? *Nat Rev Microbiol* 8:260–271 . doi: 10.1038/nrmicro2319
- Andersson SG, Kurland CG (1998) Reductive evolution of resident genomes. *Trends Microbiol* 6:263–268. doi: 10.1016/s0966-842x(98)01312-2
- Arndt D, Grant JR, Marcu A, Sajed T, Pon A, Liang Y, Wishart DS (2016) PHASTER: a better, faster version

References

- of the PHAST phage search tool. *Nucleic Acids Res* 44:W16–W21 . doi: 10.1093/nar/gkw387
- Ascalone V (1981) Assay of trimethoprim, sulfadiazine and its *N*⁴-acetyl metabolite in biological fluids by normal-phase high-performance liquid chromatography. *J Chromatogr B Biomed Sci Appl* 224:59–66 . doi: 10.1016/s0378-4347(00)80138-3
- Baeyer A, Villiger V (1899) Einwirkung des caro'schen reagens auf ketone. *Berichte der Dtsch Chem Gesellschaft* 32:3625–3633 . doi: 10.1002/cber.189903203151
- Bailly-Bechet M, Vergassola M, Rocha E (2007) Causes for the intriguing presence of tRNAs in phages. *Genome Res* 17:1486–1495 . doi: 10.1101/gr.6649807
- Bankevich A, Nurk S, Antipov D, Gurevich AA, Dvorkin M, Kulikov AS, Lesin VM, Nikolenko SI, Pham S, Prjibelski AD, Pyshkin A V., Sirotkin A V., Vyahhi N, Tesler G, Alekseyev MA, Pevzner PA (2012) SPAdes: A new genome assembly algorithm and its applications to single-cell sequencing. *J Comput Biol* 19:455–477 . doi: 10.1089/cmb.2012.0021
- Banzhaf S, Nödler K, Licha T, Krein A, Scheytt T (2012) Redox-sensitivity and mobility of selected pharmaceutical compounds in a low flow column experiment. *Sci Total Environ* 438:113–121 . doi: 10.1016/j.scitotenv.2012.08.041
- Bao Y, Chetvernin V, Tatusova T (2014) Improvements to pairwise sequence comparison (PASC): a genome-based web tool for virus classification. *Arch Virol* 159:3293–3304 . doi: 10.1007/s00705-014-2197-x
- Baquero F, Martínez JL, Cantón R (2008) Antibiotics and antibiotic resistance in water environments. *Curr Opin Biotechnol* 19:260–265 . doi: 10.1016/j.copbio.2008.05.006
- Baran W, Sochacka J, Wardas W (2006) Toxicity and biodegradability of sulfonamides and products of their photocatalytic degradation in aqueous solutions. *Chemosphere* 65:1295–1299 . doi: 10.1016/j.chemosphere.2006.04.040
- Barbieri M, Carrera J, Ayora C, Sanchez-Vila X, Licha T, Nödler K, Osorio V, Pérez S, Köck-Schulmeyer M, López de Alda M, Barceló D (2012) Formation of diclofenac and sulfamethoxazole reversible transformation products in aquifer material under denitrifying conditions: batch experiments. *Sci Total Environ* 426:256–263 . doi: 10.1016/j.scitotenv.2012.02.058
- Barnhill AE, Weeks KE, Xiong N, Day TA, Carlson SA (2010) Identification of multiresistant *Salmonella* isolates capable of subsisting on antibiotics. *Appl Environ Microbiol* 76:2678–2680 . doi: 10.1128/aem.02516-09
- Barreiros L, Nogales B, Manaia CM, Silva Ferreira AC, Pieper DH, Reis MA, Nunes OC (2003) A novel pathway for mineralization of the thiocarbamate herbicide molinate by a defined bacterial mixed culture. *Environ Microbiol* 5:944–953 . doi: 10.1046/j.1462-2920.2003.00492.x
- Batista APS, Pires FCC, Teixeira ACSC (2014) Photochemical degradation of sulfadiazine, sulfamerazine and sulfamethazine: Relevance of concentration and heterocyclic aromatic groups to degradation kinetics. *J Photochem Photobiol A Chem* 286:40–46 . doi: 10.1016/j.jphotochem.2014.04.022
- Beacham IR (1987) Silent genes in prokaryotes. *FEMS Microbiol Lett* 46:409–417 . doi: 10.1016/0378-1097(87)90046-2
- Benjamin S, Kamimura N, Takahashi K, Masai E (2016) *Achromobacter denitrificans* SP1 efficiently utilizes 16 phthalate diesters and their downstream products through protocatechuate 3,4-cleavage pathway. *Ecotoxicol Environ Saf* 134:172–178 . doi: 10.1016/j.ecoenv.2016.08.028
- Benkert P, Biasini M, Schwede T (2011) Toward the estimation of the absolute quality of individual protein structure models. *Bioinformatics* 27:343–350 . doi: 10.1093/bioinformatics/btq662
- Berendonk TU, Manaia CM, Merlin C, Fatta-Kassinos D, Cytryn E, Walsh F, Bürgmann H, Sørum H, Norström M, Pons M-N, Kreuzinger N, Huovinen P, Stefani S, Schwartz T, Kisand V, Baquero F, Martinez JL (2015) Tackling antibiotic resistance: the environmental framework. *Nat Rev Microbiol*

- 13:310–317 . doi: 10.1038/nrmicro3439
- Bhuiyan MNI, Takai R, Mitsuhashi S, Shigetomi K, Tanaka Y, Kamagata Y, Ubukata M (2015) Zincmethylpyrins and coproporphyrins, novel growth factors released by *Sphingopyxis* sp., enable laboratory cultivation of previously uncultured *Leucobacter* sp. through interspecies mutualism. *J Antibiot (Tokyo)* 69:97–103 . doi: 10.1038/ja.2015.87
- Bhullar K, Wagglechner N, Pawlowski A, Koteva K, Banks ED, Johnston MD, Barton HA, Wright GD (2012) Antibiotic resistance is prevalent in an isolated cave microbiome. *PLoS One* 7:e34953 . doi: 10.1371/journal.pone.0034953
- Birnboim HC, Doly J (1979) A rapid alkaline extraction procedure for screening recombinant plasmid DNA. *Nucleic Acids Res* 7:1513–1523. doi: 10.1371/journal.pone.0047093
- Blair JMA, Webber MA, Baylay AJ, Ogbolu DO, Piddock LJ V. (2015) Molecular mechanisms of antibiotic resistance. *Nat Rev Microbiol* 13:42–51 . doi: 10.1039/c0cc05111j
- Boetzer M, Henkel C V., Jansen HJ, Butler D, Pirovano W (2011) Scaffolding pre-assembled contigs using SSPACE. *Bioinformatics* 27:578–579 . doi: 10.1093/bioinformatics/btq683
- Borysowski J, Łobocka M, Międzybrodzki R, Weber-Dabrowska B, Górski A (2011) Potential of bacteriophages and their lysins in the treatment of MRSA. *BioDrugs* 25:347–355 . doi: 10.2165/11595610-000000000-00000
- Bosdriesz E, Magnúsdóttir S, Bruggeman FJ, Teusink B, Molenaar D (2015) Binding proteins enhance specific uptake rate by increasing the substrate-transporter encounter rate. *FEBS J* 282:2394–2407 . doi: 10.1111/febs.13289
- Bouju H, Ricken B, Beffa T, Corvini PFX, Kolvenbach BA (2012) Isolation of bacterial strains capable of sulfamethoxazole mineralization from an acclimated membrane bioreactor. *Appl Environ Microbiol* 78:277–279 . doi: 10.1128/aem.05888-11
- Bowers RM, Kyrpides NC, Stepanauskas R, Harmon-Smith M, Doud D, Reddy TBK, Schulz F, Jarett J, Rivers AR, Eloe-Fadrosch EA, Tringe SG, Ivanova NN, Copeland A, Clum A, Becraft ED, Malmstrom RR, Birren B, Podar M, Bork P, Weinstock GM, Garrity GM, Dodsworth JA, Yooseph S, Sutton G, Glöckner FO, Gilbert JA, Nelson WC, Hallam SJ, Jungbluth SP, Ettema TJG, Tighe S, Konstantinidis KT, Liu W-T, Baker BJ, Rattei T, Eisen JA, Hedlund B, McMahon KD, Fierer N, Knight R, Finn R, Cochrane G, Karsch-Mizrachi I, Tyson GW, Rinke C, Kyrpides NC, Schriml L, Garrity GM, Hugenholtz P, Sutton G, Yilmaz P, Meyer F, Glöckner FO, Gilbert JA, Knight R, Finn R, Cochrane G, Karsch-Mizrachi I, Lapidus A, Meyer F, Yilmaz P, Parks DH, Eren AM, Schriml L, Banfield JF, Hugenholtz P, Woyke T, Woyke T (2017) Minimum information about a single amplified genome (MISAG) and a metagenome-assembled genome (MIMAG) of bacteria and archaea. *Nat Biotechnol* 35:725–731 . doi: 10.1038/nbt.3893
- Bragg R, van der Westhuizen W, Lee J-Y, Coetsee E, Boucher C (2014) Bacteriophages as potential treatment option for antibiotic resistant bacteria. In: Adhikari R, Thapa S (eds) *Advances in experimental medicine and biology*. Springer, New Dehli, pp 97–110
- Brankatschk R, Bodenhausen N, Zeyer J, Bürgmann H (2012) Simple absolute quantification method correcting for quantitative PCR efficiency variations for microbial community samples. *Appl Environ Microbiol* 78:4481–4489 . doi: 10.1128/aem.07878-11
- Brettin T, Davis JJ, Disz T, Edwards RA, Gerdes S, Olsen GJ, Olson R, Overbeek R, Parrello B, Pusch GD, Shukla M, Thomason JA, Stevens R, Vonstein V, Wattam AR, Xia F (2015) RASTtk: A modular and extensible implementation of the RAST algorithm for building custom annotation pipelines and annotating batches of genomes. *Sci Rep* 5:8365 . doi: 10.1038/srep08365
- Bryant J, Chewapreecha C, Bentley SD (2012) Developing insights into the mechanisms of evolution of bacterial pathogens from whole-genome sequences. *Future Microbiol* 7:1283–1296 . doi: 10.2217/fmb.12.108
- Burton NF, Day MJ, Bull AT (1982) Distribution of bacterial plasmids in clean and polluted sites in a South

References

- Wales river. *Appl Environ Microbiol* 44:1026–9
- Bush K (1989) Characterization of beta-lactamases. *Antimicrob Agents Chemother* 33:259–263 . doi: 10.1128/aac.33.3.259
- Bush K, Jacoby GA (2010) Updated functional classification of beta-lactamases. *Antimicrob Agents Chemother* 54:969–976 . doi: 10.1128/aac.01009-09
- Caldeira JC, Peabody DS (2007) Stability and assembly *in vitro* of bacteriophage PP7 virus-like particles. *J Nanobiotechnology* 5:10 . doi: 10.1186/1477-3155-5-10
- Caracciolo AB, Topp E, Grenni P (2015) Pharmaceuticals in the environment: Biodegradation and effects on natural microbial communities. A review. *J Pharm Biomed Anal* 106:25–36 . doi: 10.1016/j.jpba.2014.11.040
- Carvalho RN, Ceriani L, Ippolito A, Lettieri T (2015) Development of the first Watch List under the Environmental Quality Standards Directive. Directive 2008/105/EC, as amended by Directive 2013/39/EU, in the field of water policy.
- Cassir N, Rolain J-M, Brouqui P (2014) A new strategy to fight antimicrobial resistance: the revival of old antibiotics. *Front Microbiol* 5:551 . doi: 10.3389/fmicb.2014.00551
- Chan BK, Abedon ST, Loc-Carrillo C (2013) Phage cocktails and the future of phage therapy. *Future Microbiol* 8:769–783 . doi: 10.2217/fmb.13.47
- Chanishvili N (2012) A literature review of the practical application of bacteriophage research. Nova Biomedical Books, New York
- Chen J, Xie S (2018) Overview of sulfonamide biodegradation and the relevant pathways and microorganisms. *Sci Total Environ* 640–641:1465–1477 . doi: 10.1016/j.scitotenv.2018.06.016
- Chen X, Hitchings MD, Mendoza JE, Balanza V, Facey PD, Dyson PJ, Bielza P, Del Sol R (2017) Comparative genomics of facultative bacterial symbionts isolated from European *Orius* species reveals an ancestral symbiotic association. *Front Microbiol* 8:1969 . doi: 10.3389/fmicb.2017.01969
- Chen Y, Zhang H, Luo Y, Song J (2012) Occurrence and assessment of veterinary antibiotics in swine manures: A case study in East China. *Chinese Sci Bull* 57:606–614 . doi: 10.1007/s11434-011-4830-3
- Choby JE, Skaar EP (2016) Heme synthesis and acquisition in bacterial pathogens. *J Mol Biol* 428:3408–3428 . doi: 10.1016/j.jmb.2016.03.018
- Chun J, Oren A, Ventosa A, Christensen H, Arahal DR, da Costa MS, Rooney AP, Yi H, Xu X-W, De Meyer S, Trujillo ME (2018) Proposed minimal standards for the use of genome data for the taxonomy of prokaryotes. *Int J Syst Evol Microbiol* 68:461–466 . doi: 10.1099/ijsem.0.002516
- Clark LC, Hodgkin J (2015) *Leucobacter musarum* subsp. *musarum* sp. nov., subsp. nov., *Leucobacter musarum* subsp. *japonicus* subsp. nov., and *Leucobacter celer* subsp. *astrifaciens* subsp. nov., three nematopathogenic bacteria isolated from *Caenorhabditis*, with an emended description of *Leucobacter celer*. *Int J Syst Evol Microbiol* 65:3977–3984 . doi: 10.1099/ijsem.0.000523
- Clarke GDP, Beiko RG, Ragan MA, Charlebois RL, Baertsch R, Hardison R, Haussler D, Miller W, Murray R, Stackebrandt E, Starr M, Truper H (2002) Inferring genome trees by using a filter to eliminate phylogenetically discordant sequences and a distance matrix based on mean normalized BLASTP scores. *J Bacteriol* 184:2072–2080 . doi: 10.1128/jb.184.8.2072-2080.2002
- Clokier MR, Millard AD, Letarov A V, Heaphy S (2011) Phages in nature. *Bacteriophage* 1:31–45 . doi: 10.4161/bact.1.1.14942
- CLSI (2018) Performance Standards for Antimicrobial Susceptibility Testing. CLSI supplement M100. Clinical and Laboratory Standards Institute, Wayne, PA

- Coenen S, Adriaenssens N, Versporten A, Muller A, Minalu G, Faes C, Vankerckhoven V, Aerts M, Hens N, Molenberghs G, Goossens H, ESAC Project Group (2011) European Surveillance of Antimicrobial Consumption (ESAC): outpatient use of tetracyclines, sulphonamides and trimethoprim, and other antibacterials in Europe (1997-2009). *J Antimicrob Chemother* 66:vi57–vi70 . doi: 10.1093/jac/dkr458
- Coenye T, Vancanneyt M, Cnockaert MC, Falsen E, Swings J, Vandamme P (2003) *Kerstersia gyiorum* gen. nov., sp. nov., a novel *Alcaligenes faecalis*-like organism isolated from human clinical samples, and reclassification of *Alcaligenes denitrificans* Ruger and Tan 1983 as *Achromobacter denitrificans* comb. *Int J Syst Evol Microbiol* 53:1825–1831 . doi: 10.1099/ijs.0.02609-0
- Conesa A, Gotz S, Garcia-Gomez JM, Terol J, Talon M, Robles M (2005) Blast2GO: a universal tool for annotation, visualization and analysis in functional genomics research. *Bioinformatics* 21:3674–3676 . doi: 10.1093/bioinformatics/bti610
- Contreras-Moreira B, Vinuesa P (2013) GET_HOMOLOGUES, a versatile software package for scalable and robust microbial pangenome analysis. *Appl Environ Microbiol* 79:7696–7701 . doi: 10.1128/aem.02411-13
- Cribb AE, Spielberg SP (1992) Sulfamethoxazole is metabolized to the hydroxylamine in humans. *Clin Pharmacol Ther* 51:522–526 . doi: 10.1038/clpt.1992.57
- Dailey HA, Dailey TA, Gerdes S, Jahn D, Jahn M, O’Brian MR, Warren MJ (2017) Prokaryotic heme biosynthesis: multiple pathways to a common essential product. *Microbiol Mol Biol Rev* 81:e00048-16 . doi: 10.1128/membr.00048-16
- Dantas G, Sommer MOA, Oluwasegun RD, Church GM (2008) Bacteria subsisting on antibiotics. *Science* 320:100–103 . doi: 10.1126/science.1155157
- Darriba D, Taboada GL, Doallo R, Posada D (2011) ProtTest 3: fast selection of best-fit models of protein evolution. *Bioinformatics* 27:1164–1165 . doi: 10.1093/bioinformatics/btr088
- de Mendiburu F (2013) agricolae: statistical procedures for agricultural research.
- De Paepe M, Taddei F (2006) Viruses’ life history: towards a mechanistic basis of a trade-off between survival and reproduction among phages. *PLoS Biol* 4:e193 . doi: 10.1371/journal.pbio.0040193
- Delaney S, Murphy R, Walsh F (2018) A comparison of methods for the extraction of plasmids capable of conferring antibiotic resistance in a human pathogen from complex broiler cecal samples. *Front Microbiol* 9:1731 . doi: 10.3389/fmicb.2018.01731
- Deng Y, Li B, Zhang T (2018) Bacteria that make a meal of sulfonamide antibiotics: blind spots and emerging opportunities. *Environ Sci Technol* 52:3854–3868 . doi: 10.1021/acs.est.7b06026
- Deng Y, Mao Y, Li B, Yang C, Zhang T (2016) Aerobic degradation of sulfadiazine by *Arthrobacter* spp.: kinetics, pathways, and genomic characterization. *Environ Sci Technol* 50:9566–9575 . doi: 10.1021/acs.est.6b02231
- Denton JF, Lugo-Martinez J, Tucker AE, Schrider DR, Warren WC, Hahn MW (2014) Extensive error in the number of genes inferred from draft genome assemblies. *PLoS Comput Biol* 10:e1003998 . doi: 10.1371/journal.pcbi.1003998
- Diaz-Torres ML, McNab R, Spratt DA, Villedieu A, Hunt N, Wilson M, Mullany P (2003) Novel tetracycline resistance determinant from the oral metagenome. *Antimicrob Agents Chemother* 47:1430–1432 . doi: 10.1128/aac.47.4.1430-1432.2003
- Dreiseikelmann B, Bunk B, Spröer C, Rohde M, Nimtz M, Wittmann J (2017) Characterization and genome comparisons of three *Achromobacter* phages of the family *Siphoviridae*. *Arch Virol* 162:2191–2201 . doi: 10.1007/s00705-017-3347-8
- Dubochet J, Adrian M, Chang JJ, Homo JC, Lepault J, McDowell AW, Schultz P (1988) Cryo-electron microscopy of vitrified specimens. *Q Rev Biophys* 21:129–228 . doi: 10.1017/s0033583500004297

References

- Dy RL, Rigano LA, Fineran PC (2018) Phage-based biocontrol strategies and their application in agriculture and aquaculture. *Biochem Soc Trans* 46:1605–1613 . doi: 10.1042/BST20180178
- Edgar RC (2004) MUSCLE: a multiple sequence alignment method with reduced time and space complexity. *BMC Bioinformatics* 5:113 . doi: 10.1186/1471-2105-5-113
- Eibes G, Debernardi G, Feijoo G, Moreira MT, Lema JM (2011) Oxidation of pharmaceutically active compounds by a ligninolytic fungal peroxidase. *Biodegradation* 22:539–550 . doi: 10.1007/s10532-010-9426-0
- El-Awaad I, Bocola M, Beuerle T, Liu B, Beerhues L (2016) Bifunctional CYP81AA proteins catalyse identical hydroxylations but alternative regioselective phenol couplings in plant xanthone biosynthesis. *Nat Commun* 7:11472 . doi: 10.1038/ncomms11472
- Ellis EL, Delbrück M (1939) The growth of bacteriophage. *J Gen Physiol* 22:365–384 . doi: 10.1085/jgp.22.3.365
- Estrela S, Trisos CH, Brown SP (2012) From metabolism to ecology: cross-feeding interactions shape the balance between polymicrobial conflict and mutualism. *Am Nat* 180:566–576 . doi: 10.1086/667887
- European Medicines Agency - EMA (2016) Sales of veterinary antimicrobial agents in 29 European countries in 2014. *European Surveillance of Veterinary Antimicrobial Consumption* (EMA/61769/2016)
- Evans TJ, Crow MA, Williamson NR, Orme W, Thomson NR, Komitopoulou E, Salmond GPC (2010) Characterization of a broad-host-range flagellum-dependent phage that mediates high-efficiency generalized transduction in, and between, *Serratia* and *Pantoea*. *Microbiology* 156:240–247 . doi: 10.1099/mic.0.032797-0
- FAO (2014) Evaluation of certain veterinary drug residues in food. Seventy-eighth report of the Joint FAO/WHO Expert Committee on Food Additives.
- Frag IF, Youssef NH, Elshahed MS (2017) Global distribution patterns and pangenomic diversity of the candidate phylum “*Latescibacteria*” (WS3). *Appl Environ Microbiol* 83:e00521-17 . doi: 10.1128/aem.00521-17
- Fenu A, Donckels BMR, Beffa T, Bemfohr C, Weemaes M (2015) Evaluating the application of *Microbacterium* sp. strain BR1 for the removal of sulfamethoxazole in full-scale membrane bioreactors. *Water Sci Technol* 72:1754–1761 . doi: 10.2166/wst.2015.397
- Finn RD, Bateman A, Clements J, Coggill P, Eberhardt RY, Eddy SR, Heger A, Hetherington K, Holm L, Mistry J, Sonnhammer ELL, Tate J, Punta M (2014) Pfam: the protein families database. *Nucleic Acids Res* 42:D222–D230 . doi: 10.1093/nar/gkt1223
- Finn RD, Coggill P, Eberhardt RY, Eddy SR, Mistry J, Mitchell AL, Potter SC, Punta M, Qureshi M, Sangrador-Vegas A, Salazar GA, Tate J, Bateman A (2016) The Pfam protein families database: towards a more sustainable future. *Nucleic Acids Res* 44:D279–D285 . doi: 10.1093/nar/gkv1344
- Forsberg KJ, Patel S, Wencewicz TA, Dantas G (2015) The tetracycline destructases: A novel family of tetracycline-inactivating enzymes. *Chem Biol* 22:888–897 . doi: 10.1016/j.chembiol.2015.05.017
- Gabriel FLP, Heidberger A, Rentsch D, Giger W, Guenther K, Kohler H-PE (2005) A novel metabolic pathway for degradation of 4-nonylphenol environmental contaminants by *Sphingomonas xenophaga* Bayram: ipso-hydroxylation and intramolecular rearrangement. *J Biol Chem* 280:15526–15533 . doi: 10.1074/jbc.m413446200
- García-Galán MJ, Silvia Díaz-Cruz M, Barceló D (2008) Identification and determination of metabolites and degradation products of sulfonamide antibiotics. *TrAC - Trends Anal Chem* 27:1008–1022 . doi: 10.1016/j.trac.2008.10.001
- Garcillán-Barcia MP, Francia MV, de La Cruz F (2009) The diversity of conjugative relaxases and its

- application in plasmid classification. *FEMS Microbiol Rev* 33:657–687 . doi: 10.1111/j.1574-6976.2009.00168.x
- Gasteiger E, Gattiker A, Hoogland C, Ivanyi I, Appel RD, Bairoch A (2003) ExPASy: The proteomics server for in-depth protein knowledge and analysis. *Nucleic Acids Res* 31:3784–3788 . doi: 10.1093/nar/gkg563
- Gauthier H, Yargeau V, Cooper DG (2010) Biodegradation of pharmaceuticals by *Rhodococcus rhodochrous* and *Aspergillus niger* by co-metabolism. *Sci Total Environ* 408:1701–1706 . doi: 10.1016/j.scitotenv.2009.12.012
- Gelband H, Miller-Petrie M, Pant S, Gandra S, Levinson J, Barter D, White A, Laxminarayan R (2015) *The State of the World's Antibiotics*. Washington DC
- Georgiou CD, Fang H, Gennis RB (1987) Identification of the *cydC* locus required for expression of the functional form of the cytochrome d terminal oxidase complex in *Escherichia coli*. *J Bacteriol* 169:2107–2112. doi: 10.1128/jb.169.5.2107-2112.1987
- Ghosh S, LaPara TM, Sadowsky MJ (2015) Transformation of tetracycline by TetX and its subsequent degradation in a heterologous host. *FEMS Microbiol Ecol* 91:fiv059 . doi: 10.1093/femsec/fiv059
- Glupczynski Y, Hansen W, Frenay J, Yourassowsky E (1988) *In vitro* susceptibility of *Alcaligenes denitrificans* subsp. *xylosoxidans* to 24 antimicrobial agents. *Antimicrob Agents Chemother* 32:276–278 . doi: 10.1128/aac.32.2.276
- Göbel A, Thomsen A, McArdell CS, Joss A, Giger W (2005) Occurrence and sorption behavior of sulfonamides, macrolides, and trimethoprim in activated sludge treatment. *Environ Sci Technol* 39:3981–3989 . doi: 10.1021/es048550a
- Göker M, García-Blázquez G, Voglmayr H, Tellería MT, Martín MP (2009) Molecular taxonomy of phytopathogenic fungi: a case study in *Peronospora*. *PLoS One* 4:e6319 . doi: 10.1371/journal.pone.0006319
- Goldman BS, Gabbert KK, Kranz RG (1996) The temperature-sensitive growth and survival phenotypes of *Escherichia coli* *cydDC* and *cydAB* strains are due to deficiencies in cytochrome bd and are corrected by exogenous catalase and reducing agents. *J Bacteriol* 178:6348–6351. doi: 10.1128/jb.178.21.6348-6351.1996
- Goodfellow M, O'Donnell AG (1993) Roots of bacterial systematics. In: Goodfellow M, O'Donnell AG (eds) *Handbook of New Bacterial Systematics*. Academic Press, London, pp 3–54
- Gorsky LD, Koop DR, Coon MJ (1984) On the stoichiometry of the oxidase and monooxygenase reactions catalyzed by liver microsomal cytochrome P-450. Products of oxygen reduction. *J Biol Chem* 259:6812–6817
- Gratia JP (2000) André Gratia: a forerunner in microbial and viral genetics. *Genetics* 156:471–476
- Grazziotin AL, Koonin E V., Kristensen DM (2017) Prokaryotic Virus Orthologous Groups (pVOGs): a resource for comparative genomics and protein family annotation. *Nucleic Acids Res* 45:D491–D498 . doi: 10.1093/nar/gkw975
- Guglielmini J, Néron B, Abby SS, Garcillán-Barcia MP, la Cruz F de, Rocha EPC (2014) Key components of the eight classes of type IV secretion systems involved in bacterial conjugation or protein secretion. *Nucleic Acids Res* 42:5715–5727 . doi: 10.1093/nar/gku194
- Gullberg E, Cao S, Berg OG, Ilbäck C, Sandegren L, Hughes D, Andersson DI (2011) Selection of resistant bacteria at very low antibiotic concentrations. *PLoS Pathog* 7:e1002158 . doi: 10.1371/journal.ppat.1002158
- Guroff G, Renson J, Udenfriend S, Daly JW, Jerina DM, Witkop B (1967) Hydroxylation-Induced Migration: The NIH Shift. *Science* 157:1524–1530 . doi: 10.1126/science.157.3796.1524
- Hamdi S, Rousseau GM, Labrie SJ, Tremblay DM, Kourda RS, Ben Slama K, Moineau S (2017)

References

- Characterization of two polyvalent phages infecting *Enterobacteriaceae*. *Sci Rep* 7:40349 . doi: 10.1038/srep40349
- Hao X, Jiang R, Chen T (2011) Clustering 16S rRNA for OTU prediction: a method of unsupervised Bayesian clustering. *Bioinformatics* 27:611–618 . doi: 10.1093/bioinformatics/btq725
- Harris HMB, Bourin MJB, Claesson MJ, O'Toole PW (2017) Phylogenomics and comparative genomics of *Lactobacillus salivarius*, a mammalian gut commensal. *Microb genomics* 3:e000115 . doi: 10.1099/mgen.0.000115
- Hays SG, Patrick WG, Ziesack M, Oxman N, Silver PA (2015) Better together: engineering and application of microbial symbioses. *Curr Opin Biotechnol* 36:40–49 . doi: 10.1016/j.copbio.2015.08.008
- Hendrix RW (2002) Bacteriophages: evolution of the majority. *Theor Popul Biol* 61:471–480 . doi: 10.1006/tpbi.2002.1590
- Heuer H, Schmitt H, Smalla K (2011) Antibiotic resistance gene spread due to manure application on agricultural fields. *Curr Opin Microbiol* 14:236–243 . doi: 10.1016/j.mib.2011.04.009
- Hibbing ME, Fuqua C, Parsek MR, Peterson SB (2010) Bacterial competition: surviving and thriving in the microbial jungle. *Nat Rev Microbiol* 8:15–25 . doi: 10.1038/nrmicro2259
- Hillas PJ, Fitzpatrick PF (1996) A mechanism for hydroxylation by tyrosine hydroxylase based on partitioning of substituted phenylalanines. *J Biol Chem* 271:6969–6975 . doi: 10.1021/bi9606861
- Hillyar CRT (2012) Genetic recombination in bacteriophage lambda. *Biosci Horizons* 5:hzs001 . doi: 10.1093/biohorizons/hzs001
- Hopwood DA (2007) How do antibiotic-producing bacteria ensure their self-resistance before antibiotic biosynthesis incapacitates them? *Mol Microbiol* 63:937–940 . doi: 10.1111/j.1365-2958.2006.05584.x
- Hu L, Flanders PM, Miller PL, Strathmann TJ (2007) Oxidation of sulfamethoxazole and related antimicrobial agents by TiO₂ photocatalysis. *Water Res* 41:2612–2626 . doi: 10.1016/j.watres.2007.02.026
- Huerta-Cepas J, Forslund K, Coelho LP, Szklarczyk D, Jensen LJ, von Mering C, Bork P (2017) Fast genome-wide functional annotation through orthology assignment by eggNOG-Mapper. *Mol Biol Evol* 34:2115–2122 . doi: 10.1093/molbev/msx148
- Huijbers MME, Montersino S, Westphal AH, Tischler D, van Berkel WJH (2014) Flavin dependent monooxygenases. *Arch Biochem Biophys* 544:2–17 . doi: 10.1016/j.abb.2013.12.005
- Hunt M, Silva N De, Otto TD, Parkhill J, Keane JA, Harris SR (2015) Circlator: automated circularization of genome assemblies using long sequencing reads. *Genome Biol* 16:294 . doi: 10.1186/s13059-015-0849-0
- Huovinen P (1987) Trimethoprim resistance. *Antimicrob Agents Chemother* 31:1451–6 . Huovinen P. Trimethoprim resistance. *Antimicrob Agents Chemother*. 1987;31(10):1451–1456. doi:10.1128/aac.31.10.1451
- Huovinen P, Sundström L, Swedberg G, Sköld O (1995) Trimethoprim and sulfonamide resistance. *Antimicrob Agents Chemother* 39:279–89 . doi: 10.1128/aac.39.2.279
- Igra-Siegman Y, Chmel H, Cobbs C (1980) Clinical and laboratory characteristics of *Achromobacter xylosoxidans* infection. *J Clin Microbiol* 11:141–5
- Ingerslev F, Halling-Sørensen B (2000) Biodegradability properties of sulfonamides in activated sludge. *Environ Toxicol Chem* 19:2467–2473 . doi: 10.1002/etc.5620191011
- Ip CLC, Loose M, Tyson JR, de Cesare M, Brown BL, Jain M, Leggett RM, Eccles DA, Zalunin V, Urban JM, Piazza P, Bowden RJ, Paten B, Mwaigwisya S, Batty EM, Simpson JT, Snutch TP, Birney E, Buck D, Goodwin S, Jansen HJ, O'Grady J, Olsen HE, MinION Analysis and Reference Consortium (2015)

- MinION Analysis and Reference Consortium: Phase 1 data release and analysis. F1000Research 4:1075 . doi: 10.12688/f1000research.7201.1
- Islas-Espinoza M, Reid BJ, Wexler M, Bond PL (2012) Soil bacterial consortia and previous exposure enhance the biodegradation of sulfonamides from pig manure. *Microb Ecol* 64:140–151 . doi: 10.1007/s00248-012-0010-5
- Jagmann N, Brachvogel H-P, Philipp B (2010) Parasitic growth of *Pseudomonas aeruginosa* in co-culture with the chitinolytic bacterium *Aeromonas hydrophila*. *Environ Microbiol* 12:1787–1802 . doi: 10.1111/j.1462-2920.2010.02271.x
- Janssen PH, Yates PS, Grinton BE, Taylor PM, Sait M (2002) Improved culturability of soil bacteria and isolation in pure culture of novel members of the divisions *Acidobacteria*, *Actinobacteria*, *Proteobacteria*, and *Verrucomicrobia*. *Appl Environ Microbiol* 68:2391–2396 . doi: 10.1128/aem.68.5.2391-2396.2002
- Jetten M, Schmid M, van de Pas-Schoonen K, Sinninghe Damsté J, Strous M (2005a) Anammox organisms: enrichment, cultivation, and environmental analysis. *Methods Enzymol* 397:34–57 . doi: 10.1016/s0076-6879(05)97003-1
- Jetten MSM, Cirpus I, Kartal B, van Niftrik L, van de Pas-Schoonen KT, Sliemers O, Haaijer S, van der Star W, Schmid M, van de Vossenberg J, Schmidt I, Harhangi H, van Loosdrecht M, Gijs Kuenen J, Op den Camp H, Strous M (2005b) 1994–2004: 10 years of research on the anaerobic oxidation of ammonium. *Biochem Soc Trans* 33:119–123 . doi: 10.1042/bst0330119
- Jia B, Raphenya AR, Alcock B, Waglechner N, Guo P, Tsang KK, Lago BA, Dave BM, Pereira S, Sharma AN, Doshi S, Courtot M, Lo R, Williams LE, Frye JG, Elsayegh T, Sardar D, Westman EL, Pawlowski AC, Johnson TA, Brinkman FSL, Wright GD, McArthur AG (2017a) CARD 2017: expansion and model-centric curation of the comprehensive antibiotic resistance database. *Nucleic Acids Res* 45:D566–D573 . doi: 10.1093/nar/gkw1004
- Jia Y, Kumar Khanal S, Zhang H, Chen G-H, Lua H (2017b) Sulfamethoxazole degradation in anaerobic sulfate-reducing bacteria sludge system. *Water Res* 119:12–20 . doi: 10.1016/j.watres.2017.04.040
- Jiang B, Li A, Cui D, Cai R, Ma F, Wang Y (2014) Biodegradation and metabolic pathway of sulfamethoxazole by *Pseudomonas psychrophila* HA-4, a newly isolated cold-adapted sulfamethoxazole-degrading bacterium. *Appl Microbiol Biotechnol* 98:4671–4681 . doi: 10.1007/s00253-013-5488-3
- Johnson M, Zaretskaya I, Raytselis Y, Merezhuk Y, McGinnis S, Madden TL (2008) NCBI BLAST: a better web interface. *Nucleic Acids Res* 36:W5–W9 . doi: 10.1093/nar/gkn201
- Jolley KA, Maiden MC (2010) BIGSdb: Scalable analysis of bacterial genome variation at the population level. *BMC Bioinformatics* 11:595 . doi: 10.1186/1471-2105-11-595
- Jończyk E, Kłak M, Międzybrodzki R, Górski A (2011) The influence of external factors on bacteriophages—review. *Folia Microbiol (Praha)* 56:191–200 . doi: 10.1007/s12223-011-0039-8
- Jones DT, Taylor WR, Thornton JM (1992) The rapid generation of mutation data matrices from protein sequences. *Comput Appl Biosci* 8:275–82
- Jung IL, Oh TJ, Kim IG (2003) Abnormal growth of polyamine-deficient *Escherichia coli* mutant is partially caused by oxidative stress-induced damage. *Arch Biochem Biophys* 418:125–132 . doi: 10.1016/j.abb.2003.08.003
- Jurczak-Kurek A, Gąsior T, Nejman-Faleńczyk B, Bloch S, Dydecka A, Topka G, Necel A, Jakubowska-Deredas M, Narajczyk M, Richert M, Mieszkowska A, Wróbel B, Węgrzyn G, Węgrzyn A (2016) Biodiversity of bacteriophages: morphological and biological properties of a large group of phages isolated from urban sewage. *Sci Rep* 6:34338 . doi: 10.1038/srep34338
- Kaas RS, Friis C, Ussery DW, Aarestrup FM (2012) Estimating variation within the genes and inferring the phylogeny of 186 sequenced diverse *Escherichia coli* genomes. *BMC Genomics* 13:577 . doi:

References

- 10.1186/1471-2164-13-577
- Kaliniene L, Klaus V, Truncaite L (2010) Low-temperature T4-like coliphages vB_EcoM-VR5, vB_EcoM-VR7 and vB_EcoM-VR20. *Arch Virol* 155:871–880 . doi: 10.1007/s00705-010-0656-6
- Kanehisa M, Furumichi M, Tanabe M, Sato Y, Morishima K (2017) KEGG: new perspectives on genomes, pathways, diseases and drugs. *Nucleic Acids Res* 45:D353–D361 . doi: 10.1093/nar/gkw1092
- Kanehisa M, Sato Y, Morishima K (2016) BlastKOALA and GhostKOALA: KEGG tools for functional characterization of genome and metagenome sequences. *J Mol Biol* 428:726–731 . doi: 10.1016/j.jmb.2015.11.006
- Karp P, Latendresse M, Paley S, Krummenacker M, Ong Q, Billington R, Kothari A, Weaver D, Lee T, Subhraveti P, Spaulding A, Fulcher C, Keseler I, Caspi R (2016) Pathway Tools version 19.0 update: software for pathway/genome informatics and systems biology. *Brief Bioinform* 17:877–890 . doi: 10.1093/bib/bbv079
- Kassotaki E, Buttiglieri G, Ferrando-Climent L, Rodriguez-Roda I, Pijuana M (2016) Enhanced sulfamethoxazole degradation through ammonia oxidizing bacteria co-metabolism and fate of transformation products. *Water Res* 94:111–119 . doi: 10.1016/j.watres.2016.02.022
- Kemper N (2008) Veterinary antibiotics in the aquatic and terrestrial environment. *Ecol Indic* 8:1–13 . doi: 10.1016/j.ecolind.2007.06.002
- Kering KK, Kibii BJ, Wei H (2019) Biocontrol of phytobacteria with bacteriophage cocktails. *Pest Manag Sci* 75:1775–1781 . doi: 10.1002/ps.5324
- Kerstens K, De Ley J (1984) Genus *Alcaligenes* Castellani and Chalmers 1919, 936^{AL}. In: Krieg NR, Holt JG (eds) *Bergey's Manual of Systematic Bacteriology*. Williams & Wilkins, Baltimore, pp 361–373
- Kindaichi T, Tsushima I, Ogasawara Y, Shimokawa M, Ozaki N, Satoh H, Okabe S (2007) *In situ* activity and spatial organization of anaerobic ammonium-oxidizing (anammox) bacteria in biofilms. *Appl Environ Microbiol* 73:4931–4939 . doi: 10.1128/aem.00156-07
- Kleindienst S, Higgins SA, Tsementzi D, Chen G, Konstantinidis KT, Mack EE, Löffler FE (2017) '*Candidatus* Dichloromethanomonas elyunquensis' gen. nov., sp. nov., a dichloromethane-degrading anaerobe of the *Peptococcaceae* family. *Syst Appl Microbiol* 40:150–159 . doi: 10.1016/j.syapm.2016.12.001
- Klenk H-P, Meier-Kolthoff JP, Göker M (2014) Taxonomic use of DNA G+C content and DNA–DNA hybridization in the genomic age. *Int J Syst Evol Microbiol* 64:352–356 . doi: 10.1099/ij.s.0.056994-0
- Kneifel H, Elmendorff K, Hegewald E, Soeder CJ (1997) Biotransformation of 1-naphthalenesulfonic acid by the green alga *Scenedesmus obliquus*. *Arch Microbiol* 167:32–37 . doi: 10.1007/s002030050413
- Koba O, Golovko O, Kodešová R, Fér M, Grabic R (2017) Antibiotics degradation in soil: A case of clindamycin, trimethoprim, sulfamethoxazole and their transformation products. *Environ Pollut* 220:1251–1263 . doi: 10.1016/j.envpol.2016.11.007
- Kolvenbach B, Schlaich N, Raoui Z, Prell J, Zühlke S, Schäffer A, Guengerich FP, Corvini PFX (2007) Degradation pathway of bisphenol A: *ipso* substitution apply to phenols containing a quaternary alpha-carbon structure in the *para* position? *Appl Environ Microbiol* 73:4776–4784 . doi: 10.1128/aem.00329-07
- Kolvenbach BA, Dobrowinski H, Fousek J, Vlcek C, Schäffer A, Gabriel FLP, Kohler H-PE, Corvini PFX (2012) An unexpected gene cluster for downstream degradation of alkylphenols in *Sphingomonas* sp. strain TTNP3. *Appl Microbiol Biotechnol* 93:1315–1324 . doi: 10.1007/s00253-011-3451-8
- Konstantinidis KT, Rosselló-Móra R, Amann R (2017) Uncultivated microbes in need of their own taxonomy. *ISME J* 11:2399–2406 . doi: 10.1038/ismej.2017.113
- Konstantinidis KT, Tiedje JM (2005) Towards a genome-based taxonomy for prokaryotes. *J Bacteriol* 187:6258–6264 . doi: 10.1128/jb.187.18.6258-6264.2005

- Koonin E V, Galperin MY (2003) Evolution of central metabolic pathways: The playground of non-orthologous gene displacement. In: Koonin E V., Galperin MY (eds) Sequence - Evolution - Function: Computational approaches in comparative genomics. Kluwer Academic, Boston, pp 295–355
- Koren S, Walenz BP, Berlin K, Miller JR, Bergman NH, Phillippy AM (2017) Canu: scalable and accurate long-read assembly via adaptive k-mer weighting and repeat separation. *Genome Res* 27:722–736 . doi: 10.1101/gr.215087.116
- Krom MD (1980) Spectrophotometric determination of ammonia: a study of a modified Berthelot reaction using salicylate and dichloroisocyanurate. *Analyst* 105:305–316 . doi: 10.1039/an9800500305
- Kropinski AM, Prangishvili D, Lavigne R (2009) Position paper: The creation of a rational scheme for the nomenclature of viruses of *Bacteria* and *Archaea*. *Environ Microbiol* 11:2775–2777 . doi: 10.1111/j.1462-2920.2009.01970.x
- Kugel S, Baunach M, Baer P, Ishida-Ito M, Sundaram S, Xu Z, Groll M, Hertweck C (2017) Cryptic indole hydroxylation by a non-canonical terpenoid cyclase parallels bacterial xenobiotic detoxification. *Nat Commun* 8:15804 . doi: 10.1038/ncomms15804
- Kulikov E, Golomidova A, Letarova M, Kostryukova E, Zelenin A, Prokhorov N, Letarov A (2014) Genomic sequencing and biological characteristics of a novel *Escherichia coli* bacteriophage 9g, a putative representative of a new *Siphoviridae* genus. *Viruses* 6:5077–5092 . doi: 10.3390/v6125077
- Kümmerer K (2009) Antibiotics in the aquatic environment – A review – Part I. *Chemosphere* 75:417–434 . doi: 10.1016/j.chemosphere.2008.11.086
- Kutateladze M, Adamia R (2010) Bacteriophages as potential new therapeutics to replace or supplement antibiotics. *Trends Biotechnol* 28:591–595 . doi: 10.1016/j.tibtech.2010.08.001
- Kyselková M, Kopecký J, Felföldi T, Čermák L, Omelka M, Grundmann GL, Moënné-Loccoz Y, Ságová-Marečková M (2008) Development of a 16S rRNA gene-based prototype microarray for the detection of selected actinomycetes genera. *Antonie van Leeuwenhoek, Int J Gen Mol Microbiol* 94:439–453 . doi: 10.1007/s10482-008-9261-z
- Lamshöft M, Sukul P, Zühlke S, Spitteller M (2007) Metabolism of ¹⁴C-labelled and non-labelled sulfadiazine after administration to pigs. *Anal Bioanal Chem* 388:1733–1745 . doi: 10.1007/s00216-007-1368-y
- Lane DJ (1991) 16S/23S rRNA sequencing. John Wiley and Sons Ltd., New York
- Larcher S, Yargeau V (2011) Biodegradation of sulfamethoxazole by individual and mixed bacteria. *Appl Microbiol Biotechnol* 91:211–218 . doi: 10.1007/s00253-011-3257-8
- Larcher S, Yargeau V (2012) Biodegradation of sulfamethoxazole: Current knowledge and perspectives. *Appl Microbiol Biotechnol* 96:309–318 . doi: 10.1007/s00253-012-4326-3
- Laskos L, Dillard JP, Seifert HS, Fyfe JA., Davies JK (1998) The pathogenic neisseriae contain an inactive *rpoN* gene and do not utilize the *pilE* σ ₅₄ promoter. *Gene* 208:95–102 . doi: 10.1016/s0378-1119(97)00664-1
- Laskov C, Herzog C, Lewandowski J, Hupfer M (2007) Miniaturized photometrical methods for the rapid analysis of phosphate, ammonium, ferrous iron, and sulfate in pore water of freshwater sediments. *Limnol Oceanogr Methods* 5:63–71 . doi: 10.4319/lom.2007.5.63
- Laviad S, Lapidus A, Copeland A, Reddy T, Huntemann M, Pati A, Ivanova NN, Markowitz VM, Pukall R, Klenk H-P, Woyke T, Kyrpides NC, Halpern M (2015) High quality draft genome sequence of *Leucobacter chironomi* strain MM2LB^T (DSM 19883^T) isolated from a *Chironomus* sp. egg mass. *Stand Genomic Sci* 10:21 . doi: 10.1186/s40793-015-0003-3
- Le SQ, Gascuel O (2008) An Improved General Amino Acid Replacement Matrix. *Mol Biol Evol* 25:1307–

References

- 1320 . doi: 10.1093/molbev/msn067
- Leangapichart T, Gautret P, Nguyen TT, Armstrong N, Rolain J-M (2018) Genome sequence of *Leucobacter massiliensis* sp. nov. isolated from human pharynx after travel to the 2014 Hajj. *New Microbes New Infect* 21:42–48 . doi: 10.1016/j.nmni.2017.10.007
- Lee HS, Sobsey MD (2011) Survival of prototype strains of somatic coliphage families in environmental waters and when exposed to UV low-pressure monochromatic radiation or heat. *Water Res* 45:3723–3734 . doi: 10.1016/j.watres.2011.04.024
- Lee J-H, Karamychev V, Kozyavkin S, Mills D, Pavlov A, Pavlova N, Polouchine N, Richardson P, Shakhova V, Slesarev A, Weimer B, O’Sullivan D (2008) Comparative genomic analysis of the gut bacterium *Bifidobacterium longum* reveals *loci* susceptible to deletion during pure culture growth. *BMC Genomics* 9:247 . doi: 10.1186/1471-2164-9-247
- Lefort V, Desper R, Gascuel O (2015) FastME 2.0: a comprehensive, accurate, and fast distance-based phylogeny inference program. *Mol Biol Evol* 32:2798–2800 . doi: 10.1093/molbev/msv150
- Lenski RE, Bouma JE (1987) Effects of segregation and selection on instability of plasmid pACYC184 in *Escherichia coli* B. *J Bacteriol* 169:5314–5316 . doi: 10.1128/jb.169.11.5314-5316.1987
- Leski TA, Bangura U, Jimmy DH, Ansumana R, Lizewski SE, Stenger DA, Taitt CR, Vora GJ (2013) Multidrug-resistant *tetX*-containing hospital isolates in Sierra Leone. *Int J Antimicrob Agents* 42:83–86 . doi: 10.1016/j.ijantimicag.2013.04.014
- Létoffé S, Heuck G, Delepelaire P, Lange N, Wandersman C (2009) Bacteria capture iron from heme by keeping tetrapyrrol skeleton intact. *Proc Natl Acad Sci U S A* 106:11719–11724 . doi: 10.1073/pnas.0903842106
- Levine R (2016) Microbial Degradation of Sulfonamide Antibiotics. University of Nebraska-Lincoln
- Li E, Yin Z, Ma Y, Li H, Lin W, Wei X, Zhao R, Jiang A, Yuan J, Zhao X (2016) Identification and molecular characterization of bacteriophage phiAxp-2 of *Achromobacter xylosoxidans*. *Sci Rep* 6:34300 . doi: 10.1038/srep34300
- Li G, Zhang T, Yang L, Cao Y, Guo X, Qin J, Yang Q, You S, Yuan G, Jiang K, Luo J, Li Z, Gao L, Jiang K, Wu L, Zheng J (2017) Complete genome sequence of *Achromobacter insolitus* type strain LMG 6003^T, a pathogen isolated from leg wound. *Pathog Dis* 75:ftx037 . doi: 10.1093/femspd/ftx037
- Li H (2013) Aligning sequence reads, clone sequences and assembly contigs with BWA-MEM. *arXiv:1303:1–3*
- Li X, Hu Y, Gong J, Zhang L, Wang G (2013) Comparative genome characterization of *Achromobacter* members reveals potential genetic determinants facilitating the adaptation to a pathogenic lifestyle. *Appl Microbiol Biotechnol* 97:6413–6425 . doi: 10.1007/s00253-013-5018-3
- Liao X, Li B, Zou R, Xie S, Yuan B (2016) Antibiotic sulfanilamide biodegradation by acclimated microbial populations. *Appl Microbiol Biotechnol* 100:2439–2447 . doi: 10.1007/s00253-015-7133-9
- Liu B, Pop M (2009) ARDB--Antibiotic resistance genes database. *Nucleic Acids Res* 37:D443-7 . doi: 10.1093/nar/gkn656
- Livak KJ, Schmittgen TD (2001) Analysis of relative gene expression data using real-time quantitative PCR and the 2^{-ΔΔCT} method. *Methods* 25:402–408 . doi: 10.1006/meth.2001.1262
- Loman NJ, Quinlan AR (2014) Poretools: a toolkit for analyzing nanopore sequence data. *Bioinformatics* 30:3399–3401 . doi: 10.1093/bioinformatics/btu555
- Lood R, Ertürk G, Mattiasson B (2017) Revisiting antibiotic resistance spreading in wastewater treatment plants - bacteriophages as a much neglected potential transmission vehicle. *Front Microbiol* 8:2298 . doi: 10.3389/fmicb.2017.02298
- Lowe TM, Chan PP (2016) tRNAscan-SE On-line: Integrating search and context for analysis of transfer

- RNA genes. *Nucleic Acids Res* 44:W54–W57 . doi: 10.1093/nar/gkw413
- Lykidis A, Chen C-L, Tringe SG, McHardy AC, Copeland A, Kyrpides NC, Hugenholtz P, Macarie H, Olmos A, Monroy O, Liu W-T (2011) Multiple syntrophic interactions in a terephthalate-degrading methanogenic consortium. *ISME J* 5:122–130 . doi: 10.1038/ismej.2010.125
- Ma B, Bao P, Wei Y, Zhu G, Yuan Z, Peng Y (2015) Suppressing nitrite-oxidizing bacteria growth to achieve nitrogen removal from domestic wastewater via anammox using intermittent aeration with low dissolved oxygen. *Sci Rep* 5:13048 . doi: 10.1038/srep13048
- Majewsky M, Wagner D, Delay M, Bräse S, Yargeau V, Horn H (2014) Antibacterial activity of sulfamethoxazole transformation products (TPs): General relevance for sulfonamide TPs modified at the *para* position. *Chem Res Toxicol* 27:1821–1828 . doi: 10.1021/tx500267x
- Makarova K, Slesarev A, Wolf Y, Sorokin A, Mirkin B, Koonin E, Pavlov A, Pavlova N, Karamychev V, Polouchine N, Shakhova V, Grigoriev I, Lou Y, Rohksar D, Lucas S, Huang K, Goodstein DM, Hawkins T, Plengvidhya V, Welker D, Hughes J, Goh Y, Benson A, Baldwin K, Lee J-H, Díaz-Muñiz I, Dosti B, Smeianov V, Wechter W, Barabote R, Lorca G, Altermann E, Barrangou R, Ganesan B, Xie Y, Rawsthorne H, Tamir D, Parker C, Breidt F, Broadbent J, Hutkins R, O’Sullivan D, Steele J, Unlu G, Saier M, Klaenhammer T, Richardson P, Kozyavkin S, Weimer B, Mills D (2006) Comparative genomics of the lactic acid bacteria. *Proc Natl Acad Sci U S A* 103:15611–15616 . doi: 10.1073/pnas.0607117103
- Maltseva O, Oriel P (1997) Monitoring of an alkaline 2,4,6-trichlorophenol-degrading enrichment culture by DNA fingerprinting methods and isolation of the responsible organism, haloalkaliphilic *Nocardioides* sp. strain M6. *Appl Environ Microbiol* 63:4145–4149
- Manaia CM, Macedo G, Fatta-Kassinos D, Nunes OC (2016) Antibiotic resistance in urban aquatic environments: can it be controlled? *Appl Microbiol Biotechnol* 100:1543–1557 . doi: 10.1007/s00253-015-7202-0
- Marchler-Bauer A, Bo Y, Han L, He J, Lanczycki CJ, Lu S, Chitsaz F, Derbyshire MK, Geer RC, Gonzales NR, Gwadz M, Hurwitz DI, Lu F, Marchler GH, Song JS, Thanki N, Wang Z, Yamashita RA, Zhang D, Zheng C, Geer LY, Bryant SH (2017) CDD/SPARCLE: functional classification of proteins via subfamily domain architectures. *Nucleic Acids Res* 45:D200–D203 . doi: 10.1093/nar/gkw1129
- Marchler-Bauer A, Derbyshire MK, Gonzales NR, Lu S, Chitsaz F, Geer LY, Geer RC, He J, Gwadz M, Hurwitz DI, Lanczycki CJ, Lu F, Marchler GH, Song JS, Thanki N, Wang Z, Yamashita RA, Zhang D, Zheng C, Bryant SH (2015) CDD: NCBI’s conserved domain database. *Nucleic Acids Res* 43:D222–D226 . doi: 10.1093/nar/gku1221
- Mareuil F, Doppelt-Azeroual O, Ménager H, Mareuil F, Doppelt-Azeroual O, Ménager H (2017) A public Galaxy platform at Pasteur used as an execution engine for web services. *F1000Research* 6:1030 . doi: 10.7490/f1000research.1114334.1
- Martin JF, Liras P (1989) Organization and expression of genes involved in the biosynthesis of antibiotics and other secondary metabolites. *Annu Rev Microbiol* 43:173–206 . doi: 10.1146/annurev.mi.43.100189.001133
- Martinez JL (2009) Environmental pollution by antibiotics and by antibiotic resistance determinants. *Environ Pollut* 157:2893–2902 . doi: 10.1016/j.envpol.2009.05.051
- Martini MC, Wibberg D, Lozano M, Torres Tejerizo G, Albicoro FJ, Jaenicke S, van Elsas JD, Petroni A, Garcillán-Barcia MP, de la Cruz F, Schlüter A, Pühler A, Pistorio M, Lagares A, Del Papa MF (2016) Genomics of high molecular weight plasmids isolated from an on-farm biopurification system. *Sci Rep* 6:28284 . doi: 10.1038/srep28284
- Masters PA, O’Byrne TA, Zurlo J, Miller DQ, Joshi N, P G, WE S (2003) Trimethoprim-sulfamethoxazole revisited. *Arch Intern Med* 163:402–410 . doi: 10.1001/archinte.163.4.402
- Mawad AMM, Hesham AE-L, Mostafa YM, Shoriet A (2016) Pyrene degrading *Achromobacter denitrificans* ASU-035: growth rate, enzymes activity, and cell surface properties. *Rend Lincei*

References

- 27:557–563 . doi: 10.1007/s12210-016-0521-y
- McCutcheon JP, Moran NA (2012) Extreme genome reduction in symbiotic bacteria. *Nat Rev Microbiol* 10:13–26 . doi: 10.1038/nrmicro2670
- McGee DJ, Radcliff FJ, Mendz GL, Ferrero RL, Mobley HL (1999) *Helicobacter pylori rocF* is required for arginase activity and acid protection *in vitro* but is not essential for colonization of mice or for urease activity. *J Bacteriol* 181:7314–7322
- Meier-Kolthoff JP, Auch AF, Klenk H-P, Göker M (2013) Genome sequence-based species delimitation with confidence intervals and improved distance functions. *BMC Bioinformatics* 14:60 . doi: 10.1186/1471-2105-14-60
- Meier-Kolthoff JP, Göker M, Kelso J (2017) VICTOR: genome-based phylogeny and classification of prokaryotic viruses. *Bioinformatics* 33:3396–3404 . doi: 10.1093/bioinformatics/btx440
- Meier-Kolthoff JP, Hahnke RL, Petersen J, Scheuner C, Michael V, Fiebig A, Rohde C, Rohde M, Fartmann B, Goodwin LA, Chertkov O, Reddy T, Pati A, Ivanova NN, Markowitz V, Kyrpides NC, Woyke T, Göker M, Klenk H-P (2014) Complete genome sequence of DSM 30083^T, the type strain (U5/41T) of *Escherichia coli*, and a proposal for delineating subspecies in microbial taxonomy. *Stand Genomic Sci* 9:2 . doi: 10.1186/1944-3277-9-2
- Merhej V, Royer-Carenzi M, Pontarotti P, Raoult D (2009) Massive comparative genomic analysis reveals convergent evolution of specialized bacteria. *Biol Direct* 4:13 . doi: 10.1186/1745-6150-4-13
- Midha S, Bansal K, Sharma S, Kumar N, Patil PP, Chaudhry V, Patil PB (2016) Genomic resource of rice seed associated bacteria. *Front Microbiol* 6:1551 . doi: 10.3389/fmicb.2015.01551
- Miethke M, Monteferrante CG, Marahiel MA, van Dijk JM (2013) The *Bacillus subtilis* EfeUOB transporter is essential for high-affinity acquisition of ferrous and ferric iron. *Biochim Biophys Acta - Mol Cell Res* 1833:2267–2278 . doi: 10.1016/j.bbamcr.2013.05.027
- Minerdi D, Zgrablic I, Castrignanò S, Catucci G, Medana C, Terlizzi ME, Gribaudo G, Gilardi G, Sadeghi SJ (2016) *Escherichia coli* overexpressing a baeyer-villiger monooxygenase from *Acinetobacter radioresistens* becomes resistant to imipenem. *Antimicrob Agents Chemother* 60:64–74 . doi: 10.1128/aac.01088-15
- Mitchell SM, Ullman JL, Teel AL, Watts RJ, Frear C (2013) The effects of the antibiotics ampicillin, florfenicol, sulfamethazine, and tylosin on biogas production and their degradation efficiency during anaerobic digestion. *Bioresour Technol* 149:244–252 . doi: 10.1016/j.biortech.2013.09.048
- Mohatt JL, Hu L, Finneran KT, Strathmann TJ (2011) Microbially mediated abiotic transformation of the antimicrobial agent sulfamethoxazole under iron-reducing soil conditions. *Environ Sci Technol* 45:4793–4801 . doi: 10.1021/es200413g
- Mohring SAI, Strzysch I, Fernandes MR, Kiffmeyer TK, Tuerk J, Hamscher G (2009) Degradation and elimination of various sulfonamides during anaerobic fermentation: A promising step on the way to sustainable pharmacy? *Environ Sci Technol* 43:2569–2574 . doi: 10.1021/es802042d
- Morais P V., Paulo C, Francisco R, Branco R, Paula Chung A, da Costa MS (2006) *Leucobacter luti* sp. nov., and *Leucobacter alluvii* sp. nov., two new species of the genus *Leucobacter* isolated under chromium stress. *Syst Appl Microbiol* 29:414–421 . doi: 10.1016/j.syapm.2005.10.005
- Moran NA (2003) Tracing the evolution of gene loss in obligate bacterial symbionts. *Curr Opin Microbiol* 6:512–518 . doi: 10.1016/j.mib.2003.08.001
- Morris BEL, Henneberger R, Huber H, Moissl-Eichinger C (2013) Microbial syntrophy: interaction for the common good. *FEMS Microbiol Rev* 37:384–406 . doi: 10.1111/1574-6976.12019
- Morris JJ, Johnson ZI, Szul MJ, Keller M, Zinser ER (2011) Dependence of the *Cyanobacterium Prochlorococcus* on hydrogen peroxide scavenging microbes for growth at the ocean's surface. *PLoS One* 6:e16805 . doi: 10.1371/journal.pone.0016805

- Morris JJ, Lenski RE, Zinser ER (2012) The black queen hypothesis: Evolution of dependencies through adaptive gene loss. *MBio* 3:e00036-12 . doi: 10.1128/mbio.00036-12
- Moura A, Soares M, Pereira C, Leitao N, Henriques I, Correia A (2009) INTEGRALL: a database and search engine for integrons, integrases and gene cassettes. *Bioinformatics* 25:1096–1098 . doi: 10.1093/bioinformatics/btp105
- Mulla SI, Hu A, Sun Q, Li J, Suanona F, Ashfaq M, Yu C-P (2018) Biodegradation of sulfamethoxazole in bacteria from three different origins. *J Environ Manage* 206:93–102 . doi: 10.1016/j.jenvman.2017.10.029
- Müller E, Schüssler W, Horn H, Lemmer H (2013) Aerobic biodegradation of the sulfonamide antibiotic sulfamethoxazole by activated sludge applied as co-substrate and sole carbon and nitrogen source. *Chemosphere* 92:969–978 . doi: 10.1016/j.chemosphere.2013.02.070
- Murray RGE, Stackebrandt E (1995) Taxonomic Note: Implementation of the Provisional Status Candidatus for Incompletely Described Procaryotes. *Int J Syst Bacteriol* 45:186–187 . doi: 10.1099/00207713-45-1-186
- Naas T, Oueslati S, Bonnin RA, Dabos ML, Zavala A, Dortet L, Retailleau P, Iorga BI (2017) Beta-lactamase database (BLDB) – structure and function. *J Enzyme Inhib Med Chem* 32:917–919 . doi: 10.1080/14756366.2017.1344235
- NCBI Resource Coordinators (2017) Database Resources of the National Center for Biotechnology Information. *Nucleic Acids Res* 45:D12–D17 . doi: 10.1093/nar/gkw1071
- Nejidat A, Saadi I, Ronen Z (2008) Effect of flagella expression on adhesion of *Achromobacter piechaudii* to chalk surfaces. *J Appl Microbiol* 105:2009–2014 . doi: 10.1111/j.1365-2672.2008.03930.x
- Nguyen PY, Silva AF, Reis AC, Nunes OC, Rodrigues AM, Rodrigues JE, Cardoso VV, Benoliel MJ, Reis MAM, Oehmen A, Carvalho G (2019) Bioaugmentation of membrane bioreactor with *Achromobacter denitrificans* strain PR1 for enhanced sulfamethoxazole removal in wastewater. *Sci Total Environ* 648:44–55 . doi: 10.1016/j.scitotenv.2018.08.100
- Nguyen PYY, Carvalho G, Reis ACC, Nunes OCC, Reis MAMAM, Oehmen A (2017) Impact of biogenic substrates on sulfamethoxazole biodegradation kinetics by *Achromobacter denitrificans* strain PR1. *Biodegradation* 28:1–13 . doi: 10.1007/s10532-017-9789-6
- Nicoloff H, Andersson DI (2016) Indirect resistance to several classes of antibiotics in cocultures with resistant bacteria expressing antibiotic-modifying or -degrading enzymes. *J Antimicrob Chemother* 71:100–110 . doi: 10.1093/jac/dkv312
- Nikolskaya II, Lopatina NG, Debov SS (1976) Methylated guanine derivative as a minor base in the DNA of phage DDVI *Shigella dysenteriae*. *Biochim Biophys Acta* 435:206–210
- Nödler K, Licha T, Barbieri M, Pérez S (2012) Evidence for the microbially mediated abiotic formation of reversible and non-reversible sulfamethoxazole transformation products during denitrification. *Water Res* 46:2131–2139 . doi: 10.1016/j.watres.2012.01.028
- Nouws JF, Firth EC, Vree TB, Baakman M (1987) Pharmacokinetics and renal clearance of sulfamethazine, sulfamerazine, and sulfadiazine and their N^4 -acetyl and hydroxy metabolites in horses. *Am J Vet Res* 48:392–402
- Okonechnikov K, Conesa A, García-Alcalde F (2015) Qualimap 2: advanced multi-sample quality control for high-throughput sequencing data. *Bioinformatics* 32:btv566 . doi: 10.1093/bioinformatics/btv566
- Oshiki M, Awata T, Kandaichi T, Satoh H, Okabe S (2013) Cultivation of planktonic anaerobic ammonium oxidation (anammox) bacteria using membrane bioreactor. *Microbes Environ* 28:436–443 . doi: 10.1264/jsm2.me13077
- Overbeek R, Olson R, Pusch GD, Olsen GJ, Davis JJ, Disz T, Edwards RA, Gerdes S, Parrello B, Shukla M,

References

- Vonstein V, Wattam AR, Xia F, Stevens R (2014) The SEED and the Rapid Annotation of microbial genomes using Subsystems Technology (RAST). *Nucleic Acids Res* 42:D206–D214 . doi: 10.1093/nar/gkt1226
- Owens N (2012) NIH Shift Literature Search. In: All Capstone Proj. <http://opus.govst.edu/capstones/72>. Accessed 18 Oct 2016
- Page AJ, Cummins CA, Hunt M, Wong VK, Reuter S, Holden MTG, Fookes M, Falush D, Keane JA, Parkhill J (2015) Roary: rapid large-scale prokaryote pan genome analysis. *Bioinformatics* 31:3691–3693 . doi: 10.1093/bioinformatics/btv421
- Pande S, Kost C (2017) Bacterial unculturability and the formation of intercellular metabolic networks. *Trends Microbiol* 25:349–361 . doi: 10.1016/j.tim.2017.02.015
- Pande S, Shitut S, Freund L, Westermann M, Bertels F, Colesie C, Bischofs IB, Kost C (2015) Metabolic cross-feeding via intercellular nanotubes among bacteria. *Nat Commun* 6:6238 . doi: 10.1038/ncomms7238
- Parks DH, Imelfort M, Skennerton CT, Hugenholtz P, Tyson GW (2015) CheckM: assessing the quality of microbial genomes recovered from isolates, single cells, and metagenomes. *Genome Res* 25:1043–1055 . doi: 10.1101/gr.186072.114
- Parte AC (2014) LPSN--list of prokaryotic names with standing in nomenclature. *Nucleic Acids Res* 42:D613–D616 . doi: 10.1093/nar/gkt1111
- Parveen N, Cornell KA (2011) Methylthioadenosine/S-adenosylhomocysteine nucleosidase, a critical enzyme for bacterial metabolism. *Mol Microbiol* 79:7–20 . doi: 10.1111/j.1365-2958.2010.07455.x
- Paterson DL, Bonomo RA (2005) Extended-spectrum beta-lactamases: a clinical update. *Clin Microbiol Rev* 18:657–686 . doi: 10.1128/cmr.18.4.657-686.2005
- Pearson WR (2013) An Introduction to Sequence Similarity (“Homology”) Searching. *Curr Protoc Bioinforma* 42:3.1.1–3.1.8 . doi: 10.1002/0471250953.bi0301s42
- Pelz O, Tesar M, Wittich R-M, Moore ERB, Timmis KN, Abraham W-R (1999) Towards elucidation of microbial community metabolic pathways: unravelling the network of carbon sharing in a pollutant-degrading bacterial consortium by immunocapture and isotopic ratio mass spectrometry. *Environ Microbiol* 1:167–174 . doi: 10.1046/j.1462-2920.1999.00023.x
- Percudani R (2013) A microbial metagenome (*Leucobacter* sp.) in *Caenorhabditis* whole genome sequences. *Bioinform Biol Insights* 7:55–72 . doi: 10.4137/bbi.s11064
- Pérez S, Eichhorn P, Aga DS (2005) Evaluating the biodegradability of sulfamethazine, sulfamethoxazole, sulfathiazole, and trimethoprim at different stages of sewage treatment. *Environ Toxicol Chem* 24:1361–1367 . doi: 10.1897/04-211r.1
- Pernthaler J, Glöckner F-O, Schönhuber W, Amann R (2001) Fluorescence in situ hybridization (FISH) with rRNA-targeted oligonucleotide probes. *Methods Microbiol* 30:207–226 . doi: 10.1016/s0580-9517(01)30046-6
- Perreten V, Boerlin P (2003) A new sulfonamide resistance gene (*sul3*) in *Escherichia coli* is widespread in the pig population of Switzerland. *Antimicrob Agents Chemother* 47:1169–1172 . doi: 10.1128/aac.47.3.1169-1172.2003
- Petrie B, Barden R, Kasprzyk-Hordern B (2015) A review on emerging contaminants in wastewaters and the environment: Current knowledge, understudied areas and recommendations for future monitoring. *Water Res* 72:3–27 . doi: 10.1016/j.watres.2014.08.053
- Pham VHT, Kim J (2012) Cultivation of unculturable soil bacteria. *Trends Biotechnol* 30:475–484 . doi: 10.1016/j.tibtech.2012.05.007
- Pirnay J-P, Verbeke G, Rose T, Jennes S, Zizi M, Huys I, Lavigne R, Merabishvili M, Vanechoutte M, Buckling A, De Vos D (2012) Introducing yesterday’s phage therapy in today’s medicine. *Future*

- Viol 7:379–390 . doi: 10.2217/fvl.12.24
- Pittman MS, Corker H, Wu G, Binet MB, Moir AJG, Poole RK (2002) Cysteine is exported from the *Escherichia coli* cytoplasm by CydDC, an ATP-binding cassette-type transporter required for cytochrome assembly. J Biol Chem 277:49841–49849 . doi: 10.1074/jbc.m205615200
- Pittman MS, Robinson HC, Poole RK (2005) A bacterial glutathione transporter (*Escherichia coli* CydDC) exports reductant to the periplasm. J Biol Chem 280:32254–32261 . doi: 10.1074/jbc.m503075200
- Pluvinage B, Dairou J, Possot OM, Martins M, Fouet A, Dupret J-M, Rodrigues-Lima F (2007) Cloning and molecular characterization of three arylamine *N*-acetyltransferase genes from *Bacillus anthracis*: Identification of unusual enzymatic properties and their contribution to sulfamethoxazole resistance. Biochemistry 46:7069–7078 . doi: 10.1021/bi700351w
- Poe M (1976) Antibacterial synergism: a proposal for chemotherapeutic potentiation between trimethoprim and sulfamethoxazole. Science 194:533–355 . doi: 10.1126/science.788154
- Ponomarova O, Patil KR (2015) Metabolic interactions in microbial communities: untangling the Gordian knot. Curr Opin Microbiol 27:37–44 . doi: 10.1016/j.mib.2015.06.014
- Poole RK, Gibson F, Wu G (1994) The *cydD* gene product, component of a heterodimeric ABC transporter, is required for assembly of periplasmic cytochrome *c* and of cytochrome *bd* in *Escherichia coli*. FEMS Microbiol Lett 117:217–223 . doi: 10.1111/j.1574-6968.1994.tb06768.x
- Poranen MM, Bamford DH, Oksanen HM (2015) Membrane-containing bacteriophages. In: eLS. John Wiley & Sons, Ltd, Chichester, UK, pp 1–11
- Pradeep S, Sarath Josh MK, Binod P, Sudha Devi R, Balachandran S, Anderson RC, Benjamin S (2015) *Achromobacter denitrificans* strain SP1 efficiently remediates di(2-ethylhexyl)phthalate. Ecotoxicol Environ Saf 112:114–121 . doi: 10.1016/j.ecoenv.2014.10.035
- Price MN, Dehal PS, Arkin AP (2010) FastTree 2 – Approximately Maximum-Likelihood trees for large alignments. PLoS One 5:e9490 . doi: 10.1371/journal.pone.0009490
- Qin Q-L, Xie B-B, Zhang X-Y, Chen X-L, Zhou B-C, Zhou J, Oren A, Zhang Y-Z (2014) A proposed genus boundary for the prokaryotes based on genomic insights. J Bacteriol 196:2210–2215 . doi: 10.1128/jb.01688-14
- Quevillon E, Silventoinen V, Pillai S, Harte N, Mulder N, Apweiler R, Lopez R (2005) InterProScan: protein domains identifier. Nucleic Acids Res 33:W116–W120 . doi: 10.1093/nar/gki442
- Radke M, Lauwigi C, Heinkele G, Múrdter TE, Letzel M (2009) Fate of the antibiotic sulfamethoxazole and its two major human metabolites in a water sediment test. Environ Sci Technol 43:3135–3141 . doi: 10.1021/es900300u
- Rambaut A, Drummond AJ, Xie D, Baele G, Suchard MA (2018) Posterior Summarization in Bayesian Phylogenetics Using Tracer 1.7. Syst Biol 67:901–904 . doi: 10.1093/sysbio/syy032
- Rang HP, Dale MM, Ritter JM, Moore PK (2003) Pharmacology, 5th edn. Churchill Livingstone, Edinburgh, UK
- Razavi M, Marathe NP, Gillings MR, Flach C-F, Kristiansson E, Joakim Larsson DG (2017) Discovery of the fourth mobile sulfonamide resistance gene. Microbiome 5:160–172 . doi: 10.1186/s40168-017-0379-y
- Reis AC, Čvančarová M, Liu Y, Lenz M, Hettich T, Kolvenbach BA, Corvini PF-X, Nunes OC (2018a) Biodegradation of sulfamethoxazole by a bacterial consortium of *Achromobacter denitrificans* PR1 and *Leucobacter* sp. GP. Appl Microbiol Biotechnol 102:10299–10314 . doi: 10.1007/s00253-018-9411-9
- Reis AC, Kroll K, Gomila M, Kolvenbach BA, Corvini PFX, Nunes OC (2017) Complete genome sequence of *Achromobacter denitrificans* PR1. Genome Announc 5:e00762-17 . doi: 10.1128/genomea.00762-17

References

- Reis PJM, Homem V, Alves A, Vilar VJP, Manaia CM, Nunes OC (2018b) Insights on sulfamethoxazole bio-transformation by environmental *Proteobacteria* isolates. *J Hazard Mater* 358:310–318 . doi: 10.1016/j.jhazmat.2018.07.012
- Reis PJM, Reis AC, Ricken B, Kolvenbach BA, Manaia CM, Corvini PFX, Nunes OC (2014) Biodegradation of sulfamethoxazole and other sulfonamides by *Achromobacter denitrificans* PR1. *J Hazard Mater* 280:741–749 . doi: 10.1016/j.jhazmat.2014.08.039
- Richter M, Rosselló-Móra R (2009) Shifting the genomic gold standard for the prokaryotic species definition. *Proc Natl Acad Sci U S A* 106:19126–19131 . doi: 10.1073/pnas.0906412106
- Ricken B, Corvini PFX, Cichocka D, Parisi M, Lenz M, Wyss D, Martínez-Lavanchy PM, Müller JA, Shahgaldian P, Tulli LG, Kohler H-PE, Kolvenbach BA (2013) *Ips*-hydroxylation and subsequent fragmentation: a novel microbial strategy to eliminate sulfonamide antibiotics. *Appl Environ Microbiol* 79:5550–5558 . doi: 10.1128/aem.00911-13
- Ricken B, Fellmann O, Kohler H-PE, Schäffer A, Corvini PF-X, Kolvenbach BA (2015a) Degradation of sulfonamide antibiotics by *Microbacterium* sp. strain BR1 – elucidating the downstream pathway. *N Biotechnol* 32:710–715 . doi: 10.1016/j.nbt.2015.03.005
- Ricken B, Kolvenbach BA, Bergesch C, Benndorf D, Kroll K, Strnad H, Vlček Č, Adaixo R, Hammes F, Shahgaldian P, Schäffer A, Kohler H-PE, Corvini PF-X (2017) FMNH₂-dependent monooxygenases initiate catabolism of sulfonamides in *Microbacterium* sp. strain BR1 subsisting on sulfonamide antibiotics. *Sci Rep* 7:15783 . doi: 10.1038/s41598-017-16132-8
- Ricken B, Kolvenbach BA, Corvini PF-X (2015b) *Ips*-substitution—the hidden gate to xenobiotic degradation pathways. *Curr Opin Biotechnol* 33:220–227 . doi: 10.1016/j.copbio.2015.03.009
- Ridderberg W, Wang M, Nørskov-Lauritsen N (2012) Multilocus sequence analysis of isolates of *Achromobacter* from patients with cystic fibrosis reveals infecting species other than *Achromobacter xylosoxidans*. *J Clin Microbiol* 50:2688–2694 . doi: 10.1128/jcm.00728-12
- Rieger PG, Meier HM, Gerle M, Vogt U, Groth T, Knackmuss HJ (2002) Xenobiotics in the environment: present and future strategies to obviate the problem of biological persistence. *J Biotechnol* 94:101–123 . doi: 10.1016/s0168-1656(01)00422-9
- Rizzo L, Manaia C, Merlin C, Schwartz T, Dagot C, Ploy MC, Michael I, Fatta-Kassinos D (2013) Urban wastewater treatment plants as hotspots for antibiotic resistant bacteria and genes spread into the environment: A review. *Sci Total Environ* 447:345–360 . doi: 10.1016/j.scitotenv.2013.01.032
- Rodriguez-R LM, Konstantinidis KT (2016) The enveomics collection: a toolbox for specialized analyses of microbial genomes and metagenomes. *PeerJ Prepr* 4:e1900v1 . doi: 10.7287/peerj.preprints.1900v1
- Rombouts S, Volckaert A, Venneman S, Declercq B, Vandenheuveld D, Allonsius CN, Van Malderghem C, Jang HB, Briers Y, Noben JP, Klumpp J, Van Vaerenbergh J, Maes M, Lavigne R (2016) Characterization of novel bacteriophages for biocontrol of bacterial blight in leek caused by *Pseudomonas syringae* pv. *porri*. *Front Microbiol* 7:279 . doi: 10.3389/fmicb.2016.00279
- Sabri NA, Schmitt H, Van der Zaan B, Gerritsen HW, Zuidema T, Rijnaarts HHM, Langenhoff AAM (2018) Prevalence of antibiotics and antibiotic resistance genes in a wastewater effluent-receiving river in the Netherlands. *J Environ Chem Eng*. doi: 10.1016/j.jece.2018.03.004
- Sahlín K, Vezzi F, Nystedt B, Lundberg J, Arvestad L (2014) BESST - Efficient scaffolding of large fragmented assemblies. *BMC Bioinformatics* 15:281 . doi: 10.1186/1471-2105-15-281
- Saitou N, Nei M (1987) The neighbor-joining method: a new method for reconstructing phylogenetic trees. *Mol Biol Evol* 4:406–425 . doi: 10.1093/oxfordjournals.molbev.a040454
- Sałek K, Zgoła-Grzeškowiak A, Kaczorek E (2013) Modification of surface and enzymatic properties of *Achromobacter denitrificans* and *Stenotrophomonas maltophilia* in association with diesel oil biodegradation enhanced with alkyl polyglucosides. *Colloids Surfaces B Biointerfaces* 111:36–42 .

- doi: 10.1016/j.colsurfb.2013.05.021
- Salmela L, Rivals E (2014) LoRDEC: accurate and efficient long read error correction. *Bioinformatics* 30:3506–3514 . doi: 10.1093/bioinformatics/btu538
- Salzberg SL (2019) Next-generation genome annotation: we still struggle to get it right. *Genome Biol* 20:92 . doi: 10.1186/s13059-019-1715-2
- Sánchez MB, Martínez JL (2015) The efflux pump SmeDEF contributes to trimethoprim-sulfamethoxazole resistance in *Stenotrophomonas maltophilia*. *Antimicrob Agents Chemother* 59:4347–4348 . doi: 10.1128/aac.00714-15
- Sander C, Schneider R (1991) Database of homology-derived protein structures and the structural meaning of sequence alignment. *Proteins Struct Funct Genet* 9:56–68 . doi: 10.1002/prot.340090107
- Sanderson JP, Hollis FJ, Maggs JL, Clarke SE, Naisbitt DJ, Park BK (2008) Nonenzymatic formation of a novel hydroxylated sulfamethoxazole derivative in human liver microsomes: Implications for bioanalysis of sulfamethoxazole metabolites. *Drug Metab Dispos* 36:2424–2428 . doi: 10.1124/dmd.108.021246
- Sanguin H, Remenant B, Dechesne A, Thioulouse J, Vogel TM, Nesme X, Moëgne-Loccoz Y, Grundmann GL (2006) Potential of a 16S rRNA-based taxonomic microarray for analyzing the rhizosphere effects of maize on *Agrobacterium* spp. and bacterial communities. *Appl Environ Microbiol* 72:4302–4312 . doi: 10.1128/aem.02686-05
- Sarmah AK, Meyer MT, Boxall ABA (2006) A global perspective on the use, sales, exposure pathways, occurrence, fate and effects of veterinary antibiotics (VAs) in the environment. *Chemosphere* 65:725–759 . doi: 10.1016/j.chemosphere.2006.03.026
- Sauter M, Moffatt B, Saechao MC, Hell R, Wirtz M (2013) Methionine salvage and S-adenosylmethionine: essential links between sulfur, ethylene and polyamine biosynthesis. *Biochem J* 451:145–154 . doi: 10.1042/bj20121744
- Sazinas P, Redgwell T, Rihtman B, Grigonyte A, Michniewski S, Scanlan DJ, Hobman J, Millard A (2018) Comparative genomics of bacteriophage of the genus *Seuratvirus*. *Genome Biol Evol* 10:72–76 . doi: 10.1093/gbe/evx275
- Schindelin J, Arganda-Carreras I, Frise E, Kaynig V, Longair M, Pietzsch T, Preibisch S, Rueden C, Saalfeld S, Schmid B, Tinevez J-Y, White DJ, Hartenstein V, Eliceiri K, Tomancak P, Cardona A (2012) Fiji: an open-source platform for biological-image analysis. *Nat Methods* 9:676–682 . doi: 10.1038/nmeth.2019
- Schink B (2002) Synergistic interactions in the microbial world. *Antonie Van Leeuwenhoek* 81:257–261 . doi: 10.1023/a:1020579004534
- Schloss PD, Handelsman J (2005) Metagenomics for studying unculturable microorganisms: cutting the Gordian knot. *Genome Biol* 6:229 . doi: 10.1186/gb-2005-6-8-229
- Schrödinger L (2002) The PyMOL molecular graphics system. Version 1.8
- Seemann T (2014) Prokka: rapid prokaryotic genome annotation. *Bioinformatics* 30:2068–2069 . doi: 10.1093/bioinformatics/btu153
- Segata N, Börnigen D, Morgan XC, Huttenhower C (2013) PhyloPhlAn is a new method for improved phylogenetic and taxonomic placement of microbes. *Nat Commun* 4:2304 . doi: 10.1038/ncomms3304
- Shao Y, Wang I-N (2008) Bacteriophage adsorption rate and optimal lysis time. *Genetics* 180:471–82 . doi: 10.1534/genetics.108.090100
- Sharp DG, Hook AE (1946) Sedimentation characters and pH stability of the T2 bacteriophage of *Escherichia coli*. *J Biol Chem* 165:259–70

References

- Shimodaira H (2002) An approximately unbiased test of phylogenetic tree selection. *Syst Biol* 51:492–508 . doi: 10.1080/10635150290069913
- Silva FJ, Latorre A, Moya A (2001) Genome size reduction through multiple events of gene disintegration in *Buchnera* APS. *Trends Genet* 17:615–618 . doi: 10.1016/s0168-9525(01)02483-0
- Silva YJ, Moreirinha C, Pereira C, Costa L, Rocha RJM, Cunha Â, Gomes NCM, Calado R, Almeida A (2016) Biological control of *Aeromonas salmonicida* infection in juvenile Senegalese sole (*Solea senegalensis*) with Phage AS-A. *Aquaculture* 450:225–233 . doi: 10.1016/j.aquaculture.2015.07.025
- Simpkin VL, Renwick MJ, Kelly R, Mossialos E (2017) Incentivising innovation in antibiotic drug discovery and development: Progress, challenges and next steps. *J Antibiot (Tokyo)* 70:1087–1096 . doi: 10.1038/ja.2017.124
- Sköld O (2000) Sulfonamide resistance: mechanisms and trends. *Drug Resist Updat* 3:155–160 . doi: 10.1054/drup.2000.0146
- Sköld O (2001) Resistance to trimethoprim and sulfonamides. *Vet Res* 32:261–273 . doi: 10.1051/vetres:2001123
- Smillie C, Garcillán-Barcia MP, Francia MV, Rocha EPC, de la Cruz F (2010) Mobility of plasmids. *Microbiol Mol Biol Rev* 74:434–452 . doi: 10.1128/mmbr.00020-10
- Solomon C, Collier J, Berg G, Glibert P (2010) Role of urea in microbial metabolism in aquatic systems: a biochemical and molecular review. *Aquat Microb Ecol* 59:67–88 . doi: 10.3354/ame01390
- Sørensen SR, Ronen Z, Aamand J (2002) Growth in coculture stimulates metabolism of the phenylurea herbicide isoproturon by *Sphingomonas* sp. strain SRS2. *Appl Environ Microbiol* 68:3478–3485 . doi: 10.1128/aem.68.7.3478-3485.2002
- Sorg RA, Lin L, van Doorn GS, Sorg M, Olson J, Nizet V, Veening J-W (2016) Collective resistance in microbial communities by intracellular antibiotic deactivation. *PLOS Biol* 14:e2000631 . doi: 10.1371/journal.pbio.2000631
- Sović I, Šikić M, Wilm A, Fenlon SN, Chen S, Nagarajan N (2016) Fast and sensitive mapping of nanopore sequencing reads with GraphMap. *Nat Commun* 7:11307 . doi: 10.1038/ncomms11307
- Spilker T, Vandamme P, Lipuma JJ (2012) A multilocus sequence typing scheme implies population structure and reveals several putative novel *Achromobacter* species. *J Clin Microbiol* 50:3010–3015 . doi: 10.1128/jcm.00814-12
- Srinivasan P, Ramasamy P (2017) Morphological characterization and biocontrol effects of *Vibrio vulnificus* phages against vibriosis in the shrimp aquaculture environment. *Microb Pathog* 111:472–480 . doi: 10.1016/j.micpath.2017.09.024
- Stackebrandt E, Goebel BM (1994) Taxonomic note: A place for DNA-DNA reassociation and 16S rRNA sequence analysis in the present species definition in bacteriology. *Int J Syst Evol Microbiol* 44:846–849 . doi: 10.1099/00207713-44-4-846
- Stewart EJ (2012) Growing unculturable bacteria. *J Bacteriol* 194:4151–4160 . doi: 10.1128/jb.00345-12
- Stolyar S, Van Dien S, Hillesland KL, Pinel N, Lie TJ, Leigh JA, Stahl DA (2007) Metabolic modeling of a mutualistic microbial community. *Mol Syst Biol* 3:92 . doi: 10.1038/msb4100131
- Stover CK, Pham XQ, Erwin AL, Mizoguchi SD, Warrenner P, Hickey MJ, Brinkman FS, Hufnagle WO, Kowalik DJ, Lagrou M, Garber RL, Goltry L, Tolentino E, Westbrook-Wadman S, Yuan Y, Brody LL, Coulter SN, Folger KR, Kas A, Larbig K, Lim R, Smith K, Spencer D, Wong GK, Wu Z, Paulsen IT, Reizer J, Saier MH, Hancock RE, Lory S, Olson M V (2000) Complete genome sequence of *Pseudomonas aeruginosa* PAO1, an opportunistic pathogen. *Nature* 406:959–964 . doi: 10.1038/35023079
- Sturm G, Jacobs J, Sproer C, Schumann P, Gescher J (2011) *Leucobacter chromiirestiens* sp. nov., a

- chromate-resistant strain. *Int J Syst Evol Microbiol* 61:956–960 . doi: 10.1099/ijms.0.022780-0
- Su T, Deng H, Benskin JP, Radke M (2016) Biodegradation of sulfamethoxazole photo-transformation products in a water/sediment test. *Chemosphere* 148:518–525 . doi: 10.1016/j.chemosphere.2016.01.049
- Suchard MA, Lemey P, Baele G, Ayres DL, Drummond AJ, Rambaut A (2018) Bayesian phylogenetic and phylodynamic data integration using BEAST 1.10. *Virus Evol* 4:vey016 . doi: 10.1093/ve/vey016
- Sun LN, Pan DD, Wu XW, Yang ED, Hua RM, Li QX (2018) *Leucobacter triazinivorans* sp. nov., a s-triazine herbicide prometryn-degrading bacterium isolated from sludge. *Int J Syst Evol Microbiol* 68:204–210 . doi: 10.1099/ijsem.0.002483
- Suzuki S, Hoa PTP (2012) Distribution of Quinolones, Sulfonamides, Tetracyclines in Aquatic Environment and Antibiotic Resistance in Indochina. *Front Microbiol* 3:67 . doi: 10.3389/fmicb.2012.00067
- Takai R, Shigetomi K, Kamagata Y, Ubukata M (2017) Growth mechanism of uncultured actinobacterial strain *Leucobacter* sp. ASN212 by zinc coproporphyrin. *Heterocycles* 95:145–151 . doi: 10.3987/com-16-s(s)31
- Takenaka S, Okugawa S, Kadowaki M, Murakami S, Aoki K (2003) The metabolic pathway of 4-aminophenol in *Burkholderia* sp. strain AK-5 differs from that of aniline and aniline with C-4 substituents. *Appl Environ Microbiol* 69:5410–3 . doi: 10.1128/aem.69.9.5410-5413.2003
- Tamura K, Nei M (1993) Estimation of the number of nucleotide substitutions in the control region of mitochondrial DNA in humans and chimpanzees. *Mol Biol Evol* 10:512–526 . doi: 10.1093/oxfordjournals.molbev.a040023
- Tamura K, Stecher G, Peterson D, Filipski A, Kumar S (2013) MEGA6: Molecular Evolutionary Genetics Analysis Version 6.0. *Mol Biol Evol* 30:2725–2729 . doi: 10.1093/molbev/mst197
- Tappe W, Herbst M, Hofmann D, Koepfchen S, Kummer S, Thiele B, Groeneweg J (2013) Degradation of sulfadiazine by *Microbacterium lacus* strain SDZm4, isolated from lysimeters previously manured with slurry from sulfadiazine-medicated pigs. *Appl Environ Microbiol* 79:2572–2577 . doi: 10.1128/aem.03636-12
- Tappe W, Hofmann D, Disko U, Koepfchen S, Kummer S, Vereecken H (2015) A novel isolated *Terrabacter*-like bacterium can mineralize 2-aminopyrimidine, the principal metabolite of microbial sulfadiazine degradation. *Biodegradation* 26:139–150 . doi: 10.1007/s10532-015-9722-9
- Tatro ET, Purnajo I, Richman DD, Smith DM, Gianella S (2014) Antibody response to *Achromobacter xylosoxidans* during HIV infection is associated with lower CD4 levels and increased lymphocyte activation. *Clin Vaccine Immunol* 21:46–50 . doi: 10.1128/cvi.00553-13
- Tatusova T, DiCuccio M, Badretdin A, Chetvernin V, Nawrocki EP, Zaslavsky L, Lomsadze A, Pruitt KD, Borodovsky M, Ostell J (2016) NCBI prokaryotic genome annotation pipeline. *Nucleic Acids Res* 44:6614–6624 . doi: 10.1093/nar/gkw569
- Taupp M, Heckel F, Harmsen D, Schreier P (2006) Biohydroxylation of *N,N*-dialkylarylamines by the isolated topsoil bacterium *Bacillus megaterium*. *Enzyme Microb Technol* 38:1013–1016 . doi: 10.1016/j.enzmictec.2005.11.021
- Team RC (2015a) R: A language and environment for statistical computing. R Found. Stat. Comput.
- Team Rs (2015b) RStudio: Integrated development for R.
- Teuber M (2001) Veterinary use and antibiotic resistance. *Curr Opin Microbiol* 4:493–499 . doi: 10.1016/s1369-5274(00)00241-1
- The Gene Ontology Consortium (2015) Gene Ontology Consortium: going forward. *Nucleic Acids Res* 43:D1049–D1056 . doi: 10.1093/nar/gku1179
- Thiaville JJ, Kellner SM, Yuan Y, Hutinet G, Thiaville PC, Jumpathong W, Mohapatra S, Brochier-Armanet

References

- C, Letarov A V., Hillebrand R, Malik CK, Rizzo CJ, Dedon PC, de Crécy-Lagard V (2016) Novel genomic island modifies DNA with 7-deazaguanine derivatives. *Proc Natl Acad Sci* 113:E1452–E1459 . doi: 10.1073/pnas.1518570113
- Thrash JC, Temperton B, Swan BK, Landry ZC, Woyke T, DeLong EF, Stepanauskas R, Giovannoni SJ (2014) Single-cell enabled comparative genomics of a deep ocean SAR11 bathytype. *ISME J* 8:1440–1451 . doi: 10.1038/ismej.2013.243
- Timmis KN, Pieper DH (1999) Bacteria designed for bioremediation. *Trends Biotechnol* 17:200–204 . doi: 10.1016/s0167-7799(98)01295-5
- Topp E, Chapman R, Devers-Lamrani M, Hartmann A, Marti R, Martin-Laurent F, Sabourin L, Scott A, Sumarah M (2012) Accelerated biodegradation of veterinary antibiotics in agricultural soil following long-term exposure, and isolation of a sulfamethazine-degrading *Microbacterium* sp. *J Environ Qual* 42:173–178 . doi: 10.2134/jeq2012.0162
- Topp E, Renaud J, Sumarah M, Sabourin L (2016) Reduced persistence of the macrolide antibiotics erythromycin, clarithromycin and azithromycin in agricultural soil following several years of exposure in the field. *Sci Total Environ* 562:136–144 . doi: 10.1016/j.scitotenv.2016.03.210
- Tripp HJ (2013) The unique metabolism of SAR11 aquatic bacteria. *J Microbiol* 51:147–153 . doi: 10.1007/s12275-013-2671-2
- Turner S, Pryer KM, Miao VPW, Palmer JD (1999) Investigating deep phylogenetic relationships among cyanobacteria and plastids by small subunit rRNA sequence analysis. *J Eukaryot Microbiol* 46:327–338 . doi: 10.1111/j.1550-7408.1999.tb04612.x
- Ullrich R, Hofrichter M (2007) Enzymatic hydroxylation of aromatic compounds. *Cell Mol Life Sci* 64:271–293 . doi: 10.1007/s00018-007-6362-1
- Vaillancourt FH, Bolin JT, Eltis LD (2006) The ins and outs of ring-cleaving dioxygenases. *Crit Rev Biochem Mol Biol* 41:241–267 . doi: 10.1080/10409230600817422
- Van Boeckel TP, Gandra S, Ashok A, Caudron Q, Grenfell BT, Levin SA, Laxminarayan R (2014) Global antibiotic consumption 2000 to 2010: an analysis of national pharmaceutical sales data. *Lancet Infect Dis* 14:742–750 . doi: 10.1016/s1473-3099(14)70780-7
- Van Goethem MW, Pierneef R, Bezuidt OKI, Van De Peer Y, Cowan DA, Makhalyane TP (2018) A reservoir of “historical” antibiotic resistance genes in remote pristine Antarctic soils. *Microbiome* 6:40 . doi: 10.1186/s40168-018-0424-5
- van Hoek AHAM, Mevius D, Guerra B, Mullany P, Roberts AP, Aarts HJM (2011) Acquired antibiotic resistance genes: an overview. *Front Microbiol* 2:203 . doi: 10.3389/fmicb.2011.00203
- Vandamme PA, Peeters C, Inganäs E, Cnockaert M, Houf K, Spilker T, Moore ERB, LiPuma JJ (2016) Taxonomic dissection of *Achromobacter denitrificans* Coenye et al. 2003 and proposal of *Achromobacter agilis* sp. nov., nom. rev., *Achromobacter pestifer* sp. nov., nom. rev., *Achromobacter kerstersii* sp. nov. and *Achromobacter deleyi* sp. nov. *Int J Syst Evol Microbiol* 66:3708–3717 . doi: 10.1099/ijsem.0.001254
- Vartoukian SR, Adamowska A, Lawlor M, Moazzez R, Dewhirst FE, Wade WG (2016) *In vitro* cultivation of ‘unculturable’ oral bacteria, facilitated by community culture and media supplementation with siderophores. *PLoS One* 11:e0146926 . doi: 10.1371/journal.pone.0146926
- Ventola CL (2015) The antibiotic resistance crisis: part 1: causes and threats. *P T* 40:277–283
- Vila-Costa M, Gioia R, Aceña J, Pérez S, Casamayor EO, Dachs J (2017) Degradation of sulfonamides as a microbial resistance mechanism. *Water Res* 115:309–317 . doi: 10.1016/j.watres.2017.03.007
- Volkers G, Palm GJ, Weiss MS, Wright GD, Hinrichs W (2011) Structural basis for a new tetracycline resistance mechanism relying on the TetX monooxygenase. *FEBS Lett* 585:1061–1066 . doi: 10.1016/j.febslet.2011.03.012

- Wada A, Kono M, Kawauchi S, Takagi Y, Morikawa T, Funakoshi K (2012) Rapid discrimination of Gram-positive and Gram-negative bacteria in liquid samples by using NaOH-sodium dodecyl sulfate solution and flow cytometry. *PLoS One* 7:e47093 . doi: 10.1371/journal.pone.0047093
- Walker BJ, Abeel T, Shea T, Priest M, Abouelliel A, Sakthikumar S, Cuomo CA, Zeng Q, Wortman J, Young SK, Earl AM (2014) Pilon: an integrated tool for comprehensive microbial variant detection and genome assembly improvement. *PLoS One* 9:e112963 . doi: 10.1371/journal.pone.0112963
- Wang L, Liu Y, Ma J, Zhao F (2016) Rapid degradation of sulphamethoxazole and the further transformation of 3-amino-5-methylisoxazole in a microbial fuel cell. *Water Res* 88:322–328 . doi: 10.1016/j.watres.2015.10.030
- Wang Q, Garrity GM, Tiedje JM, Cole JR (2007) Naive Bayesian classifier for rapid assignment of rRNA sequences into the new bacterial taxonomy. *Appl Environ Microbiol* 73:5261–5267 . doi: 10.1128/aem.00062-07
- Wang S, Hu Y, Wang J (2018) Biodegradation of typical pharmaceutical compounds by a novel strain *Acinetobacter* sp. *J Environ Manage* 217:240–246 . doi: 10.1016/j.jenvman.2018.03.096
- Waterhouse A, Bertoni M, Bienert S, Studer G, Tauriello G, Gumienny R, Heer FT, de Beer TAP, Rempfer C, Bordoli L, Lepore R, Schwede T (2018) SWISS-MODEL: homology modelling of protein structures and complexes. *Nucleic Acids Res* 46:W296–W303 . doi: 10.1093/nar/gky427
- Welte T (2016) New antibiotic development: the need *versus* the costs. *Lancet Infect Dis* 16:386–387 . doi: 10.1016/s1473-3099(16)00068-2
- Wernegreen JJ (2015) Endosymbiont evolution: predictions from theory and surprises from genomes. *Ann N Y Acad Sci* 1360:16–35 . doi: 10.1111/nyas.12740
- Whelan S, Goldman N (2001) A General Empirical Model of Protein Evolution Derived from Multiple Protein Families Using a Maximum-Likelihood Approach. *Mol Biol Evol* 18:691–699 . doi: 10.1093/oxfordjournals.molbev.a003851
- Widder S, Allen RJ, Pfeiffer T, Curtis TP, Wiuf C, Sloan WT, Cordero OX, Brown SP, Momeni B, Shou W, Kettle H, Flint HJ, Haas AF, Laroche B, Kreft J-U, Rainey PB, Freilich S, Schuster S, Milferstedt K, van der Meer JR, Großkopf T, Huisman J, Free A, Picioreanu C, Quince C, Klapper I, Labarthe S, Smets BF, Wang H, Soyer OS, Soyer OS (2016) Challenges in microbial ecology: building predictive understanding of community function and dynamics. *ISME J* 10:2557–2568 . doi: 10.1038/ismej.2016.45
- Wintermute EH, Silver PA (2010) Dynamics in the mixed microbial concourse. *Genes Dev* 24:2603–2614 . doi: 10.1101/gad.1985210
- Wittmann J, Dreiseikelmann B, Rohde C, Rohde M, Sikorski J (2014a) Isolation and characterization of numerous novel phages targeting diverse strains of the ubiquitous and opportunistic pathogen *Achromobacter xylosoxidans*. *PLoS One* 9:e86935 . doi: 10.1371/journal.pone.0086935
- Wittmann J, Dreiseikelmann B, Rohde M, Meier-Kolthoff JP, Bunk B, Rohde C (2014b) First genome sequences of *Achromobacter* phages reveal new members of the N4 family. *Viol J* 11:14 . doi: 10.1186/1743-422x-11-14
- Woappi Y, Gabani P, Singh A, Singh O V. (2014) Antibiotrophs: The complexity of antibiotic-subsisting and antibiotic-resistant microorganisms. *Crit Rev Microbiol* 42:17–30 . doi: 10.3109/1040841x.2013.875982
- Wolf S, Schmidt S, Müller-Hannemann M, Neumann S (2010) *In silico* fragmentation for computer assisted identification of metabolite mass spectra. *BMC Bioinformatics* 11:148 . doi: 10.1186/1471-2105-11-148
- Wright ES, Yilmaz LS, Noguera DR (2012) DECIPHER, a search-based approach to chimera identification for 16S rRNA sequences. *Appl Environ Microbiol* 78:717–725 . doi: 10.1128/aem.06516-11

References

- Wright GD (2005) Bacterial resistance to antibiotics: Enzymatic degradation and modification. *Adv Drug Deliv Rev* 57:1451–1470 . doi: 10.1016/j.addr.2005.04.002
- Wu J-H, Wu F-Y, Chuang H-P, Chen W-Y, Huang H-J, Chen S-H, Liu W-T (2013) Community and proteomic analysis of methanogenic consortia degrading terephthalate. *Appl Environ Microbiol* 79:105–112 . doi: 10.1128/aem.02327-12
- Yagi H, Jerina DM, Kasperek GJ, Bruce TC (1972) A novel mechanism for the NIH-shift. *Proc Natl Acad Sci USA* 69:1985–1986 . doi: 10.1073/pnas.69.7.1985
- Yamashita M, Murahashi H, Tomita T, Hirata A (2000) Effect of alcohols on *Escherichia coli* phages. *Biocontrol Sci* 5:9–16
- Yang C-W, Hsiao W-C, Fan C-H, Chang B-V (2016) Bacterial communities associated with sulfonamide antibiotics degradation in sludge-amended soil. *Environ Sci Pollut Res Int* 23:19754–19763 . doi: 10.1007/s11356-016-7187-y
- Yang N, Wan J, Zhao S, Wang Y (2015) Removal of concentrated sulfamethazine by acclimatized aerobic sludge and possible metabolic products. *PeerJ* 3:e1359 . doi: 10.7717/peerj.1359
- Yang W, Moore IF, Koteva KP, Bareich DC, Hughes DW, Wright GD (2004) TetX is a flavin-dependent monooxygenase conferring resistance to tetracycline antibiotics. *J Biol Chem* 279:52346–52352 . doi: 10.1074/jbc.M409573200
- Ye J, Coulouris G, Zaretskaya I, Cutcutache I, Rozen S, Madden TL (2012) Primer-BLAST: A tool to design target-specific primers for polymerase chain reaction. *BMC Bioinformatics* 13:134 . doi: 10.1186/1471-2105-13-134
- Yoon S-H, Ha S-M, Kwon S, Lim J, Kim Y, Seo H, Chun J (2017) Introducing EzBioCloud: a taxonomically united database of 16S rRNA gene sequences and whole-genome assemblies. *Int J Syst Evol Microbiol* 67:1613–1617 . doi: 10.1099/ijsem.0.001755
- Yoshida R, Oikawa S, Ogawa Y, Miyakoshi Y, Ooida M, Asanuma K, Shimizu H (1998) Mutagenicity of *p*-aminophenol in *E. coli* WP2uvrA/pKM101 and its relevance to oxidative DNA damage. *Mutat Res* 415:139–150 . doi: 10.1016/S1383-5718(98)00058-8
- Youssef NH, Farag IF, Rinke C, Hallam SJ, Woyke T, Elshahed MS (2015) *In silico* analysis of the metabolic potential and niche specialization of candidate phylum “*Latescibacteria*” (WS3). *PLoS One* 10:e0127499 . doi: 10.1371/journal.pone.0127499
- Yun J-H, Cho Y-J, Chun J, Hyun D-W, Bae J-W (2014) Genome sequence of the chromate-resistant bacterium *Leucobacter salsicius* type strain M1-8^T. *Stand Genomic Sci* 9:495–504 . doi: 10.4056/sigs.4708537
- Zakharieva O, Grodzicki M, Trautwein AX, Veeger C, Rietjens IMC. (1998) Molecular orbital study of porphyrin–substrate interactions in cytochrome P450 catalysed aromatic hydroxylation of substituted anilines. *Biophys Chem* 73:189–203 . doi: 10.1016/s0301-4622(98)00111-2
- Zankari E, Hasman H, Cosentino S, Vestergaard M, Rasmussen S, Lund O, Aarestrup FM, Larsen M V. (2012) Identification of acquired antimicrobial resistance genes. *J Antimicrob Chemother* 67:2640–2644 . doi: 10.1093/jac/dks261
- Zhang T, Li B (2011) Occurrence, transformation, and fate of antibiotics in municipal wastewater treatment plants. *Crit Rev Environ Sci Technol* 41:951–998 . doi: 10.1080/10643380903392692
- Zhang Y-B, Zhou J, Xu Q-M, Cheng J-S, Luo Y-L, Yuan Y-J (2016) Exogenous cofactors for the improvement of bioremoval and biotransformation of sulfamethoxazole by *Alcaligenes faecalis*. *Sci Total Environ* 565:547–556 . doi: 10.1016/j.scitotenv.2016.05.063
- Zhang Z, Schwartz S, Wagner L, Miller W (2000) A greedy algorithm for aligning DNA sequences. *J Comput Biol* 7:203–214 . doi: 10.1089/10665270050081478